222
Advances in Polymer Science

Advances in Polymer Science

Recently Published and Forthcoming Volumes

Inclusion Polymers

Volume Editor: Gerhard Wenz

With contributions by

S. Amajjahe · S. Choi · A.E. Kaifer · R. Katoono · J. Li ·
H. Ritter · A.E. Tonelli · W. Wang · G. Wenz · N. Yui ·
A. Yamashita

Advances in Polymer Science
Also Available Electronically

For all customers who have a standing order to Advances in Polymer Science, we offer the electronic version via SpringerLink free of charge. Please contact your librarian who can receive a password or free access to the full articles by registering at:

springerlink.com

If you do not have a subscription, you can still view the tables of contents of the volumes and the abstract of each article by going to the SpringerLink Home page, clicking on "Browse by Online Libraries", then "Chemical Sciences", and finally choose Advances in Polymer Science.

You will find information about the

– Editorial Board
– Aims and Scope
– Instructions for Authors
– Sample Contribution

at springer.com using the search function.

Color figures are published in full color within the electronic version on SpringerLink.

Preface

Since Hermann Staudinger coined the concept of macromolecules as covalently linked very large molecular entities in 1922, the main focus of ongoing research has been on the synthesis of polymers and copolymers leading to a great variety of stable, structural, and functional materials. On the other hand, during the last 15 years the knowledge about supramolecular self-organization of polymers with low molecular-weight compounds by reversible non-covalent interactions gained increasing attention. In particular, the interactions of cyclic molecules, called hosts, with polymers became increasingly attractive, since the properties of polymers such as solubility or crystallinity can be altered without the need of chemical reactions. In contrast to regular polymers or copolymers, supramolecular structures comprised of polymers and ring-shaped hosts are not totally stable. Therefore they can show programmable lifetimes or adapt specifically to different environments. In this respect polymeric supramolecular structures resemble living systems more than regular polymers.

This volume is mainly devoted to a very fascinating class of ring-shaped cyclic $\alpha(1\rightarrow4)$ linked oligo-glucans, named *cyclodextrins*. Cyclodextrins are industrially produced from the renewable resource starch. They are especially suitable for the self-assembly of water based supramolecular structures, and they are highly biocompatible. Cyclodextrins are able to complex both monomers and polymers which offer suitable hydrophobic binding sites. The driving forces are mainly van der Waals and hydrophobic interactions. This complexation process is called *inclusion* and the resulting supramolecular structures *inclusion compounds*. In addition, Chapter 6 of this volume is devoted to another interesting host, a cyclic urea compound called cucurbituril, which is able to recognize cationic guest molecules in aqueous solution.

In the first chapter I shall describe basic principles of molecular recognition of monomers and polymers by cyclodextrins (G. Wenz, in Volume 222, Chapter 1) and try to provide an overview of inclusion polymers with cyclodextrins. The following chapters are more specialized. They are about functional cyclodextrin polyrotaxanes for drug delivery (N. Yui, R. Katoono, A. Yamashita, in Volume 222, Chapter 2), cyclodextrin inclusion polymers forming hydrogels (J. Li,

in Volume 222, Chapter 3), molecular processing of polymers with cyclodextrins (A.E. Tonelli, in Volume 222, Chapter 4), polymerization of included monomers and behaviour of resulting polymers (S.W. Choi, S. Amajjahe, H. Ritter, in Volume 222, Chapter 5), and cucurbituril and cyclodextrin complexes of dendrimers (W. Wang, A.E. Kaifer, in Volume 222, Chapter 6).

We have described the versatile field of inclusion polymers from several directions and have tried to contribute to some broader application of cyclic host molecules for the variation of physical and chemical properties of polymers. Hopefully, this volume will be beneficial to readers of the polymer community who like to enter the fascinating field of supramolecular polymer chemistry.

Saarbrücken, Spring 2009   *Gerhard Wenz*

Contents

Recognition of Monomers and Polymers by Cyclodextrins

Gerhard Wenz

Abstract Cyclodextrins (CDs), cyclic oligomers consisting of 6, 7, 8, or more $\alpha(1 \rightarrow 4)$-linked glucose units, are readily available, water-soluble organic host compounds that are able to complex organic guest molecules if the latter contain a suitable hydrophobic binding site. The main driving forces are nonpolar interactions such as hydrophobic and van der Waals interactions. CDs are able to recognize the thickness, polarity, and chirality of monomeric and polymeric guest molecules. In addition, functional groups can be covalently attached to CDs to modify or improve the molecular recognition capability of CDs. In this review, the binding potentials of the most important CDs and CD derivatives are summarized, and general rules for the recognition of monomeric and polymeric guests are derived. A supramolecular tool box of water-soluble hosts and guests is provided, which allows the assembly of many sophisticated supramolecular structures, as well as rotaxanes and polyrotaxanes.

Contents

G. Wenz
Organische Makromolekulare Chemie, Saarland University, Campus Saarbrücken, C 4.2,
66123 Saarbrücken, Germany
e-mail: g.wenz@mx.uni-saarland.de

Abbreviations

α-CD	α-Cyclodextrin
β-CD	β-Cyclodextrin
γ-CD	γ-Cyclodextrin
CD	Cyclodextrin
CE	Capillary electrophoresis
DMF	N,N-Dimethylformamide
DMSO	Dimethylsulfoxide
DS	Degree of substitution
FITC	Fluoresceine-4-isothiocyanate
GPC	Gel permeation chromatography
IC	Inclusion compounds
ITC	Isothermal titration calorimetry
LCST	Lower critical solution temperature
NMR	Nuclear magnetic resonance spectroscopy
NOE	Nuclear-Overhauser-effect
OLED	Organic light emitting diode
PCL	Polycaprolactone
PDLA	Poly(D-lactide)

PDMS   Polydimethylsiloxane
PEO   Polyethylene glycol
PIBMA   Poly(isobutene-*alt*-maleic acid)
PPO   Polypropylene glycol
PLLA   Poly(L-lactide)
PTHF   Polytetrahydrofuran, poly(tetramethylene oxide)
r.t.   Room temperature
THF   Tetrahydrofuran
UV–vis UV–vis spectroscopy
WAXS   Wide angle X-ray scattering

1 Introduction

The recognition of one person from a crowd of people requires the distinction of certain human attributes, such as tallness, voice, hair color, or gestures. Recognition becomes more selective when increasing numbers of these attributes are checked for various persons. Our society would not function without the ability to recognize certain people. Recognition is one of the most important prerequisites of the development of the human culture, since it allows creation, transformation, and collection of information. The information content of a system increases with the selectivity of recognition of one event out of many others. Therefore, selectivity gained by recognition allows for writing of information into and reading from a system, which would be otherwise random, arbitrary and chaotic [1].

The recognition of one molecule out of a crowd of many other molecules requires distinction of certain molecular attributes, such as size, polarity, hydrogen bond pattern, chirality, or other physicochemical properties. If several attributes can be checked simultaneously, recognition becomes more selective. Recognition between an enzyme and a substrate was described first by Emil Fischer as the well-known *lock and key principle* [2]. Molecular recognition between complementary DNA strands [3] or protein ligand interactions [4] is very important for the molecular function of living systems.

Recognition between two sorts of molecules, A and B, is caused by reversible, noncovalent interactions such as Coulomb, van der Waals, and solvophobic interactions, as well as hydrogen bonds. D.J. Cram coined the terms host and guest for two complementary molecules [5]. The complex of both is called a *host–guest complex* or, according to Lehn, *supramolecular structure* or *super molecule* [6]. Supramolecular structures may also be composed of more than two molecules. Selectivity of recognition increases as hosts and guests fit together better. Binding constants increase with increasing preorganization of a host for a certain guest [7].

Intelligent molecular systems can be created based on host–guest recognition, which can self-organize and behave differently than nonorganized matter. Supramolecular structures formed by molecular recognition can be used to create molecular systems with specific functions, such as motors or stimulus-responsive

artificial muscles [8, 9], surfaces with photo-switchable polarities [10], intelligent drug carriers [11], or high density information storage systems [12, 13].

Therefore, supramolecular structures will be of great importance for the development of new technologies in the near future. Despite there being a plethora of secondary literature available about molecular recognition of monomeric guests by organic host molecules, little systematic and comprehensive knowledge is available about molecular recognition of polymers. Therefore, I wish to address this topic in this chapter, focusing on one important class of organic host molecules, namely, the cyclodextrins (CDs). CDs form complexes, so-called "Einschlussverbindungen" [14], or inclusion compounds (ICs), with hydrophobic or amphiphilic guests. Among other hosts [15], such as crown ethers [16], cryptands [17], spherands [7], cucurbiturils [18], cyclic amides [19], and cyclic peptides [20], CDs offer several advantages:

- CDs are produced on an industrial scale in high purity (>5,000 tons per year)
- CDs form supramolecular structures in water
- CDs are highly biocompatible, biodegradable and show low toxicity
- CDs can be selectively modified
- CDs already have some industrial applications [21]

Since the literature about CDs is rapidly expanding ($\sim$45,000 references in the CAS database from September 2008), this review is focused on stating basic principles exemplified by original literature. Older literature about CDs has already been summarized in several review articles dealing with CDs in general [22, 23], CD crystallography [24, 25], CD derivatives [26], stabilities of CD ICs [27], CD rotaxanes [28], and CD polyrotaxanes [29–31].

2 Cyclodextrins and Cyclodextrin Derivatives

2.1 Cyclodextrins

CDs are cyclic oligomers consisting of 6, 7, 8, or more $\alpha(1 \rightarrow 4)$ linked anhydroglucose units called α-, β-, γ-CDs, and so on, respectively (see Fig. 1). They were discovered by Villiers [32], identified by Schardinger [33], and systematically investigated by Freudenberg [34] and Cramer [35]. They are produced by enzymatic degradation of starch by CD glucosyltransferases (CGTases), already on an industrial scale. The ring sizes $n = 6$, 7, and 8 are isolated from the reaction mixture with high purities by specific precipitation agents (n-octanol, toluene, and cyclohexadec-8-en-1-one for α-, β-, and γ-CD, respectively) [23]. Since there are no precipitation agents available for the higher oligomers, these oligomers still need to be isolated by chromatographic methods. Nevertheless, even the structure of the 26-membered ring is known [24]. In addition, the five-membered cyclic oligomer, cyclomaltopentaose, has been obtained by chemical synthesis in small quantities [36]. We shall focus in

Fig. 1 Schematic drawings
of cyclodextrins (CDs), $n =$
6, 7, 8 for α-, β-, γ-CD,
respectively
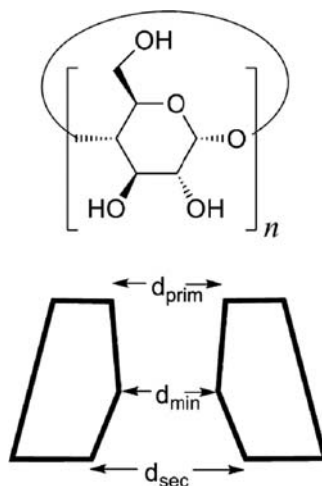
Table 1 Inner widths of cyclodextrins obtained by molecular modeling

Cyclodextrin	n	d_{prim} [Å] CPK[a]	d_{sec} [Å] CPK[a]	d_{min} [Å] AM1[b]
α-CD	6	4.7	5.2	4.4
β-CD	7	6.0	6.4	5.8
γ-CD	8	7.5	8.3	7.4

[a]Measured from CPK models [22]
[b]Calculated by Gaussian03 [42] and MolShape [40]

the review mainly on the hosts α-, β-, and γ-CDs because of their ready availability. These CDs are moderately to highly soluble in water (see Table 2) [37] and highly soluble in strongly polar organic solvents like DMF, DMSO, and pyridine.

As shown by X-ray and neutron beam crystallography, α-CD, β-CD, and γ-CD molecules look like hollow truncated cones (Fig. 1) [24]. The primary C-atoms C-6 are located at the narrow side, called the primary rim, while the secondary C-atoms C-2 and C-3 are located at the wide side, called the secondary rim. Since the glucose moieties cannot rotate within these rings because of steric constraints, no conformational isomers are possible, unlike for calixarenes [38]. Furthermore, the CD macrocycles are rigidified by intramolecular hydrogen bonds between the secondary hydroxyl groups [39]. The diameters of the internal cavities range from about 4.5 to 8 nm, depending on the ring size (see Table 1). These cavities are not cylindrically shaped but conical with a constriction in the middle, as depicted in Fig. 1 [22,40,41]. The heights of α-CD, β-CD, and γ-CD molecules are very similar and around 0.8–0.9 nm [24].

2.2 Cyclodextrin Derivatives

The hydroxyl groups at the primary (C-6) and the two secondary positions (C-2, C-3) are prone to displacement reactions at the O- or C-atoms leading to CD derivatives [26]. There are several motivations for the derivatization of CDs:

- Improvement of solubility in water
- Improvement of solubility in organic solvents
- Improvement of molecular recognition potential
- Reduction of toxicity

Derivatizations can be performed in well-defined regioselective ways, in which 1, 2, 2n, or 3n ($n = 6$, 7, or 8 for α-CD, β-CD, or γ-CD, respectively) substituents were attached at certain positions of the CD scaffold [26]. In addition, CDs have also been derivatized statistically at various positions. Statistical derivatizations require much less effort for synthesis and purification and give rise to higher yields than regioselective ones, but the products are difficult to reproduce and to characterize because of their heterogeneity. All synthetic methods will be briefly summarized subsequently. Those derivatives used most often are listed in Table 2.

The main entry for CD derivatives, mono-substituted at the C-6 position, are the tosylates for α-CD and β-CD and 2,4,6-triisopropylbenzene sulfonate for γ-CD [43–45]. The 6-*O*-sulfonates of CDs can be converted to functional CD derivatives,

Table 2 The supramolecular toolbox: CDs and common CD derivatives and their solubilities in water

Abbreviation	Ring size, n	Substituents	Positions	Degree of substitution per CD	Aqueous solubility at 25°C, %	Aqueous solubility at 60°C, %
α-CD	6	No		0	13	>33
β-CD	7	No		0	1.8	9
γ-CD	8	No		0	26	>50
RAMEA	6	Methyl	All	10	>50	>50
RAMEB	7	Methyl	All	12–13	>50	>50
DIMEB	7	Methyl	2,6-O	14	>50	1.8
TRIMEB	7	Methyl	All	21	29	2.6
HPα-CD	6	Hydroxypropyl	All	3–5	>50	>50
HPβ-CD	7	Hydroxypropyl	All	4–5	>50	>50
HPγ-CD	7	Hydroxypropyl	All	4–6	>50	>50
Tosyl-β-CD	7	Tosyl	6-O	1	0.06	0.6
NH$_2$-β-CD	7	Amino	6-C	1	7.5	>30
SBE7-β-CD	7	Sulfonatobutyl	All	7	>50	>50
SET7-β-CD	7	Sulfonatoethylthio	6-C	7	>50	>50
AET7-β-CD	7	Aminoethylthio	6-C	7	>50	>50

such as the 6-azido [46], 6-amino [44], or 6-thioether [47] by nucleophilic displacement reactions. Additionally, different regio-isomers (AB, AC, or AD) of CDs, disubstituted at O-6 [48, 49], and trisubstituted at O-6 [50] can be obtained by a reaction of β-CD with sulfonyl chlorides. Furthermore, sulfonates at the secondary hydroxyl groups can be synthesized and readily transferred to the 2,3-anhydro-CDs, which can further react with nucleophiles to furnish β-CD derivatives functionalized at the secondary rim [51]. On the other hand, hepta-2,3,6-tri-*O*-methyl-β-CD and hepta-2,3,6-tri-*O*-benzyl-β-CD can be regioselectively dealkylated at two well-defined primary positions with DIBAL [52, 53]. The resulting free OH groups can be further modified to other functional groups [54, 55]. Per-6-iodo-6-deoxy-CDs, readily available by reaction of CDs and triphenylphosphine/I_2 [56], are the key intermediates for the synthesis of CD derivatives with *n* substituents at the primary rim by nucleophilic displacement reactions. Substitution by azide and subsequent reduction furnishes the corresponding per-6-amino-6-deoxy-CD derivatives [57]. Reaction of the per-6-iodo-6-deox-CDs with thiol functions leads to various *n* functional thioethers, such as heptaamines, heptacarboxylates, and heptasulfonates [47, 58]. Several glycoclusters bearing *n* sugar groups (mannose, glucose, galactose) at the primary rim were synthesized this way, as well [59].

All regioisomers of per-*O*-methyl-CDs (2-*O*-, 3-*O*-, 6-*O*-) and per-di-*O*-methyl-β-CDs (2,6-di-*O*-, 2,3-di-*O*-, 3,6-di-*O*-) have been synthesized by regioselective methods using protecting group chemistry [60–63]. Analogous functional β-CD derivatives bearing 7, 14, or 21 carboxymethyl groups, as well as 7 amino and 7 carboxymethyl groups, were synthesized by Kraus et al. via the corresponding allyl ethers [64–67].

In addition to the regioselectively derivatized CDs, a number of statistically substituted CDs are in use. Highly water-soluble statistic derivatives are obtained by reaction of CDs with methyl halides [68], with epoxides (e.g., ethylene oxide, propylene oxide [69, 70], or allyl glycidylether [71]), and with cyclic sulfates (e.g., butane sultone [72]). Statistical allyl ethers were converted to sulfonates by addition of sulfite [71]. Monochlorotriazinyl-β-CD is another available reactive CD. Since these synthetic procedures are rather simple compared to the regioselective ones, many of these statistical compounds are available at the technical scale.

The solubilities of native CDs in water are moderate, with β-CD showing the lowest solubility, as shown in Table 2 [37]. Solubilities generally increase drastically with increasing temperature. Only methylation leads to lower solubilities at elevated temperatures. In other words, methylated CDs show a lower critical solution temperature (LCST). Hydroxypropyl-CDs are highly water-soluble at any temperature [69, 70]. Ethylated CDs are amphiphilic [73], while alkylated CDs with alkyl chain lengths >2 are already insoluble in water, but soluble in organic solvents like chloroform or toluene [74]. Both anionic CD derivatives like SBE-β-CD or SET7-β-CD and cationic CD derivatives like AET-β-CD are also highly water-soluble and therefore well suited for the solubilization of hydrophobic guest molecules [47, 58, 75].

2.3   Cyclodextrin Dimers and Polymers

Since space is limited within the internal cavities of α-, β-, and γ-CDs, it was desirable to connect two and more CD rings to achieve some cooperativity in binding large guests. Two α-CD rings had been connected by one or two bridges at the primary rims [76]. Two β-CD had been connected, as well, via one or two bonds to a dimer by Breslow et al. [49, 77–81]. Recently, a heterodimer of α-CD and β-CD was also synthesized [82].

CD polymers can be synthesized (1) by radical polymerization of monofunctional CD monomers, (2) by polymer-analogous reaction of polymers with CDs, and (3) by partial crosslinking of CDs, as exemplified below.

α-CD and β-CD, both conjugated with an acryloyl group, were polymerized by radical initiators [83]. Similarly, phenylacetylene [84] and polyphenylene ethynylene [85] backbones with pendant α-CD, β-CD, and γ-CD groups were synthesized by polymerization of the respective CD monomers. Polymer-analogous reaction turned out to be a highly efficient method of CD polymer synthesis. Native CDs were attached via an ester bond to alternating poly(maleic anhydride) copolymers in high yields to produce water-soluble poly CD maleates [86–89]. α-CD and β-CD were also conjugated to polyallylamine [90], poly(ethyleneimine) dendrimers [91], chitosane [92, 93], and alginate [94]. Similarly, 6-amino-β-CD was attached via an amide bond to a succinylated α-CD-PEO polyrotaxane [95].

Crosslinking of α-CD with epichlorohydrin in aqueous solution under well controlled conditions furnished hyperbranched water-soluble α-CD polymers [96, 97]. On the other hand, template directed crosslinking of α-CD, threaded on PEG, gave rise to linear CD polymers with two to three bridges between every two neighboring rings, or so-called molecular tubes, as shown in Fig. 2 [98–101].

3   Recognition of Monomeric Guests by CDs and CD Derivatives

3.1   General Remarks

The following section exemplifies how different molecular attributes of a guest, such as length and thickness, chirality, functional groups, and end groups are recognized by CDs and CD derivatives. Molecular recognition is always controlled by interactive forces between the guest and the host, as described below.

The internal cavities of CDs are mainly hydrophobic and able to attract guest molecules by hydrophobic, van der Waals, and other dispersive interactions [102]. Since these interactions are strongly distance dependent [103], thickness recognition is especially pronounced. The dominance of solvophobic interactions is evident in the fact that the inclusion of guests in CDs occurs preferentially in aqueous solutions. The addition of small amounts of organic solvents to aqueous solutions is enough to render ICs significantly less stable [104]. These attractive interactions are mainly controlled by space filling: the more the hydrophobic part of the guest fills
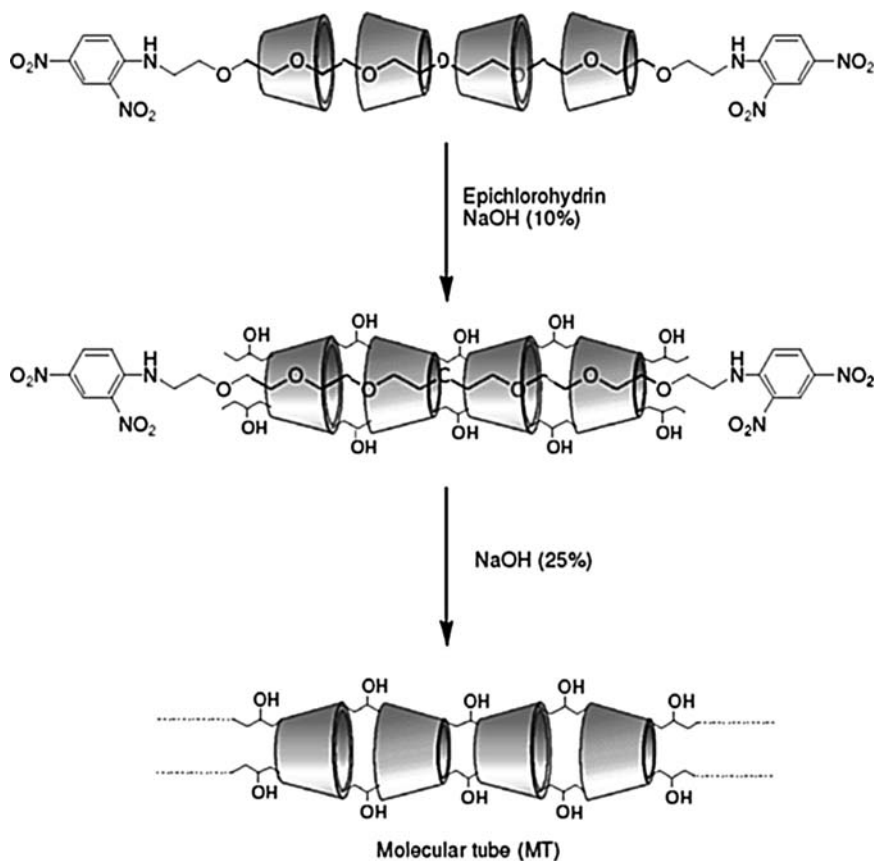
Fig. 2 Template directed synthesis of molecular tubes (MT) Harada et al.

the internal space of the CD host, the stronger the host–guest interaction. Therefore, the hydrophobic area of the guest mainly determines the nonspecific attractive interactions. For example, binding free energy values $-\Delta G^0$ of several homologous series of guests in β-CD linearly increase by $2.8 \pm 0.6 \, \text{kJ mol}^{-1}$ per methylene group [27, 105].

Molecular recognition of guests by CDs is not only controlled by interactions between CD and guest but also indirectly by interactions between CDs and between guests. Four different types of CD ICs can be classified, as depicted in Fig. 3. ICs of type I consist of a native CD and a hydrophobic guest. These ICs are generally insoluble in water, since channel ICs are formed by hydrogen bonds between the hydroxyl groups of the CDs and hydrophobic interactions between the guests. In general, at least one hydrophilic group at the guest leads to the formation of soluble ICs of type II. Solubility of the guest is increased by IC formation because the hydrophobic part of the guest is masked by the CD. So-called *bola-amphiphiles* [106, 107], amphiphilic molecules with two terminal hydrophilic groups, form ICs
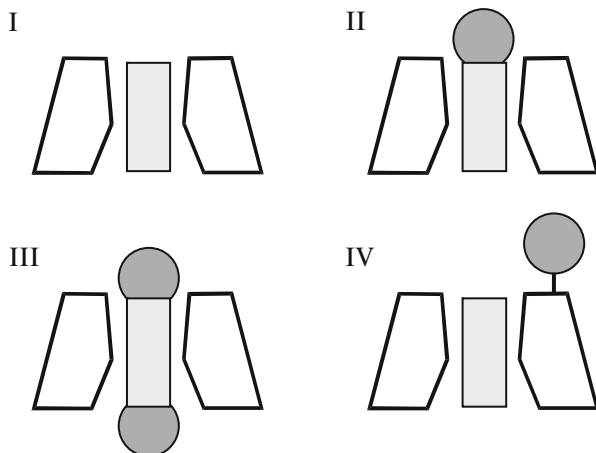
Fig. 3 Classification of CD ICs: type I: hydrophobic guest, insoluble channel IC, type II: amphiphilic guest, solubilization of a guest, type III: bola-amphiphilic guest, homogenous IC formation, type IV: charged CD derivative, solubilization of a hydrophobic guest

of type III under homogenous conditions, since all of CD, guest, and IC are highly water-soluble. Furthermore, charged CD derivatives form water-soluble ICs of type IV even with hydrophobic guests. In ICs of types II–IV, repulsive interactions between the hydrophilic groups and solvation effects prevent the formation of water insoluble channel ICs typical for type I.

For the quantification of molecular recognition, binding constant K and binding free energy ΔG^0 are defined by (1) and (2), respectively. Since determination of K requires at least measurable concentrations of each component, K and ΔG^0 can only be accurately determined for ICs of types II–IV:

$$K = \frac{[CD \cdot G]}{[CD][G]}, \tag{1}$$

$$\Delta G^0 = -RT \ln K. \tag{2}$$

Molecular recognition is not only limited to differentiation of binding free energies ΔG^0, called *thermodynamic recognition*, but can also originate from differentiation of the kinetics of IC formation and dissociation, denoted as *kinetic recognition*. Activation energies of both complex formation and dissociation influence the binding kinetics, which can influence binding selectivities in nonequilibrium states. Kinetic recognition occurs especially for bola-amphiphiles because the bulky end groups can significantly hinder formation and dissociation of the ICs. Inclusion becomes an activated process controlled by an activation energy, which increases with increasing size of the bulky end groups (see Fig. 4). Activation energies $E_A = \Delta H^{\neq}$ are determined according to the Arrhenius equation from the temperature dependence of the respective rate constants. Activation free energies, $\Delta G^{\neq}$, are directly
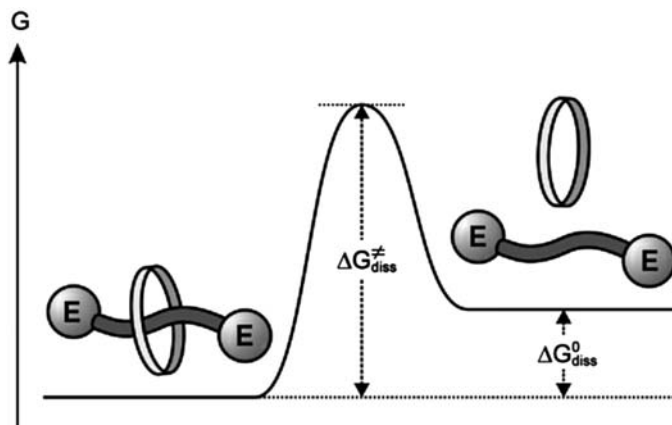
Fig. 4 Energy diagram for the dissociation of the IC of a bola-amphiphile, E: hydrophilic end group, $\Delta G_{\text{diss}}^{\neq}$: activation free energy of dissociation, $\Delta G_{\text{diss}}^{0} = -\Delta G^{0}$: free energy of dissociation (reprinted with permission from [31], copyright of the American Chemical Society)

calculated from the corresponding rate constants k using the Eyring theory [108] (3), with Planck's constant h and Boltzmann's constant k_{B}. Both activation energies are often in the same range. Those ICs in which dissociation is sterically hindered are *pseudorotaxanes*, and those where activation energy exceeds 50 RT (the 50-fold average thermal energy) are *rotaxanes* [31]:

$$\Delta G^{\neq} = -RT \ln \frac{k\text{h}}{k_{\text{B}}T}. \qquad (3)$$

3.2 Thermodynamic Recognition of the Size of a Guest

Due to their well-defined internal diameters (see Table 1) and their rigid structure, CDs are able to recognize the thicknesses of various guest molecules. Thermodynamic thickness recognition of some often used guests by α-, β-, and γ-CDs is summarized in Table 3. α-CD is capable of complexing linear aliphatic chains. Benzene, naphthalene, adamantane, or ferrocene moieties fit well within β-CD. γ-CD can accommodate pyrene or two azobenzene moieties. $-\Delta G^{0}$ values of 30 kJ mol^{-1} can be reached if the guest fits well inside a CD cavity. More detailed information about ICs of α-, β-, and γ-CDs is provided subsequently.

3.2.1 ICs of α-CD

The minimal internal diameter of α-CD, $d = 4.4$ Å, limits the formation of ICs mainly to linear alkyl chains. For example, α-CD forms crystalline ICs with

Table 3 Recognition of the thicknesses of guests by CDs according to their binding free energies ΔG^0 in kJ mol^{-1} at pH 7

Guest	$-\Delta G^0$/kJ mol^{-1} α-CD	$-\Delta G^0$/kJ mol^{-1} β-CD	$-\Delta G^0$/kJ mol^{-1} γ-CD	Ref.
1,10-Decandiol	22	19	<10	[109, 110]
1-Adamantane-carboxylate	13	26	21	[111]
4-*tert*-Butybenzoate	13	24	<10	[58, 112]
2-Naphthalene sulfonate	15	31	7	[113]
Pyrene	12	15	17	[114]
methyl orange anion	23	19	41[a]	[115]

[a]2:1 Complex formed
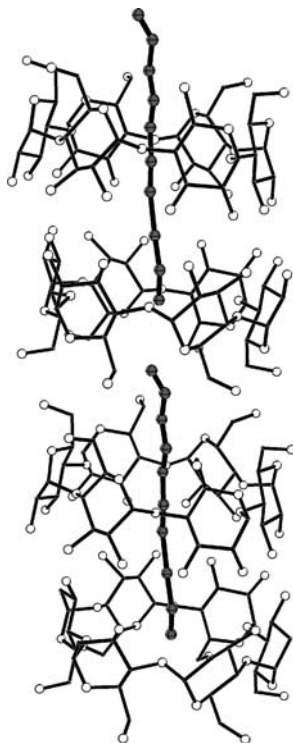
Fig. 5 Crystal structure of the channel IC of *n*-decane in α-CD [116]

n-alkanes insoluble in water. These ICs show a channel structure in which CDs are oriented in a nearly parallel fashion, and the alkane is confined within the channel, as exemplified in Fig. 5. The α-CD rings are connected by hydrogen bonds between the primary rims and the secondary rims each. Since the alkyl chain nearly fills the α-CD cavity, the internal water molecules of native α-CDs are totally ejected by the guest. Most C–C bonds of the guest are in the *trans* conformation.
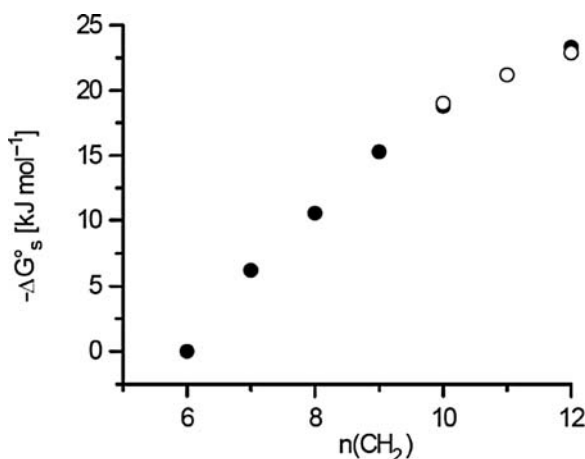
Fig. 6 Binding free energies $-\Delta G^0$ as a function of the lengths of the hydrophobic binding sites, quantified by the number of methylene groups $n(CH_2)$, for (*filled circle*) bola-amphiphiles, α, ω-diaminoalkanes, and (*open circle*) poly-bolaamphiphiles, poly(imino-oligomethylene)s at pH 6.7 and 25 °C, determined by ITC [119]

Some limited mobility of the alkanes was detected by solid state DNMR as a function of temperature [117]. This mobility explains why alkanes such as pentane can be driven out of the ICs by heating, leaving behind empty channel structures that differ from the well known native herringbone type structures of CDs [118].

There is no binding data of *n*-alkanes available, since the α-CD type I ICs are insoluble in water. Hydrophilic groups, such as carboxylate, amino, or hydroxyl groups, at one or both ends of linear alkyl chains render the ICs water-soluble and allow the determination of binding data [27]. The binding free energies ΔG^0 are becoming linearly more negative with increasing number *n* of methylene groups, as shown for the homologous series of α, ω-diamino alkanes in Fig. 6.

For *n* = 6 or less, no binding was found at all because the highly hydrophilic protonated amino groups avoid staying inside the hydrophobic CD cavity [119]. For comparison, the corresponding α, ω-diols are able to form ICs with shorter spacer lengths, since the hydroxyl groups are less hydrophilic than the protonated amino groups [109]. For short spacer lengths *n*, repulsive interactions between end-groups of bola-amphiphiles and α-CD are pronounced, but they level off with increasing *n*. If *n* is 12 or greater, even two α-CDs can thread onto bola-amphiphiles [120]. At present, no systematic binding data is available for amphiphilic guest molecules with unsaturated and branched alkyl chains, such as isoprenoids.

Benzene or cyclohexane rings can still pass through the α-CD ring, but they are already too thick to be complexed within the center of the α-CD cavity. Therefore, only rather unstable ICs are formed, in which the ring is situated at the wider secondary rim of the α-CD cavity. They are called *shallow ICs*. Benzoic acid derivatives are complexed exceptionally well and deeply, since the COOH group prefers to remain in the cavity [121]. Biphenyl derivatives are not bound at all as well as the dibromo–diphenylethane derivative in Fig. 7.

Fig. 7 Recognition of bola-amphiphiles by α-CD (Reprinted with permission of [40], copyright of Wiley)
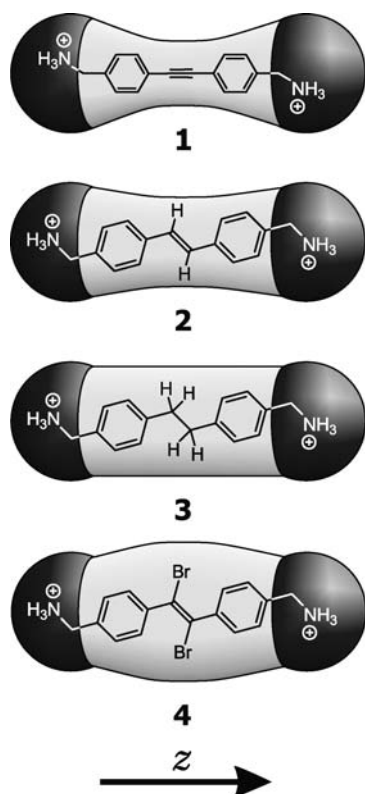
On the other hand, stilbene and tolane derivatives are tightly complexed by α-CD, since the narrow parts (waists) of these guests fit perfectly within the constriction of the host [40]. Interestingly, the values of ΔG^0 of tolane derivatives are more negative than the ones of corresponding stilbene derivatives, despite the space filling of the α-CD cavity is better with the stilbene moiety. Perfect space filling is accompanied with a high loss of entropy, which counteracts the attractive forces. The slimmer tolane moiety is bound better because it loses less entropy due to a looser fit. Consequently, a loose fit between host and guest supports binding as long as no water molecules can intrude in the empty space between host and guest. The preference of a slightly loose fit was also found earlier [122].

3.2.2 ICs of β-CD

Since the internal diameter of β-CD is 5.8 Å, it is able to accommodate guest molecules that are thicker than the ones complexed by α-CD. Hydrophobic moieties such as benzene [123], naphthalene [113, 124], anthracene [125], adamantane [126, 127], and ferrocene [128] are bound well by the β-CD cavity. Again, hydrophilic groups have to be attached to these hydrophobic binding sites to insure water

Fig. 8 Structure of bile salts
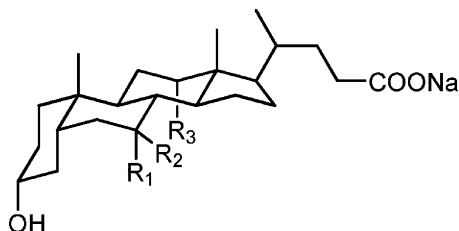
Table 4 Recognition of the pattern of hydroxylation of bile salts by β-CD [129]

Steroid	R^1	R^2	R^3	$-\Delta G^0$/kJ mol^{-1}
Cholate	OH	H	OH	21
Deoxycholate	H	H	OH	20
Chenodeoxycholate	OH	H	H	30
Ursodeoxycholate	H	OH	H	34
Lithocholate	H	H	H	36

solubility of the ICs. Binding constants K of up to $10^5\,M^{-1}$ are reached with un-substituted β-CD for the guest 1-adamantyl ammonium [27]. The bola-amphiphilic guest 4,4′-bis(imidazolyl-methylen)-biphenyl is already long enough for being complexed by two β-CD molecules, while the corresponding benzene derivative is only complexed by a single one. Furthermore, amphiphilic steroids such as bile salts cholate, deoxycholate, and lithocholate depicted in Fig. 8 form very stable complexes with β-CD. The binding data collected in Table 4 show that hydroxyl groups at the center of the guest diminish binding, while the highest $-\Delta G^0$ of 36 kJ mol^{-1} was found for lithocholate, the guest with no hydroxyls at positions 7 and 12 [129]. This example shows that a large continuous hydrophobic surface is necessary at the guest to achieve a strong affinity to CDs. The hydrophilic hydroxyl groups seem to prevent a deep inclusion of the guest within the host.

If many hydroxypropyl groups, or one or more ionic substituents, are attached to β-CD, fully hydrophobic guests can be solubilized in water by formation of type IV ICs. For example, sulfobutyl-β-CD SBE7-β-CD is even able to solubilize steroids like testosterone in water [75]. Naphthalene was solubilized in water by 3-sulfonatopropyl-oxy-hydroxypropyl-β-CD [71]. Hepta-6-aminoethyl-thio-β-CD, AET7-β-CD, renders the anticancer drug camptothecin soluble in water to a high degree. In every case, the highly hydrophilic ionic group at the β-CD prevents formation of water-insoluble channel ICs.

3.2.3 ICs of γ-CD

γ-CD possesses an internal diameter that is even larger than the previously discussed CDs, $d = 7.4\,\text{Å}$ (see Table 1), allowing inclusion of large guests such as polycyclic aromatics, e.g., pyrene [130, 131], perylene [132], and even C$_{60}$ [133, 134].

Furthermore, γ-CD can complex two guests at the same time. For example, two stilbene [135], naphthalene [136], or anthracene [137] moieties can fit in the γ-CD cavity. Attractive interactions between the end groups of two included guests enhance the stability of the ICs [136]. Because of the close proximity between two included guests, bimolecular reactions like $[2+2]$-cycloadditions [135] and Diels–Alder-reactions [138–140] are strongly accelerated by these ICs.

3.3 Thermodynamic Recognition of Chiral Guests

Since CD hosts are chiral molecules, enantiomers of a chiral guest can indeed be distinguished due to diastereomeric interactions, but differences in binding free energy $\Delta\Delta G_{R,S}$ are generally small $(0.1–2\,\text{kJ mol}^{-1})$ because CDs deviate only slightly from a cylindrical shape. The influence of substituents at β-CD on $\Delta\Delta G_{R,S}$ was systematically investigated for amino acids and their *N*-protected derivatives, shown in Table 5.

For native β-CD, chiral recognition is very small; alkyl substituents lead to an increase, while mono phenylseleno derivatives show exceptionally high selectivities, with $\Delta\Delta G_{R,S}$ of up to $8\,\text{kJ mol}^{-1}$. One polar substituent appears to have the greatest disturbance of the symmetry of the CD, providing a suitable asymmetric environment for the chiral guest. For example, 6-monoamino-β-CD and 6-*O*-carboxymethyl-β-CD show stronger chiral selectivity for amino acids than native β-CD does [144–147], while disubstituted β-CD derivatives performed even better [148]. This idea was already expressed by the three-point rule by Kano, which states that the guest has to strongly interact at least at three points with the host to gain high enantioselectivity [149].

Despite the values of $\Delta\Delta G_{R,S}^0$ being generally small, they are large enough to be resolved by high performance chromatographic methods such as gas and liquid chromatography. Thousands of successful separations of enantiomers by CD

Table 5 Chiral recognition of enantiomeric guest molecules by β-CD derivatives

Host	Guest	Method	$\Delta\Delta G_{R,S}$	Ref.
Mono-[6-(*o*-tolylseleno)-6-deoxy]-β-CD	Alanine	UV–vis	8.10	[141]
Mono-[6-(phenylseleno)-6-deoxy]-β-CD	Alanine	UV–vis	3.40	[141]
TRIMEB	AQC[a]-alanine	CE	0.16	[142]
β-CD polymer	AQC-alanine	CE	0.11	[142]
HP-β-CD	AQC-alanine	CE	0.10	[142]
DIMEB	AQC-alanine	CE	0.10	[142]
β-CD	AQC-alanine	CE	0.05	[142]
6-*O*-(4-chlorophenyl)-β-CD	Camphor	ITC	3.44	[143]
β-CD	Camphor	ITC	1.25	[143]

[a]AQC = 6-aminoquinolyl-carboxy derivative of amino acid

bonded phases using high performance liquid chromatography [150, 151], gas chromatography [152–154], or capillary electrophoreses [155] have been reported in the literature [156].

3.4 Thermodynamic Recognition of Polar Guests by CD Derivatives

Binding selectivities can be increased by polar interactions, e.g., Coulomb interactions or hydrogen bonds, between functional groups of CD derivatives and functional groups at the guest. Recently, we demonstrated the superior binding properties of hepta-6-S-6-deoxy-β-CD derivatives towards the cancer treatment drug camptothecin [47].

The contribution of Coulomb interactions to the binding of charged guests with statistically substituted sulfobutyl ether β-CD derivatives [75] and charged hepta-6-S-6-deoxy-β-CD derivatives, e.g., AET7-β-CD and SET7-β-CD, has already been demonstrated [58]. We found binding constants K exceeding $10^6\,\mathrm{M}^{-1}$ for complexes of the heptacationic β-CD derivative AET7-β-CD and negatively charged derivatives of $tert$-butyl benzene, listed in Table 6. The orientations of charged guests in the CD cavity are also influenced by Coulomb interactions, exemplified in Fig. 9. Coulomb repulsion forces the guest into a "downward" orientation, while Coulomb attraction forces the guest into an "upward" orientation.

Binding free energy ΔG^0 was strongly dependent on the solvent, and it could be subdivided into two parts: (1) the part ΔG^{00}, due to nonpolar interactions, called *binding affinity*, and (2) the part $\Delta\Delta G^0$, due to polar interactions, called *binding selectivity*, by comparison of the binding data of neutral and charged guest molecules, respectively. On one hand, binding affinity *increased* with increasing salt concentration. This increase of affinity is due to increasing hydrophobic interactions, the so-called salting out effect [124]. On the other hand, binding selectivity *decreased* with increasing salt concentration because of the shielding effects of ion clouds

Table 6 Molecular recognition between charged hosts[a] and guests [58]

Functional group	Number of functional groups	$-\Delta G^0/\mathrm{kJ\,mol}^{-1}$ for cationic guest[b]	$-\Delta G^0/\mathrm{kJ\,mol}^{-1}$ for anionic guest[c]
$S-CH_2COO^-$	1	23	22
$S-CH_2NH_3{}^+$	1	22	25
$S-CH_2COO^-$	7	35	22
$S-CH_2NH_3{}^+$	7	23	37

[a]6-Deoxy-β-CD derivatives
[b]4-$tert$-Butyl-1-guanidinium-benzene
[c]4-$tert$-Butyl-benezenesulfonic acid
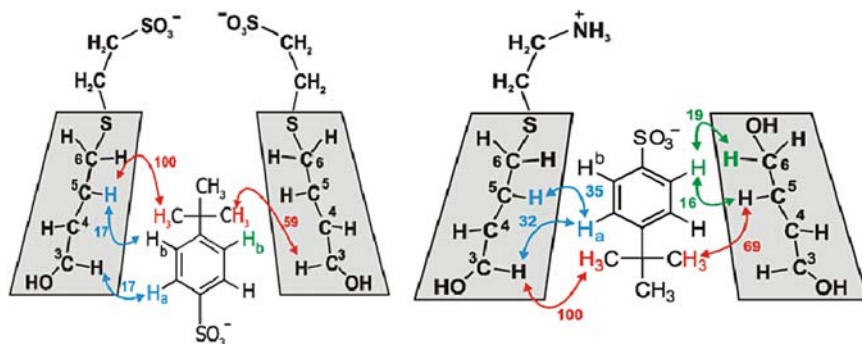
Fig. 9 Influence of charged groups at β-CD (*left*: SET7-β-CD, *right*: AET1-β-CD) on the orientations of the anionic guest *tert*-butylbenzenesulfonate in the CD cavity, as determined by ROESY NMR spectroscopy (Reprinted with permission of [58], copyright of Wiley)

formed around the functional groups, which diminish Coulomb interactions. This shielding effect can be quantitatively described by the Debye–Hückel–Onsager theory [58].

3.5 Thermodynamic Recognition of Guests by CD Dimers and CD Polymers

CD dimers are ditopic hosts, providing two connected cavities that can accommodate a guest with two binding sites for CDs, a ditopic guest. Since the complexation of the two sites is synergetic, high binding free energies ΔG^0_2 can be expected, ranging up to twice the value of ΔG^0_1 of the corresponding monotopic CD IC. This maximum value of $\Delta G^0_2 = 2\Delta G^0_1$ is never reached because the CD dimer and the guest lose conformational entropy upon complex formation, as shown in Table 7 [79, 81, 157]. Therefore, the excess binding free energy $\Delta G^0_2 - \Delta G^0_1$ of CD dimers decreases with increasing flexibility of the linker between the two CDs, as shown by comparison of the excess binding free energies, $\Delta G^0_2 - \Delta G^0_1$, calculated from ΔG^0_2 of entries 1, 5, 7, and 9 diminished by ΔG^0_1 of the corresponding monotopic complexes (entries 2, 4, 6, and 8, respectively) in Table 6.

In general, CD polymers perform worse than CD dimers, since the CD rings are connected to each other by rather flexible covalent bonds, as shown by comparison of entries 3 and 1 in Table 7. Nevertheless, CD polymers can be advantageous over CD dimers, especially because of their better availabilities and solubilities in water. For example, the fullerene C_{60} can be solubilized by CD polymers [159]. Ditopic binding between a ditopic guest and a CD polymer might be hampered by a mismatch of the distance of the binding sites in the guest and the distance of the CD cavities at the polymer. Therefore, it appears to be favorable to conjugate CD rings to a polyrotaxane, since these CD rings can migrate along the polymer thread to adopt the proper distance for binding the ditopic guest. Dissociation free energies

Table 7 Comparison of binding potentials of β-CD, β-CD dimers and a β-CD polymer

No.	Spacer	DP CD	Guest	$-\Delta G^0$/kJ mol^{-1}	Ref.
1	$-S-$	Dimer	Cholesterol	39	[158]
2	No	Monomer	Cholesterol	24	[158]
3	$-OCH_2 - CHOH - CH_2 - O-$	Polymer	Cholesterol	27	[158]
4	No	Monomer	Cholate	21	[129]
5	$-OCH_2CH_2NHCH_2CH_2O-$	Dimer	Cholate	31	[129]
6	No	Monomer	Lithocholate	36	[129]
7	$-OCH_2CH_2NHCH_2CH_2O-$	Dimer	Lithocholate	40	[129]
8	$-S-S-$	Dimer	*tert*-Butylphenol	24	[77]
9	$-S-S-$	Dimer	*tert*-Butylphenyl-*tert*-butylbenzoate	46	[77]
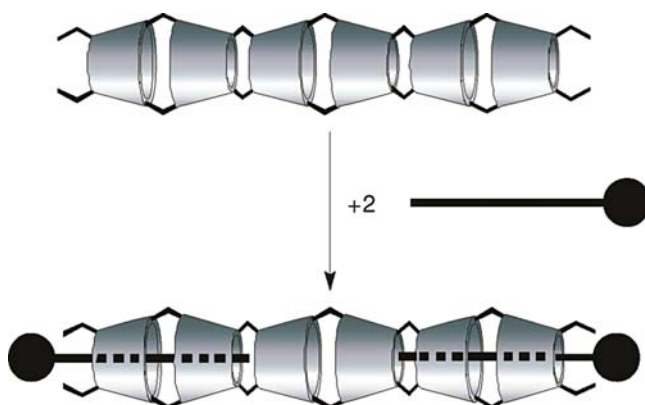
Fig. 10 Inclusion of dodecyl sulfonate by CD molecular tube [160]

$-\Delta G^0$ for the guest pyrene are significantly higher for β-CD conjugated to a polyrotaxane, $-\Delta G^0 = 19\,\mathrm{kJ\,mol^{-1}}$, compared with β-CD conjugated to a regular polymer, $-\Delta G^0 = 15\,\mathrm{kJ\,mol^{-1}}$, and native β-CD, $-\Delta G^0 = 14\,\mathrm{kJ\,mol^{-1}}$ [95].

Moreover, CD molecular tubes should be very promising ditopic and multitopic hosts because of their high rigidity due to multifold linkages between the CD rings. Indeed, very stable complexes were found for the α-CD molecular tube and the guest dodecyl sulfonate with $-\Delta G^0 = 29\,\mathrm{kJ\,mol^{-1}}$. Only two guests were complexed by one α-CD molecular tube because the anionic end groups of the guests prefer to remain outside the tube, as shown in Fig. 10 [160].

3.6 Steric Effects on Thermodynamic Recognition

Steric effects between hosts and guests generally lead to very high selectivities, since repulsive energies steeply increase with decreasing intermolecular distance *r*

according to the Lennard–Jones potential $V \sim r^{-12}$. As a consequence, guests not fitting in a CD cavity show depressed values of $-\Delta G^0$. For example β-CD binds 3-nitroaniline much weaker ($-\Delta G^0 = 9\,\text{kJ mol}^{-1}$) than the well fitting 4-nitroaniline ($-\Delta G^0 = 14\,\text{kJ mol}^{-1}$) [161]. Similarly, *m*-substituted benzoic acids form less stable ICs than *p*-substituted ones [123]. The interaction of α-CD with stilbene derivatives is even photo switchable: the *cis* isomer is more weakly bound, with $-\Delta G^0 = 14\,\text{kJ mol}^{-1}$, than the *trans* isomer, with $-\Delta G^0 = 18\,\text{kJ mol}^{-1}$ [135]. At this point, little is known about the flexibility of CDs and CD derivatives to adapt to a certain size of a guest.

3.7 Kinetic Recognition by Steric Effects

Steric hindrance exerts a very strong influence on the kinetics of the inclusion of bola-amphiphiles. Before the CD ring reaches the hydrophobic binding site, it must overcome an activation barrier in passing the bulky hydrophilic end group. Due to this steric hindrance, both the formation and the dissociation of ICs of bola-amphiphiles are exceptionally slow (see Table 8).

Since the half-lives of ICs of these bola-amphiphiles range from minutes to hours, they are termed pseudorotaxanes. We denominate the bulky end groups that control the kinetic stabilities as "*pseudostoppers*," in analogy to the term "stoppers" applicable to rotaxane formation. From the first order rate constants of dissociation, k_{diss}, Eyring's free activation energies, $\Delta G^{\neq}_{\text{diss}}$, were calculated according to (3) and listed in Table 8. Additionally, the Arrhenius activation energies can be derived from the temperature dependence of k_{diss}. These had been uptill now in reasonable agreement with $\Delta G^{\neq}_{\text{diss}}$. The activation energies increase with increasing size of the pseudostoppers. Therefore, the strong influence of steric effects is obvious. The activation energy of dissociation $\Delta G^{\neq}_{\text{diss}}$ increases with the length of the hydrophobic binding site, since the binding free energy $-\Delta G^0$ also increases. On the other hand,

Table 8 Kinetic recognition of the size of end groups of bola-amphiphiles by α-CD; k_{diss}, first order dissociation rate constant; $\Delta G^{\neq}_{\text{diss}}$, Eyring's free activation energy of dissociation

Binding site	$-\Delta G^0/\text{kJ mol}^{-1}$	End group[a]	$k_{\text{diss}}/\text{s}^{-1}$	$\Delta G^{\neq}_{\text{diss}}/\text{kJ mol}^{-1}$	Ref.
$-(CH_2)_9-$	13	NMe₃	3.90×10^{-4}	92	[162]
$-(CH_2)_{10}-$	15	NMe₃	8.65×10^{-5}	96	[163]
$-(CH_2)_{11}-$	20	NMe₃	1.60×10^{-5}	100	[162]
$-(CH_2)_{12}-$	22	NMe₃	9.00×10^{-6}	102	[162]
$-(CH_2)_{10}-$	17	NMe₂Et	2.70×10^{-6}	105	[163]
$-(CH_2)_{12}-$	10	C(OH)MeEt	1.45×10^{-3}	89	[164]
$-(CH_2)_{12}-$	15	C(OH)MeBu	3.45×10^{-4}	93	[164]
$-(CH_2)_{10}-$	17	2-MePyr	9.50×10^{-8}	113	[165]
$-(CH_2)_{10}-$	16	2,5-Me₂Pyr	8.50×10^{-8}	113	[165]

[a]Smaller, rate determining end group, if there are two different end groups

the activation energy of IC formation $\Delta G^{\neq}_{form} = \Delta G^{\neq}_{diss} + \Delta G^0$ remains nearly constant, which is reasonable, considering that the thermodynamic stability of the IC should not influence its formation rate. The largest currently known pseudostopper is the 2,5-dimethylpyridinium group, which causes a remarkable half-life of the IC of 48 days [165]. Pseudostoppers might prove to be very useful in the future, since they allow the design of supramolecular structures with a programmed lifetime. Since their formation rate is highly temperature dependent, they can be easily formed at elevated temperatures. Currently, pseudostoppers are only known for the smallest ring size, α-CD.

3.8 Directional Control by Steric Effects

Since the CD molecule has a conical shape in which the primary rim is narrow and the secondary side is wide, steric hindrance should depend on the direction of threading. If the bulky end group approaches the CD cavity from the primary rim, inclusion should be more hindered than for the approach from the secondary rim. Consequently, big pseudostoppers should force CD rings to thread with a preferential orientation. Preferential orientation can indeed be detected for unsymmetrical bola-amphiphiles composed from a pseudostopper and a real stopper, as shown in Fig. 11 and Table 9.

Orientational selectivity depends on the size of the pseudostopper: the smaller trimethyl ammonium group gives rise to a preference of 2:1 for the end group approaching the wide side α-CD [163]. The preference ratio reaches 7:1 for the bigger
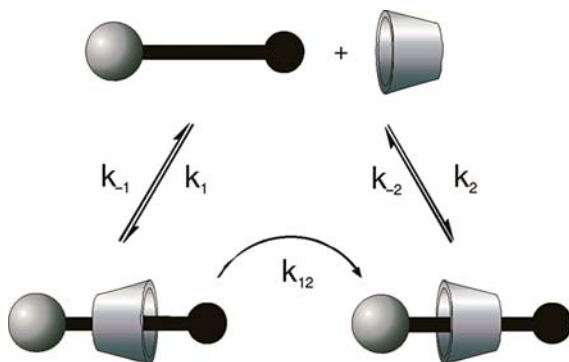
Fig. 11 Control of the orientation of CD during threading onto unsymmetrical bola-amphiphiles [166]

Table 9 Control of the orientations of α-CD rings threaded onto asymmetric bola-amphiphiles

Stopper	Pseudostopper	Orientational selectivity	$-\Delta\Delta G_{orient}$ kJ mol^{-1}	Ref.
3,5-Dimethyl-pyridinium	2-Me-pyridinium	7:1	6	[165, 167]
Quinuclidinium	4-*tert*-Butylpyridinium	3:1	3	[166]
3,5-Dimethyl-pyridinium	NMe$_3$	2:1	2	[163]

2-methylpyridinium group, equivalent to $\Delta\Delta G_{\text{orient}}$ of 6 kJ mol^{-1} [165]. These selectivities were based on the formation kinetics, which solely depend on the size of the pseudostopper. The thermodynamic selectivities controlling the final distribution of products might be different, since they also depend on interactions of the CD with the binding site and the stopper. Examples are known where the CD rings changed their mind: they began by threading in one direction (kinetically controlled) but, in the end, they threaded in the other direction (thermodynamically controlled) [166, 168].

3.9   Formation of Rotaxanes

[n]-Rotaxanes are molecular entities consisting of one or more rings and one or more axes, where the axes are confined inside the rings by bulky substituents (so-called *stoppers*) at both ends of the axes. The number of interlocked components is represented by n [169, 170]. This number is implicitly 2 if it is not specified. In contrast to the aforementioned pseudostoppers, stoppers completely prevent dissociation of a rotaxane. Since rotaxanes are not in dynamic equilibrium with their components, they cannot be classified as supramolecular structures. Nevertheless, they are briefly described with focus on molecular recognition they are readily synthesized from ICs by attachment of stoppers. This coupling reaction, called 'rotaxanation,' has to proceed in high yield, preferably in aqueous solution, since the use of inert organic solvents immediately causes dissociation of most ICs. Details of rotaxane synthesis have been summarized elsewhere [31, 171].

A stopper for α-CD has to significantly exceed the internal diameter of α-CD, $d = 4.4$ Å. The smallest known stopper groups for α-CD are 3,5-dimethylphenyl [172], 3,5-dimethylpyridinium, and 3,5-phenyldicarboxylate [173] groups. It is striking that the 2,5-dimethylpyridinium group can still pass through α-CD, being a pseudostopper, whilst the 3,5 isomer cannot, already being a stopper. This difference demonstrates the high sensitivity of steric interactions. Beside the above-mentioned blocking groups, larger ones such as TEMPO [174], picryl [175], naphthalene disulfonate [176], Fe- [177] Co- [178], and Pt- [179] complexes have also been employed as stoppers for rotaxanation of α-CD.

Since the internal diameter of β-CD, $d = 5.8$ Å, is larger than the one of α-CD, larger stoppers, such as *m*-terphenyl [125] or β-CD [180, 181], must also be used. Alternatively, an axis molecule containing azobenzene was functionalized at both ends with 4,4′-bipyridinium groups. After complexation of the azo benzene moiety with α-CD, the 4,4′-bipyridinium groups were complexed with the cyclic host cucurbituril- [7], acting as a supramolecular stopper because of its very high binding constant (shown in Fig. 12) [182]. This work shows a very striking example of *orthogonal molecular recognition*: the azobenzene moiety is selectively recognized by α-CD, while the 4,4′-bipyridine group is selectively recognized by cucurbituril-[7]. Orthogonal recognition, known from natural systems such as base pairing of RNA and DNA, remains one of the challenges in supramolecular chemistry.
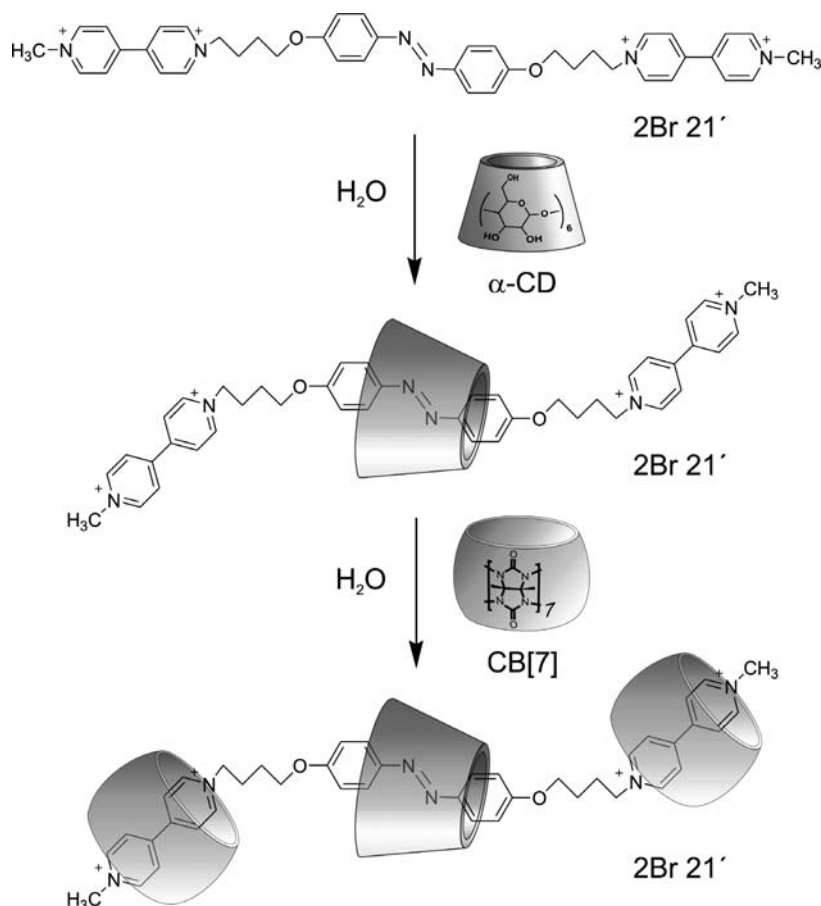
Fig. 12 Supra molecular stoppering of a β-CD inclusion compound by cucurbituril [182]

Finally, γ-CD, with an internal diameter of 7.4 Å, requires very large stoppers for rotaxane synthesis. Therefore, only a few γ-CD rotaxanes are presently known. The Anderson group showed that *m*-terphenyl-4, 4′dicarboxylic acid is sufficiently large. They were able to synthesize a [2]-rotaxane from the IC of γ-CD and a stilbene derivative using this stopper. The [2]-rotaxane obtained had sufficient space remaining to accommodate another axis molecule that could be stopped, as well to furnish the first [3]-rotaxane with two axes through one CD ring. Both homo- and hetero- [3]-rotaxanes with two equal and two different axes, respectively, could be synthesized this way, as shown in Fig. 13 [183].

In principle, CD rotaxanes can be used for molecular information processing if they are reversibly switchable between two states, such as CD [2]-rotaxanes comprising two different binding sites within their axes, as shown in Fig. 14. In the "off" state, the threaded CD recognizes the better binding site and settles there. Once the
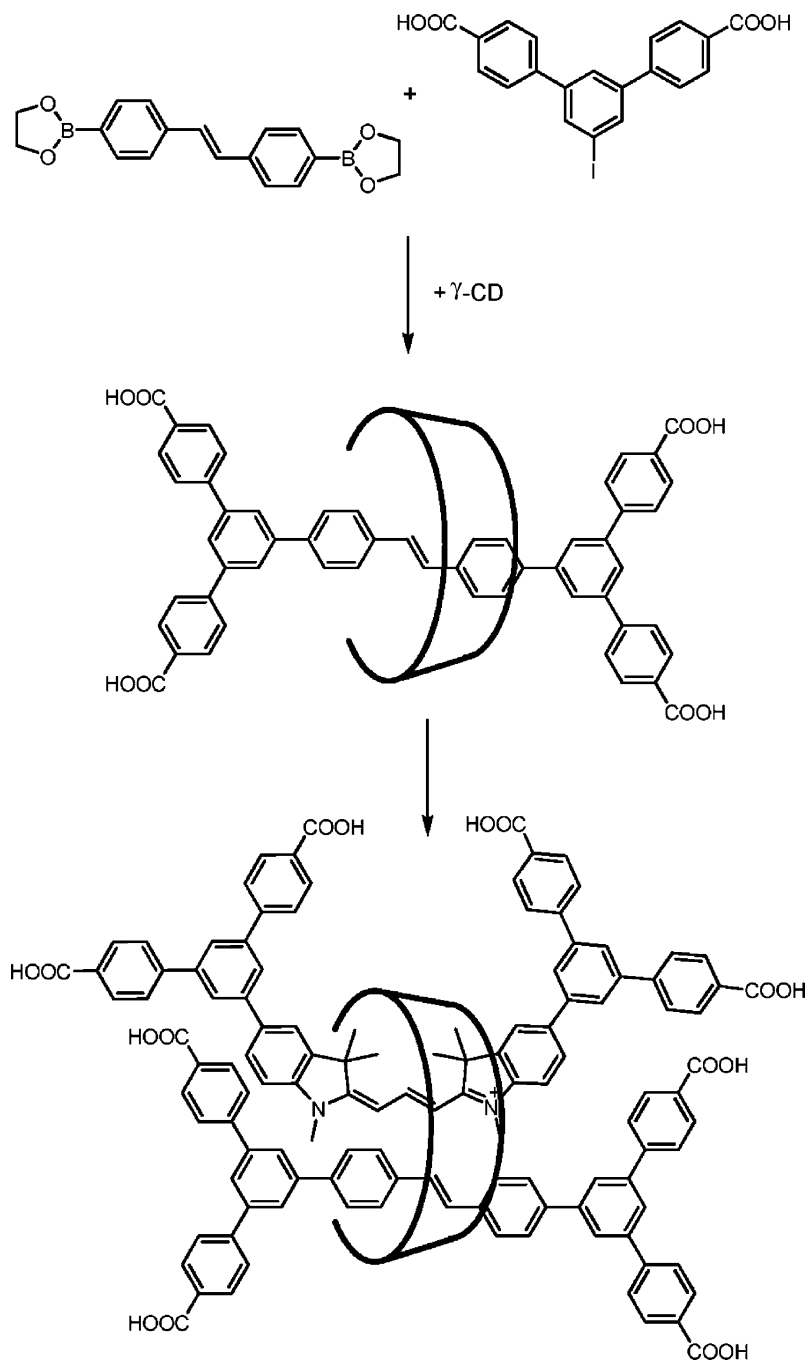
Fig. 13 Stepwise synthesis of a [3]-rotaxane from γ-CD [183]
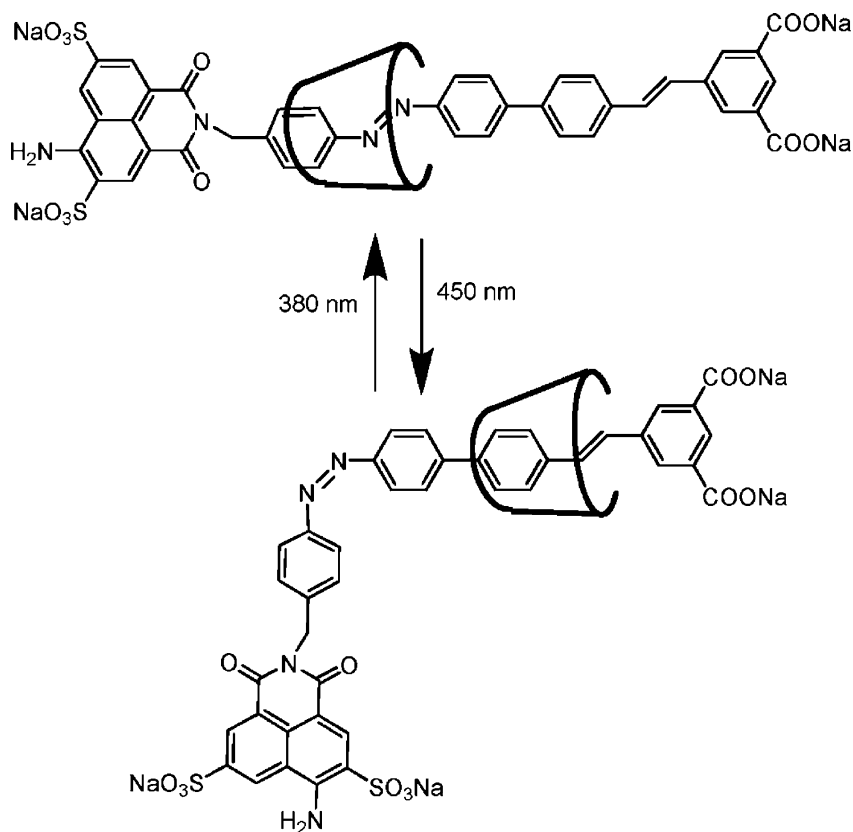
Fig. 14 [2]-Rotaxane, switchable by light [184]

Table 10 Stimulus-responsive, switchable α-CD [2]-rotaxanes

Binding site 1	Binding site 2	"On" stimulus	"Off" stimulus	Ref.
Tetrathiafulvalene	1,2,3-Triazole	$-e^-, +0.32\,V$	$+e^-, +0.22\,V$	[185]
Azobenzene	Biphenyl	$h\nu$, 365 nm	Δ, 60°C	[186]
Azobenzene	Stilbene	$h\nu$, 380 nm	$h\nu$, 450 nm	[184]
Stilbene	Azobenzene	$h\nu$, 313 nm	$h\nu$, 280 nm	[184]
Azobenzene	$-CH_2-CH_2-$	$h\nu$, 360 nm	$h\nu$, 430 nm	[187]

structure of this binding site is changed by an external stimulus, such as light or an electron, the CD ring moves to the other binding site. This places the system in the "on" state until it is switched off by another external stimulus. Then the ring will move back to its original position. Several switchable CD rotaxanes are already known and summarized in Table 10. Switching was highly reversible in most cases.

4   Recognition of Polymers with Pending Binding Sites

4.1   Recognition of Guest Polymers by Monomeric CDs

Guest moieties attached as side chains to a polymer backbone are complexed by CD hosts in the same fashion as corresponding monomeric guests, as depicted in Fig. 15. Again, the size of the hydrophobic binding site of a polymer is recognized by the CD cavity. In general, the observed binding free energies for the guest polymers are somewhat lower than the ones for the monomeric guests (see Table 11). This might be due to repulsion between CD rings complexing adjacent binding sites because of steric constants.

   The first example of the inclusion of a guest polymer was reported by Harada's group. *n*-Alkyl and *tert*-butyl groups were attached to a polyacrylamide chain. Polymeric ICs were formed with α-CD and β-CD, respectively. Similarly, *tert*-butyl-phenyl and adamantanyl groups were attached to poly(maleicacid-*alt*-methylvinylether) and poly(maleic acid-*alt*-isobutylene), respectively [189, 190]. Dissociation free energies of these polymers with β-CD were in the range of $-\Delta G^0 = 22$–$25\,\mathrm{kJ\,mol^{-1}}$, compared to $-\Delta G^0 = 24$–$26\,\mathrm{kJ\,mol^{-1}}$ for the corresponding monomeric guests. It is also evident from the data in Table 11 that $-\Delta G^0$ decreases with increasing degree of substitution of the pending binding sites at the

+ CD
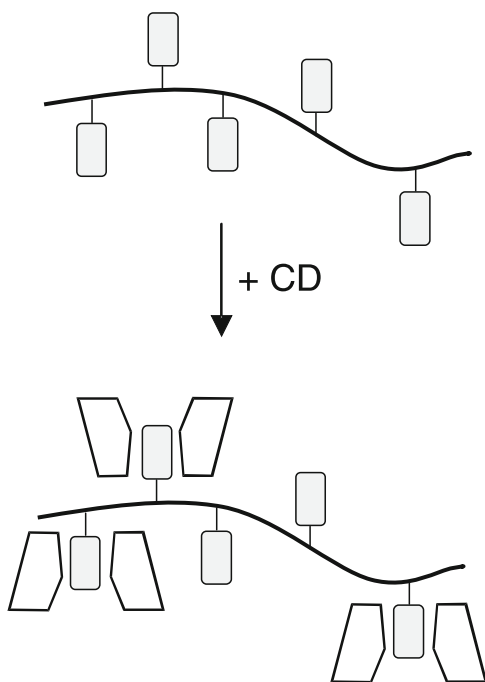
Fig. 15 Schematic drawing of inclusion of side chain guest polymers by CDs

Table 11 Recognition of binding sites conjugated as side chains to polymers

Polymer backbone	Binding site	DS	CD	$-\Delta G^0$/kJ mol^{-1}	Ref.
Hydroxypropyl-methylcellulose	Azobenzene	0.0035	α-CD	20	[188]
Hydroxypropyl-methylcellulose	Azobenzene	0.031	α-CD	17	[188]
Poly(maleic acid-*alt*-isobutene)	*tert*-Butylanilide	0.08	β-CD	25	[189]
Poly(maleic acid-*alt*-isobutene)	1-Adamantane-amide	0.1	β-CD	22	[190]
Poly(maleic acid-*alt*-isobutene)	1-Adamantane-amide	0.2	β-CD	21	[190]
Polyacrylamide	*n*-Dodecyl	0.17	α-CD	17	[191]
Polyacrylamide	*tert*-Butyl	0.17	β-CD	14	[191]

polymer backbone. This decrease of complex stability may also be due to steric hindrance of complexation between adjacent binding sites.

Amphiphilic polymers tend to aggregate and to form gels or micelles. The inclusion of hydrophobic groups at such polymers generally leads to an increase of solubility and a reduction of viscosity in water. One commercial application was patented by Rohm and Haas, in which viscosity of an associative thickener was controlled by addition of CDs [192, 193]. Hydrophobically modified polyurethanes form highly viscous aqueous solutions, which are very difficult to handle. Addition of CDs, especially RAMEB, dramatically reduces the viscosity and allows for preparation of highly concentrated stock solutions. Complexation of the hydrophobic groups eliminates the polymer–polymer interactions. The high viscosity can be restored on demand by addition of sodium dodecyl sulfate (SDS). Since SDS is a competitive guest forming more stable ICs than the polymer, bound CDs are removed from the polymer chain. As a consequence, the liberated hydrophobic sites of the polymer aggregate, causing a large increase in viscosity (see Fig. 16).

Both RAMEB and SDS are called *rheology modifiers*, since they greatly increase and decrease viscosity. Since their discovery, CD-based rheology modifiers have been found for a great variety of associative polymers, such as α-CD for dodecylamido–polyacrylic acid [194], HP-β-CD for hexadecyl modified hydroxyethyl-cellulose [195], and RAMEB for adamantane modified polyacrylamide [196].

The IC of RAMEB and an adamantane modified polyacrylamide is thermosensitive: heating of the aqueous solution of the IC of this guest polymer leads to a very steep increase of both viscosity and turbidity at a certain temperature, which is due to temperature induced decomplexation, followed by an aggregation of the polymer [196].

In addition, photosensitive associative hydrogel systems have been constructed based on dodecyl modified polyacrylic acid, α-CD, and a photoresponsive competitive guest 4,4′-azodibenzoic acid. This guest can be switched from the *trans* to the *cis* state by light back and forth. Since only the *trans* state is complexed by α-CD, gel formation can be switched on and off by light [197]. Thus, molecular recognition and photo switching together induce changes of macroscopic material properties.

Fig. 16 CDs as rheology
modifiers: addition of CD
reduces viscosity because
it breaks intermolecular
hydrophobic interactions;
addition of SDS (sodium do-
decyl sulfate) regenerates the
original hydrogel [192, 193]
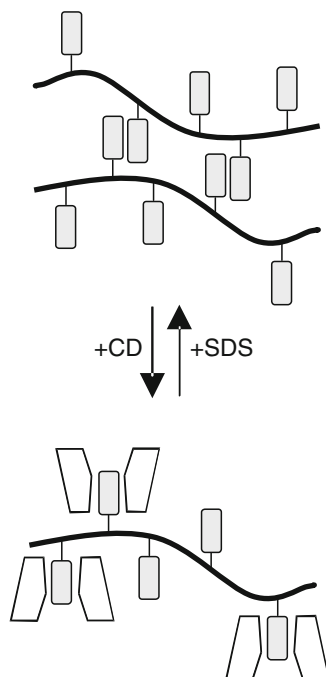
4.2 Recognition of Guest Polymers by Dimeric and Polymeric CDs

The interaction of CD dimers or CD polymers with side chain guest polymers leads
to the reversible formation of three-dimensional supramolecular networks, as shown
in Fig. 17.

The first supramolecular networks of CD polymers and guest dimers or
guest polymers were described in 1996 [87, 198]. Sebille's group used β-CD
epichlorohydrin polymers and adamantane terminated PEO [198–200], while we
combined β-CD conjugated to poly(isobutene-*alt*-maleic acid) PIBMA and *tert*-
butyl aniline conjugated to PIBMA [87, 88, 201, 202]. With both systems, viscosity
increased by four to five orders of magnitude after mixing solutions of the two
components because of formation of crosslinked host–guest complexes. Molecular
recognition between polymer bound CD and guest moieties was clearly demon-
strated by a continuous variation plot of the viscosity shown in Fig. 18, which
revealed a maximum of viscosity at a 1:1 stoichiometry of β-CD and guest moi-
eties [190]. Viscosity decreased with increasing shear rate, possibly because of
mechanical ruptures of the host–guest interactions.

Gel formation could be switched off either by dilution with water or by addi-
tion of monomeric β-CD or guest [190]. Several other polymeric systems, with
complementary binding sites conjugated to polyacrylic acid [194, 203], polyacryl
amide [204], and chitosan [205–207] backbones, have been described subsequently,
all with similar properties. Compared to regular covalent networks, these noncova-
lent, supramolecular networks offer several advantages:

Fig. 17 Formation of supramolecular networks from CD polymers and guest polymers
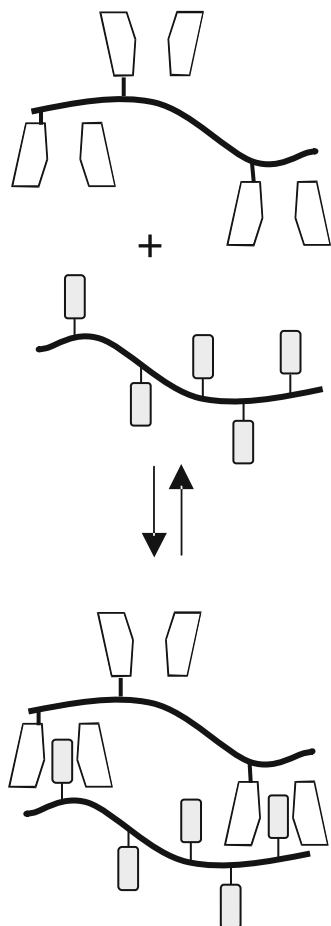
- CD supramolecular networks are uniform and transparent
- Supramolecular network formation is reversible
- Supramolecular networks can adapt to a certain form, e.g., in a mold
- Supramolecular network formation can be switched on and off by an external stimmulus
- Supramolecular networks can be dissolved by high dilution
- Supramolecular networks are water-based and biocompatible

Therefore, these gelling systems based on two components might find interesting applications in the future. These and other CD based gels have been described by Li et al. [208].

A remarkably different system comprised of a β-CD polymer and a guest polymer was recently described by Gref et al. [209]. They mixed aqueous solutions of neutral β-CD epichlorohydrin polymer and a neutral lauryl ester of dextran, both of high molecular weights, and received no macroscopic gels but well-defined and
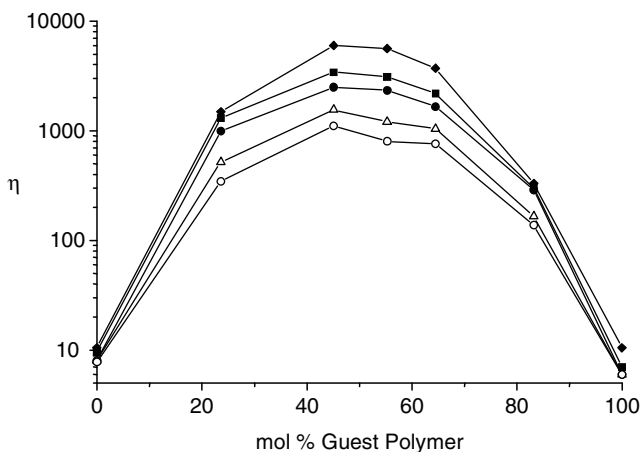
Fig. 18 Viscosities of mixtures of a β-CD polymer (β-cyclodextrinyl-PIBMA) and a guest poly-
mer (*tert*-butyl anilide of PIBMA) as functions of the molar fraction of guest groups in water for
different shear rates D (s^{-1}) of 66 (*filled diamonds*), 131 (*filled squares*), 196 (*filled circles*), 393
(*open triangles*), and 590 (*open circles*) at constant total polymer concentration of 2 wt% [202]

stable nanoparticles with diameters of about 200 nm. These nanoparticles may be
very interesting as carriers for targeted drug delivery.

4.3 Recognition of Guest Polymers by CDs Attached to Surfaces

CDs arranged in a two-dimensional order at a surface are also able to interact
with side chain guest polymers. Amphiphilic β-CD derivatives were organized as
double layers in spherical vesicles. These ordered CDs complexed hydrophobic
tert-butyl-anilid conjugated to PIBMA, leading to vesicles wrapped by the poly-
mer. These vesicles are stabilized by supramolecular interactions and resemble cells
protected by a cyto-skeleton, as shown in Fig. 19. The binding free energy for the
guest polymer with this two-dimensional β-CD array, $-\Delta G^0 = 36\,\text{kJ mol}^{-1}$, is much
higher than for the same polymer with monomeric β-CD, $-\Delta G^0 = 23\,\text{kJ mol}^{-1}$,
demonstrating the high cooperativity of binding [210].

Furthermore, β-CD heptathioethers were immobilized at planar gold surfaces in
regular hexagonal arrays, so-called molecular print boards [211]. Dimers, polymers,
and dendrimers with two and more attached adamantane or ferrocene binding sites
are nearly irreversibly complexed by these β-CD arrays because of the cooperativity
of the binding events and negligible entropic loss due to the high rigidity of the CD
array. The polymer coil may first bind with a small number of binding sites before
being compressed to a flat conformation, which allows more host–guest interactions,
as depicted in Fig. 20 [212–215]. These molecular CD print boards may find very
interesting applications for the assembly of molecular devices by ink jet printing or
dip pen nanolithography.
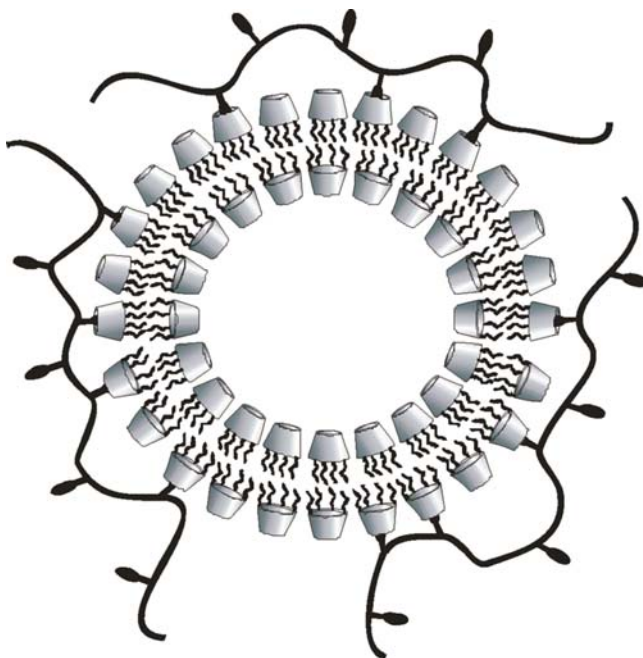
Fig. 19 Cyclodextrin vesicles stabilized by complexation of the guest polymer, *tert*-butylanilid-PIBMA [210]
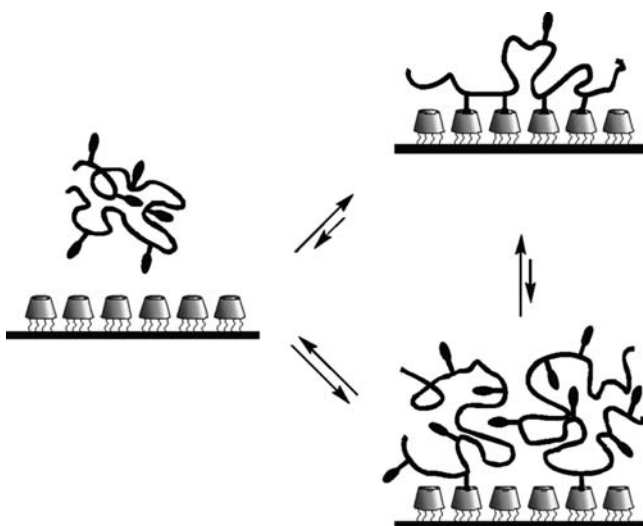
Fig. 20 Schematic representation of different binding modes for guest polymers with planar CD arrays [213]

5 Recognition of Linear Polymers with Binding Sites in the Main Chain

5.1 General Considerations

Complexation of a polymer main chain by CDs differs significantly from complexations of polymer side chains. Complexations of side chains occur in parallel, while complexation of a main chain is a serial process in which consecutive steps are dependent on each other. Since complexation of a main chain polymer, so-called threading, requires a one-dimensional transport of CD rings along the chain, it requires much more time than complexation of a side chain polymer. While the first segments of a polymer chain are rapidly complexed, migration along the polymer is slow and a molecular version of a "traffic jam" can occur.

The linear alignment of threaded CD rings allows attractive interactions between the rings. Native CD rings can each form intermolecular hydrogen bonds between the primary hydroxyls and the secondary hydroxyls. Therefore, alternating head-to-head and tail-to-tail orientations of threaded rings are usually found as soon as the complete polymer chain is covered by CDs, as shown in Fig. 21a. These attractive interactions between threaded CD rings deliver a major contribution to the binding free energy [216]. The rodlike polymer complexes further organize into water-insoluble crystals, so-called channel structures, similar to type I ICs of hydrophobic monomeric guests described in Sect. 3.1.

On the other hand, bulky hydrophilic groups within the polymer chain prevent a dense coverage of the polymer (see Fig. 21b) and therefore lead to water-soluble ICs.

5.2 Recognition of the Thickness of a Polymer Chain

The formation of insoluble channel ICs is a very common feature for the interaction of various polymers with α-, β-, and γ-CDs. The recognition of the thickness of a polymer by the internal diameter of the CD is demonstrated by the data of Table 12. Selectivities of IC formation for polymers are even higher than for similar
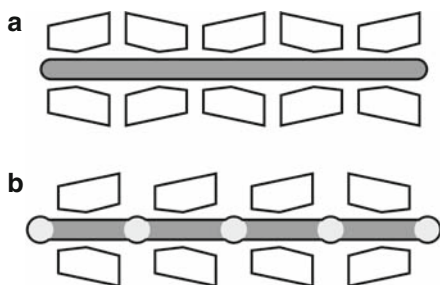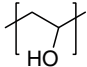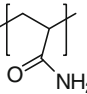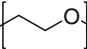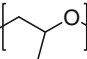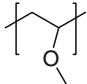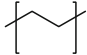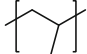
Fig. 21 a,b Schematic representation of different structures of polymer main chain ICs. **a** Channel ICs. **b** ICs of poly(bola-amphiphiles) (reprinted with permission from [31], copyright of the American Chemical Society)

Table 12 Yields of IC formation for various polymers as a function of the CD ring size [217]

Polymer	Structure	MW g^{-1} mol^{-1}	α-CD (%)	β-CD (%)	γ-CD (%)
PVA		22,000	0	0	0
PAAm		10,000	0	0	0
PEG		1,000	92	0	Trace
PPG		1,000	0	96	80
PMeVE		2,000	0	0	82
PE		563	63	0	0
PP		800	0	40	7
PIB		800	0	8	90

monomers, possibly because of the high cooperativity of the inclusion process. The formation rate of channel type ICs decreases with increasing molecular weight and decreasing solubility of the polymer. Therefore, an upper molecular weight limit often exists for IC formation between 3,000 and 20,000 g mol^{-1}. Some more detailed information about IC formation of polymers is given below.

5.2.1   IC Formation of α-CD

The formation of an IC of a polymer main chain was clearly evidenced for the first time by the Harada group in 1990 [218]. They observed precipitation of the polymeric IC a few minutes after mixing saturated aqueous solutions of α-CD and poly(ethylene oxide) (PEO) in high yield. Later, they found that threading occurs even after mixing α-CD and PEO without any solvent present [219]. The stoichiometry of this IC is about one α-CD ring per two PEO units. Since the length of two oxyethylene units is similar to the height of an α-CD torus (8 Å), the authors anticipated complete coverage of the PEO chain with α-CD rings. This hypothesis was confirmed by X-ray diffraction data and solid state NMR-spectroscopy, proving a channel structure [220, 221]. Interestingly, the PEO dimer does not form any IC

with α-CD, probably because of the terminal OH groups, which are too hydrophilic to intrude into the cavity [222]. Formation of the channel structure starts with the trimer, from which an X-ray structure is known [223]. Strong intermolecular hydrogen bonds within the channel structure appear to be necessary to gain sufficient complex stability. This also explains why any substituent at the α-CD ring prevents precipitation of the PEO complex, since this substituent prevents dense packing of CD rings along the PEO thread.

It was found meanwhile that nearly every slim unbranched polymer chain, such as poly(trimethylene oxide) [224], poly(1,3-dioxolane) [225], poly(tetramethylene oxide) [226], poly(ethylene imine) [227], poly(3-hydroxy propionate), poly (4-hydroxybutyrate) and poly(6-hydroxyhexanoate) [228, 229], poly(butylene succinate) [229], polyadipates [230], nylon-6 [231], and even oligomers of polyethylene [232], form α-CD ICs with channel structures. In all of these cases, inclusion is a heterogeneous process, since the guest polymer and its CD complex are almost insoluble in water. Therefore, extensive sonication had to be applied to accelerate the diffusion process. The polymer was also dissolved in an organic solvent, e.g., nylon-6 in formic acid, and this solution was added to the solution of α-CD [231]. Alternatively, a monomer, such as 11-aminoundecanoic acid, was included in α-CD and polymerized to nylon-11 by solid state polycondensation within the channels of the IC. Thus, the IC of nylon-11 was formed under conservation of the crystal packing [233–235].

In contrast to monomeric α-CD derivatives, molecular tube (α-CD-MT) shows a high binding affinity to poly(tetramethylene oxide) moieties, which might be due to the high cooperativity of binding exerted by the α-CD rings, rigidly preorganized within the MT. Since these ICs are water-soluble, binding free energies could be determined by ITC. Values of $-\Delta G^0 = 33 \, \text{kJ mol}^{-1}$ were reached [236].

5.2.2 IC Formation of β-CD

The more spacious β-CD, with its internal diameter of 5.8 Å, is able to complex polymers thicker than PEO. It forms insoluble ICs with channel structures with polypropylene glycol (PPO) [237], and even poly(tetrafluorethylenoxide-*co*-difluormethylenoxide) [238]. This does not mean that slim polymers, such as poly(trimethylene oxide), are complexed less by β-CD, but less stable ICs are formed, in which the polymer does not completely fill the cavity. The structure of the IC is shown in Fig. 22 [239]. Poly(dimethylsiloxane) [217, 240] and poly(dimethylsilane) [241, 242] are also complexed by β-CD when their molecular weights are less than $400 \, \text{g mol}^{-1}$.

Polyconjugated polymers, such as polyaniline [243, 244] and polythiophene [245, 246], seem to be complexed in β-CD, as well. Because of the low solubilities of these polymers, polymerization and inclusion have to be performed simultaneously. These so-called *molecular wires* are promising electrical and photonic materials [247].

Fig. 22 Structure of poly(trimethylene oxide) complexed in β-CD; the *dotted lines* are intermolecular hydrogen bonds; the *circles* are water molecules
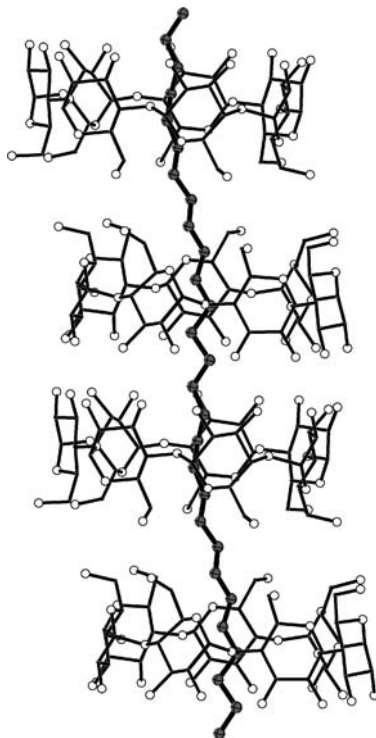
5.2.3 IC Formation of γ-CD

The largest commercially available CD, with a minimum internal diameter of 7.4 Å, γ-CD is wide enough to complex rather thick polymers, such as polyisobutylene [248], polymethylvinylether [249], polystyrene [250, 251], polyvinyl chloride [252], polysiloxanes and polysilanes of molecular weights 1,000–3,000 g mol^{-1} [217, 253], poly(perfluorpropylene oxide) [238], and *N*-acetylethylenimine [254], leading to water-insoluble ICs with channel structures. PEO chains are slim enough to form a double stranded IC in γ-CD [255, 256]. However, preparation of these complexes is very difficult because the loss of entropy for the two PEO chains is very high. Naphthalene groups terminating the PEO chains facilitate simultaneous threading of two PEO chains through one γ-CD ring, since they preorganize properly by forming dimeric aggregates in aqueous solution [255]. Similar double stranded ICs of poly(caprolactone-*b*-THF-*b*-caprolacton) triblock-copolymers in γ-CD have been found subsequently [257].

5.3 Site-Selective Complexation of Block Copolymers

As already shown in Table 12, α-CD prefers complexation of nonbranched aliphatic chains, such as *n*-alkyl or oxy-alkyl chains, while β-CD prefers thicker polymers,
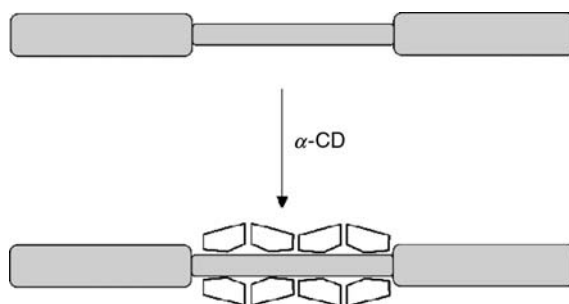
Fig. 23 Schematic drawing of site-selective complexation of PPO-PEO-PPO triblock-copolymer by α-CD

such as PPO. On the other hand, PPO can still thread through α-CD, and β-CD can form a loose complex with PEO, but both of these ICs are unfavorable. Selectivity of IC formation is unveiled by competition experiments using block-copolymers. For example, triblock-copolymers of PEO and PPO were complexed by α-CD. The location of the threaded α-CD-rings can be checked by NOE spectroscopy or by indirect methods such as X-ray diffraction or DSC. As a result, the α-CDs are concentrated at the PEO segments even for PPO–PEO–PPO triblock-copolymers, for which α-CD rings have to pass the bulky PPO blocks, as shown in Fig. 23. Threading times strongly increase here with the lengths of the PPO blocks [258]. On the other hand, β-CD selectively complexes the PPO segments of these block-copolymers [259]. Consequently, the CD-rings can recognize the appropriate segments; such complexation is called *site-selective*. There are many examples of site-selective complexations, e.g., α-CD selectively binds the PEO segments of PEO-poly(3-hydroxybutyrate)-PEO [260] and PEO-poly(*N,N*-dimethylaminoethyl-methacrylate) [261] and the PCL blocks of PCL–PTHF–PCL [257] and PCL–PPO–PCL [262]. Site-selective complexation can be quite useful, since it allows selective masking of the hydrophobicity of a segment in a block-copolymer for some time. In addition, the partially complexed block-copolymers remain more soluble than the fully complexed homopolymers. For example, PEO-poly(*N,N*-dimethylaminoethyl-methacrylate) selectively complexed at the PEO blocks by α-CD forms nanoparticles [261].

5.4 Enantioselective Recognition of Chiral Polymers

Since the CD molecule is chiral, it could recognize the winding of a chiral polymer, functioning like a nut threading onto a bolt. Since the spatial differences of two corresponding enantiomers are small, the fit between the CD nut and the polymer bolt should be as tight as possible to allow chiral recognition. The first example of a stereoselective inclusion of a polymer was given by the Tonelli group [263]. They found that isotactic poly(3-hydroxybutyrate) is included in α-CD, while atactic poly(3-hydroxybutyrate) is not. The first enantioselective inclusion
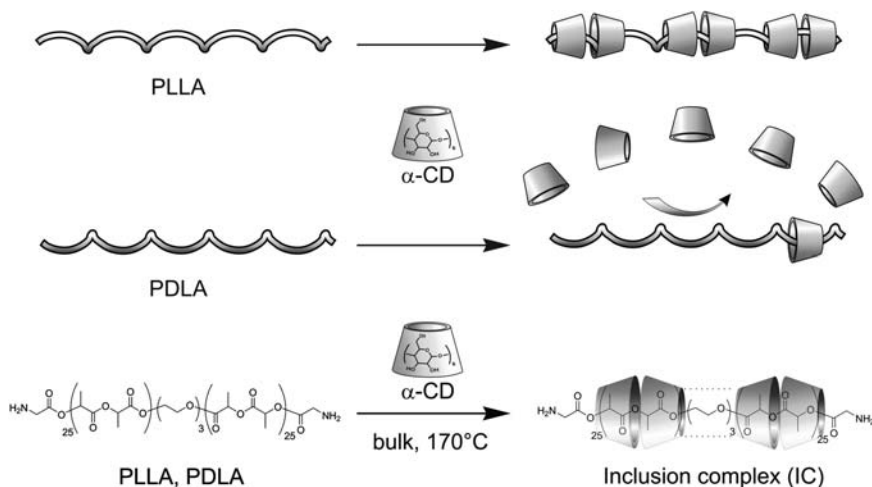
Fig. 24 Schematic drawing of enantioselective complexation of polylactides by α-CD [264]

of a polymer was observed by Yui et al. for isotactic polylactides, which indeed resemble molecular screws by forming 3_{10}-helices. Poly(L-lactide) (PLLA) with α-CD forms an IC of high coverage (42%) at 170°C, which is stable enough even to survive dissolution in DMSO (depicted in Fig. 24). Conversely, the other enantiomer poly(D-lactide) (PDLA) is only complexed by a few α-CD rings, leading to a very low coverage of 7%. Because of its wrong screw sense, this polymer does not fit in the α-CD ring [264]. From the coverages of both enantiomeric polymers, the estimated chiral recognition, $\Delta\Delta G_{R,S} \geq 7\,\mathrm{kJ\,mol^{-1}}$, is higher than the ones observed for enantiomeric monomers, as listed in Table 5. This very high enantioselectivity is indeed remarkable. It might be due to the cooperativity of binding caused by the hydrogen bonds between adjacent α-CD rings within the IC. In the future, molecular machines [265, 266] might be constructed which make use of the unidirectional rotation of an α-CD nut moving along the PLLA screw.

5.5 Recognition of the Polarity of the Polymer

Since the major driving force of inclusion is hydrophobic interaction, stabilities of ICs depend strongly on the polarity of the polymer. The more hydrophobic the polymer is, the higher is the affinity of CDs towards it. On the other hand, solubility in water decreases with increasing hydrophobicity of the polymer. Since affinity and solubility have to be compromised, an optimum of polarity of the polymer should exist for complexation by CDs. It is difficult to quantify the binding free energies of CD channel inclusion compounds, since they are insoluble in water. Stabilities of these polymeric ICs can be qualitatively compared by competition experiments. For example, PLLA and PCL were competitively included in α-CD. The IC of PCL was
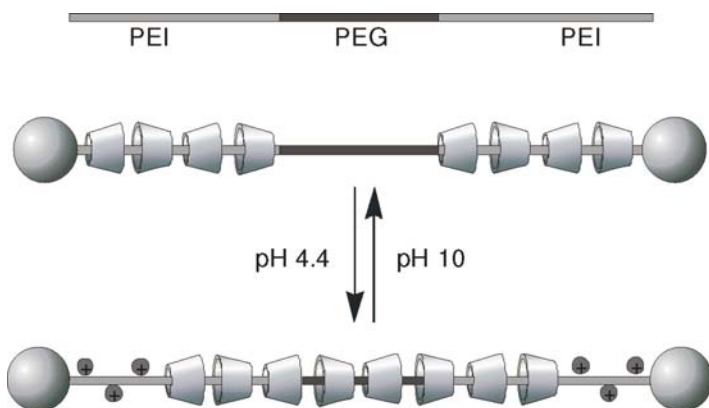
Fig. 25 pH dependent coverage of PEI–PEO–PEI

nearly exclusively formed, which means that the caproate groups are better binding sites for α-CD than lactate groups because caproate is less polar than lactate [267].

Polyethylenimine (PEI) only forms ICs with α-CD and γ-CD at rather basic conditions, pH > 8, since only the nonprotonated PEI is sufficiently hydrophobic to be included in these CDs. These ICs are insoluble in water and behave similarly to the ICs of PEG. Protonated PEI is not included at all by CDs, since it is too polar [227]. Interestingly a triblock-copolymer PEI–PEO–PEI becomes homogenously covered by α-CD at a pH of 10. As soon as the pH is lowered to pH 4.4, α-CD rings escape from the PEI segments to the PEO segments, as shown in Fig. 25 [268].

If anthracene stoppers are attached, this pH driven locomotion of the CD rings becomes completely reversible and can be monitored in situ using fluorescence resonance energy transfer (FRET) of suitable fluorescent probes attached to the CD rings and to both ends of the polymer [269].

5.6 Recognition of the Hydrophobic Segment Lengths of Poly(bola-amphiphile)s

Since longer alkylene segments in polyamines should lead to more stable ICs, we investigated the interaction of α-CD with a homologous series of poly(imino-oligomethylene)s, PI-6, PI-8, PI-10, PI-11, and PI-12 (formulas shown in Fig. 26) in aqueous solution at pH 4.8 [270, 271]. With the exception of PI-6, these formed water-soluble ICs under homogenous conditions. Because of their similarity to bola-amphiphiles, these polymers were classified as *poly(bola-amphiphile)s*. The high solubility of the ICs is caused by the bulky hydrophilic groups within the polymers, which prevent a dense packing of threaded CD-rings that would otherwise lead to an insoluble channel structure. Threading kinetics of α-CD rings onto these polymers could be followed in situ by solution ^{1}H-NMR spectroscopy. Binding free

PI-11   [119, 272]

PI-3,10   [119]

PI-6,10   [119]

PMI-11   [273]

PMNO-11   [273]

I-11   [274]

I-6,10   [275, 276]

PP-10   [277]
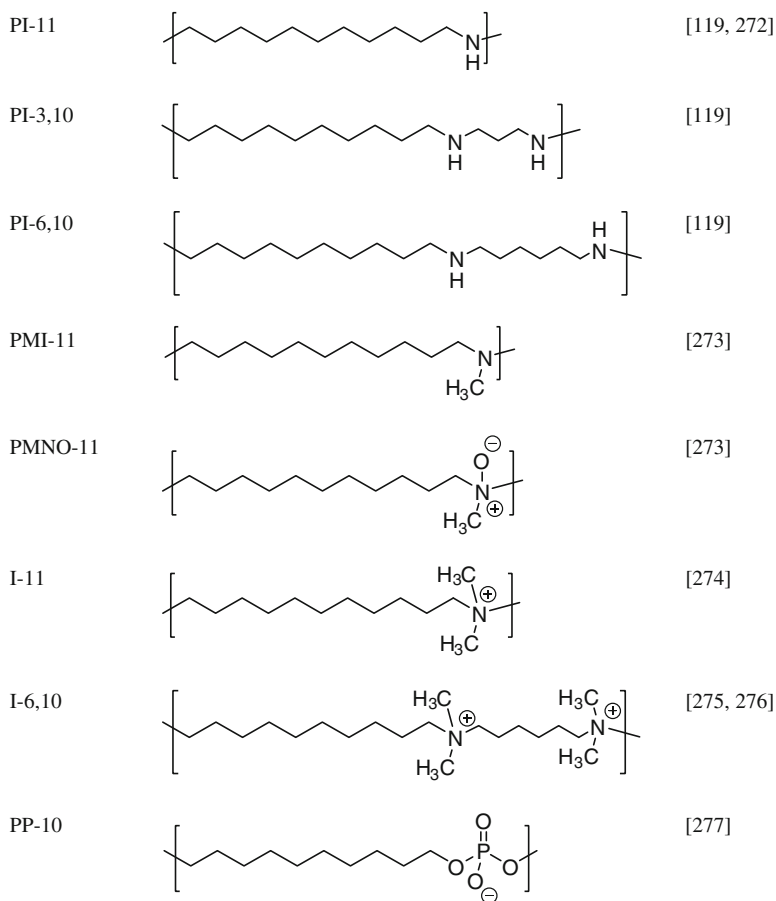
Fig. 26 Poly(bola-amphiphile)s that form water-soluble ICs with α-CD

energies $-\Delta G^0$ could be calculated from the limiting conversions of the threading processes or by ITC. The $-\Delta G^0$ values of the poly(bola-amphiphile)s increase with the lengths of the hydrophobic segments and are nearly identical to those of the monomeric bola-amphiphiles, as depicted in Fig. 6. Polymer PI-6 was not complexed at all by α-CD at pH 4.6, while the most stable IC was obtained for PI-12. From a thermodynamic point of view, these poly(bola-amphiphile)s behave very similarly to their monomeric counterparts.

Thus, molecular recognition of poly(bola-amphiphile)s mainly depends on the structure of one limited binding site and not on the structure of the polymer as a whole. Consequently, the knowledge about molecular recognition of monomeric bola-amphiphiles can be brought forward to understand molecular recognition of polymeric bola-amphiphiles.

Besides poly(imino-oligomethylene)s PI-*n* [272], many other poly(bola-amphiphile)s, such as poly(*N*-methyl-imino-oligomethylene)s PMI-*n* [273], poly

(N,N-dimethyl-iminium-oligomethylene)s (also called ionenes) I-n [278], poly(N, N-4,4′-bipyridinium-oligomethylene)s [279], PV-n poly(N-methyl-imino-oligo methylene-N-oxide)s PMINO-n [273], and poly(oligomethylene-phosphate)s PP-n [277] summarized in Fig. 26, also form water-soluble ICs with α-CD if the length of the hydrophobic segments is sufficient ($n \geq 10$). Binding free energies range from $-\Delta G^0 = 14$ to $20 \, \text{kJ mol}^{-1}$, increasing with n. This minimum segment length is necessary to allow the ionic groups to stay completely out of the α-CD cavity so that they do not disturb inclusion. Inclusion of poly(bola-amphiphile)s is mainly driven by hydrophobic interactions. The separation of the threaded CD rings by the ionic groups does not allow any additional stabilization of the IC by hydrogen bonds between the rings, as described for the channel inclusion compounds. Beside α-CD, β-CD and γ-CD, as well as CD derivatives, are able to thread onto these poly(bola-amphiphile)s under homogenous conditions [275, 280, 281]. In addition, there is no upper limit of the molecular weight for the formation of ICs, since threading is a homogenous process. Functional CDs and poly(bola-amphiphile)s can form a supramolecular toolbox for the design of functional pseudopolyrotaxanes.

5.7 Kinetic Recognition of Bulky Groups within Poly(bola-amphiphile)s

In Sect. 3.6 we have described how the bulky ionic end groups of monomeric bola-amphiphiles can strongly influence formation and dissociation rates of CD ICs. The same is true for polymeric bola-amphiphiles. The kinetics of IC formation could be measured in real time by ^{1}H NMR spectroscopy, since complexation is a homogenous process. Inclusion times are extremely dependent on the sizes of the hydrophilic groups within the polymer. Threading α-CD onto a secondary polyamine, poly(imino-undecamethylene), was completed after only about 1 h at r.t. [270]. Threading onto a quaternary polyamine, poly(N,N-dimethylammonio-hexamethylene-$N′,N′$-dimethylammonio-decamethylene), took more than 2 years at r.t. [278]. Inclusion kinetics could be quantitatively described by an empirical function, a so-called stretched exponential $y = y_\infty(1 - e^{-\sqrt{kt}})$ with the yield of complexation y and the limiting yield y_∞. The time t_{90} for reaching 90% of the limiting yield was calculated from the rate constant k according to $t_{90} = (\ln 10)^2/k$. Results are listed in Table 13 [273].

The polymers with large hydrophilic groups had to be measured at elevated temperatures ($60 \, °C$), since otherwise kinetics are too slow. Kinetics become much faster at higher temperatures, indicating that threading is an activated process. The time t_{90} strongly depends on the size of the bulky groups within the polymer chain. It ranges from a few minutes for the imino group to several weeks for the more bulky dimethylammonium group. If there are two bulky dimethylammonium groups in close proximity to each other, the steric barrier becomes even higher, and the threading time t_{90} is about 2 months at $60 \, °C$.

Table 13 Threading times t_{90} for reaching 90% of final yield for various poly(bola-amphiphiles) $-(CH_2)_n - X-$ [273]

X	n	t_{90}/h at 25°C	t_{90}/h at 60°C	d/Å	Ref.
$-NH_2^+-$ [a]	11	0.47		4.28	[273]
$-N^+HMe-$ [a]	11	10.8	0.16	5.06	[273]
$-N^+MeO^--$	11		58	5.49	[273]
$-N^+Me_2-$	11		413	5.73	[273]
$-N^+Me_2(CH_2)_6 N^+Me_2-$	10		1,370	5.73	[278]

[a]At pH 4.6
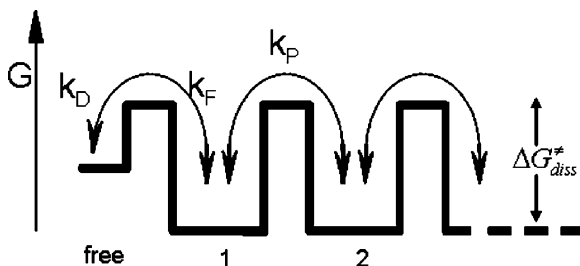
Fig. 27 Model for the threading poly(bola-amphiphile)s; rate constants are: k_D for dissociation, k_F for formation, and k_P for propagation (reprinted with permission from [278], copyright of the American Chemical Society)
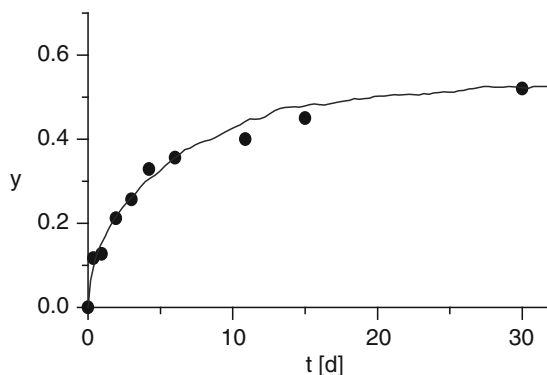
Fig. 28 Kinetics of the inclusion of ionene-6,10 (points) by α-CD, line calculated by the simulation program Abakus (reprinted with permission from [278], copyright of the American Chemical Society)

The slow rate of the threading process can be rationalized on a molecular level as a hopping process of the CD rings over the periodic potential caused by the repulsive interactions exerted by the bulky hydrophilic groups, illustrated in Fig. 27.

Threading kinetics was quantitatively described by the Monte Carlo simulation program Abakus [278]. As shown in Fig. 28, the agreement of experimental data and the Abakus fit is reasonably good, demonstrating the validity of the kinetic model.

The binding constant K and the propagation rate constant k_p are obtained as fitting parameters. The time a CD ring rests on a segment, $\tau_{1/2} = \ln 2/k_p$, was derived from the rate constant k_p. From the temperature dependence of this rate constant, the activation energies E_a were estimated by Arrhenius plots. The obtained activation energies of propagation over dimethyl ammonium groups ($E_a = 90 \, \text{kJ} \, \text{mol}^{-1}$) were on the same order of magnitude as the activation free energy for the corresponding monomeric bola-amphiphile, 1,10-bis-trimethylammonium-decane, already listed in Table 8.

The diameters d of the hydrophilic groups of poly(bola-amphiphile)s were calculated by semiempirical quantum mechanical calculations and are listed in Table 13 [273]. They correlate well with the threading times t_{90}. That means that the diameter d of the hydrophilic groups in poly(bola-amphiphile)s is sensitively recognized by α-CD-rings.

Most α-CD complexes of above-mentioned poly(bola-amphiphile)s are stable enough to be isolated; therefore, they are classified as pseudopolyrotaxanes. Dissociation kinetics of CD pseudorotaxanes can easily be detected by following the CD concentration during dialysis or ultrafiltration, by which free α-CD rings are continuously removed, as depicted in Fig. 29.

The polymers that are rapidly complexed by α-CD also dissociate rapidly. Those polymer ICs, like those of ionenes, which require high temperatures and long threading times to be formed, are almost kinetically stable at r.t.

Threading and dissociation rates of polymeric secondary amines PI-11 and PI-3,10 are highly dependent on the pH: at high pH, threading of PI-3,10 is im-
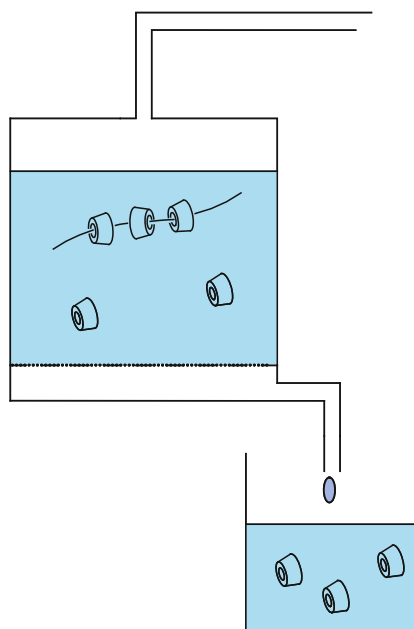
Fig. 29 Schematic drawing of the ultrafiltration system for the measurement of the dissociation kinetics of polymer ICs. Concentrations of CD both in the filtrate and the retentate were determined from the optical rotations of the solutions
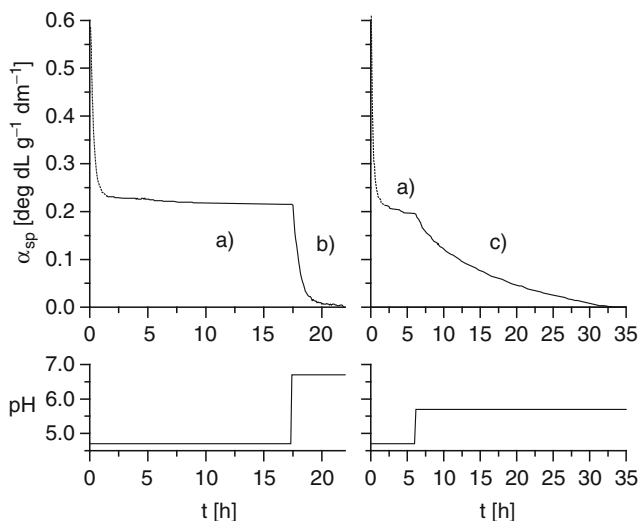
Fig. 30 pH dependence of dissociation of the IC of PI-3,10 and α-CD as measured by the decay of specific optical rotation α_{sp} of α-CD in the retentate during dialysis [271]

measurably fast; at pH 3, it takes several days. Therefore, the rate of threading can be controlled by the pH [282]. A change of pH seems to influence strongly steric hindrance of threading: protonated imino groups significantly hinder threading, while neutral ones do not. Since the steric hindrance of a single proton cannot cause this strong effect, the change of the charge also has to be taken into account. Cationic protonated imino groups attract water molecules, forming a solvation shell, which might exert the observed pronounced steric hindrance. Additionally, the rate of dissociation of the IC can be switched by small variations of the pH, as shown in Fig. 30. At pH 4.6, the IC of PI-3,10 is almost stable, demonstrated by a nearly horizontal line.

The decay at the beginning was due to excess free α-CD still present from the preparation of the IC. Raising the pH from 4.6 to 6.6 causes the immediate release of all threaded CD rings, while raising the pH to 5.6 leads to a much slower release, requiring about 1 day for liberation of the threaded rings [271]. These switchable pseudopolyrotaxanes might be useful for delivery and pH programmed release within organisms of drugs bound to threaded CD rings.

Complexation and dissociation of poly(bola-amphiphile)s by the larger ring, β-CD, is too fast to allow isolation of the ICs. In addition, this complexation is not detectable by ^{1}HNMR, since there is no complexation induced shift of the signals due to the loose fit of the polymers in β-CD. α-CD rings can be used as stoppers to stabilize the β-CD IC. Much higher coverages of the polymer by CD rings are found after subsequent threading of β-CD and α-CD than for α-CD alone, shown in Fig. 31. Apparently, a stable triblock copolyrotaxane with the sequence (α-CD)$_n$ (β-CD)$_m$ (α-CD)$_n$ of threaded rings has been formed [276].
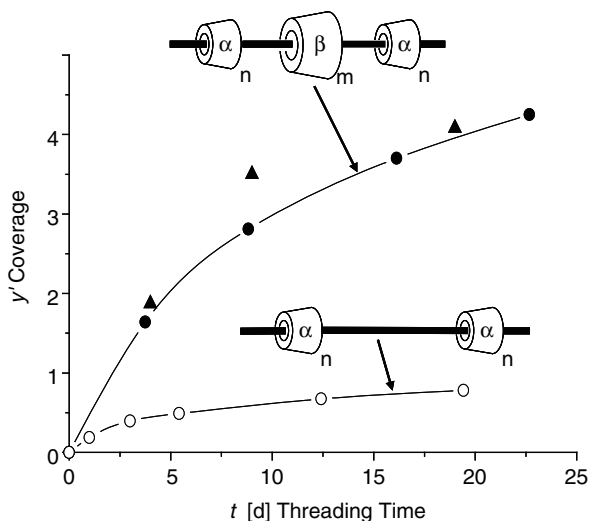
Fig. 31 Formation of (α-CD)$_n$ (β-CD)$_m$ (α-CD)$_n$ triblock pseudopolyrotaxane by sequential threading of (1) β-CD and (2) α-CD onto I-10,6. (*filled circles, filled triangles*) Coverage y' (total number of anhydroglucose units of α-CD and β-CD per repeat of I-10,6) as a function of threading time for α-CD, (*open circles*) control, coverage of threading α-CD solely [276]

Since threaded α-CD rings could not be distinguished from threaded β-CD rings by NMR, β-CD rings had to be labeled to prove unambiguously the structure of the triblock copolyrotaxanes. Therefore, 6-amino-6-deoxy-β-CD was covalently labeled with fluorescein isothiocyanate. The fluorescent β-CD derivative FITC-β-CD was threaded onto the polymer I-10,6. α-CD was threaded afterwards to stabilize the supramolecular structure. The resulting pseudopolyrotaxane was purified from free α-CD and FITC-β-CD rings by ultrafiltration. The fluorescence of the isolated product clearly proved that the sequential threading protocol of FITC-β-CD and α-CD onto I-10,6 had worked out as proposed [280]. The α-CD rings acted as supramolecular stoppers for the β-CD rings.

5.8 Synthesis of Polyrotaxanes from Main Chain Pseudopolyrotaxanes

The pseudopolyrotaxanes described above can be converted to polyrotaxanes by the attachment of bulky groups, which completely prevent dissociation of threaded rings. Bulky groups can be attached either (1) along the chain or (2) at both chain ends.

First, CD polyrotaxanes were synthesized by us by polymer analogous reaction of the amino groups of the PI-11/α-CD pseudopolyrotaxane with nicotinoyl chloride. A 25% conversion of the imino groups led to a permanent 67% coverage of

the polymer. The stability of the so-formed polyrotaxane was tested by extensive ultrafiltration, during which the α-CD rings remained on the polymer chain for longer than 1 week [272]. Polyrotaxanes of β-CD and PI-11 were synthesized in an analogous way. Since the nicotinoyl stoppers were too small to block β-CD, a larger reagent, 2,4-dinitrofluor-5-aniline, had to be used for the synthesis of the β-CD polyrotaxane [119].
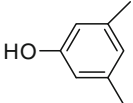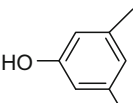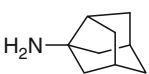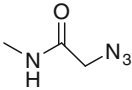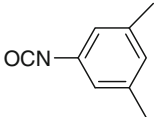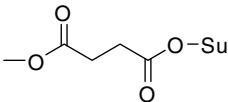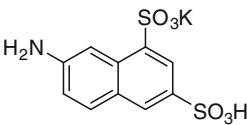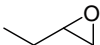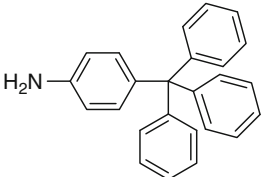
The ICs of PEO by α-CD were also converted to polyrotaxanes by the attachment of various blocking groups at the chain ends. Since the reactivity of the terminal hydroxyl groups is low, chain ends were functionalized prior to complexation by α-CD. Terminal amino groups were used by Harada's group in the first synthesis of a PEO-α-CD polyrotaxane. These were coupled with 2,4-dinitrofluorobenzene to furnish the polyrotaxane in 60% yield, since this end group was large enough to completely prevent dissociation of threaded rings even in organic solvents like DMSO [283]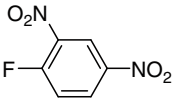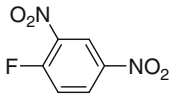. For low molecular weight PEG $(1,450\,\mathrm{g\,mol^{-1}})$, coverage of 91% per diethylene glycol repeat unit was reached, equivalent to 15 threaded rings per chain. For polymer threats of higher molecular weight, coverage was lower, e.g., 31% for molecular weight of $20,000\,\mathrm{g\,mol^{-1}}$, equivalent to 70 threaded rings [284].

Subsequently, further rotaxanation reactions, shown in Table 14, were developed, offering several advantages. A high reactivity of the functional chain end with the stopper reagent is very important because dissociation of threaded rings occurs during the reaction, especially when the reaction is performed in an organic solvent like DMF or DMSO, in which the ICs are not stable.

Similarly, the readily accessible PEO tosylates were stopped by etherification with 3,5-dimethylphenol [286]. As already observed for the synthesis of monomeric α-CD rotaxanes, a 1,3-disubstituted phenyl group or an adamantane group is already large enough to completely block dissociation of threaded α-CD rings. Modern click chemistry, using the Huisgen $[2+3]$ cycloaddition of azides and propargyl derivatives, also appears to be very effective for polyrotaxane synthesis [288]. Oligopeptide stoppers offer the advantage of being enzymatically cleavable on demand by proteases. This might be useful for the controlled release of drugs attached to the threaded α-CD rings [293]. The achievable coverage of the polymer chain with CD rings usually decreases with increasing molecular weight of the polymer thread for all stoppering reactions investigated to date.

Bigger stoppers, such as naphthalene-6,8-disulfonic acid [290] or tetraphenylmethane [292], are necessary for blocking the larger β-CD rings. For the synthesis of a β-CD polyrotaxane, a PEO–PPO–PEO triblock polymer functionalized with terminal amino groups was regioselectively complexed at the PPO block with β-CD and stoppered with fluorescein-4-isothiocyanate. The hydrophilic PEO blocks offer the advantage of increasing solubility in water, since they are scarcely covered by β-CD rings. Five β-CD rings were threaded within the polyrotaxane. The fluorescein blocking group was large enough to prevent their dissociation. At room temperature, these five β-CD rings were distributed over the full length of the polyrotaxane axis, while they were concentrated at the PPO segment at elevated temperatures [291, 294].

Table 14 Synthesis of polyrotaxanes by terminal coupling of stopper groups at polymer ICs with X coverage, number of CD rings per two polymer repeat units

Polymer	MW g mol^{-1}	End group	CD	Reagent	X%	Ref.
PEG	1,450	$-NH_2$	α	2,4-dinitrofluorobenzene (O_2N, F, NO_2)	91	[285]
PEG	20,000	$-NH_2$	α	2,4-dinitrofluorobenzene (O_2N, F, NO_2)	31	[285]
PEG	1,500	$-O-Tos$	α	3,5-dimethylphenol (HO-)	70	[286]
PEG	20,000	$-O-Tos$	α	3,5-dimethylphenol (HO-)	19	[286]
PEG	35,000	$-COOH$	α	aminoadamantane (H_2N-)	22	[287]
PEG	1,500	(azido acetamide, N_3)	α	$H\!\equiv\!\!-CH_2 \cdot O\!-\!R$	75	[288]
PTHF	1,100	$-NH_2$	α	3,5-dimethylphenyl isocyanate (OCN-)	96[a]	[289]
PEG–PPG–PEG	4,200	(succinimidyl succinate, $O-Su$)	β	amino naphthalene sulfonate (H_2N-, SO_3K, SO_3H)	49	[290]
PEG–PPG–PEG	4,200	$-NH_2$	β	FITC	12	[291]
PDMS	1,250	(epoxide, O)	β	4-aminotrityl (H_2N-)	28	[292]

[a]Per single repeat unit

Su: N-succinimide; FITC: fluorescein-4-isothiocyanate

Finding stoppers for γ-CD is difficult, because of its large diameter. Therefore β-CD and γ-CD were cothreaded on a polymer and rotaxanated by stoppers which block β-CD rings. Since the threaded γ-CD rings cannot overtake β-CD rings, they were blocked as well [275].

6 Conclusions and Outlook

It was shown that CDs and CD derivatives are very versatile hosts for the recognition of various monomeric and polymeric guests. Experience collected from binding studies with monomeric guests can often be applied and generalized for polymeric guests as well. Side chain and main chain guest polymers behave quite differently. While the recognition events happen in parallel for side chain guest polymers, they occur sequentially for main chain guest polymers. Slow inclusion of bola-amphiphiles and poly(bola-amphiphile)s offers certain advantages in comparison to other guests, since the ICs with them are kinetically stable for a defined time. Complex molecular architectures can be created without the necessity of covalent chemistry in water by using a supramolecular tool box.

Recognition potential of CDs can be greatly enhanced by regioselective derivatization of CDs. Recognition of polymers by CD derivatives is still an open field. Recognition might also be combined with catalytic activity of CDs or functional CD derivatives. Catalytic CDs might selectively bind to certain regions of destination of a block-copolymer to perform a specific reaction. Additionally, molecular machines might be created that exploit switchable site-selective binding.

Since molecular recognition of CDs and guests functions in water, it can also be combined with bio-molecular recognition. Ligands for certain cell specific receptors, such as lactose, were already linked to CD polyrotaxanes. These functional polyrotaxanes selectively bound to the human receptor protein galectin-1, inhibiting agglutination with T-cells already at low concentrations [295–297]. Therefore, CD polyrotaxanes might be very useful as vehicles for targeted drug delivery.

Since CDs are highly biocompatible, readily available, and easy to functionalize, and since they self-organize in a rather predictable way in aqueous solutions, they will become one of the most important supramolecular building blocks of the future.

References

1. Eigen M (1971) Naturwissenschaften 58:465
2. Fischer E (1894) Ber Dtsch Chem Ges 27:2985
3. Watson JD, Crick FHC (1953) Nature 171:737
4. Houk KN, Leach AG, Kim SP, Zhang XY (2003) Angew Chem Int Ed 42:4872

5. Cram DJ (1988) J Inclusion Phenom Macrocyc Chem 6:397
6. Lehn J-M (1988) Angew Chem Int Ed 27:89
7. Cram DJ (1986) Angew Chem Int Ed 25:1039
8. Dietrich-Buchecker C, Jimenez-Molero MC, Sartor V, Sauvage JP (2003) Pure Appl Chem 75:1383
9. Leigh DA, Wong JKY, Dehez F, Zerbetto F (2003) Nature 424:174
10. Berna J, Leigh DA, Lubomska M, Mendoza SM, Perez EM, Rudolf P, Teobaldi G, Zerbetto F (2005) Nat Mater 4:704
11. Moon C, Kwon YM, Lee WK, Park YJ, Yang VC (2007) J Control Release 124:43
12. Vignon SA, Jarrosson T, Iijima T, Tseng H-R, Sanders JKM, Stoddart JF (2004) J Am Chem Soc 126:9884
13. Green JE, Choi JW, Boukai A, Bunimovich Y, Johnston-Halperin E, DeIonno E, Luo Y, Sheriff BA, Xu K, Shin YS, Tseng HR, Stoddart JF, Heath JR (2007) Nature 445:414
14. Freudenberg K, Meyer-Delius M (1938) Ber Dtsch Chem Ges 71:1596
15. Oshovsky GV, Reinhoudt DN, Verboom W (2007) Angew Chem Int Ed 46:2366
16. Pedersen CJ (1988) Angew Chem Int Ed 27:1021
17. Lehn JM (1978) Acc Chem Res 11:49
18. Kim K (2002) Chem Soc Rev 31:96
19. Lukin O, Vogtle F (2005) Angew Chem Int Ed 44:1456
20. Rodriguez-Docampo Z, Pascu SI, Kubik S, Otto S (2006) J Am Chem Soc 128:11206
21. Hedges AR (1998) Chem Rev 98:2035
22. Saenger W (1980) Angew Chem Int Ed 19:344
23. Wenz G (1994) Angew Chem Int Ed 33:803
24. Saenger W, Jacob J, Gessler K, Steiner T, Hoffmann D, Sanbe H, Koizumi K, Smith SM, Takaha T (1998) Chem Rev 98:1787
25. Harata K (1998) Chem Rev 98:1803
26. Khan AR, Forgo P, Stine KJ, D'Souza VT (1998) Chem Rev 98:1977
27. Rekharsky MV, Inoue Y (1998) Chem Rev 98:1875
28. Stoddart JF (1998) Chem Rev 98:1959
29. Harada A (1997) Adv Polym Sci 133:141
30. Harada A, Hashidzume A, Takashima Y (2006) Adv Polym Sci 201:1
31. Wenz G, Han B-H, Müller A (2006) Chem Rev 106:782
32. Villiers A (1891) Compt Rend Acad Sci 112:536
33. Schardinger F (1903) Z Untersuch Nahr u Genussm 6:865
34. Freudenberg K, Jakobi R (1935) Liebigs Ann 518:102
35. Freudenberg K, Cramer F (1950) Chem Ber 83:296
36. Nakagawa T, Ueno K, Kashiw M, Watanabe J (1994) Tetrahedron Lett 35:1921
37. Jozwiakowski MJ, Connors KA (1985) Carbohydr Res 143:51
38. de Namor AFD, Cleverley RM, Zapata-Ormachea ML (1998) Chem Rev 98:2495
39. Zabel V, Saenger W, Mason SA (1986) J Am Chem Soc 108:3664
40. Müller A, Wenz G (2007) Chem – Eur J 13:2218
41. Lichtenthaler FW, Immel S (1994) Tetrahedron Asymmetry 5:2045
42. Frisch MJT, Schlegel HB, Scuseria GE, Robb MA, Cheeseman JR, Montgomery JA Jr, Vreven T, Kudin KN, Burant JC, Millam JM, Iyengar SS, Tomasi J, Barone V, Mennucci B, Cossi M, Scalmani G, Rega N, Petersson GA, Nakatsuji H, Hada M, Ehara M, Toyota K, Fukuda R, Hasegawa J, Ishida M, Nakajima T, Honda Y, Kitao O, Nakai H, Klene M, Li X, Knox JE, Hratchian HP, Cross JB, Adamo C, Jaramillo J, Gomperts R, Stratmann RE, Yazyev O, Austin AJ, Cammi R, Pomelli C, Ochterski JW, Ayala PY, Morokuma K, Voth GA, Salvador P, Dannenberg JJ, Zakrzewski VG, Dapprich S, Daniels AD, Strain MC, Farkas O, Malick DK, Rabuck AD, Raghavachari K, Foresman JB, Ortiz JV, Cui Q, Baboul AG, Clifford S, Cioslowski J, Stefanov BB, Liu G, Liashenko A, Piskorz P, Komaromi I, Martin RL, Fox DJ, Keith T, Al-Laham MA, Peng CY, Nanayakkara A, Challacombe M, Gill PMW, Johnson B, Chen W, Wong MW, Gonzalez C, Pople JA (2003) Program Gaussian03, Revision b.03, Pittsburgh, PA

43. Defaye J, Crouzy S, Evrard N, Law H (1999) WO9961483
44. Tang W, Ng SC (2008) Nat Protocols 3:691
45. Palin R, Grove SJA, Prosser AB, Zhang M-Q (2001) Tetrahedron Lett 42:8897
46. Djedaini-Pilard F, Desalos J, Perly B (1993) Tetrahedron Lett 34:2457
47. Steffen A, Thiele C, Tietze S, Strassnig C, Kämper A, Lengauer T, Wenz G, Apostolakis J (2007) Chem Eur J 13:6801–6809
48. Ueno A, Minato S, Osa T (1992) Anal Chem 64:2562
49. Yuan D-Q, Immel S, Koga K, Yamaguchi M, Fujita K (2003) Chem Eur J 9:3501
50. Atsumi M, Izumida M, Yuan D-Q, Fujita K (2000) Tetrahedron Lett 41:8117
51. Yuan D-Q, Tahara T, Chen W-H, Okabe Y, Yang C, Yagi Y, Nogami Y, Fukudome M, Fujita K (2003) J Org Chem 68:9456
52. Bistri O, Sinay P, Sollogoub M (2005) Tetrahedron Lett 46:7757
53. du Roizel B, Baltaze J-P, Sinay P (2002) Tetrahedron Lett 43:2371
54. Bistri O, Sinay P, Sollogoub M (2006) Tetrahedron Lett 47:4137
55. Bistri O, Sinay P, Sollogoub M (2006) Chem Commun:1112
56. Gadelle A, Defaye J (1991) Angew Chem Int Ed 30:78
57. Ashton PR, Koniger R, Stoddart JF, Alker D, Harding VD (1996) J Org Chem 61:903
58. Wenz G, Strassnig G, Thiele C, Engelke A, Morgenstern B, Hegetschweiler K (2008) Chem Eur J 14:7202
59. Garcia-López JJ, Hernández-Mateo F, Isac-Garcia J, Kim JM, Roy R, Santoyo-González F, Vargas-Berenguel A (1999) J Org Chem 64:522
60. Takeo K, Mitoh H, Uemura K (1989) Carbohydr Res 187:203
61. Cousin H, Cardinael P, Oulyadi H, Pannecoucke X, Combret JC (2001) Tetrahedron Asymmetry 12:81
62. Ashton PR, Boyd SE, Gattuso G, Hartwell EY, Königer R, Spencer N, Stoddart JF (1995) J Org Chem 60:3898
63. Uccello-Barretta G, Sicoll G, Balzano F, Salvadori P (2005) Carbohydr Res 340:271
64. Kraus T, Budesinsky M, Zavada J (1997) Carbohydr Res 304:81
65. Kraus T, Budesinsky M, Zavada J (2001) J Org Chem 66:4595
66. Kraus T, Budesinsky M, Cisarova I, Zavada J (2002) Angew Chem Int Ed 41:1715
67. Kraus T, Budesinsky M, Cisarova I, Zavada J (2004) Eur J Org Chem:4060
68. Wimmer T (1995) EP0646602A1
69. Brauns U, Mueller BWW (1985) DE3346123A1
70. Muller BW, Brauns U (1986) J Pharm Sci 75:571
71. Wenz G, Höfler T (1999) Carbohydr Res 322:153
72. Stella VJ, Rajewski R (1994) Wo9402518
73. Uekama K, Hirashima N, Horiuchi Y, Hirayama F, Ijitsu T, Ueno M (1987) J Pharm Sci 76:660
74. Wenz G (1991) Carbohydr Res 214:257
75. Zia V, Rajewski RA, Stella VJ (2001) Pharm Res 18:667
76. Lecourt T, Mallet J-M, Sinay P (2002) Tetrahedron Lett 43:5533
77. Breslow R, Greenspoon N, Guo T, Zarzycki R (1989) J Am Chem Soc 111:8296
78. Okabe Y, Yamamura H, Obe KI, Ohta K, Kawai M, Fujita K (1995) J Chem Soc Chem Commun:581
79. Breslow R, Halfon S, Zhang BL (1995) Tetrahedron 51:377
80. Yuan DQ, Koga K, Kouno I, Fujioka T, Fukudome M, Fujita K (2007) Chem Commun:828
81. Liu Y, Chen Y (2006) Acc Chem Res 39:681
82. Bistri O, Lecourt T, Mallet J-M, Sollogoub M, Sinay P (2004) Chem Biodiversity 1:129
83. Harada A, Furue M, Nozakura SI (1976) Macromolecules 9:701
84. Maeda K, Mochizuki H, Watanabe M, Yashima E (2006) J Am Chem Soc 128:7639
85. Ogoshi T, Takashima Y, Yamaguchi H, Harada A (2006) Chem Commun:3702
86. Weickenmeier M, Wenz G (1996) Macromol Rapid Commun 17:731
87. Huff J, Kistenmacher A, Schornick G, Weickenmeier M, Wenz G (1996) DEDE 19612768A1
88. Wenz G, Weickenmeier M, Huff J (2000) ACS Symp Ser 765:271
89. Renard E, Volet G, Amiel C (2005) Polym Int 54:594

90. Seo T, Kajihara T, Iijima T (1987) Makromol Chem 188:2071
91. Suh J, Hah SS, Lee SH (1997) Bioorganic Chem 25:63
92. Tojima T, Katsura H, Han S-M, Tanida F, Nishi N, Tokura S, Sakairi N (1998) J Polym Sci 36:1965
93. Sakairi N, Furusaki E, Ueno Y, Nishi N, Tokura S (1996) Carbohydr Polym 29:29
94. Pluemsab W, Sakairi N, Furuike T (2005) Polymer 46:9778
95. Choi HS, Takahashi A, Ooya T, Yui N (2006) ChemPhysChem 7:1668
96. Renard E, Barnathan G, Deratani A, Sebille B (1997) Macromol Symp 122:229
97. Renard E, Deratani A, Volet G, Sébille B (1997) Eur Polym J 33:49
98. Harada A, Li J, Kamachi M (1993) Nature 364:516
99. Choi B-K, Suwa Y, Hashizume T, Terada Y, Ito K, Shimomura T (2005) Jp2005272664
100. Harada A, Okada M, Kawaguchi Y, Kamachi M (1999) Polym Adv Technol 10:3
101. Ceccato M, LoNostro P, Rossi C, Bonechi C, Donati A, Baglioni P (1997) J Phys Chem B 101:5094
102. Liu L, Guo Q-X (2002) J Inclusion Phenom Macrocyc Chem 42:1
103. Meyer EA, Castellano RK, Diederich F (2003) Angew Chem Int Ed 42:1210
104. Connors KA (1997) Chem Rev 97:1325
105. Eftink MR, Andy ML, Bystrom K, Perlmutter HD, Kristol DS (1989) J Am Chem Soc 111:6765
106. Fuhrhop JH, Boettcher C, Spiroski D (1993) J Am Chem Soc 115:1600
107. Fuoss RM, Chu VFH (1951) J Am Chem Soc 73:949
108. Eyring H (1935) J Chem Phys 3:107
109. Bastos M, Briggner LE, Shehatta I, Wadsö I (1990) J Chem Thermodyn 22:1181
110. Shehatta I (1996) React Funct Polym 28:183
111. Cromwell WC, Bystrom K, Eftink MR (1985) J Phys Chem 89:326
112. Wenz G (2008) unpublished data
113. Inoue Y, Hakushi T, Liu Y, Tong L-H, Shen B-J, Jin D-S (1993) J Am Chem Soc 115:475
114. Blyshak LA, Warner IM, Patonay G (1990) Anal Chim Acta 232:239
115. Miyajima K, Komatsu H, Inoue K, Handa T, Nakagaki M (1990) Bull Chem Soc Jpn 63:6
116. Klüfers P, Wenz G, Goel P (1997) unpublished data
117. Schmider J, Fritsch G, Haisch T, Muller K (2001) Mol Cryst Liquid Cryst Sci Technol A Mol Cryst Liquid Cryst 356:99
118. Wenz G, Steinbrunn M (1998) WO9838222A2
119. Keller B (1994) Dissertation, Universität Karlsruhe, Germany
120. Eliadou K, Yannakopoulou K, Rontoyianni A, Mavridis IM (1999) J Org Chem 64:6217
121. Simova S, Schneider H-J (2000) Perkin 2:1717
122. Schneider HJ, Blatter T, Simova S (1991) J Am Chem Soc 113:1996
123. Höfler T, Wenz G (1996) J Inclusion Phenom Macro Chem 25:81
124. Sau S, Solanki B, Orprecio R, Van Stam J, Evans CH (2004) J Inclusion Phenom Macrocyc Chem 48:173
125. Stone MT, Anderson HL (2007) Chem Commun:2387
126. Gelb RI, Schwartz LM (1989) J Inclusion Phenom Mol Recog Chem 7:537
127. Briggner LE, Ni X-R, Tempesti F, Wadsö I (1986) Thermochim Acta 109:139
128. Godínez LA, Patel S, Criss CM, Kaifer AE (1995) J Phys Chem 99:17449
129. de Jong MR, Engbersen JFJ, Huskens J, Reinhoudt DN (2000) Chem Eur J 6:4034
130. Kano K, Matsumoto H, Yoshimura Y, Hashimoto S (1988) J Am Chem Soc 110:204
131. Kano K, Matsumoto H, Hashimoto S, Sisido M, Imanishi Y (1985) J Am Chem Soc 107:6117
132. Pistolis G, Malliaris A (2004) J Phys Chem B 108:2846
133. Yoshida ZI, Takekuma H, Takekuma SI, Matsubara Y (1994) Angew Chem Int Ed 33:1597
134. Buvari-Barcza A, Rohonczy J, Rozlosnik N, Gilanyi T, Szabo B, Lovas G, Braun T, Samu J, Barcza L (2001) J Chem Soc Perkin Trans 2:191
135. Herrmann W, Wehrle S, Wenz G (1997) Chem Commun:1709
136. Tan WH, Ishikura T, Maruta A, Yamamoto T, Matsui Y (1998) Bull Chem Soc Jpn 71:2323
137. Belosludov R, Hiwada T, Kawazoe Y, Ohno K, Yoshinari T, Ohnishi A, Nagasaka S-I (1999) J Solid State Chem 144:263

138. Schneider HJ, Sangwan NK (1987) Angew Chem 99:924
139. Sternbach DD, Rossana DM (1982) J Am Chem Soc 104:5853
140. Kim SP, Leach AG, Houk KN (2002) J Org Chem 67:4250
141. Liu Y, Li B, Wada T, Inoue Y (1999) Supramol Chem 10:173
142. CladrowaRunge S, Rizzi A (1997) J Chromatogr A 759:157
143. Liu Y, Yang EC, Yang YW, Zhang HY, Fan Z, Ding F, Cao R (2004) J Org Chem 69:173
144. Kitae T, Nakayama T, Kano K (1998) J Chem Soc Perkin Trans 2:207
145. Rekharsky M, Yamamura H, Kawai M, Inoue Y (2001) J Am Chem Soc 123:5360
146. Rekharsky MV, Inoue Y (2002) J Am Chem Soc 124:813
147. Hacket F, Simova S, Schneider H (2001) J Phys Org Chem 14:159
148. Yamamura H, Rekharsky MV, Ishihara Y, Kawai M, Inoue Y (2004) J Am Chem Soc 126:14224
149. Kano K (1997) J Phys Org Chem 10:286
150. Armstrong DW, Demond W (1984) J Chromatogr Sci 22:411
151. Armstrong DW, Ward TJ, Armstrong RD, Beesley TE (1986) Science 232:1132
152. Konig WA, Lutz S, Wenz G (1988) Angew Chem Int Ed 27:979
153. Ehlers J, König WA, Lutz S, Wenz G, tom Dieck H (1988) Angew Chem Int E Engl 27:1556
154. Schurig V, Nowotny HP (1990) Angew Chem Int Ed 29:939
155. Fanali S (2000) J Chromatogr A 875:89
156. Li S, Purdy WC (1992) Chem Rev 92:1457
157. Hasegawa Y, Miyauchi M, Takashima Y, Yamaguchi H, Harada A (2005) Macromolecules 38:3724
158. Breslow R, Zhang B (1996) J Am Chem Soc 118:8495
159. Hu H-C, Liu Y, Zhang D-D, Wang L-F (1999) J Inclusion Phenom Macrocyc Chem 33:295
160. Ikeda T, Hirota E, Qoya T, Yui N (2001) Langmuir 17:234
161. Harata K (1981) Bioorg Chem 10:255
162. Lyon AP, Banton NJ, Macartney DH (1998) Can J Chem 76:843
163. Baer AJ, Macartney DH (2005) Org Biomol Chem 3:1448
164. Smith AC, Macartney DH (1998) J Org Chem 63:9243
165. Oshikiri T, Takashima Y, Yamaguchi H, Harada A (2007) Chem Eur J 13:7091
166. Baer AJ, Macartney DH (2007) Supramol Chem 19:537
167. Yamaguchi H, Oshikiri T, Harada A (2006) J Phys Condens Matter 18:S1809
168. Park JW, Song HJ, Cho YJ, Park KK (2007) J Phys Chem C 111:18605
169. Safarowsky O, Windisch B, Mohry A, Vögtle F (2000) J für Praktische Chemie-Pract Appl Appl Chem 342:437
170. Wilks ES (2003) Polym Prepr 4:1278
171. Nepogodiev SA, Stoddart JF (1998) J Am Chem Soc 98:1959
172. Craig MR, Claridge TDW, Hutchings MG, Anderson HL (1999) Chem Commun 1537
173. Park JS, Wilson JN, Hardcastle KI, Bunz UHF, Srinivasarao M (2006) J Am Chem Soc 128:7714
174. Mezzina E, Franchi P, Lucarini M (2007) J Inclusion Phenom Macrocyc Chem 57:179
175. Onagi H, Carrozzini B, Cascarano GL, Easton CJ, Edwards AJ, Lincoln SF, Rae AD (2003) Chem Eur J 9:5971
176. Wang Q-C, Ma X, Qu D-H, Tian H (2006) Chem Eur J 12:1088
177. Baer AJ, Macartney DH (2000) Inorg Chem 39:1410
178. Ogino H (1981) J Am Chem Soc 103:1303
179. Suzaki Y, Taira T, Osakada K (2006) Dalton Trans 5345
180. Sakamoto K, Takashima Y, Yamaguchi H, Harada A (2007) J Org Chem 72:459
181. Skinner PJ, Blair S, Kataky R, Parker D (2000) New J Chem 24:265
182. Ma X, Wang Q, Qu D, Xu Y, Ji F, Tian H (2007) Adv Funct Mater 17:829
183. Klotz EJF, Claridge TDW, Anderson HL (2006) J Am Chem Soc 128:15374
184. Qu D-H, Ji F-Y, Wang Q-C, Tian H (2006) Adv Mater 18:2035
185. Zhao Y-L, Dichtel WR, Trabolsi A, Saha S, Aprahamian I, Stoddart JF (2008) J Am Chem Soc 130:11294
186. Qu DH, Wang QC, Tian H (2005) Mol Cryst Liquid Cryst 430:59

187. Murakami H, Kawabuchi A, Kotoo K, Kunitake M, Nakashima N (1997) J Am Chem Soc 119:7605
188. Zheng PJ, Wang C, Hu X, Tam KC, Li L (2005) Macromolecules 38:2859
189. Weickenmeier M, Wenz G, Huff J (1997) Macromol Rapid Commun 18:1117
190. Weickenmeier M (1998) Dissertation, Karlsruhe, Germany
191. Harada A, Adachi H, Kawaguchi Y, Kamachi M, Harada (1997) Macromolecules 30:5181
192. Eisenhart EK, Merritt RF, Johnson EA (1991) EP0460896A2
193. Lau W, Shah VM (1994) EP614950A1
194. Tomatsu I, Hashidzume A, Harada A (2005) Macromol Rapid Commun 26:825
195. Beheshti N, Bu H, Zhu K, Kjoniksen A-L, Knudsen KD, Pamies R, Hernandez Cifre JG, Garcia de la Torre J, Nystroem B (2006) J Phys Chem B 110:6601
196. Kretschmann O, Steffens C, Ritter H (2007) Angew Chem Int Ed 46:2708
197. Tomatsu I, Hashidzume A, Harada A (2005) Macromolecules 38:5223
198. Amiel C, Sebille B (1996) J Inclusion Phenom Mol Recognit Chem 25:61
199. Amiel C, Sebille B (1997) Rev Inst Fr Pet 52:248
200. Amiel C, Sebille B (1999) Adv Colloid Interf Sci 79:105
201. Weickenmeier M, Wenz G, Huff J (1997) Macromol Rapid Commun 18:1117
202. Weickenmeier M (1998) Dissertation, University of Karlsruhe, Germany
203. Guo XH, Abdala AA, May BL, Lincoln SF, Khan SA, Prud'homme RK (2005) Macromolecules 38:3037
204. Takashima Y, Nakayama T, Miyauchi M, Kawaguchi Y, Yamaguchi H, Harada A (2004) Chem Lett 33:890
205. Bistri O, Mazeau K, Auzély-Velty R, Sollogoub M (2007) Chem Eur J 13:8847
206. Auzely-Velty R, Rinaudo M (2002) Macromolecules 35:7955
207. Lecourt T, Sinay P, Chassenieux C, Rinaudo M, Auzely-Velty R (2004) Macromolecules 37:4635
208. Li J (2009) Adv Polym Sci same volume, in press
209. Gref R, Amiel C, Molinard K, Daoud-Mahammed S, Sebille B, Gillet B, Beloeil J-C, Ringard C, Rosilio V, Poupaert J, Couvreur P (2006) J Control Release 111:316
210. Ravoo BJ, Jacquier J-C, Wenz G (2003) Angew Chem Int Ed 42:2066
211. Schönherr H, Beulen MWJ, Bügler J, Huskens J, van Veggel FCJM, Reinhoudt DN, Vancso GJ (2000) J Am Chem Soc 122:4963
212. Ludden MJW, Mulder A, Tampe R, Reinhoudt DN, Huskens J (2007) Angew Chem Int Ed 46:4104
213. Crespo-Biel O, Peter M, Bruinink CM, Ravoo BJ, Reinhoudt DN, Huskens J (2005) Chem Eur J 11:2426
214. Ludden MJW, Li X, Greve J, van Amerongen A, Escalante M, Subramaniam V, Reinhoudt DN, Huskens J (2008) J Am Chem Soc 130:6964
215. Ling XY, Reinhoudt DN, Huskens J (2008) Chem Mat 20:3574
216. Horsky J (2000) Macromol Theory Simul 9:759
217. Okumura H, Kawaguchi Y, Harada A (2001) Macromolecules 34:6338
218. Harada A, Kamachi M (1990) Macromolecules 23:2821
219. Harada A, Okada M, Kawaguchi Y (2005) Chem Lett 34:542
220. Harada A, Li J, Kamachi M (1993) Macromolecules 26:5698
221. Harada A, Kamachi M (1994) Macromolecules 27:4538
222. Harada A, Li J, Kamachi M (1994) Macromolecules 27:4538
223. Harada A, Li J, Kamachi M, Kitagawa Y, Katsube Y (1998) Carbohydr Res 305:127
224. Harada A, Okada M, Kamachi M (1995) Acta Polym 46:453
225. Li JY, Yan DY (2001) Macromolecules 34:1542
226. Harada A (1997) Carbohydr Polym 34:183
227. Choi HS, Ooya T, Lee SC, Sasaki S, Kurisawa M, Uyama H, Yui N (2004) Macromolecules 37:6705
228. Shin K, Dong T, He Y, Taguchi Y, Oishi A, Nishida H, Inoue Y (2004) Macromol Biosci 4:1075
229. Dong T, Kai W, Pan P, Cao A, Inoue Y (2007) Macromolecules 40:7244

230. Harada A, Nishiyama T, Kawaguchi Y, Okada M, Kamachi M (1997) Macromolecules 30:7115
231. Huang L, Allen E, Tonelli AE (1999) Polymer 40:3211
232. Li J, Harada A, Kamachi M (1994) Bull Chem Soc Jpn 67:2808
233. Wenz G, Steinbrunn MB (1997) De19608354
234. Steinbrunn MB, Landfester K, Wenz G (1997) Tetrahedron 53:15575
235. Steinbrunn MB, Wenz G (1996) Angew Chem Int Ed 35:2139
236. Ikeda T, Lee WK, Ooya T, Yui N (2003) J Phys Chem B 107:14
237. Harada A, Kamachi M (1990) J Chem Soc Chem Commun 19:1322
238. Jiao H, Goh SH, Valiyaveettil S, Zheng JW (2003) Macromolecules 36:4241
239. Kamitori S, Matsuzaka O, Kondo S, Muraoka S, Okuyama K, Noguchi K, Okada M, Harada A (2000) Macromolecules 33:1500
240. Harada A, Okumura H, Okada M, Kawaguchi Y (2000) Macromolecules 33:4297
241. Okumura H, Kawaguchi Y, Harada A (2003) Macromolecules 36:6422
242. Okumura H, Kawaguchi Y, Harada A (2002) Macromol Rapid Commun 23:781
243. Shimomura T, Yoshida K, Ito K, Hayakawa R (2000) Polym Adv Technol 11:837
244. Yoshida K-i, Shimomura T, Ito K, Hayakawa R (1999) Langmuir 15:910
245. Yamaguchi I, Kashiwagi K, Yamamoto T (2004) Macromol Rapid Commun 25:1163
246. van den Boogaard M, Bonnet G, Van't Hof P, Wang Y, Brochon C, van Hutten P, Lapp A, Hadziioannou G (2004) Chem Mater 16:4383
247. Belosludov RV, Farajian AA, Kikuchi Y, Mizuseki H, Kawazoe Y (2006) Comput Mater Sci 36:130
248. Harada A, Li J, Suzuki S, Kamachi M (1993) Macromolecules 26:5267
249. Harada A, Li J, Kamachi M (1993) Chem Lett:237
250. Uyar T, Rusa M, Tonelli AE (2004) Macromol Rapid Commun 25:1382
251. Uyar T, Gracz HS, Rusa M, Shin ID, El-Shafei A, Tonelli AE (2006) Polymer 47:6948
252. Martinez G, Gomez MA, Villar-Rodil S, Garrido L, Tonelli AE, Balik CM (2007) J Polym Sci A Polym Chem 45:2503
253. Sanji T, Kato M, Tanaka M (2005) Macromolecules 38:4034
254. Rusa M, Wang X, Tonelli AE (2004) Macromolecules 37:6898
255. Harada A, Li J, Kamachi M (1994) Nature 370:126
256. Panova IG, Gerasimov VI, Kalashnikov FA, Topchieva IN (1998) Vysokomolekulyarnye Soedineniya Seriya A Seriya B 40:2077
257. Li J, Chen B, Wang X, Goh SH (2004) Polymer 45:1777
258. Li J, Ni XP, Zhou ZH, Leong KW (2003) J Am Chem Soc 125:1788
259. Ooya T, Ito A, Yui N (2005) Macromol Biosci 5:379
260. Li X, Li J, Leong KW (2003) Macromolecules 36:1209
261. Huang J, Ren L, Zhu H, Chen Y (2006) Macromol Chem Phys 207:1764
262. Shuai XT, Porbeni FE, Wei M, Bullions T, Tonelli AE (2002) Macromolecules 35:2401
263. Shuai XT, Probeni FE, Wei M, Bullions T, Tonelli AE (2002) Macromolecules 35:3778
264. Ohya Y, Takamido S, Nagahama K, Ouchi T, Ooya T, Katoono R, Yui N (2007) Macromolecules 40:6441
265. Kinbara K, Aida T (2005) Chem Rev 105:1377
266. Balzani V, Credi A, Raymo FM, Stoddart JF (2000) Angew Chem Int Ed 39:3349
267. Rusa CC, Fox J, Tonelli AE (2003) Macromolecules 36:2742
268. Choi HS, Ooya T, Yui N (2006) Macromol Biosci 6:420
269. Choi HS, Hirasawa A, Ooya T, Kajihara D, Hohsaka T, Yui N (2006) Chem Phys Chem 7:1671
270. Wenz G, Keller B (1992) Angew Chem Int Ed 31:197
271. Keller B (1994), Dissertation, University of Mainz, Germany
272. Wenz G, Keller B (1992) Angew Chem Int Ed 31:197
273. Wenz G, Gruber C, Keller B, Schilli C, Albuzat T, Mueller A (2006) Macromolecules 39:8021
274. Gruber C (2002), Dissertation, University of Karlsruhe, Germany
275. Herrmann W, Schneider M, Wenz G (1997) Angew Chem Int Ed 36:2511
276. Herrmann W (1997) Dissertation, Universität Karlsruhe, Germany

277. Baudendistel N (2001) Diploma Thesis, University of Karlsruhe, Germany
278. Herrmann W, Keller B, Wenz G (1997) Macromolecules 30:4966
279. Meier LP, Heule M, Caseri WR, Shelden RA, Suter UW, Wenz G, Keller B (1996) Macromolecules 29:718
280. Krauter I, Herrmann W, Wenz G (1996) J Inclusion Phenom Mol Recog Chem 25:93
281. Kelch S, Caseri WR, Shelden RA, Suter UW, Wenz G, Keller B (2000) Langmuir 16:5311
282. Wenz G, Keller B (1994) Macromol Symp 87:11
283. Harada A, Li J, Kamachi M (1992) Nature 356:325
284. Harada A, Li J, Nakamitsu T, Kamachi M (1993) J Org Chem 58:7524
285. Harada A (1996) Supramol Sci 3:19
286. Zhao TJ, Beckham HW (2003) Macromolecules 36:9859
287. Araki J, Zhao C, Ito K (2005) Macromolecules 38:7524
288. Loethen S, Ooya T, Choi HS, Yui N, Thompson DH (2006) Biomacromolecules 7:2501
289. Arai T, Takata T (2007) Chem Lett 36:418
290. Fujita H, Ooya T, Kurisawa M, Mori H, Terano M, Yui N (1996) Macromol Rapid Commun 17:509
291. Fujita H, Ooya T, Yui N (1999) Macromol Chem Phys 200:706
292. Marangoci N, Farcas A, Pinteala M, Harabagiu V, Simionescu BC, Sukhanova T, Bronnikov S, Grigoryev A, Gubanova G, Perminova M, Perichaud A (2008) High Perform Polym 20:251
293. Ooya T, Yui N (1998) Macromol Chem Phys 199:2311
294. Fujita H, Ooya T, Yui N (1999) Macromolecules 32:2534
295. Belitsky JM, Nelson A, Hernandez JD, Baum LG, Stoddart JF (2007) Chem Biol 14:1140
296. Nelson A, Belitsky JM, Vidal S, Joiner CS, Baum LG, Stoddart JF (2004) J Am Chem Soc 126:11914
297. Nelson A, Stoddart JF (2003) Org Lett 5:3783

Functional Cyclodextrin Polyrotaxanes for Drug Delivery

Nobuhiko Yui, Ryo Katoono, and Atsushi Yamashita

Dedicated to Professor Naoya Ogata on the occasion of his 77th birthday (Kiju)

Abstract The mobility of cyclodextrins (CDs) threaded onto a linear polymeric chain and the dethreading of the CDs from the chain are the most fascinating features seen in polyrotaxanes. These structural characteristics are very promising for their possible applications in drug delivery. Enhanced multivalent interaction between ligand–receptor systems by using ligand–conjugated polyrotaxanes would be just one of the excellent properties related to the CD mobility. Gene delivery using cytocleavable polyrotaxanes is a more practical but highly crucial issue in drug delivery. Complexation of the polyrotaxanes with DNA and its intracellular DNA release ingeniously utilizes both CD mobility and polyrotaxane dissociation to achieve effective gene delivery. Such a supramolecular approach using CD-containing polyrotaxanes is expected to exploit a new paradigm of biomaterials.

Keywords CD mobility, Gene delivery, Multivalent interaction, Saccharide/protein interaction, Supramolecular dissociation

Contents

N. Yui (✉) and R. Katoono
School of Materials Science, Japan Advanced Institute of Science and Technology, Asahidai, Nomi, Ishikawa 923-1292, Japan and
JST CREST, 5 Sanbancho, Chiyoda, Tokyo 102-0075, Japan
e-mail: yui@jaist.ac.jp, katoono@jaist.ac.jp

A. Yamashita
School of Materials Science, Japan Advanced Institute of Science and Technology, Asahidai, Nomi, Ishikawa 923-1292, Japan
e-mail: a-yamata@jaist.ac.jp

1 Introduction

One of the structural features seen in polyrotaxanes is the absence of any covalent binding between cyclic compounds and a linear polymeric chain capped with bulky end-groups at both terminals [1]. It looks like a necklace: the cyclic compounds are mechanically locked by the linear polymeric chain. The cyclic compounds in a polyrotaxane can slide and/or rotate along the axial polymeric chain if the polyrotaxane is soluble in a certain solvent. Furthermore, such mechanical locking between the cyclic compounds and the linear polymeric chain will be opened once one of the terminal bulky end-groups is cleaved by any external conditions. These characteristics are only observable in and specific to polyrotaxanes and are never seen in conventional polymeric architectures (Fig. 1).

The first report on preparing a polymeric inclusion complex (polypseudorotaxane) using cyclodextrin (CD) was published by Ogata and his coworkers in 1976 [2]. They prepared several inclusion complexes consisting of an aromatic or aliphatic diamine with β-CD and then applied the complex to polycondensation reactions with an acid chloride such as isophthaloyl and terephthaloyl dichloride to prepare CD-included polyamides. In 1990, Harada and Kamachi reported a very straightforward method to prepare an inclusion complex (pseudopolyrotaxane) between α-CD and a linear polymeric chain such as poly(ethylene glycol) (PEG) of various molecular weights in aqueous conditions [3]. They found that one can obtain pseudopolyrotaxanes as a precipitate within a short period of time if the saturated aqueous solution of α-CD is directly mixed with aqueous solutions of PEG at room temperature. This unexpected finding led to explore quite a new paradigm of the world of polyrotaxane as functional polymers. At almost the same period of time, Wenz and his coworker reported the first polyrotaxane synthesis from α-CD and a polyamine [4]. Harada and Kamachi have analyzed not only the formation of a variety of pseudopolyrotaxanes, but also the preparation of polyrotaxanes and their related architectures, and their significant efforts contributed much to the progress in understanding polyrotaxanes using CDs [5].

From the viewpoint of biomaterials which are to be utilized in contact with a living body, the combination of α-CD and PEG as building-blocks allowed us to envision the novel design of biologically inert and/or biodegradable polymers. CDs have been approved by the FDA as food additives and as drug formulations, and PEG is a worldwide-used water-soluble polymer for conjugating biologically active agents such as drugs and proteins. It is thus easily established that biodegradable polyrotaxanes consisting of α-CD molecules and a PEG chain capped with bulky end-groups via biodegradable linkages have much potential in drug delivery.
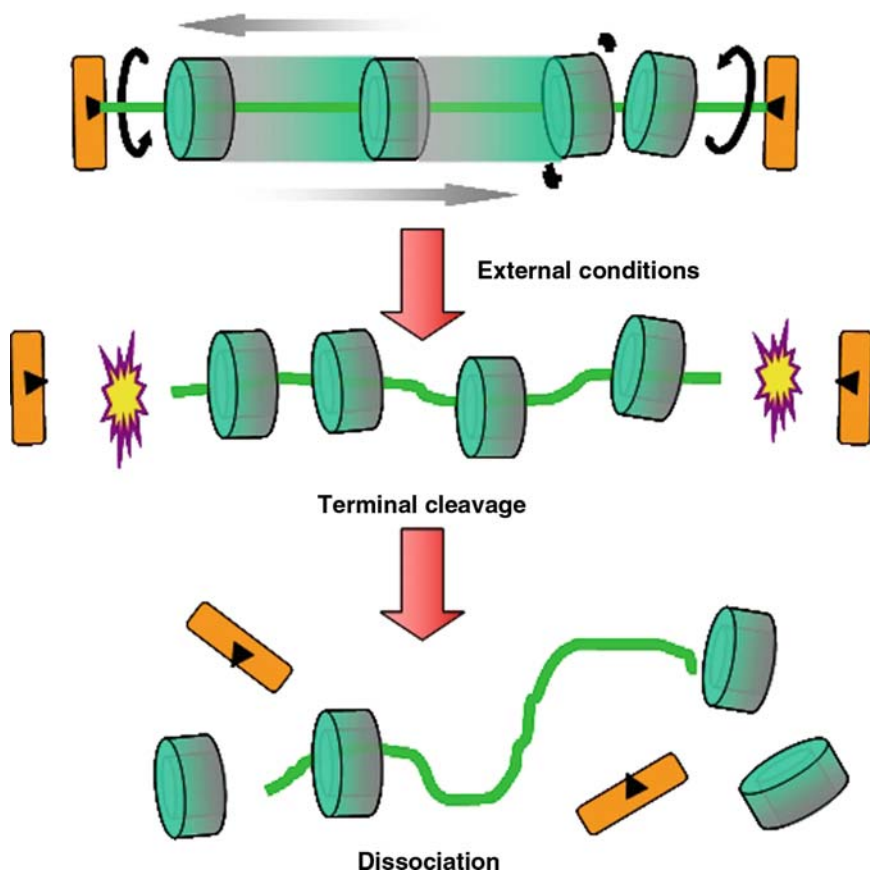
Fig. 1 Images of the mobility of mechanically interlocked cyclic compounds and stimuli responsive dissociation of the polyrotaxanes

Supramolecular dissociation of the polyrotaxanes into constituent molecules such as α-CD and PEG was quite a new image as a mode of biodegradation in a living body. This insight was the first step to initiate our studies on polyrotaxanes as biomaterials 15 years ago [6].

In general, the most important strategy when initiating the design of materials using polyrotaxanes lies in the effectiveness of such a supramolecular structure regarding their functionality. If the functionality of the polyrotaxanes were already achieved in conventional materials, the use of polyrotaxanes would of course not make any sense. Quite a new functionality which has never been achieved in previous studies should be thoroughly considered as it is strongly required for initiating and proposing a new concept. From this point of view, it should be noted that the characteristics of polyrotaxanes depicted in Fig. 1 are so fascinating that they create a paradigm shift in materials science [7]. Of course, one should thoroughly consider the following three issues when initiating the design of materials: (1) the strategy

of designing the functionality of biomaterials, (2) the tactics of preparing new architectures which fit the design concept, and (3) the logistics of cost performance and feasibility. When taking these issues into account, polyrotaxanes will constitute one of the greatest challenges to achieving far-reaching applications in the future. From these perspectives, the fact that polyrotaxanes have a lot of supramolecular characteristics including the mobility of cyclic compounds threaded onto a linear polymeric chain and the perfect dissociation at specific sites in a living body seems to constitute a sophisticated paradigm.

This chapter deals with CD-based functional polyrotaxanes for drug delivery, our main achievements over the last decade. First, we present an overview of the perspectives of polyrotaxane preparations for biomaterials applications. Then we highlight recent topics of our studies on drug delivery using CD-based polyrotaxanes. In particular, we describe a concept for enhancing multivalent interaction of a ligand-mobile polyrotaxane with receptor proteins. This issue is significantly related to receptor-mediated drug delivery and to modulation of cellular and tissue metabolism. The efficiency of such ligand–conjugated polyrotaxanes is also demonstrated in the design of inhibitors which are recognized by intestinal transporters in mammalian tissues but neither absorbed into the tissue nor exhibiting any toxicity. Finally, in order to expand this concept to more practical applications, we also introduce our studies on cytocleavable polyrotaxanes for gene delivery as an ultimate modern therapy. The dynamic motion of polyrotaxanes would contribute significantly to forming a polyplex with DNA to be delivered into target cells, and dissociating the polyrotaxane structure in intracellular environments is an effective way to release DNA for transfection at the nucleus.

2 Preparation and Properties of Polyrotaxanes for Biomedical Use

A large number of methods for the preparation of polyrotaxanes using CDs have been made available, and reported elsewhere [8,9]. In particular, one of the common strategies to prepare polyrotaxanes has been the capping of both terminals of pseudopolyrotaxanes with bulky groups, since Harada and Kamachi reported a unique preparation method of pseudopolyrotaxanes and polyrotaxanes [3, 5]. In order to design polyrotaxanes for medical and pharmaceutical applications, special attention should be paid to their biocompatibility as well as to their nontoxicity. For instance, assuming that polyrotaxanes will be used as a drug carrier, they should be water-soluble as well as functional for drug conjugation. If their molecular weight is higher than 10,000, in order to be excreted from urine, their digestion or degradation in a living body may be considered. Of course, biological inertness during their usage is also one of the necessary conditions to perform their functionality in contact with a living body. In this section, we describe a common preparation of polyrotaxanes for use in a living body by capping pseudopolyrotaxanes with amino acid derivatives as bulky end-groups via a condensation reaction, and a chemical modification of CD
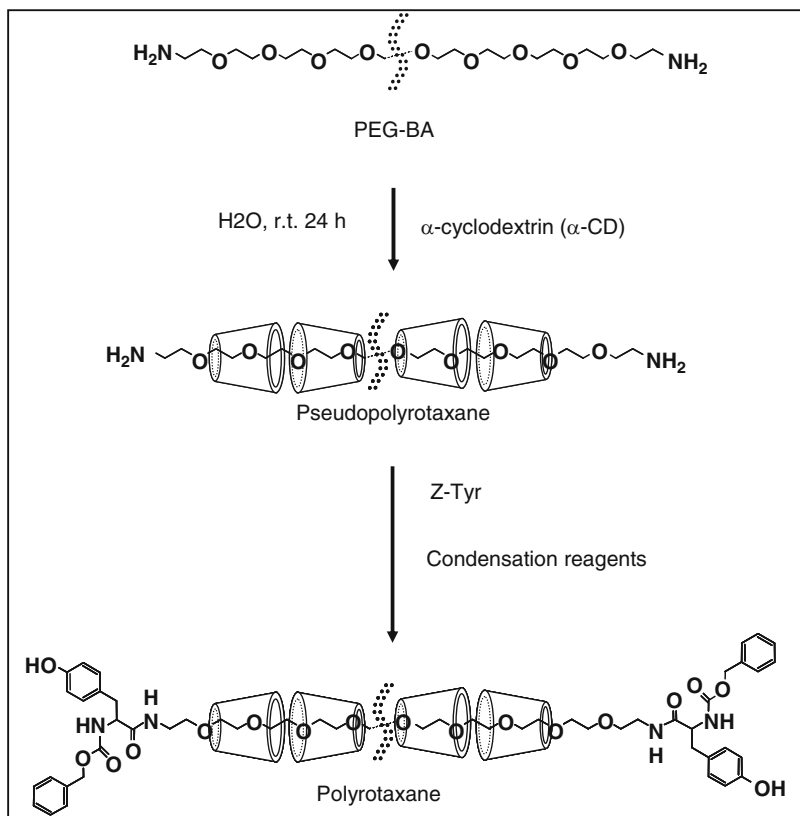
Fig. 2 Synthetic scheme of polyrotaxanes, in which α-CDs are threaded onto a PEG chain capped with Z-L-Tyr

molecules in polyrotaxanes for improving water-solubility and/or for functionalizing by conjugation of biologically-active agents.

Basically, the preparation of polyrotaxanes for biological applications consists of the following two steps: the preparation of a pseudopolyrotaxane by mixing α-CD and PEG-bis(amine) (PEG-BA) in water, and a subsequent capping reaction with amino acid derivatives such as *N*-benzyloxycarbonyl-L-tyrosine (Z-Tyr) (Fig. 2). In the first step, of course, pseudopolyrotaxanes consisting of α-CD and PEG–BA are commonly prepared according to the method reported by Harada and his coworkers as mentioned above. In the second step, Z-Tyr is allowed to react with the terminal amino groups of PEG–BA in pseudopolyrotaxanes by using a variety of suitable condensing agents in DMF or MeOH. When biologically labile linkages such as disulfide bond are introduced into the polyrotaxane, an SS-introduced PEG–BA is employed in place of PEG–BA mentioned in the above protocol.

Purification of the polyrotaxanes is one of the important aspects in preparing biomaterials. In the course of the polyrotaxane preparations mentioned above,

contamination from unthreaded CD and other chemicals is highly problematic and is to be completely removed. Usually, purification of polyrotaxanes by reprecipitation and dialysis in DMSO and water is very promising in removing these undesirable contaminants. Also, GPC measurements in DMSO or in suitable aqueous solutions are helpful to verify the purification of polyrotaxanes. Finally, chemical composition such as the number of threading CD molecules in the obtained polyrotaxane is calculated from the ratio of peak integrations for both C(1) protons in α-CD around 4.8 ppm and methylene protons in PEG around 3.5 ppm in the NMR spectrum measured in $D_2O/NaOD$, as shown later (Fig. 14).

Water solubility of polyrotaxanes is a critical issue when considering their medical and pharmaceutical applications, such as drug delivery. In general, polyrotaxanes prepared following the above-mentioned methods are poorly soluble in water, illustrated by the fact that the insolubility of pseudopolyrotaxanes in water enabled their isolation with ease. In order to endow intact polyrotaxanes with water solubility, a variation of the chemical modifications which have been previously reported for CD chemistry [10] is applicable. In particular, charged functional groups such as amino and carboxyl groups can be introduced at the hydroxyl groups of CDs through suitable spacers, since such chemical modifications are useful not only for improving water solubility but also for further functionalizing polyrotaxanes with biologically-active moieties in the following step. For the introduction of carboxyl groups, CD-containing polyrotaxanes are allowed to react with dicarboxylic acid anhydrides such as succinic anhydride in pyridine. A variety of biologically active agents can be introduced at these groups in the polyrotaxanes via condensation reactions. The dialysis against water, GPC and NMR measurements in water are conventional steps to ascertain purification and chemical compositions. These protocols are depicted in Fig. 3.

3 Enhancing Multivalent Ligand–Receptor Interactions Using Polyrotaxanes

Control of the binding of biologically active agents or ligands to receptor sites of proteins on the plasma membranes of cells is a crucial factor for modulating receptor-mediated cellular metabolism as well as endocytosis for drug delivery. One of the important aspects in this event is how effectively and specifically the binding on membrane proteins using very low quantities of the agents or ligands can be achieved. In this perspective, a "multivalent interaction" using a functional polymer has been proposed and extensively studied over the last decades [11]. The term of multivalency is defined as a way to bind simultaneously multiple copies of ligands with receptor sites of proteins. This approach is believed to be promising for enhancing the binding constant of ligand–receptor interaction, and is expected to exploit significant improvements of such applications as targeting drugs, drug-mediated drug delivery and tissue regenerations (Fig. 4).
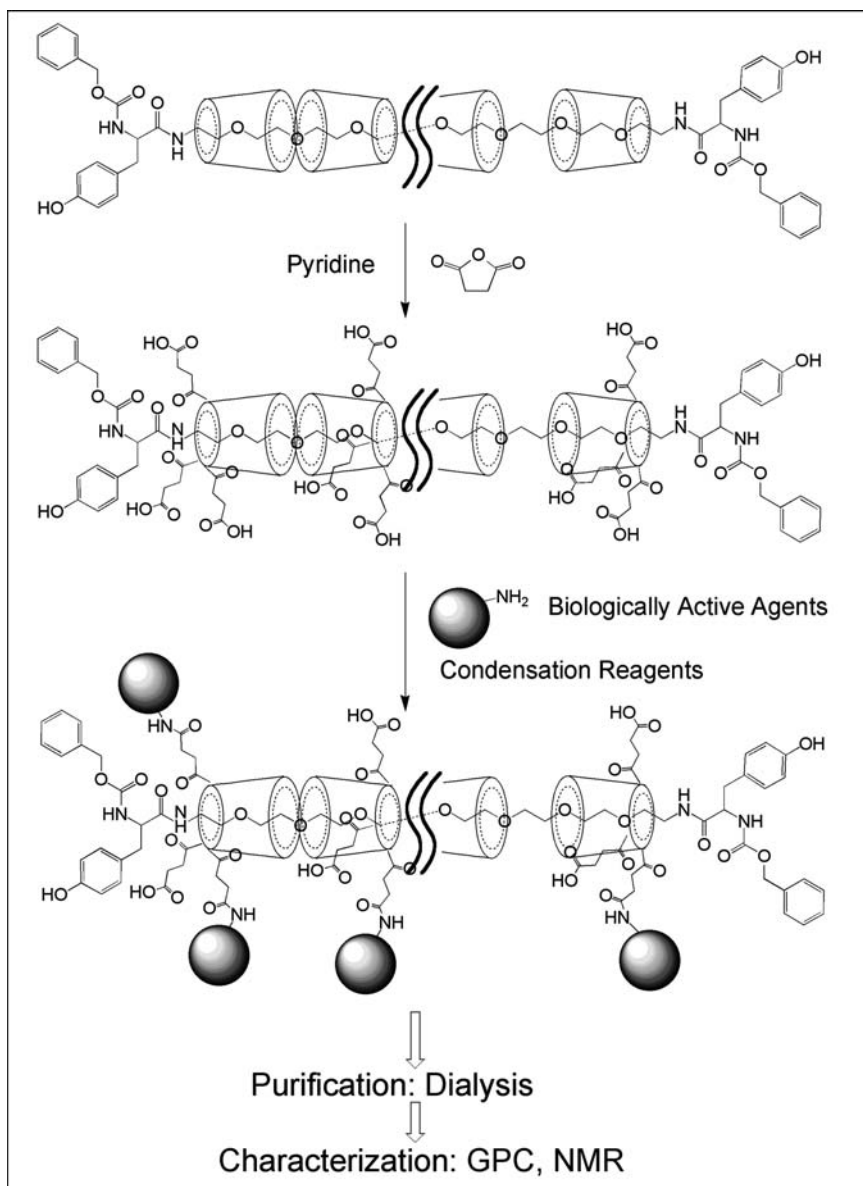
Fig. 3 Synthetic scheme of synthesis of functional polyrotaxanes, in which carboxyl groups were introduced into hydroxyl groups in CDs

A variety of functional polymers has been designed and demonstrated to be a tool of multivalent ligand-immobilized polymers. However, the binding constant using such polymers was not as enhanced as expected. Such unsatisfying results using a functional polymer were mainly attributed to a spatial mismatch between the
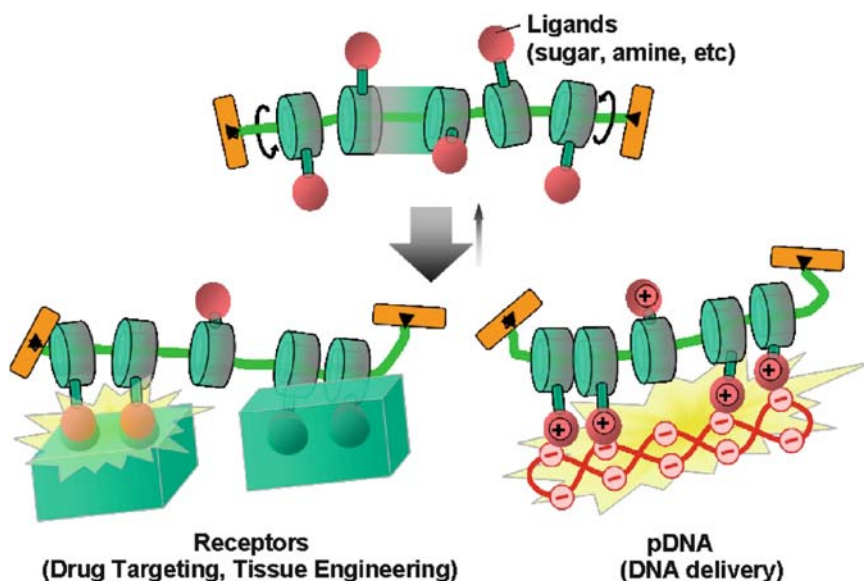
Fig. 4 Mobile cyclic compounds enhance molecular recognition. Cyclic compounds can rotate and/or slide along a polymeric chain in the structure of polyrotaxanes, and the mobility of ligands linked by the cyclic compounds play a key role in enhancing multivalent interaction with biomacromolecules. This concept can be used in sugar recognition and plasmid DNA polyplex formation [7]

ligand–polymers and receptor sites of proteins. Increasing the number of ligands in the polymer eventually causes an excessively large density of ligands, and this excess density is thermodynamically unfavorable to multivalent interactions between the ligands and receptors [12, 13].

From these perspectives, we tried to enhance the multivalent interactions using polyrotaxanes. As mentioned above, the most striking features observed in polyrotaxanes is the freely mobile nature of cyclic compounds threaded onto a linear polymeric chain capped with bulky end-groups. Thus, we believe that polyrotaxanes are advantageous in deriving thermodynamic benefits for enhancing multivalent interaction with biological systems. Freely mobile ligands conjugated to the cyclic compounds in polyrotaxanes would effectively bind to receptor proteins in a multivalent manner, which is based on the enthalpic gain due to enhanced opportunity of the binding for increasing internal energy of the bond molecules via their excellent mobility close to low molecular-weight compounds (Fig. **5 a,**ba). Although the multivalent event is entropically unfavorable, the enthalpic gain would overcompensate it in comparison with conventional ligand–polymer conjugates (Fig. **5 a,**bb).

In order to prove our hypothesis, we examined the interaction of ligand–immobilized polyrotaxanes with receptor proteins [14–17]. For instance, we studied the multivalent interaction of saccharide–conjugated polyrotaxanes with a lectin, a model receptor protein. A series of the maltose–conjugated polyrotaxanes with
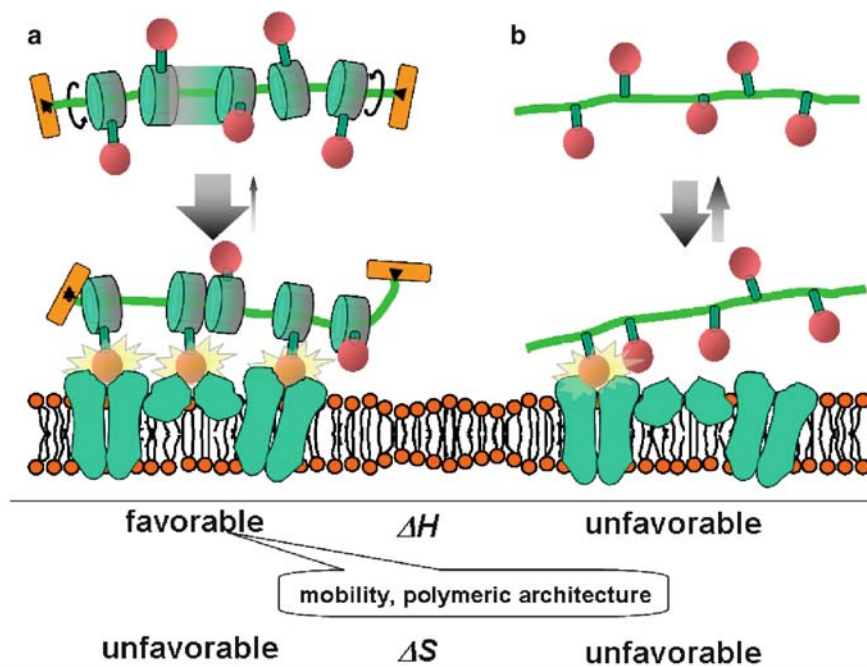
Fig. 5 a,b The effects of the mobile motion of the cyclic compounds in polyrotaxanes on binding receptor proteins in a multivalent manner: Image of binding/dissociating equilibrium **a** between a ligand–polyrotaxane conjugate and receptor sites, and **b** between a ligand–immobilized-polymer and receptors [7]

different numbers of threading α-CD molecules (50, 85, and 120) was prepared from an inclusion complex consisting of α-CD and an α,ω-diamino-PEG with an average molecular weight of 20,000. Here, approximately 220 molecules of α-CD can be theoretically threaded onto this PEG chain, assuming that two repeating units of ethylene glycols are included into the cavity of an α-CD molecule. At first, polyrotaxanes with different number of threading α-CDs were prepared by capping both amino groups in the inclusion complex with Z-protected L-tyrosine in the presence of benzotriazol-1-yloxytris(dimethylamino)phosphonium hexafluorophospate (BOP reagent), 1-hydroxybenzotriazole (HOBt), and N,N-diisopropylethylamine (DIEA) in DMSO/DMF, and were then allowed to react with succinic anhydride, resulting in carboxypropanoyl-modified polyrotaxanes (C-PRxs). Then, β-maltosylamine was conjugated with the carboxyl groups of C-PRxs in the presence of BOP reagent, HOBt, and DIEA. In these polyrotaxanes, the number of maltose groups conjugated to α-CD molecules was varied to some extent.[1]

---

[1] The number of maltose groups was not determined exactly due to the lack of attention to some issues about the purification and assignment.
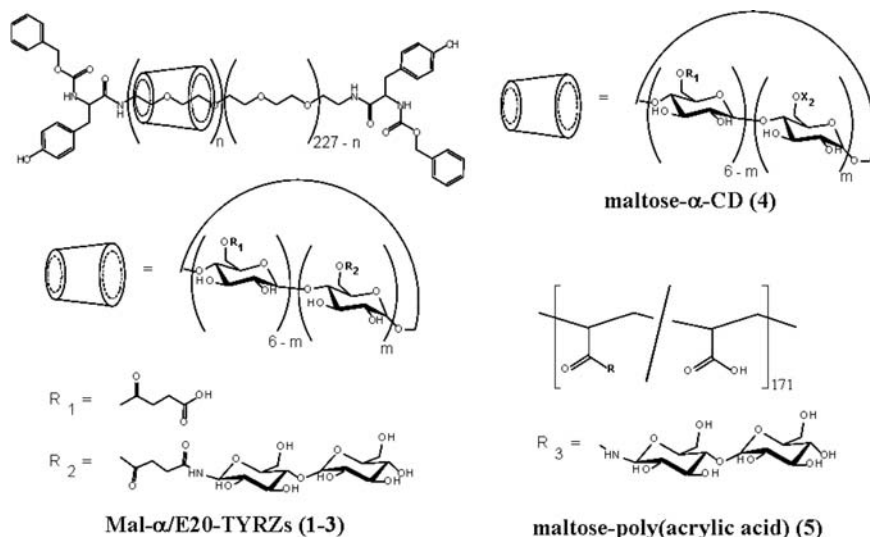
Fig. 6 Chemical structure of maltose–polyrotaxane conjugates consisting of α-CDs, PEG, benzyloxycarbonyl–tyrosine and maltose (Mal-α/E20-TYRZs, **1–3**), maltose-α-CD (**4**), and maltose-poly(acrylic acid) (**5**) conjugates [14]

The interaction of maltose–conjugated polyrotaxanes with their receptor proteins was evaluated by estimating the inhibitory effect of the polyrotaxanes on Concanavalin A-induced hemagglutination of red blood cells (Fig. 6). The minimum inhibitory concentration (MIC) of the maltose unit was determined as a measure of the relative potency vs the lectin. The maltose–conjugated polyrotaxanes were found to exhibit a much stronger inhibitory effect than maltose itself, up to 3,000 times larger. We also found that maltose-conjugated poly(acrylic acid)s have a much smaller inhibitory effect than the polyrotaxane conjugates. These results highlight the remarkable effect of polyrotaxanes on ligand–receptor multivalent interactions.

These results suggest the importance of structural aspects of polyrotaxanes, such as the mobility of α-CD molecules along the PEG chain including sliding or rotational motion, play a crucial role in binding of Con A. Indeed, we examined NMR measurements of the spin-lattice relaxation time (T_1) and the spin-spin relaxation time (T_2) for C(1) protons of α-CD, maltosyl C(1) and PEG methylene protons in maltose-polyrotaxane conjugates, which reveal that the mobility of α-CD in the polyrotaxane governs the molecular motion of maltosyl groups in α-CD molecules in polyrotaxane.

It is worth mentioning that the inhibitory effect of maltose-polyrotaxane conjugates on Con A-induced hemagglutination was found to be closely related to the T_2 values of maltosyl groups (Fig. 7). The T_2 value of maltosyl C(1) proton in the polyrotaxane exhibiting the greatest potency was almost the same as that in maltose–conjugated α-CD. This finding strongly supports our suggestion that the high mobility of maltose ligands on α-CD threaded onto the PEG chain contributes significantly to enhancing the multivalent binding with Con A. The T_2 of methylene
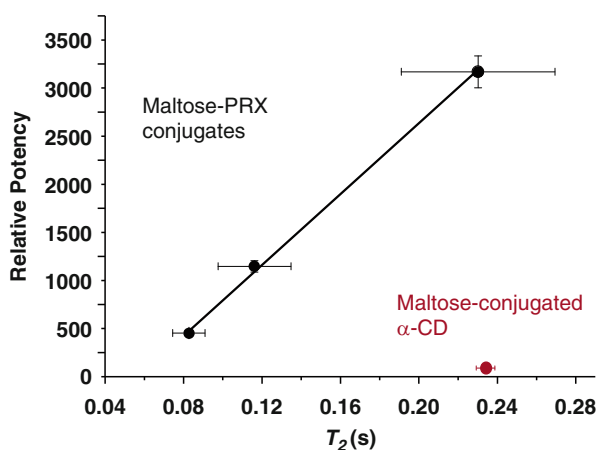
Fig. 7 Relationship between the T_2 value of maltosyl C(1) protons in the polyrotaxane and the relative potency of Con-A-induced hemagglutination inhibition based on the MIC of the maltose unit

protons in the PEG chain tends to become longer with a decrease of the number of α-CD molecules in polyrotaxanes, suggesting that the PEG chain is more flexible in the regions where their ethylene glycol units are exposed to the aqueous medium.

These findings suggest that the mechanically threaded structure of polyrotaxanes with controlled number of threading α-CD molecules can have favorable thermodynamic effects on multivalent interactions. Finally, we have established the concept that the combination of multiple copies of ligands and their supramolecular mobility along the mechanically threaded polyrotaxane structure should contribute to the novel design of polymeric architectures aiming at enhanced multivalent interactions.

Alternatively, Stoddart and his coworkers prepared water-soluble pseudopolyrotaxanes consisting of lactose-appended α-/β-CDs threaded onto hydrophobic polymers such as poly(tetrahydro)pyrane and poly(propylene)glycol, respectively [18], and subsequently examined the binding of these self-assembled pseudopolyrotaxanes with lectins [19]. In their studies, they demonstrated great enhancement on multivalent interaction between lactose and lectin by using the lactose–conjugated pseudopolyrotaxanes, and suggested a flexible and dynamic ligand, including highly mobile ligands as a result of the CD rotating about the polymer chain, creating a new dimension for the study of protein–carbohydrate interactions.

4 Inhibitory Effect of Ligand–Conjugated Polyrotaxanes on Intestinal Transports

One of the possible applications directly related to multivalent ligand–receptor interactions will be the design of polymeric inhibitors which specifically bind receptors existing on cellular membranes to inhibit the uptake of biological substrates via the receptors. For example, there are many kinds of intestinal membrane transporters for

the specific uptake of digested food (proteins and carbohydrates) as well as drugs such as antibiotics. The restriction of these uptakes is strongly required for patients suffering from chronic renal diseases. In this sense, it is useful, for improving their quality of life, to achieve temporal inhibition of the uptake using an inhibitor. In particular, we note that such an inhibitor should be specifically recognized by a transporter without being absorbed to preclude kidney damage. From these points of view, it is obvious that ligand–conjugated polyrotaxane can be advantageous as a multivalent ligand–conjugated polymer.

First we prepared dipeptide–conjugated polyrotaxanes and studied their inhibitory effect on digested peptide uptake by intestinal human peptide transporter (hPEPT1) [20]. Here, Val–Lys as a dipeptide was conjugated to α-CD threaded onto a PEG 4,000 in polyrotaxanes, and we examined the inhibitory effect of the polyrotaxanes on the uptake of a model dipeptide via hPEPT1 using hPEPT1-expressing HeLa cells. The uptake of the model dipeptide was significantly inhibited by the polyrotaxanes, and the inhibition was much greater than dipeptide–conjugated reference samples such as dextran and α-CD. Also, we found that the effect of the polyrotaxanes was significantly enhanced by preincubation with hPEPT1-expressing cells (30 min before adding the model dipeptide), although the inhibitory effect of dipeptide–conjugated α-CD on the uptake was reduced by the preincubation. These results suggest that the supramolecular structure of the polyrotaxanes contributes to inhibiting the uptake via hPEPT1 in a multivalent manner. Furthermore, we confirmed that the inhibitory effect is dependent upon the molecular weight of the PEG chain in the polyrotaxanes when the average molecular weight of PEG was changed between 4,000 and 100,000. At the same concentration of dipeptide, the highest molecular weight of PEG (M_n: 100,000) showed the best inhibitory effect. After selecting the optimum molecular weight, dependence of hPEPT1 expression was also examined by changing the amount of the expressed hPEPT1 (10, 20, 60 μg per 15-cm dish). When the amount of expressed hPEPT1 on HeLa cell surface was the highest (60 μg per 15-cm dish), the dipeptide–conjugated polyrotaxane was found to exhibit the greatest inhibitory effect on the uptake of [^{3}H]Gly–Sar. This result suggests that high expression level of hPEPT1 was essential for inducing multivalent interaction [21].

In *vivo* performance of biomaterials after in vitro studies is one of the important steps for proving their applicability. When we applied the dipeptide–conjugated polyrotaxanes to an in *vivo* model using mice, the result was not as striking as expected. We considered this failure is due to insufficient blockage of the binding sites of the hPEPT1 located on the intestinal membrane: it is not so easy to occupy fully all the binding sites of the transporter with dipeptide molecules conjugated to the polyrotaxane. It is also well known that the activity of hPEPT1 is governed by proton concentration at the membrane. In order to maintain the binding with hPEPT1 via the multivalent interaction and then decrease the surrounding proton concentration on the intestinal membrane to complete the inhibition of the uptake, a polyrotaxane conjugated with dipeptide as well as sodium carboxlylate was prepared as a revised sample. This polyrotaxane was found to decrease the pH of the intestinal tract significantly and to cause the inhibition of the dipeptide uptake in mice [21].

Presumably, the polyrotaxane can bind the intestinal membranes via multivalent interaction with hPEPT1 and effectively contribute to decreasing the local pH on the membrane, resulting in a significant inhibition of the uptake in mice. These results clearly indicate the efficacy of the ligand–conjugated polyrotaxanes as an inhibitor in intestinal uptake in *vivo*.

Furthermore, we prepared 2-(N,N-dimethylamino)ethylcarbamoyl (DMAEC)-polyrotaxanes and examined their inhibitory effect on the uptake of cations via carnitine/organic cation transporter, OCTN2, existing on the intestinal membrane and in tissues [22]. The DMAEC-polyrotaxanes were prepared by treating polyrotaxane with carbonyldiimidazole (CDI) in DMSO, followed by condensation with N,N-dimethylethylenediamine. The inhibitory effect was evaluated in terms of the uptake of L-carnitine in OCTN2-transfected HEK293/PDZK1 cells. The DMAEC-polyrotaxanes prepared from a PEG 20,000 were found to inhibit completely the uptake, although DMAEC-CD, the constituent molecule, and the polyrotaxanes with a shorter PEG 4,000 showed far less inhibition (Fig. 8). This result indicates that DMAEC groups along the polyrotaxanes are actually recognized simultaneously with multiple copies of OCTN2 on the cell surfaces, resulting in the complete inhibition of L-carnitine uptake.

Another interesting feature seen in the cationic polyrotaxanes in this study is their very low cytotoxicity. In general, cationic polymers such as polyarylamine (PAAm, Nitoo Boseki Co. Ltd., Japan; -$(CH_2CH(CH_2NH_2))_n$-) have been known to show high cytotoxicity when applied to native tissues and cells, due to nonspecific interaction with plasma proteins, sometimes leading to intracellular
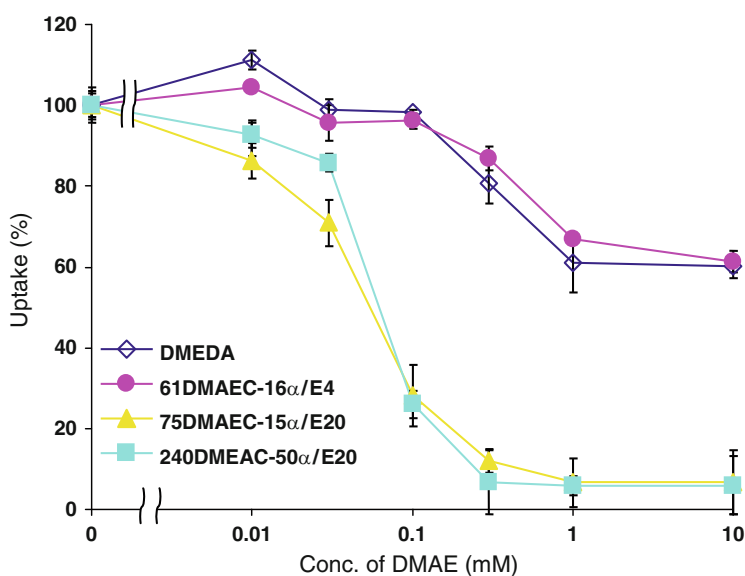

Fig. 8 Inhibitory effects of cationic polyrotaxanes (61DMAEC-16α/E4, 75DMAEC-15α/E20, 240DMAEC-50α/E20) on OCTN$_2$-mediated carnitine uptake in HEK293/PDZK$_1$ cells: HEK293/PDZK$_1$ cells were transiently transfected with YFP-OCTN$_2$, and the uptake of L-[^{3}H]carnitine was measured for 3 min in the presence of each compound [22]
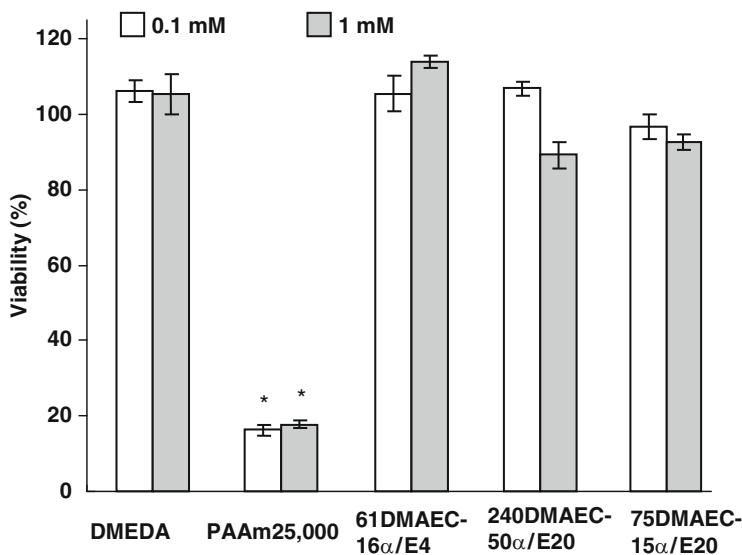
Fig. 9 Viability of HEK293/PDZK$_1$ cells in the presence of cationic polyrotaxanes (61DMAEC-16α/E4, 75DMAEC-15α/E20, 240DMAEC-50α/E20) and of cationic polymer (PAAm25,000) assessed by MTT assay. *Statistically significant difference from the control ($p < 0.05$)

damage, including mitochondrial energy transfer. Indeed, the PAAm inhibited the uptake markedly, but showed very high cytotoxicity in terms of the MTT assay. The MTT assay used here measures the reduction of a tetrazolium compound (MTT) to an insoluble formazan product by the mitochondria of living cells [23]. Thus, this result suggests that the inhibition observed for PAAm is not due to the specific binding with OCTN2 but to a nonspecific binding with plasma proteins, resulting in undesirable cytotoxicity through mitochondrial metabolism. However, our designed DMAEC-polyrotaxanes showed less cytotoxicity in term of the MTT assay, and the cell viability was almost the same as that of a control (Fig. 9). Presumably, the lower density of DMAEC groups along the polyrotaxane structure is considered to prevent intracellular uptake (endocytosis) of the polyrotaxane accompanied by electrostatic interactions with plasma proteins. The mobility as well as low density of DMAEC groups along the polyrotaxane structure appears to prevent cytotoxicity. These results strongly suggest that the cationic polyrotaxanes which we designed are promising candidates for an effective inhibition of cation transport via OCTN2 with less cytotoxicity.

5 Designing Cytocleavable Polyrotaxanes for Intracellular Gene Delivery

In order to expand our concept of "mobile" ligands seen in polyrotaxanes to more practical applications, we have focused on the design of cytocleavable polyrotaxanes as a nonviral gene carrier. Gene delivery using polycations is one of the greatest
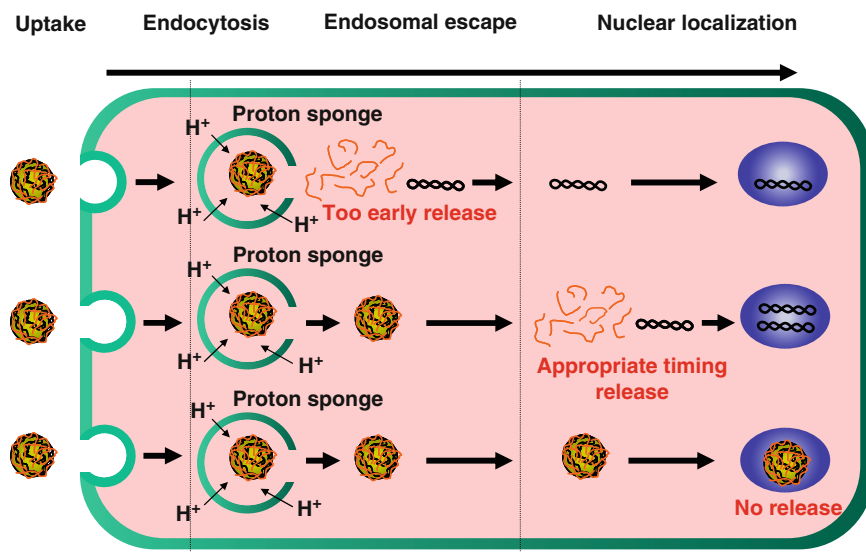
Fig. 10 Images of differences in intracellular trafficking and pDNA release timing

challenges for inventing nonviral gene carrier systems instead of toxic virus-based vector systems [24–26]. Polycations have been widely believed to form a polyion complex (polyplex) with anionic DNA to deliver it to target cells via endocytosis, eventually leading to the nucleus. However, several difficulties have arisen in this strategy: how, when, and where the DNA polyplexes must be dissociated to deliver and release the DNA (Fig. 10), in particular for the polyplex to escape from endosomal/lysosomal digestion to release the DNA into the cytoplasm, and finally to reach the nucleus through the nucleus membrane. The cytotoxicity of polycations has also been seriously pointed out during this research. For instance, high molecular-weight polycations such as polyethyleneimine (PEI) have been studied as nonviral gene vectors that effectively form a polyplex with plasmid DNA (pDNA), whereas low molecular-weight polycations are very advantageous in terms of pDNA release from the polyplex as well as of a low cytotoxicity [27].

In order to solve such a controversy, the introduction of biodegradable moieties into polycations to dissociate the polyplex has been recently proposed elsewhere [28–31]. For example, introducing many disulfide (SS) linkages into the main chain of polycations has been reported as a key for controlling intracellular gene delivery, because the pDNA polyplex is dissociated in the cytoplasm through the cleavage of disulfide linkages. However, excess amount of the disulfide linkers can induce the over stabilization of polyplex. Kissel and his coworkers reported that the transfection activity decreases with an increase in the SS crosslinking degree in a polyplex, due to decreasing the amount of released DNA [32].

From these perspectives, we designed a cytocleavable polyrotaxane that has a necklace-like structure between many α-CDs with attached cationic groups and
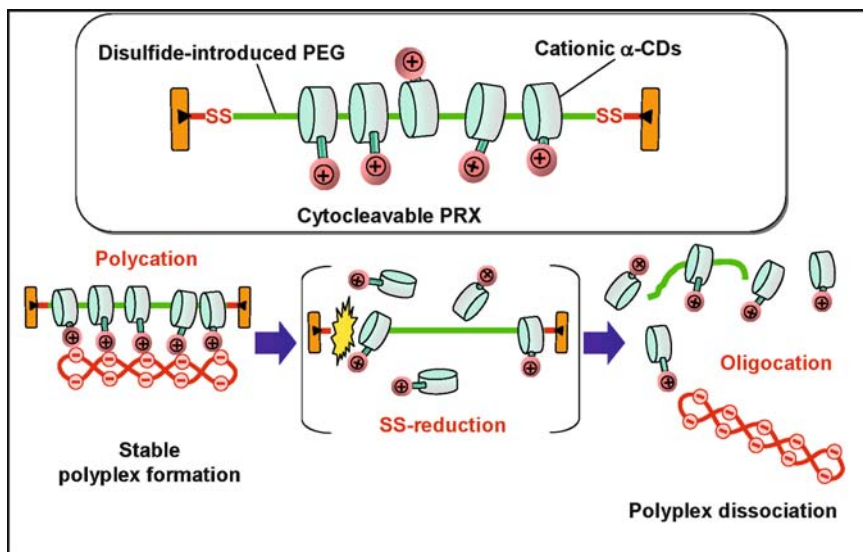
Fig. 11 Polyplex formation and pDNA release accompanied by the supramolecular dissociation of DMAEC-SS-polyrotaxanes

an SS-terminated PEG chain [33, 34]. Here, DMAEC-α-CDs are threaded onto a PEG chain ($M_n = 4,000$) capped with Z-Tyr via SS linkages that exist only at both terminals of the PEG chain (DMAEC-SS-PRX). Also, we expect that the polyrotaxane shows sufficient cleavage of SS linkages under reducible conditions. The SS cleavage will lead to triggering pDNA release via the dissociation of the noncovalent linkages between α-CDs and PEG, looking like a necklace broken into pieces (Fig. 11).

In our design of polyrotaxanes here, the respective numbers of threaded α-CDs and DMAEC groups per polyrotaxane were estimated to be around 23 and 40 for DMAEC-SS-PRx, 30 and 40 for DMAEC-PRx from their ^{1}H-NMR spectra. The complexation of DMAEC-(SS)-PRXs with pDNA was compared with that of a linear PEI with a M_n of 22,000 (LPEI22k) in terms of gel electrophoresis. A band for free pDNA in the electrophoresis was disappeared upon complexation with a smaller quantity of amino groups in the polyplex with the polyrotaxane than with the LPEI.

In vitro pDNA dissociation experiments in the presence of 10 mM dithiothreitol (DTT) as a reducing agent confirmed that pDNA is perfectly released from the DMAEC-SS-PRX polyplex in the presence of a counter polyanion (Dextran sulfate, $M_n = 25,000$). However, the polyplex of DMAEC-PRX, which has no SS linkages, is stable in the same conditions. Since the DMAEC-α-CD release was confirmed in the same reducible condition by GPC, we consider that the SS cleavage under the reducible condition led to the dissociation of the polyplex via PEG dethreading from DMAEC-α-CD cavities, and an interexchange with polyanions caused the pDNA release.

The intracellular trafficking was measured through a quantitative three-dimensional analysis using a confocal laser scanning microscope (CLSM) technique. It is surprising that the DMAEC-SS-PRX polyplex (the N/P ratio was around 5) completely escaped from the endosome and/or the lysosome 90 min after the transfection. We note that ca. 30% of the pDNA cluster was found in the nucleus, as it was clearly shown by the CLSM image. In the case of the LPEI22k polyplex, the pDNA cluster was not located in the nucleus, and ca. 30% of the pDNA was still located in the endosome and/or the lysosome for the same incubation time. Therefore, the high localization of the pDNA cluster in the nucleus is due to rapid endosomal escape of the DMAEC-SS-PRX polyplex.

Furthermore, the DMAEC-SS-PRX polyplex affects the transfection of pDNA using NIH3T3 cells. The transfection of the DMAEC-SS-PRX polyplex is likely to be independent of the N/P ratio, whereas that of the LPEI polyplex is apparently dependent on this ratio. These results suggest that the transfection of the DMAEC-SS-PRX polyplex is independent of the amount of free polycations. It is obvious that the SS cleavage played a key role in the gene expression, since the transfection of the DMAEC-SS-PRX polyplex was much higher than that of the DMAEC-PRX (Fig. 12). Also, we found that the DMAEC-SS-PRX exhibited low cytotoxicity independently of the N/P ratio, whereas the LPEI showed a higher cytotoxicity with an increase in the N/P ratio (Fig. 13). This result indicates that the supramolecular dissociation of the polyrotaxane into the constituent molecules with low molecular weights can contribute to the elimination of the cytotoxicity that is usually observed for high molecular weight polycations.
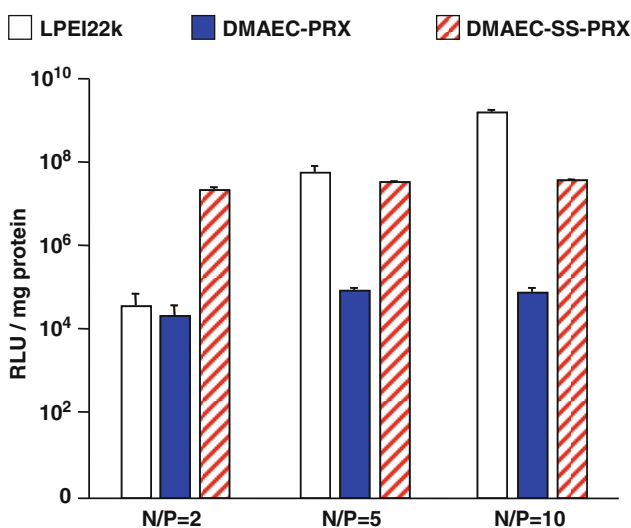

Fig. 12 Transfection activities of the DMAEC-SS-polyrotaxanes, DMAEC-polyrotaxanes, and the LPEI22k at different N/P ratios in NIH/3T3 cells. Luciferase activity in the NIH/3T3 cells was measured at 48 h after the addition of the polyplexes. Results were expressed as relative lights units (RLU) per mg of cell protein
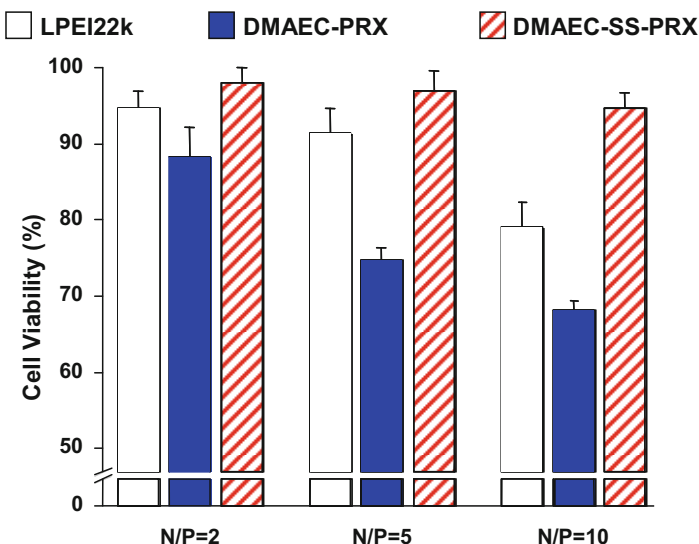
Fig. 13 Cells viability of the DMAEC-SS-polyrotaxanes, DMAEC-polyrotaxanes and LPEI22k at different N/P ratios measured via the MTT assay

The finding as observed above is likely due to the mobile motion of α-CDs in the necklace-like structure of the polyrotaxane. The pDNA dissociation of the polyplex occurred through the SS cleavage in the polyrotaxane and the subsequent interexchange with polyanions. This is presumably due to a reduction on the potency of the multivalent interaction between the cationic polyrotaxane and the anionic pDNA through the supramolecular dissociation. A rapid endosomal escape and pDNA delivery to the nucleus using such cytocleavable polyrotaxanes can be achieved through systematic analyses of polyrotaxane structures.

From this point of view, we further investigated pDNA transfection as well as polyion complexation with pDNA using a variety of DMAEC-SS-PRXs with different numbers of DMAEC groups (the number of α-CDs in the polyrotaxane was fixed to be 18) (Fig. 14) [35]. Positively charged polyplex with pDNA was observed for all the DMAEC-SS-PRXs when the N/P ratio was over 1, although the LPEI22k polyplex showed still negative value. This finding seems to be one of the unique characteristics of the polyrotaxanes related to their structures (Fig. 15). These data suggest that the DMAEC-SS-PRXs can form a polyplex with pDNA in small quantity of cationic groups. Therefore, it is likely that the driving force for complexation of the DMAEC-SS-PRX with the pDNA should be not only an electrostatic interaction but also any other factors.

The ethidium bromide assay revealed that the compaction of pDNA was significantly influenced by the number of DMAEC groups in DMAEC-SS-PRXs: a larger number of DMAEC groups in the DMAEC-SS-PRXs resulted in more tightly packed polyplex formation (Fig. 16). However, the highest transfection of pDNA was observed for a DMAEC-SS-PRX at appropriate number of DMAEC groups
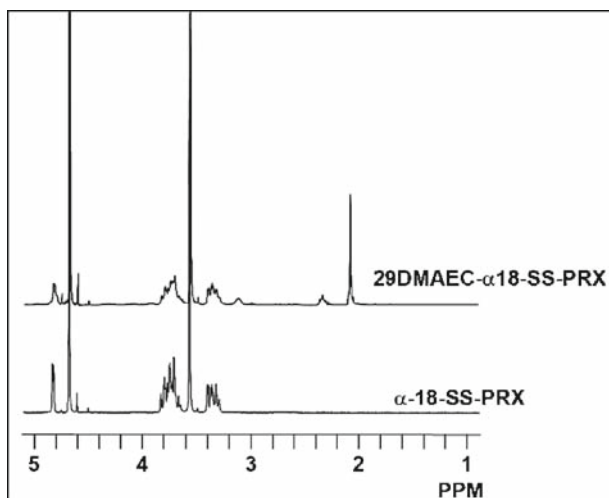
Fig. 14 NMR spectrums of α 18-SS-polyrotaxane and 29DMAEC-α 18-SS-polyrotaxane in NaOD/D$_2$O
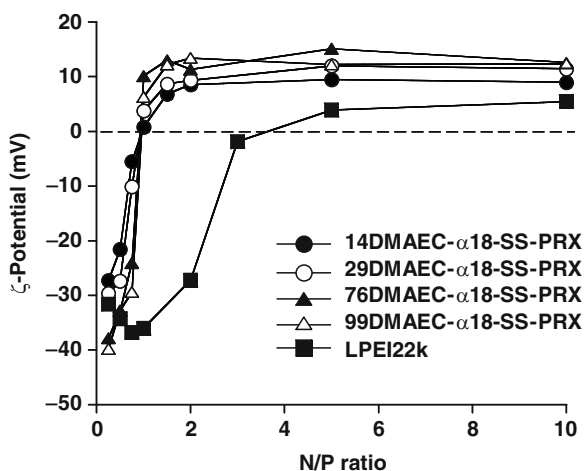

Fig. 15 ζ-Potential of the pDNA polyplexes with DMAEC-α 18-SS-polyrotaxanes for various N/P ratios

(Fig. 17). In particular, from the CLSM analysis it was observed that the DMAEC-SS-PRX with the lowest number of DMAEC groups exhibited a much faster pDNA release in cytoplasm. These results strongly suggest the importance of timing for DNA release under a reducible condition as well as of the stability of the pDNA polyplex before lysosomal and/or endosomal escape in the course of DNA delivery into the nucleus. Finally, we conclude that both polyplex stability and intracellular pDNA release for transfection were achieved by optimizing the number of DMAEC groups in the DMAEC-SS-PRXs [35].
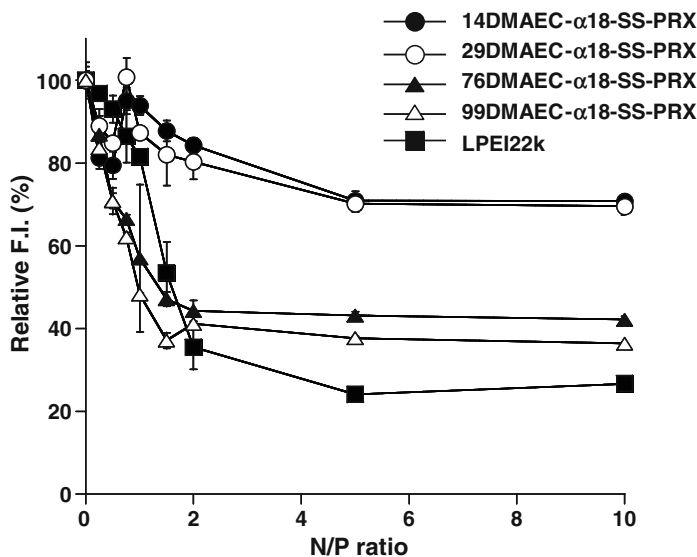
Fig. 16 Ethidium bromide displacement assay of the DMAEC-α 18-SS-polyrotaxanes polyplex and the LPEI22k polyplex. The recorded fluorescent intensities (F.I.) were expressed relative to the fluorescence intensity of the DNA–EtBr solution in the absence of polycation, after subtracting the fluorescence of EtBr in the absence of DNA under the same buffer conditions
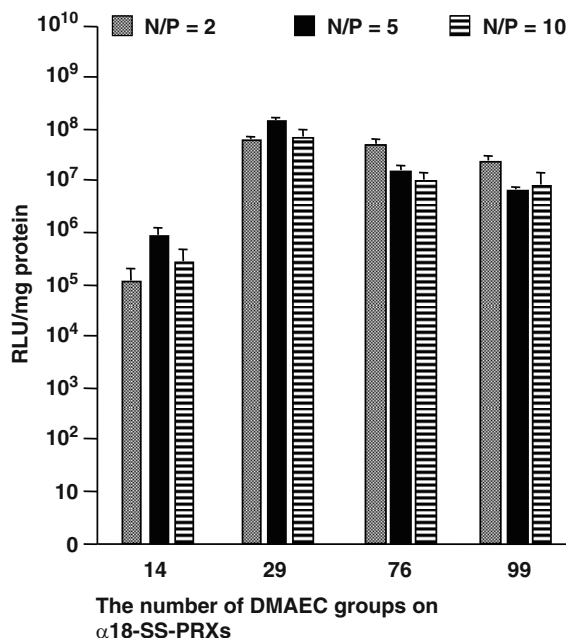

Fig. 17 Transfection activities of the DMAEC-α 18-SS-polyrotaxanes. Luciferase activity in the NIH/3T3 cells was measured 48 h after the addition of polyplexes. Results were expressed as relative light units (RLU) per mg of cell protein

6 Future Aspects

Further studies on the design of polyrotaxanes exploit not only a far-reaching technology of nonviral gene delivery, but also a variety of practical applications for beneficial biomedical devices and tools. Controlling the mobility of cyclic compounds threaded onto a linear polymeric chain and the interlocked structure seen in polyrotaxanes will convincingly lead to a paradigm shift in biomaterials design, and such a supramolecular approach becomes more important not only in biomaterials but also in any other functional materials.

Stimuli-responsive control of the mobility of cyclic compounds along a polymeric chain is distinctive as one of our future works on supramolecular biomaterials. We have already demonstrated the pH-responsive control of the α-CD mobility along a PEI–PEG–PEI triblock-copolymer capped with bulky end-groups [36–38]. The majority of α-CDs were found to be located at the center-block (PEG) in the copolymer in acidic conditions, although they were freely mobile along the copolymer in basic environment. Not only the location but also the mobility of α-CDs could be controlled by a pH change within a physiological range of pH 5–8. Such a control of the mobility of ligands along the polymeric chain can lead to either modulate the K value in the interaction with receptor proteins, or to control the fluidity (clustering) of receptor proteins on plasma membranes. This method can exploit the extracellular modulation of cytoplasmic metabolism at target cells and/or into tissues.

Another important aspect of the design of polyrotaxanes as biomaterials will be to create two- or three-dimensional architectures for cellular and tissue modulation. Regarding this issue, we are now preparing polyrotaxane surfaces which exhibit the mobility of CDs along a linear polymeric chain fixed both terminals to a solid substrate such as Si and/or Au. We strongly expect this unique surface to enhance specific binding with certain proteins and cells through a multivalent ligand–receptor interaction as well as to prevent nonspecific interaction with
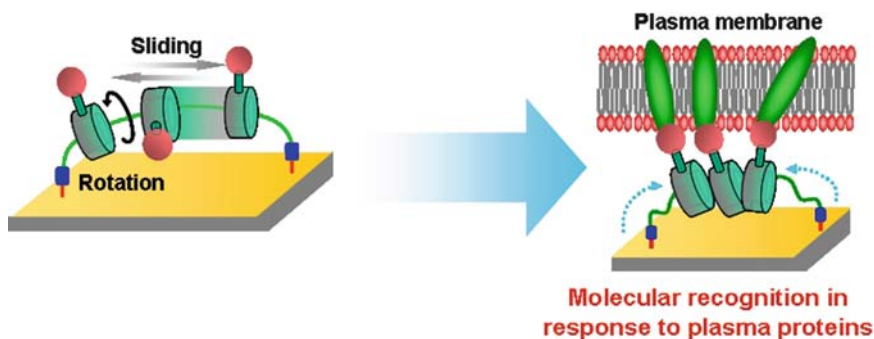

Fig. 18 Modulation of cellular metabolism and tissues via a multivalent binding of plasma membrane proteins with ligand conjugated polyrotaxanes immobilized on solid substrates at the terminal groups

biological molecules such as proteins, as illustrated in Fig. 18. In such a case, any reactive groups toward the Au surface, such as thiol, are introduced into the end-capping molecule of Z-Tyr, prior to the capping reaction of the pseudopolyrotaxanes.

7 Conclusions

Our recent studies on polyrotaxanes as biomaterials have been summarized in this chapter. The mobility of cyclic compounds along a linear polymeric chain is one of the fascinating characteristics seen in polyrotaxanes, and we have clarified that a modulating multivalent interaction with biological systems is strongly related to this unique feature. Another important issue regarding polyrotaxanes is the easiness in dissociating the supramolecular structures into pieces when cleaving one of the bulky end-groups at the terminals. This allows us to modulate the binding constant with biological systems, and is actually useful when designing cytocleavable polyrotaxanes as nonviral DNA vectors.

References

 1. Wenz G, Han BH, Muller A (2006) Chem Rev 106:782–817
 2. Ogata N, Sanui K, Wada J (1976) J Polym Sci Polym Lett Ed 14:459–462
 3. Harada A, Kamachi M (1990) Macromolecules 23:2821–2823 and references therein
 4. Wenz G, Keller B (1992) Angew Chem Int Ed 31:197–199
 5. Harada A, Li J, Kamachi M (1992) Nature 356:325–327
 6. Ooya T, Mori H, Terano M, Yui N (1995) Macromol Rapid Commun 16:259–263
 7. Yui N, Ooya T (2006) Chem Eur J 12:6730–6737
 8. Wenz G (1994) Angew Chem Int Ed 33:803–822
 9. Loethen S, Kim JM, Thompson DH (2007) Polym Rev 47:383–418
10. Khan AR, Forgo P, Stine KJ, D'Souza VT (1998) Chem Rev 98:1977–1996
11. Mammen M, Choi SK, Whitesides GM (1998) Angew Chem Int Ed 37:2754–2794
12. Cairo CW, Gestwicki JE, Kanai M, Kiessling LL (2002) J Am Chem Soc 124:1615–1619
13. Gestwicki JE, Cairo CW, Strong LE, Oetjen KA, Kiessling LL (2002) J Am Chem Soc 124:14922–14933
14. Ooya T, Eguchi M, Yui N (2003) J Am Chem Soc 125:13016–13017

15. Ooya T, Utsunomiya H, Eguchi M, Yui N (2005) Bioconjugate Chem 16:62–69
16. Hirose H, Sano H, Mizutani G, Eguchi M, Ooya T, Yui N (2004) Langmuir 20:2852–2854
17. Hirose H, Sano H, Mizutani G, Eguchi M, Ooya T, Yui N (2006) Polym J 38:1093–1097
18. Nelson A, Stoddart JF (2003) Org Lett 5:3783–3786
19. Nelson A, Belitsky JM, Vidal S, Joiner CS, Baum LG, Stoddart JF (2004) J Am Chem Soc 126:11914–11922
20. Yui N, Ooya T, Kawashima T, Saito Y, Tamai I, Sai Y, Tsuji A (2002) Bioconjugate Chem 13:582–587
21. Eguchi M (2003) Dissertation, Japan Advanced Institute of Science and Technology, Tokyo
22. Utsunomiya H, Katoono R, Yui N, Sugiura T, Kubo Y, Kato Y, Tsuji A (2008) Macromol Biosci 8:655–669
23. Mosmann T (1983) J Immunol Methods 65:55–63
24. Wolff JA (2002) Nat Biotechnol 20:768–769
25. Nori A, Kopecek J (2005) Adv Drug Deliv Rev 57:609–636
26. Nishiyama N, Iriyama A, Jang W, Miyata K, Itaka K, Inoue Y, Takahashi H, Yanagi Y, Tamaki Y, Koyama H, Kataoka K (2005) Nat Mater 4:934–941
27. Kunath K, von Harpe A, Fischer D, Petersen H, Bickel U, Voigt K, Kissel T (2003) J Control Release 89:113–125
28. Saito G, Swanson JA, Lee KD (2003) Adv Drug Deliv Rev 55:199–215
29. Gosselin MA, Guo W, Lee RJ (2001) Bioconjugate Chem 12:989–994
30. Miyata K, Kakizawa Y, Nishiyama N, Harada A, Yamasaki Y, Koyama H, Kataoka K (2004) J Am Chem Soc 126:2355–2361
31. Oupicky D, Carlisle RC, Seymour LW (2001) Gene Ther 8:713–724
32. Neu M, Germershaus O, Mao S, Voigt KH, Behe M, Kissel T (2007) J Control Release 118:370–380
33. Ooya T, Choi HS, Yamashita A, Yui N, Sugaya Y, Kano A, Maruyama A, Akita H, Ito R, Kogure K, Harashima H (2006) J Am Chem Soc 128:3852–3853
34. Yamashita A, Yui N, Ooya T, Kano A, Maruyama A, Akita H, Kogure K, Harashima H (2006) Nat Protocols 1:2861–2869
35. Yamashita A, Katoono R, Yui N, Ooya T, Maruyama A, Akita H, Kogure K, Harashima H (2008) J Control Rel 131:137–144
36. Lee SC, Choi HS, Ooya T, Yui N (2004) Macromolecules 37:7464–7468
37. Choi HS, Lee SC, Yamamoto K, Yui N (2005) Macromolecules 38:9878–9881
38. Choi HS, Hirasawa A, Ooya T, Kajihara D, Hohsaka T, Yui N (2006) Chem Phys Chem 7:1671–1673

Cyclodextrin Inclusion Polymers Forming Hydrogels

Jun Li

Abstract This chapter reviews the advances in the developments of supramolecular hydrogels based on the polypseudorotaxanes and polyrotaxanes formed by inclusion complexes of cyclodextrins threading onto polymer chains. Both physical and chemical supramolecular hydrogels of many different types are discussed with respect to their preparation, structure, property, and gelation mechanism. A large number of physical supramolecular hydrogels were formed induced by self-assembly of densely packed cyclodextrin rings threaded on polymer or copolymer chains acting as physical crosslinking points. The thermo-reversible and thixotropic properties of these physical supramolecular hydrogels have inspired their applications as injectable drug delivery systems. Chemical supramolecular hydrogels synthesized from polypseudorotaxanes and polyrotaxanes were based on the chemical crosslinking of either the cyclodextrin molecules or the included polymer chains. The chemical supramolecular hydrogels were often made biodegradable through incorporation of hydrolyzable threading polymers, end caps, or crosslinkers, for their potential applications as biomaterials.

Keywords Biomaterials, Cyclodextrin, Drug delivery, Hydrogel, Inclusion complex, Polyrotaxane, Supramolecule

Contents

J. Li
Division of Bioengineering, Faculty of Engineering, National University of Singapore, 7 Engineering Drive 1, Singapore 117574, Singapore
e-mail: bielj@nus.edu.sg

Institute of Materials Research and Engineering, A*STAR (Agency for Science, Technology and Research), 3 Research Link, Singapore 117602, Singapore

1 Introduction

Hydrogels are three-dimensional crosslinked macromolecular networks formed by hydrophilic polymers swollen in water. The three-dimensional networks can retain large volumes of water in the crosslinked structures. The extent of swelling and the content of water are largely dependant on the hydrophilicity of the polymer chains and the crosslinking density. The crosslinks can be formed by either covalent bonds or physical cohesion forces between the polymer segments such as ionic bonds, hydrogen bonds, van der Waals forces, and hydrophobic interactions [1–4]. Polymeric hydrogels have been of great interest relative to biomaterials applications because of their favorable biocompatibility [5, 6]. High in water content, they are attractive for delivery of delicate bioactive agents such as proteins [2, 7, 8]. For example, chemically crosslinked poly(ethylene oxide) (PEO) hydrogels have been extensively studied for this purpose [9–11].

Cyclodextrins (CDs) are a series of natural cyclic oligosaccharides composed of 6, 7, or 8 D(+)-glucose units linked by α-1,4-linkages, and named α-, β-, or γ-CD, respectively (Fig. 1). The geometry of CDs gives a hydrophobic inner cavity having a depth of ca. 8.0 Å, and an internal diameter of ca. 4.5, 7.0, and 8.5 Å for α-, β-, and γ-CD, respectively [12]. Various molecules fit into the cavity of CDs to form supramolecular inclusion complexes, which have been extensively studied as models for understanding the mechanism of molecular recognition [13–15].

The overwhelming interest on the developments of CD inclusion polymers arose since the discovery of α-CD inclusion complexes with PEO of different molecular weights [16] and the subsequent synthesis of the polyrotaxanes composed of multiple α-CD rings threaded and entrapped on a polymer chain (Fig. 2) [17,18]. So far, a large number of reports have been published on the CD-based polypseudorotaxanes and polyrotaxanes [12, 18–49] and their applications in biomaterials [50–58].

Fig. 1 Structure of α-CD
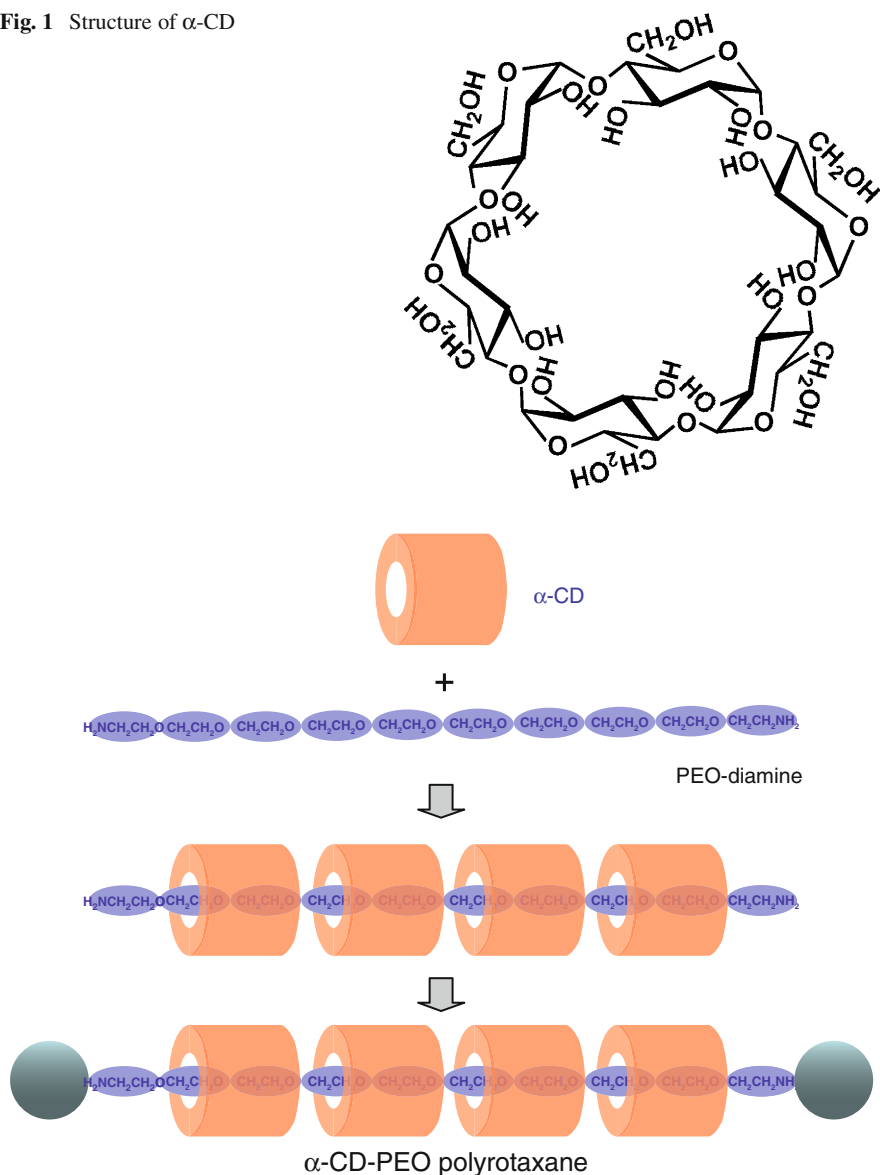
Fig. 2 The synthesis of polyrotaxane composed of multiple α-CD rings threaded and entrapped on a PEO chain [17]

The first report on a CD inclusion polymer forming hydrogels dates back to 1994, which describes the discovery of the sol–gel transition during the inclusion complex formation between α-CD and high molecular weight PEO in aqueous solution [59]. The gelation was induced by the partially formed α-CD–PEO inclusion complexes, which self-assembled into water-insoluble domains acting as a kind of

physical crosslinking. This review will update the developments of hydrogels based on the inclusion complexes, both polypseudorotaxanes and polyrotaxanes, formed between CDs and various polymers and copolymers. There are basically two classes of CD inclusion complex hydrogels: the physical hydrogels formed from polypseudorotaxanes induced by the self-assembly of inclusion complex domains acting as the physical crosslinks and the chemical hydrogels crosslinked through intermolecular covalent bonding either between CD molecules or between included polymers.

There are also physical hydrogels self-assembled from modified CDs in the absence of polymers [60], or physical hydrogels obtained by reversible inclusion compound formation between CD polymers and guest dimmers [61] or guest-containing copolymers [62–64], and between CD dimmers and thermosensitive guest-containing copolymers [65]. Another interesting thermosensitive pseudo-block copolymer system with controllable low critical solution temperature (LCST) based on CD-star polymer and guest-bearing PEO was reported recently [66]. These CD-based systems do not involve the inclusion complexation of polymer chains in CD cavities, and are out of the scope of this review. Readers can refer to the relevant literature for the details.

2   Physical Hydrogels Formed by Polypseudorotaxanes and Polypseudorotaxanes

2.1   *Gelation Induced by Inclusion Complexation Between α-CD and PEO*

2.1.1   Hydrogels of α-CD and PEO Homopolymer

The formation of inclusion complexes between α-CD and PEO of medium or low MW is accompanied by the precipitation of the formed polypseudorotaxanes from the aqueous solutions. The polypseudorotaxane precipitates are crystals that are self-assembled from the inclusion complexes. This phenomenon indicates that the formation of the polypseudorotaxanes altered the water solubility of their components, i.e., α-CD and PEO, which are both very hydrophilic and water-soluble. However, the α-CD–PEO polypseudorotaxanes are less water-soluble.

When high molecular PEO (MW higher than 3,500) is used to form polypseudorotaxanes with α-CD, the PEO chains thread into α-CD from the two ends to form inclusion complexes, which subsequently self-assemble into crystalline and water-insoluble domains, while the middle segments of PEO still remain uncomplexed and hydrophilic. As a result, the polypseudorotaxanes of α-CD and high molecular PEO form hydrogels (Fig. 3) [59]. This is an interesting class of supramolecular hydrogels in which only physical crosslinking is involved. The hydrogels of α-CD and high molecular PEO were further studied in terms of their structures, properties, and applications as an injectable drug delivery system [67]. Table 1 lists the α-CD–PEO
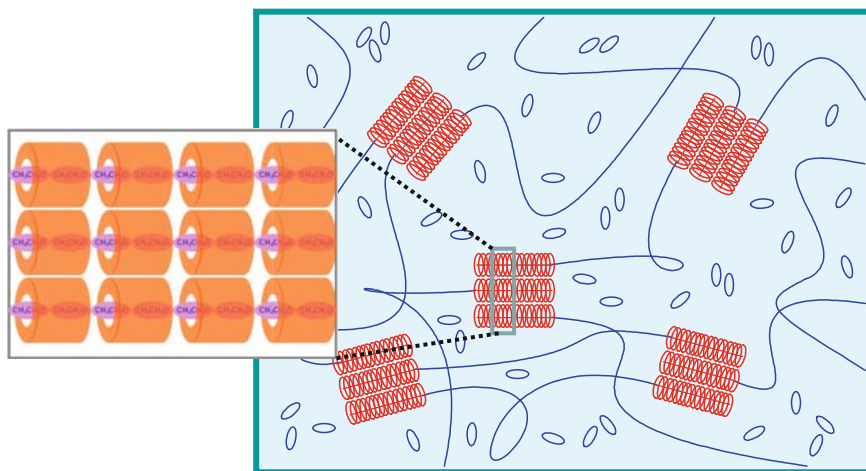
Fig. 3 Hydrogel formed between α-CD and high molecular weight PEO based on the partially formed self-assembled inclusion complex domains as physical crosslinks [59]

Table 1 Preparation of α-CD–PEO hydrogels [67]

α-CD–PEO hydrogel[a]	Average MW of PEO	Gel composition	
		α-CD (g mL^{-1})	PEO (g mL^{-1})
Gel-8K-60	8,000	0.0967	0.133
Gel-10K-60	10,000	0.0967	0.133
Gel-20K-60	20,000	0.0967	0.133
Gel-35K-20	35,000	0.0967	0.044
Gel-35K-40	35,000	0.0967	0.088
Gel-35K-60	35,000	0.0967	0.133
Gel-35K-80	35,000	0.0967	0.177
Gel-35K-100	35,000	0.0967	0.222
Gel-100K-60	100,000	0.0967	0.133

[a]The hydrogels were prepared by mixing 0.3 mL of α-CD aqueous solution (0.145 g mL^{-1}) with 0.15 mL of PEO solution. The first and second numbers denote the number–average MW of PEO and the amount of PEO used in the hydrogel preparation in mg, respectively. For example, Gel-10K-60 means 60 mg of PEO with number–average MW of 10,000 was used

hydrogels studied in that work, including the molecular weights of PEO and the gel compositions. Mixture of the PEO and α-CD solutions became opaque within minutes or hours of contact, depending on the concentrations of PEO and α-CD, as well as on the molecular weight of PEO. It may take even longer until the gel forms. For most compositions, the supramolecular hydrogels turned fluid upon heating at above 70 °C.

The threading of α-CD on the PEO chains and formation of inclusion complexes and their supramolecular self-assembly in the hydrogels were confirmed

with wide-angle X-ray diffraction studies of the hydrogels in comparison with other
inclusion complexes of α-CD with propionic acid and PEO of low molecular weight
(MW 1,000) (Fig. 4) [67]. In Fig. 4a, the pattern of α-CD–propionic acid com-
plex represents a cage-type structure of α-CD inclusion complexes. In Fig. 4b, the
pattern of crystalline α-CD–PEO (MW 1,000) complex with a number of sharp
reflections represents the channel-type structure of necklace-like stoichiometric in-
clusion complex of α-CD and low molecular weight PEO, which is totally different
from that of α-CD–propionic acid complex. In particular, the sharp reflection at
$2\theta = 19.4°$ ($d = 4.57$ Å) is a characteristic peak for the channel-type α-CD inclu-
sion complexes. In Fig. 4c–e, the characteristic peak as well as a similar pattern to
α-CD–PEO (MW 1,000) complex are observed, suggesting the gel system contains
necklace-like inclusion complexes formed by α-CD densely threaded on parts of
the PEO segments, and its self-assembling acts as physical cross-links and provides
the primary driving force for the gelation of the solutions of α-CD and the high
molecular weight PEOs. The patterns in Fig. 4c–e are quite broad as compared to
that of the crystalline stoichiometric α-CD–PEO (MW 1,000) complex. This is in
accordance with the fact that the crystalline domains within the hydrogel are rather
small. The hydrogel contains large amorphous domains of PEO chains besides the
crystalline ones. The amorphous domains are necessary for the hydrogel to retain
large volumes of water in its supramolecular structure.

The gel formation can be confirmed visually [59], or be traced with the viscosity of the PEO/α-CD systems, which increased significantly during the gelation [67]. The gelation kinetics is dependent on the concentrations of the polymer and cyclodextrin, as well as on the molecular weight of the PEO used. Generally, the higher the molecular weight, the slower the gelation process, because the PEO must thread through α-CD at the two ends, and the concentration of the ends becomes lower with increasing molecular weight PEO [59].

2.1.2   Hydrogels of α-CD and PEO Block Copolymers

Since α-CD and high molecular weight PEO can form supramolecular hydrogels where the gelation is induced by inclusion complex domains formed by the partially complexed PEO segments, a block copolymer comprising a flanking PEO block is also possible to form a hydrogel with α-CD. A number of works on supramolecular hydrogel formation between α-CD and triblock or diblock copolymers comprising PEO block and other thermosensitive or biodegradable polymer blocks were reported [68–72].

Although PEO–PPO–PEO triblock copolymers (also known as Pluronics) form hydrogels at high concentrations and elevated temperatures, it was found that α-CD could aid the formation of hydrogels of PEO–PPO–PEO triblock copolymers with 25 wt% or more of PEO segment at much lower copolymer concentrations [68]. The hydrogel formation was traced by the changes in viscosity of the solutions. The viscosity of a solution containing 13 wt% of copolymer $EO_{10}PO_{44}EO_{10}$ and 9.7 wt% of α-CD reached up to 10^4 cP at 22 °C, while that of the same solution without a-CD remained at a level lower than a few hundred cP. The studies also tested the viscosities of the same copolymer $EO_{10}PO_{44}EO_{10}$ solution at 13 wt%, or the same solution with 9.7 wt% of D(+)-glucose at 4 and 22 °C, respectively. The viscosities of the two solutions at both temperatures were found to remain unchanged with time at a low level.

The inclusion complexes formed by α-CD and PEO blocks of Pluronics are thought to aggregate into microcrystals, which act as physical crosslinks and induce formation of a supramolecualr polymer network, consequently resulting in the gelation of the solutions. The micellization of the PPO block is also important in the gelation of the copolymer and α-CD solutions. At the elevated temperatures, the hydrophobic interaction between the PPO segments of Pluronic facilitates the formation of the polymer network. This is why a solution of Pluronic and α-CD could not form hydrogels at 4 °C, at which temperature the interaction between PPO segments of Pluronic is weak and the micelles tend to dissociate. Therefore, the driving force for the gelation of Pluronic and α-CD solutions is a combination of the inclusion complexation between α-CD and PEO blocks and the micellization of the PPO block of Pluronic copolymer.

The inclusion complex formation between PEO blocks of the Pluronic copolymers and α-CD in the hydrogels was confirmed with wide-angle X-ray diffraction studies of the hydrogels [68]. The effect of α-CD to aid the gelation of

PEO–PPO–PEO copolymer aqueous solutions was further evidenced by the phase diagrams of the mixtures of PEO–PPO–PEO copolymer and α-CD aqueous solution [70]. Figure 5 presents the temperature–polymer concentration phase diagrams of PEO–PPO–PEO copolymer $EO_{13}PO_{30}EO_{13}$ aqueous solutions at the absence and presence of α-CD with different α-CD concentrations. The regions marked with gel indicate that the formulations of $EO_{13}PO_{30}EO_{13}$ and α-CD aqueous solutions form a hydrogel, which remains intact when the tube is inverted upside down. The regions marked with sol indicate that the formulations are either a clear or turbid solution, or a mixture containing partially gel and fluid portions, which will flow when the tube is inverted. The region where the pure $EO_{13}PO_{30}EO_{13}$ can form a hydrogel is very small (α-CD 0%), while the concentration must be very high. With increase in α-CD concentration, the gelation regions become larger and larger, and the lowest concentration at which the copolymer can form hydrogel becomes much lower with higher α-CD concentrations. When plotting the lowest gelation concentrations of $EO_{13}PO_{30}EO_{13}$ as function of α-CD concentration at $31\,^{\circ}C$, it was found that, with the increase in α-CD concentration, the lowest copolymer gelation concentration decreased from 50 to about 20%. It is clear that the partially formation of inclusion complexes between the EO blocks of $EO_{13}PO_{30}EO_{13}$ with α-CD largely changed the hydrophobicity of the PEO–PPO–PEO copolymer, and significantly lowered its gelation concentration.

A biodegradable poly(ethylene oxide)-poly[(R)-3-hydroxybutyrate]-poly (ethylene oxide) (PEO–PHB–PEO) triblock copolymer was synthesized [73] and used to form supramolecular hydrogel with α-CD (Fig. 6) [71]. It was found that the preferential inclusion complexation of α-CD with the PEO block together with the hydrophobic interaction between the middle PHB blocks cooperatively result in a self-assembly system that induces a strong macromolecular network. The strong intermolecular hydrophobic interaction between the middle PHB blocks of PEO–PHB–PEO triblock copolymer was proved by their very low critical micellization concentration (cmc) values (Table 2) [74, 75]. Although the two copolymers were water-soluble, they formed micelles in aqueous solution at very low concentrations. The cmc values of PEO–PHB–PEO triblock copolymers were found to be significantly smaller than their counterparts of Pluronic PEO–PPO–PEO or PEO–PLLA–PEO triblock copolymers with similar compositions [71, 74–76].

Despite the formation of micelles, 13 wt% of aqueous solution of both polymers did not form hydrogels. However, aqueous solutions containing 13 wt% of either PEO–PHB–PEO copolymers and 9.7 wt% of α-CD formed hydrogels at room temperature. In other words, α-CD aided the gel formation for PEO–PHB–PEO triblock copolymers at a low copolymer concentration. Here the inclusion complexes formed by α-CD and PEO blocks of PEO–PHB–PEO triblock copolymers are thought to aggregate into microcrystals, which act as physical crosslinks and induce formation of a supramolecular polymer network, consequently resulting in the gelation of the solutions. The micellization of the PHB block is also important in the gelation process. The hydrophobic interactions between the PHB blocks facilitate the formation of the polymer network. Therefore, the gelation of the aqueous solutions of PEO–PHB–PEO triblock copolymers and α-CD is the result of a cooperation of the
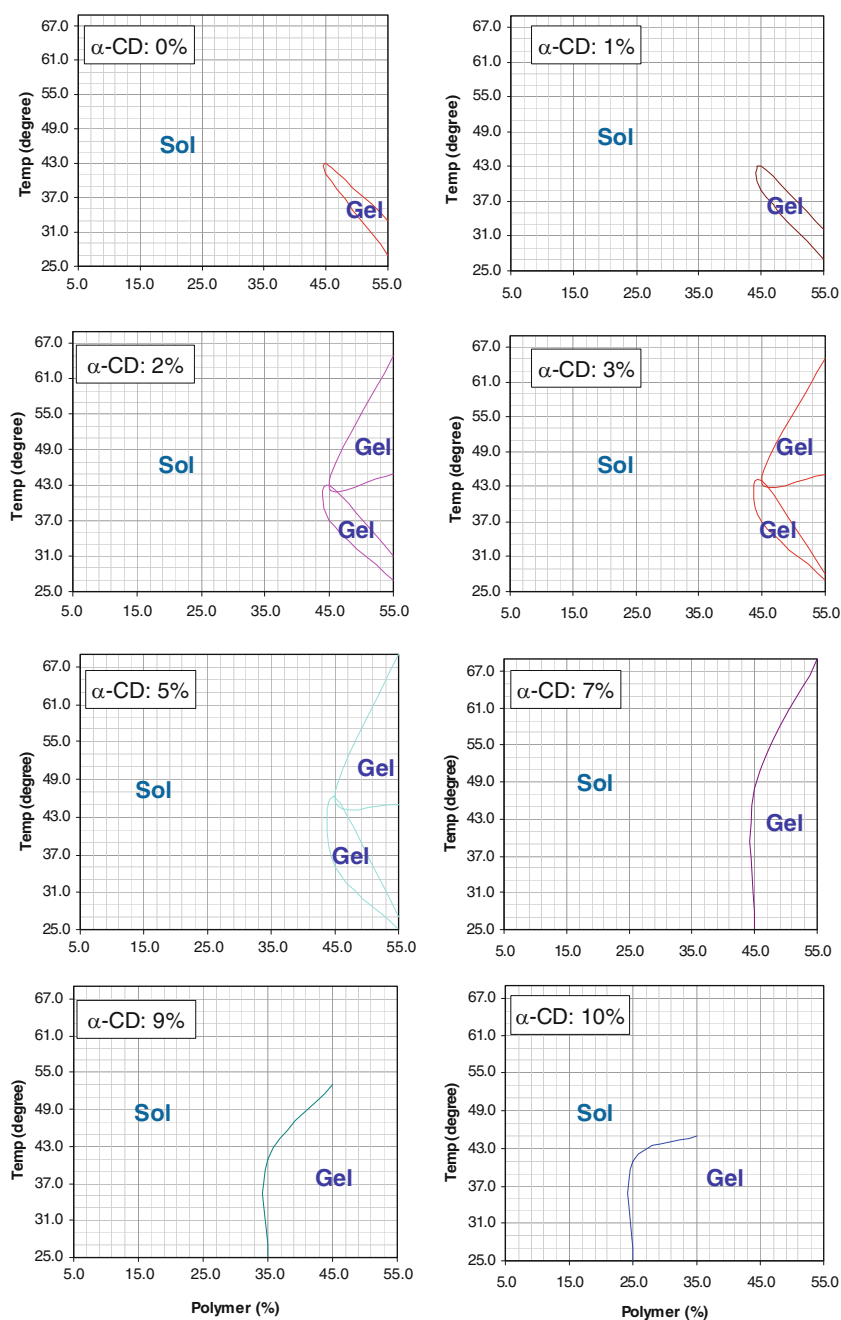
Fig. 5 The temperature–polymer concentration phase diagrams of PEO–PPO–PEO copolymer $EO_{13}PO_{30}EO_{13}$ aqueous solutions at the absence and presence of α-CD with different α-CD concentrations [70]
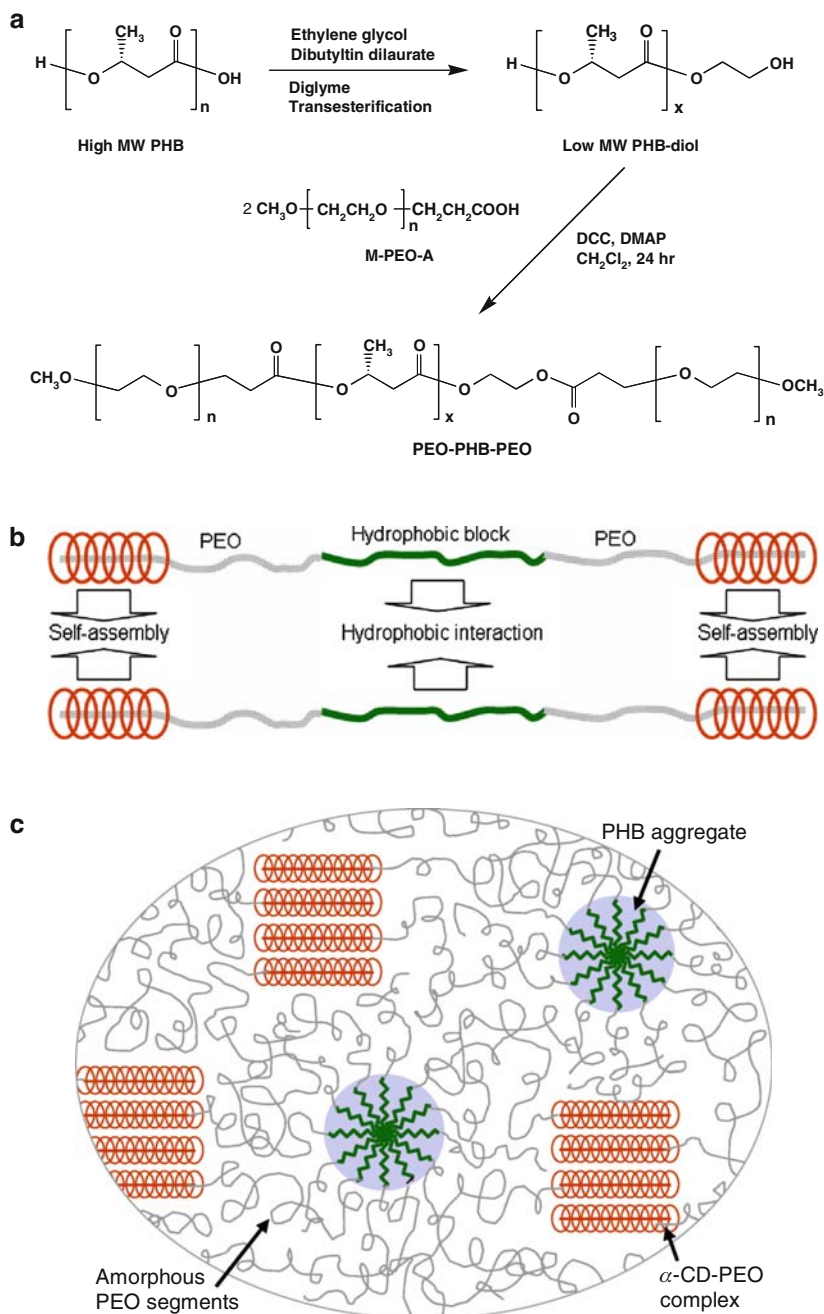
Fig. 6 a–c The synthesis of PEO–PHB–PEO triblock copolymer **a**, and the schematic illustrations of the proposed structures of a-CD–PEO–PHB–PEO inclusion complex **b**, and a-CD–PEO–PHB–PEO supramolecular hydrogel **c** [71]

Table 2 PEO–PHB–PEO triblock copolymers used for preparation of hydrogels with α-CD [71]

Triblock copolymer[a]	M_n	Block length (M_n)		cmc[b] (g L^{-1})
		PEO	PHB	
PEO–PHB–PEO(5000–1750–5000)	11,270	4,830	1,750	5.7×10^{-2}
PEO–PHB–PEO(5000-3140-5000)	12,160	4,830	3,140	2.7×10^{-2}

[a]The numbers in the parentheses show the indicative block length of each block in g mol^{-1}
[b]Critical micellization concentration (cmc) determined by dye absorption experiments for PEO–PHB–PEO copolymers at 23 °C

inclusion complexation between α-CD and PEO blocks and the micellization of the PHB block of the triblock copolymers.

Based on the results of the X-ray diffraction studies, the structure of the α-CDPEO–PHB–PEO supramolecular hydrogels was proposed (Fig. 6c). In the α-CD–PEO–PHB–PEO complexes (Fig. 6b), PEO chains penetrate α-CD rings from both ends, and then form necklace-like inclusion complexes. The molecular weight of each PEO block is ca. 5,000 Da in the supramolecular hydrogels. Only a length of PEO segments of about molecular weight 2,000 Da or less from each end of the copolymers could be included by α-CD rings based on the studies on complex formation between α-CD and PEO–PHB–PEO triblock copolymers with PEO length of 2,000 Da, where only crystalline solid complexes formed [30, 37]. The hypothesis was also supported by the number of α-CD rings threaded on a PEO chain and capped by bulky groups at the two ends, as described in the study on synthesis of α-CD–PEO polyrotaxanes [17]. In the courses of preparation of polyrotaxanes, a maximum average number of 23 α-CD rings, corresponding to a length of PEO molecular weight 2,000 Da, were trapped over a PEO chain, even if the molecular weight of PEO used was more than 3,000 Da. In the cases of PEO–PHB–PEO block copolymers with PEO block length of 5,000 Da, the PEO segments covered by α-CD rings should be shorter than 2,000 Da from each end because the cooperative gelation process may hinder α-CD further threading over the PEO blocks. The partial inclusion complexation of α-CD with PEO block together with the hydrophobic interaction between the middle PHB blocks cooperatively result in a self-assembly system that induces a strong network and gives a novel supramolecular hydrogel.

Another supramolecular hydrogel was formed between α-CD and biodegradable amphiphilic poly(ethylene oxide)-*b*-poly(ε-caprolactone) (PEO–PCL) diblock copolymer [72]. In this study, a PEO–PCL diblock copolymer of molecular weight of 5,000 for PEO and 5,000 for PCL was used. A turbid solution was obtained after dispersing this diblock copolymer into water under sonicating and stirring, and no gelation was observed. However, a viscous mixture was obtained when α-CD aqueous solution was employed instead of the pure water. The viscous mixture could further transfer to homogeneous hydrogel in a few minutes. It was assumed that the gelation is induced by the supramolecular self-assembly of the PEO–PCL diblock polymer chains partially included by α-CD. It was proposed that the PEO block is preferentially complexed by α-CD, while the complexed hydrophobic PCL block forms aggregates due to the hydrophobic interaction.

2.1.3 Hydrogels of α-CD and PEO-Grafted Copolymers

Based on similar principles to the hydrogels formation between α-CD and various block copolymers comprising a PEO block, there were a few reports on hydrogel formation between α-CD and PEO-grafted hydrophilic polymers CD [77–80].

Supramolecular hydrogels were prepared based on the inclusion complexation between PEO-grafted dextrans and α-CD in aqueous media (Fig. 7) [77]. The gel–sol transition was reversible with hysteresis. The transition temperature was controllable by variation in the polymer concentration and the PEO content in the graft copolymers as well as the stoichiometric ratio between the guest and host molecules. The X-ray diffraction data indicated that the hydrogel contains a channel-type crystalline structure, demonstrated by a strong reflection at $2\theta = 20°$ ($d = 4.44$ Å). The authors suggested that the supramolecular hydrogels comprise a mico-phase separated structure consisting of hydrophobic and channel-type crystalline PEO inclusion complex domains and hydrated dextran matrices.

In a similar way, supramolecular hydrogels were prepared on the basis of inclusion complex formation between PEO-grafted chitosans and α-CD [78]. A series of PEO-grafted chitosans were synthesized by coupling reactions between chitosan and monocarboxylated PEO using water-soluble carbodiimide as coupling agent. The PEO side-chains on the chitosan backbones were found to form inclusion complexes with α-CD, resulting in the formation of channel type crystalline micro-domains, which play a role of physical crosslinking for the hydrated chitosan chains. The gelation property was affected by several factors including the PEO content in the polymers, the solution concentration, the mixing ratio of host and guest molecules, temperature, pH, etc. All the hydrogels in acidic conditions exhibited thermo-reversible gel–sol transitions. The authors proposed that the supramolecular hydrogels comprise a phase-separated structure that consists of hydrophobic crystalline inclusion complexes domains formed by the α-CD and the grafted PEO segments, and the hydrated chitosan matrices below the pKa.

α-CD inclusion complex formation of highly densely PEO-grafted polymer brushes and resulting hydrogel formation were reported (Fig. 8) [79]. The polymers grafted with PEO macromonomers were prepared through the "grafting from" approach by atom transfer radical polymerization (ATRP) of poly(ethylene glycol) methyl ether methacrylate, PEOMA, from a well-defined poly(macroinitiator), poly(2-(2-bromoisobutyryloxy)ethyl methacrylate) (PBIEM). The inclusion complexation and hydrogel formation of this type of polymer brush with α-CD were studied. The column-type crystalline structures of the hydrogels were confirmed by XRD measurement. The mechanism for the hydrogel formation was proposed by the authors as follows. The polymer brush PBIEM-g-P(PEOMA) with very higher densely grafted PEO chains formed hydrogels with α-CD due to the density of grafted PEO segments. The PEO segments that located at the outer end of the side chains could be threaded relatively easily and formed column inclusion complex aggregates to give a physical crosslinking point. The formed inclusion complex columns are parallel to the main chain, and the orientation of the inclusion complex columns for the polymer brush may promote the physical crosslinking for the
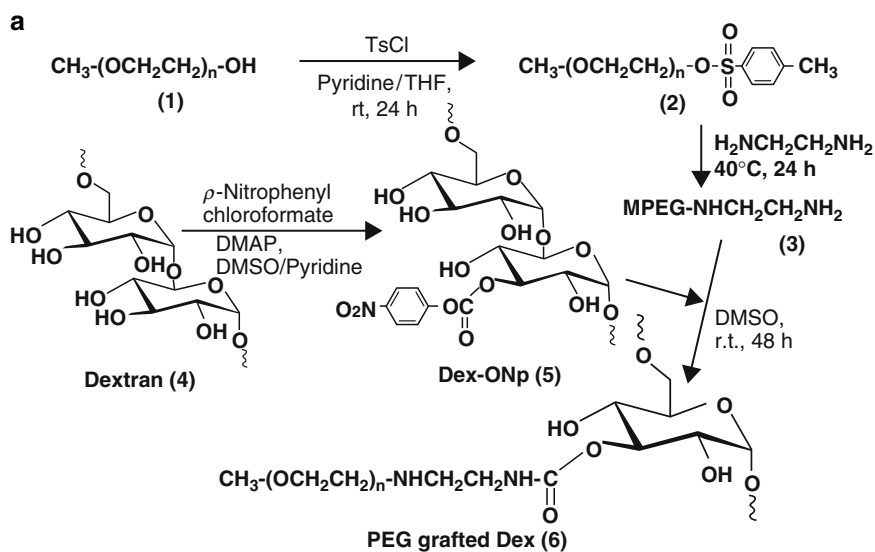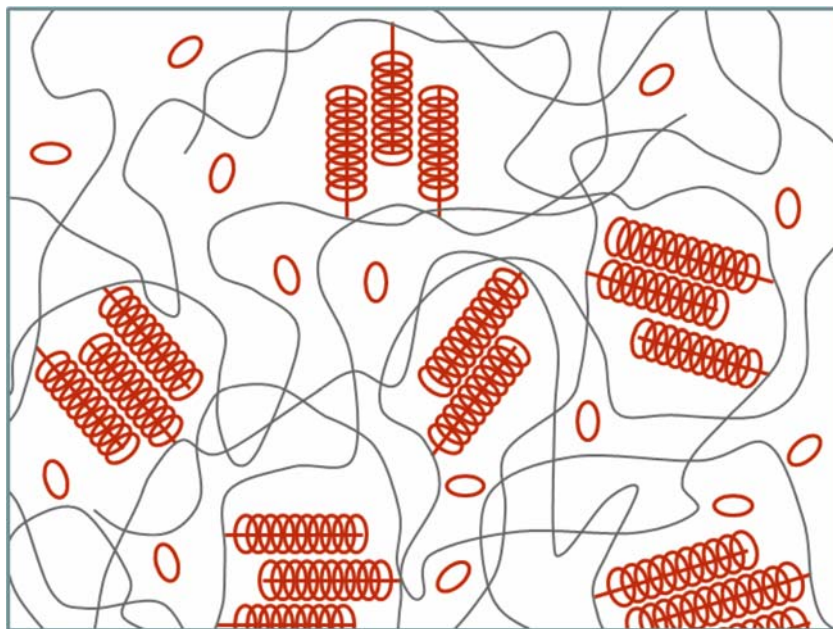
a

b

Fig. 7 The synthesis route for PEO-grafted dextran **a** and the schematic illustration of proposed structure of supramolecular hydrogel by inclusion complexation between PEO-grafted dextran and α-CD **b** [77]
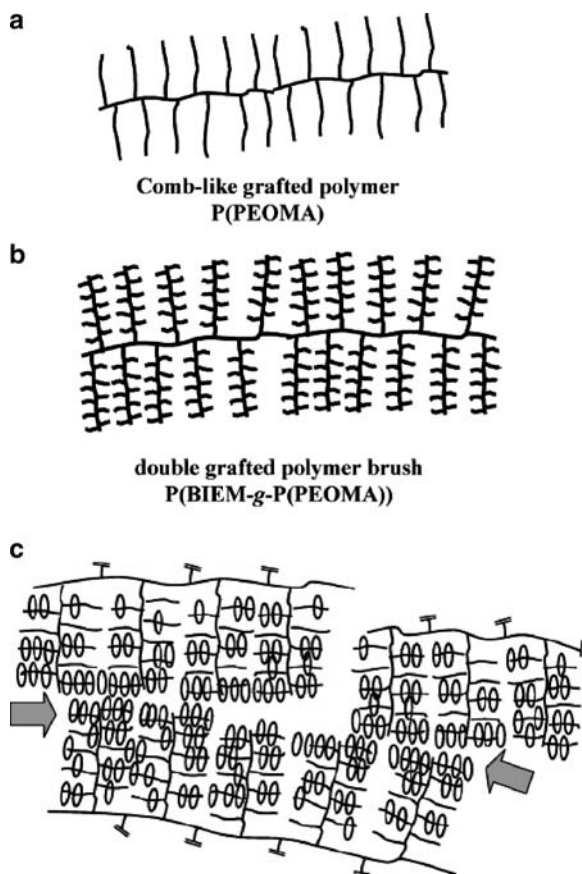
Fig. 8 a–c The schematic illustrations of comb-like PEO-grafted polymer P(PEOMA) **a**, double grafted polymer brush P(BIEM-g-P(PEOMA)) **b**, and structure of hydrogel formed from polymer brush P(BIEM-g-P(PEOMA)) and α-CD **c**. *Arrows* indicate the crosslinking points [79]

gelation (Fig. 8c, arrows). On the other hand, owing to the steric hindrance, the PEO segments attached close to the backbone were very crowded and difficult to be threaded by α-CD. Therefore, some PEO segments were free of complexation and were swollen by water. The combination of above two factors induced formation supramolecular networks of the hydrogels.

The preparation of supramolecular hydrogels formed between α-CD and Pluronic copolymers hybridized with single-walled carbon nanotubes (SWNTs) was reported as well (Fig. 9) [80]. Such hydrogel hybridized with SWNTs was prepared by mixing an aqueous solution of α-CD with an aqueous dispersion of SWNTs stabilized by Pluronic copolymer. In the hydrogels, the SWNTs were well dispersed through interaction of their walls with the PPO blocks of Pluronic copolymer. In other words, the PPO blocks are aggregated to the SWNTs while the PEO blocks look like grafted chains of the SWNTs. Therefore, the
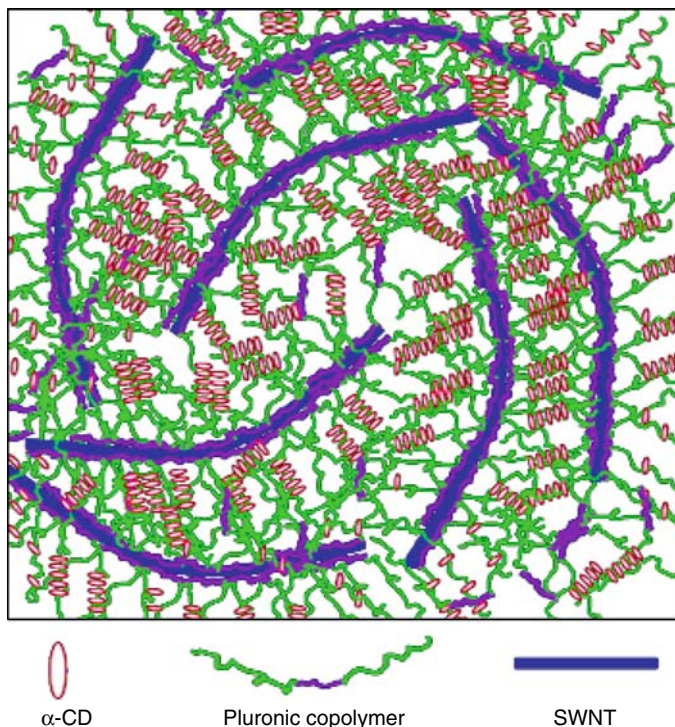
α-CD   Pluronic copolymer   SWNT

Fig. 9 Proposed structure of the supramolecular hydrogel formed between α-CD and Pluronic copolymer in the presence of well-dispersed single-walled carbon nanotubes (SWNTs) [80]

Pluronic copolymer plays dual roles in dispersing SWNTs as well as forming inclusion complexes with α-CD in the hydrogels. Although the introduction of well-dispersed SWNTs changed the gelation mechanism as compared to that of the native hydrogels between Pluronic copolymers and α-CD, the study showed that there was no obvious influence on the structure and morphology. The resultant hybrid hydrogel retained the basic characteristics of the supramolecular hydrogels, especially the shear-thinning and reversible temperature-responsive properties.

2.2 Gelation Induced by Inclusion Complexation Between α-CD and PEI

It was reported that a series of linear polyethylenimines (PEIs) with various molecular weights were synthesized and used to prepare polypseudorotaxanes with α-CD [81]. The PEIs were found to form stable polypseudorotaxanes at suitable pH and/or temperature, because PEIs have ionizable secondary amino groups ($pKa = 8.9$), which play a role of an energy barrier for the polypseudorotaxane formation.

Some of the polypseudorotaxanes with 40–55% of α-CD coverage could form hy-drogels, similar to that of the gelation of the polypseudorotaxanes of α-CD and PEO of high molecular weight where a PEO chain is partially included by α-CD [59].

To decrease the energy barrier for polypseudorotaxane formation, the PEIs and α-CD solutions were mixed at 60 °C. After adjusting the pH to 11.0, the mixture was cooled down gradually. At a certain temperature (the gelation temperature), the so-lutions became turbid and formed a gel-like network. It was found to be interesting that the hydrogels could undergo a transition from gel state to crystalline precipitate state during a repeated heating and cooling processes (Fig. 10) [81].

On slow heating up to the gel-melting temperature, the formed hydrogels be-came soft and transparent. Stirring at this temperature led to further threading of α-CD onto the PEI chains. With a decrease in temperature after this process, the solutions did not form hydrogels but became turbid. Repeated heating and cooling processes resulted in crystalline precipitates after several cycles. It was found that the coverage of the PEI chains by α-CD was significantly increased in the crystalline precipitates [81].
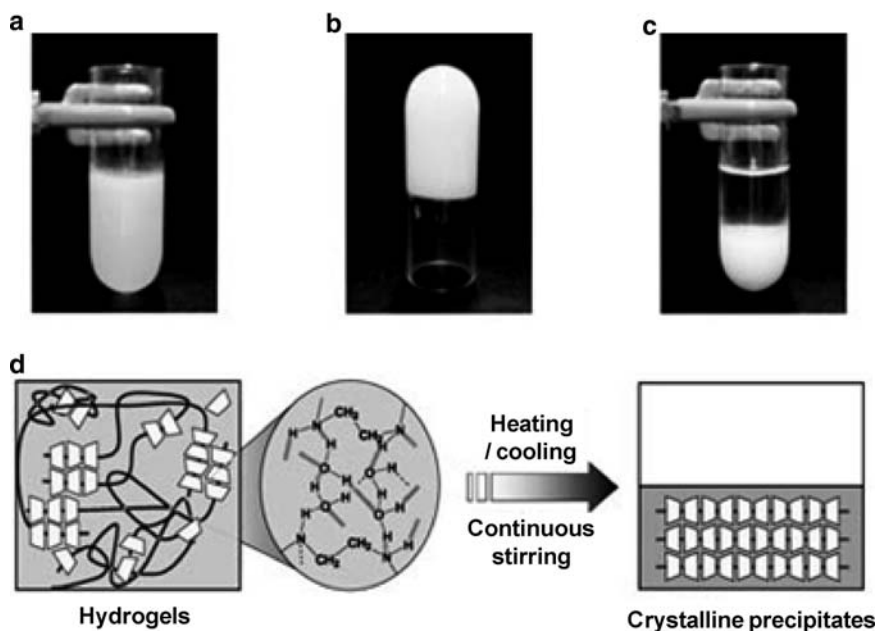

Fig. 10 a–d Optical images of polypseudorotaxane formed by α-CD and PEI: gel-like network formed at gelation temperature **a**, equilibrated hydrogel at gelation temperature **b**, and crystalline precipitate formed by thermal process **c**; and the schematic illustration of the transition process from the hydrogels to the crystalline precipitates **d** [81]

2.3 Gelation Induced by Inclusion Complexation Between α-CD and Grafted PL

A pH-sensitive and thermo-reversible supramolecular hydrogel system formed between α-CD and poly(ε-lysine) (PL)-grafted dextran was reported [82]. The PL grafting chains could form inclusion complexes with α-CD. The gelation was induced from a phase-separated structure comprising hydrated dextrans and hydrophobically aggregated inclusion complexes in buffer solution at pH 10.0. A rapid phase transition from gel to sol was observed upon decreasing the pH value to 4.0, which resulted from the dissociation of the inclusion complexes because of the protonation of the guest PL polymer chains.

2.4 Gelation Induced by Inclusion Complexation Between β-CD and Grafted PPO

Poly(propylene oxide) (PPO)-grafted dextran was synthesized and used to form inclusion complexes and supramolecular hydrogels with β-CD [83]. In this work, the average number of grafted PPO per dextran was in the range of 1.1–38.5 per polymer chain. The supramolecular hydrogels were formed induced by the formation of inclusion complexes between the grafted PPO and β-CD. Similar to the hydrogels formed by α-CD and PEO-grafted dextran [77], the supramolecular hydrogels between β-CD and PPO-grafted dextran comprise a microphase separated structure consisting of the hydrophobic and channel-type crystalline inclusion complex domains as the physical crosslinks and the hydrated dextran matrices which contain a large amount of water in the structure. The significance of this β-CD inclusion complex hydrogel system is that the gelation process is very fast.

2.5 Gelation Induced by Double Chain Inclusion Complexation between γ-CD and Grafted PEI

It was found that the large γ-CD molecule can include two chains of PEO into its cavity to form double-strand polypseudorotaxanes [22]. For developing a supramolecular network which can lead to formation of hydrogels, a PEO–PEI-grafted dextran (PEO–PEI–dex) was synthesized and used to form supramolecular hydrogels with γ-CD based on the double-strand inclusion complexation (Fig. 11) [84]. When adding γ-CD to the aqueous solution of PEO–PEI–dex, double strands of the PEG–PEI chains grafted on dextran backbones can intrude into the inner cavity of γ-CD, in either the same or opposite directions, which leads to formation of double-strand inclusion complexes with either a parallel or antiparallel direction. Therefore, the whole hydrogel system consists of a phase separated structure of the double-strand inclusion complex domains and the hydrated dextran
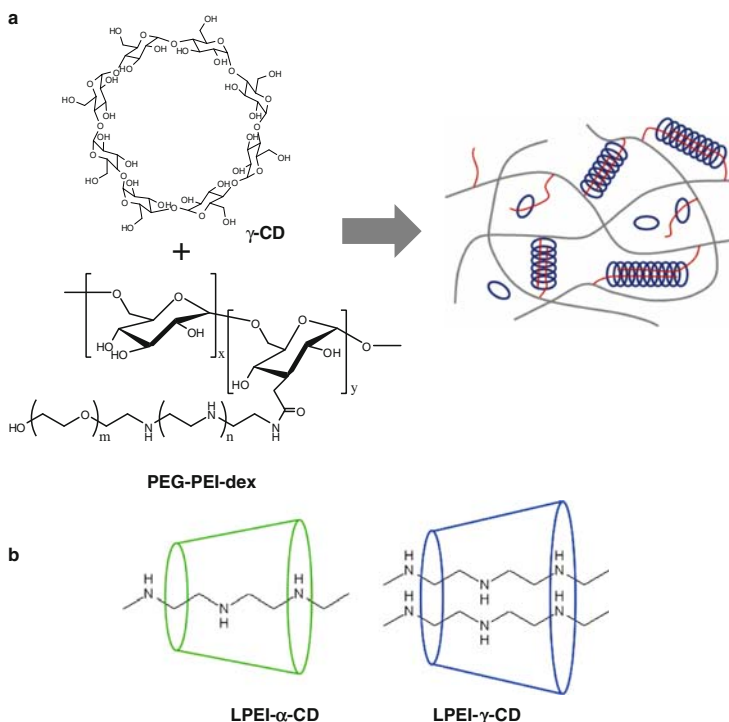
Fig. 11 a,b Schematic representation for the formation of PEO–PEI–dex·γ-CD networks. **a** A supramolecular network is formed via the double-strand complex between γ-CD and double strands of the PEO–PEI chains. The double-strand complexes are either of the parallel or antiparallel type. **b** α-CD and γ-CD include single and double strands of PEI, respectively. Stoichiometric ratios of α-CD or γ-CD to the repeating unit of PEI are 1:2 and 1:4, respectively [84]

matrices. The PEI segments can be protonated at low pH, which increases their hydrophilicity and leads to dissociation of the inclusion complexes. Therefore, the supramolecular hydrogels formed between PEO–PEI–dex and γ-CD are pH-sensitive. Their viscosity changes depending on the pH as shown in Fig. 12 [84]. It is commented that, although PEO–PEI–dex and α-CD will not form double-strand inclusion complexes, the single-strand inclusion complex may still form self-assembled crystalline domains, which can play a role of physical crosslinking and lead to the formation of a hydrogel as reported elsewhere [77, 78, 82].

2.6 Supramolecular Hydrogels as Injectable Drug Delivery Systems

Polymeric hydrogels have been attractive biomaterials for drug delivery, particularly for controlled release of delicate bioactive agents such as proteins and peptides. However, chemically crosslinked hydrogels can be applied only as implantables,
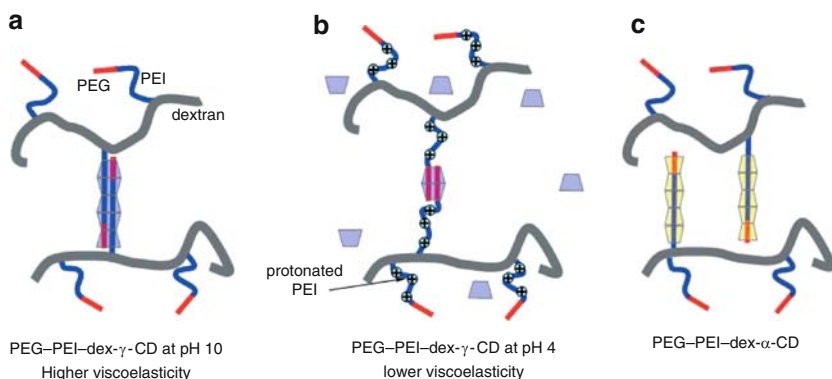
Fig. 12 a–c Proposed structures of supramolecular networks under different conditions. **a** PEO–PEI–dex·γ-CD network is formed with a full double-strand complex at pH 10. **b** The full double-stand complex of PEO–PEI–dex·γ-CD network is transformed to a partial double-stand complex at pH 4 owing to protonation of the PEI chains. **c** PEO–PEI–dex·α-CD networks do not form any double-strand complex at pH 10 [84]

and the incorporation of drugs by sorption may be time-consuming and limiting in the loading level. In addition, the cross-linking reaction may conjugate the drug to the hydrogel or impair the chemical integrity of the drug. Therefore, a delivery system where gelation and drug loading can be achieved simultaneously, taking place in an aqueous environment and without covalent crosslinking, would be attractive. Since both PEO and CDs are known to be biocompatible and bioabsorbable, the supramolecular hydrogels formed between CDs and PEO or its copolymers could be excellent candidates a new class of bioabsorbable physical hydrogels for controlled drug delivery [67].

Generally, the supramolecular hydrogels of CDs and polymers based on the formation of inclusion complexes which play the role of physical crosslinking are thermo-reversible. [59, 67, 68, 77–79]. The supramolecular hydrogels were also found to be thixotropic and reversible. For example, the viscosity of the hydrogel form between α-CD and PEO greatly diminished as it was agitated (Fig. 13a). This property renders the hydrogel formulation injectable even through a fine needle. The diminished viscosity of the hydrogels eventually restored towards its original value, in most cases within hours, when there was no more agitation (Fig. 13b). The thixotropic and thermo-reversible properties of the gel afforded us with a unique injectable hydrogel drug delivery system. One can first incorporate bioactive agents, such as drugs, proteins, vaccines, or plasmid DNA, into the hydrogel in a syringe at room temperature without any contact with organic solvents. The drug-loaded hydrogel formulation can then be injected into the tissue under pressure because of the thixotropic property. After restoration of the gelation in situ, the hydrogel serves as a depot for controlled release (Fig. 14) [50]. As compared to implantable hydrogels, the injectable hydrogel will be much more attractive.
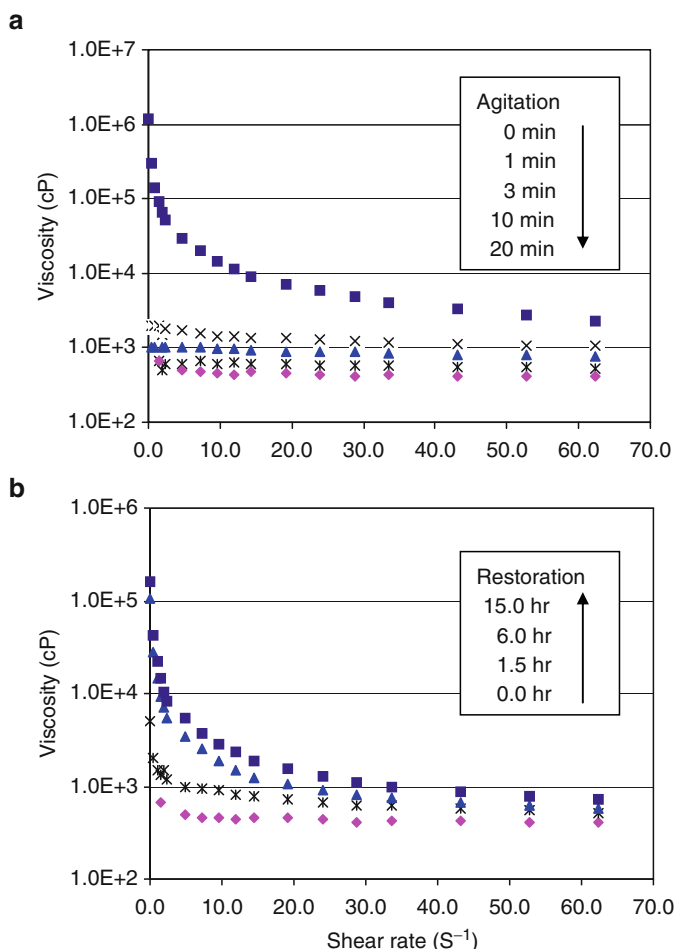
a

b

Fig. 13 a, b Changes of the viscosities of Gel-20K-60 as a function of agitation time at a shear rate of $120 \, s^{-1}$ **a**, and restoration of the viscosities of the gel after 20 min agitation at a shear rate of $120 \, s^{-1}$ **b** [67]

The effect of the injection through needles on the viscosity of the hydrogels was studied (Table 3) [67]. The viscosity dropped significantly after injection from the syringes. Inducing a higher shear rate, the finer needle caused a steeper decrease in viscosity of the hydrogel. The maximum speeds at which the hydrogels can be injected through a syringe of different needle sizes were also reported [67]. The hydrogels formed from PEOs of higher molecular weights were more difficult to be injected though fine needles. Injection of Gel-35K-60 through a 27G needle was limited to only $0.09 \, mL \, min^{-1}$.

Since the formation of the hydrogels is induced by the supramolecular self-assembling in aqueous solution, and there is no any chemical crosslinking reagents,
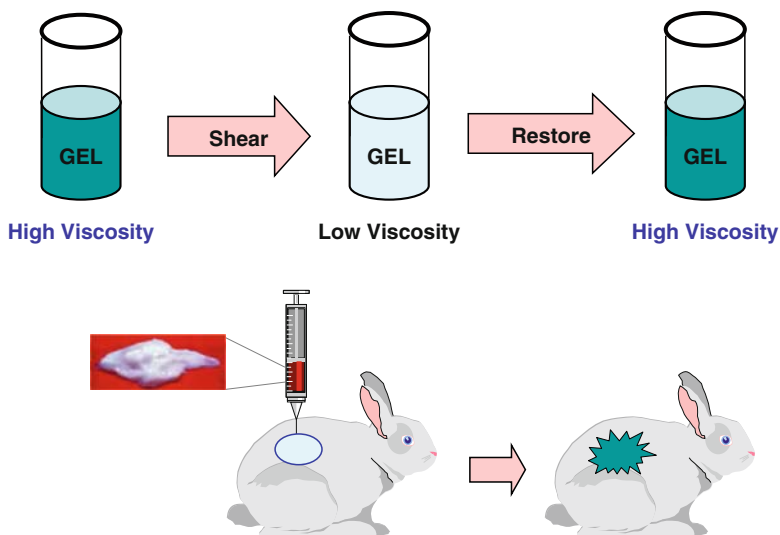
Fig. 14 Injectable drug delivery system based on supramolecular hydrogels formed by α-CD and PEO [50]

Table 3 Maximum speeds at which the hydrogels can be injected though needles of different sizes [67]

Needle size[a]	Maximum injection speed of hydrogel (mL min^{-1})			
	Gel-8K-60	Gel-10K-60	Gel-20K-60	Gel-35K-60
18G × 1.5 in	–[b]	75.1	32.8	8.93
19G × 1.5 in	–[b]	47.5	15.3	3.15
21G × 1.5 in	33.9	13.8	5.72	1.66
22G × 1.5 in	22.6	4.35	3.41	0.72
27G × 0.5 in	2.61	1.01	0.36	0.09

[a]Terumo 6-mL syringes were used for the experiments

[b]The injection speed is higher than 100 mL min^{-1}

bioactive agents, the drugs, can be incorporated into the hydrogel in situ at room temperature without any contact with organic solvents. The drug carrier properties of the supramolecular hydrogels were evaluated in vitro using a model system [67]. Fluorescein isothiocyanate labeled dextran (dextran-FITC) was physically entrapped in the hydrogels and their in vitro release properties were characterized. Figure 15 shows the in vitro release profiles of dextran-FITC from the hydrogels with PEO of different molecular weights or different PEO concentrations. The release rate decreases sharply with an increase in the molecular weight of PEO up to 35,000, presumably because of the chain entanglement effect and different complex stability (Fig. 15a). The release rate is quite steady with time for gels formed with PEO 35,000 (Gel-35K-60) and 100,000 (Gel-100K-60). Although Gel-100K-60 shows the most sustained release kinetics, it was studied here mostly for
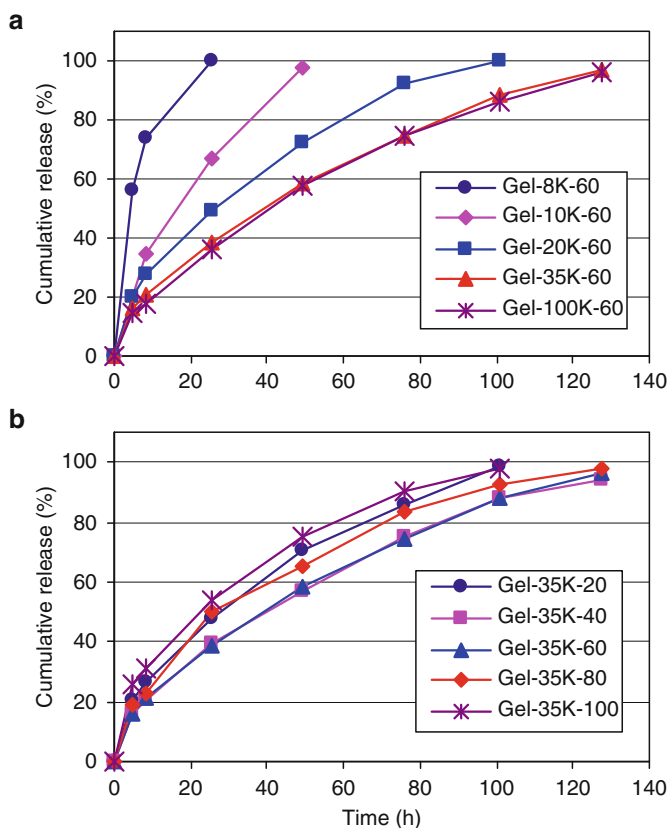
Fig. 15 a,b In vitro release profiles for dextran-FITC (MW 20,000) released from α-CD–PEO hydrogels formed from PEO of different molecular weights **a** and different concentrations **b**. Refer to Table 1 for the compositions of the hydrogels [67]

understanding of the structure–property relationship as PEO at this large would be undesirable for in *vivo* applications due to the difficulty of its clearance from the body. When α-CD used was fixed at $0.0967\,\mathrm{g\,mL^{-1}}$, hydrogel compositions with PEO of 0.133–$0.177\,\mathrm{g\,mL^{-1}}$ (Gel-35K-60 and Gel-35K-80) gave the most sustained release profiles (Fig. 15b). Compositions with PEG contents outside this range resulted in more rapid release. Therefore, the optimal formulations of the α-CD–PEO hydrogels for sustained release of drugs may be those of Gel-20K-60 and Gel-35K-60.

Hydrogels formed by PEO block copolymers have previously been proposed as sustained release matrix [85, 86]. The α-CD–PEO hydrogel delivery system differs in that the gelation relies on the formation of a polymer inclusion complex induced by the PEO-threaded CDs. The properties of the supramolecular hydrogel can be fine-tuned with the composition, molecular weight and chemical structure of the polymer or copolymers.

Although the α-CD–PEO hydrogels were demonstrated as a potential injectable drug delivery system, we are facing some challenges in applying the hydrogels in clinical applications. Generally, the release kinetics is too fast, and only suitable for short-term drug release with a time span of less than 1 week, because the dissociation of the hydrogel in aqueous environment is rapid due to the hydrophilic nature of PEO. In addition, the use of high molecular weight PEO of more than 10,000 in *vivo* will be problematic, because PEO is not biodegradable, and the high molecular weigh PEO is not suitable for filtration through human kidney membrane due to the large hydrodynamic radius.

To overcome the above mentioned problems, the supramolecular hydrogels self-assembled between α-CD and the biodegradable PEO–PHB–PEO triblock copolymers were studied for controlled drug delivery applications. It was found that the preferential inclusion complexation of α-CD with PEO block together with the hydrophobic interaction between the middle PHB blocks cooperatively result in a self-assembly system that induces a strong macromolecular network to give a supramolecular hydrogel system which is suitable for long-term sustained release of drugs [71].

The in vitro controlled release properties of the α-CD–PEO–PHB–PEO hydrogels were studied using fluorescein isothiocyanate labeled dextran (dextran-FITC) as a model macromolecular drug. Table 4 lists the dextran-FITC encapsulated α-CD–PEO–PHB–PEO hydrogels with different compositions that were used for the in vitro release kinetics studies. The α-CD–PEO (35,000 Da) hydrogel formulation was used as a comparison. Figure 16 shows the in vitro release profiles for dextran-FITC released from the supramolecular hydrogels. Both PEO–PHB–PEO triblock copolymers at 13 wt% in water were solutions, and could not sustain release of dextran-FITC because they dispersed in large quantity of water or PBS buffer in seconds. The α-CD–PEO homopolymer hydrogel even with very high PEO molecular weight (35,000 Da) dissociated and dissolved in PBS within 5 days (Fig. 16a, Gel-1) [67]. However, the α-CD–PEO–PHB–PEO (5000–3140–5000) hydrogels with reasonably high α-CD concentration (9.7 wt%, Fig. 16e, Gel-5) showed excellent controlled release property, sustaining the release of dextran-FITC for more than 1 month. The hydrogels with lower α-CD concentrations resulted in much faster release kinetics (Fig. 16c, Gel-3, and Fig. 4d, Gel-4), indicating

Table 4 α-CD-PEO–PHB–PEO supramolecular hydrogel formulations used for in vitro controlled release studies [71]

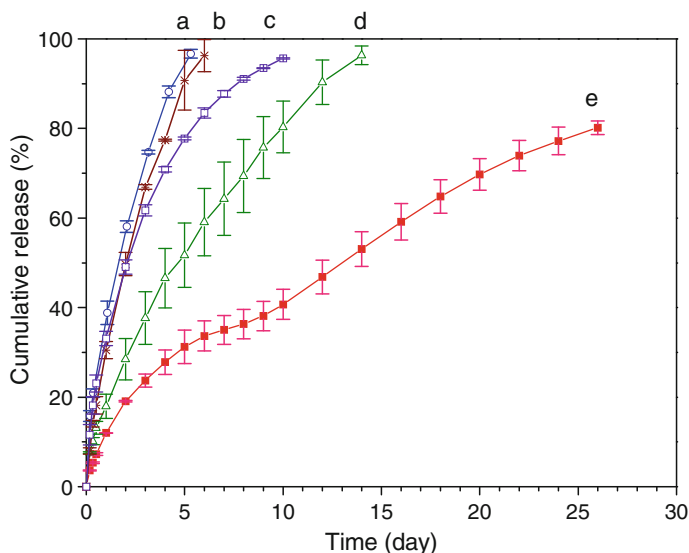| Hydrogel formulation	Polymer used	Gel composition (wt%)			
		α-CD	Polymer	Dextran–FITC	H$_2$O
Gel-1	PEO(35000)	9.7	13.3	0.66	76.3
Gel-2	PEO–PHB–PEO(5000-1750-5000)	9.7	13.3	0.66	76.3
Gel-3	PEO–PHB–PEO(5000-3140-5000)	5.4	13.3	0.66	80.6
Gel-4	PEO–PHB–PEO(5000-3140-5000)	7.9	13.3	0.66	78.1
Gel-5	PEO–PHB–PEO(5000-3140-5000)	9.7	13.3	0.66	76.3

Fig. 16 a–e In vitro release profiles for dextran-FITC released from α-CD–PEO–PHB–PEO hydrogels with different compositions in comparison with α-CD–PEO hydrogel: **a** Gel-1; **b** Gel-2; **c** Gel-3; **d** Gel-4; **e** Gel-5 [71]. The compositions of the hydrogels are listed in Table 4

that the complexation between α-CD and the PEO blocks play a key role in formation of a stable supramolecular hydrogel. Interestingly, α-CD–PEO–PHB–PEO (5000–1750–5000) hydrogel with shorter PHB block only sustained the release of dextran-FITC for 6 days (Figs. 16 and 2b, Gel-2), although its α-CD concentration was high (9.7 wt%). The results indicate that the PHB block length is also critical for the stability of the supramolecular hydrogels, which further support the hypothesis that the cooperation effect of both α-CD complexation with PEO segments and the hydrophobic interaction between PHB blocks results in the formation of hydrogels with strong supramolecular networks as well as the long-term sustained release property that many simple triblock copolymer delivery systems could not achieve. These findings implicate that, the properties of the supramolecular hydrogels can be fine-tuned not only with different lengths of PHB block, but also with different copolymers, which may open up a wide range of possible biomedical applications. Although there were supramolecular hydrogel formation between α-CD with homo-PEO [59, 67], the α-CD–PEO–PHB–PEO hydrogels were different because there was the cooperative effect of the self-assembly of inclusion complexes of α-CD with PEO segments and the hydrophobic interaction between the PHB segments, which led to the formation of a strong hydrogel network. Not only are lower molecular weights of the copolymer needed in the α-CD–PEO–PHB–PEO hydrogels for sustained release, but also the biodegradable PEO–PHB–PEO copolymers will have the advantage that the hydrogel formulations will be bioabsorbable after the drug delivery and dissociation of the hydrogels into their components [71].

Recently, another supramolecular hydrogel formed between α-CD and biodegradable and amphiphilic PEO–PCL diblock copolymer was also studied for controlled drug delivery. The hydrogel was found to have significantly improved sustained release property compared to α-CD–PEO supramolecular hydrogels. The release of dextran-FITC from α-CD–PEO–PCL hydrogels could be lasted for 1 month even though the molecular weight of PEO block is only 5,000, which is attributed to the strong hydrophobic interaction between uncovered PCL blocks. Thus, the requirement of high molecular weight PEO for long term delivery system is avoided [72].

It was found that the α-CD–PEO–PCL hydrogel showed similar performance to those formed by PEO–PHB–PEO triblock copolymers and α-CD in controlled release of macromolecular drugs [71]. So, the α-CD–PEO–PCL hydrogel can be an alternative to achieve the sustained release using different copolymers. Particularly, PEO–PCL diblock copolymer is easier to synthesize and commercially available, thus it is attractive for further application studies using the α-CD–PEO–PCL hydrogels.

2.7 Gelation Induced by Physical Interaction of Threaded Methylated CDs in Polyrotaxanes

Recently a polyrotaxane composed of multiple methylated α-CD rings threaded on a high molecular weight PEO chain and end-capped by bulky adamantyl groups was synthesized (Fig. 17) and investigated in terms of its thermo-reversible sol–gel transition and hydrogel formation [87].

The aqueous solutions of the polyrotaxane of methylated α-CD (MePR), where the degree of substitution (DS) of the methylated α-CD, the number of modified
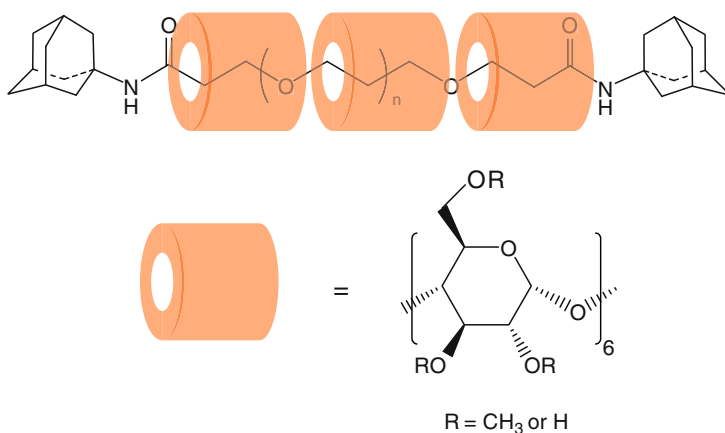

$R = CH_3$ or H

Fig. 17 Molecular structure of polyrotaxane formed by methylated α-CD (MePR) [87]

hydroxyl groups per glucose unit, was 2.8, showed a lower critical solution temperature (LCST) and form an elastic hydrogel with increasing temperature. When the concentrations of the MePR was 2 wt%, the solution became turbid at 40 °C. The MePR solution of 4 wt% formed a hydrogel at 20 °C, and became a sol at lower temperature. The X-ray diffraction investigation revealed that the localization and highly ordered arrangement of methylated α-CD along the PEG chain in the gel increased with increasing temperature. The arrangement of methylated α-CD was also reflected by the changes in elasticity and long relaxation behavior of the solution around the sol–gel transition.

Based on the investigations by the authors using X-ray diffraction, microdifferential scanning calorimetry, and rheometry, they proposed a mechanism for the sol–gel transition of the MePR/water system (Fig. 18) [87]. The crystal-like crosslinks of MePR in water are originated from the regularly ordered structure of methylated α-CDs along a PEG chain. The thermal gelation of MePR solution is induced not merely by the hydrophobic association among methylated α-CD, but also by the strong crystal-like aggregation as proved by the X-ray diffraction study.

3 Chemical Hydrogels Formed by Polypseudorotaxanes and Polyrotaxanes

3.1 Gelation Induced by Chemical Crosslinking of CDs

Through chemically crosslinking the α-CD molecules in polyrotaxanes, a class of supramolecular networks which are also called "sliding gels" has been developed (Fig. 19) [88], where cyanuric chloride, divinyl-sulfone, and bifunctional PEO were used as the chemical crosslinking agents [88–95].

Okumura and Ito reported the synthesis of sliding gels by chemically crosslinking α-CD molecules in the polyrotaxanes formed by multiple α-CD rings threaded on a PEO chain and end-capped by 2,4-dinitro-phenyl groups, using cyanuric chloride as the crosslinking agent. The crosslinking points are also described as figure-of-eight crosslinks (Fig. 20) [89]. The resultant sliding gels are transparent gels with good tensility, low viscosity, and large swellability in water. It is interesting that the threading PEO polymer chains in the gels are neither covalently crosslinked like in a chemical gel, nor physically crosslinked by weak cohesion forces like in a physical gel. Instead, they are topologically interlocked by the figure-of-eight cross-links. It is expected that this kind of special crosslink can pass along the polymer chains freely to equalize the 'tension' of the threading polymer chains like a pulley. Therefore, the nanoscale heterogeneity in structure and stress may be automatically equalized in the gel. Another example of sliding gels was reported by Hadzziioannou and coworkers, where the α-CD molecules in the polyrotaxanes were crosslinked by using divinyl-sulfone as the crosslinking agent (Fig. 21) [88].
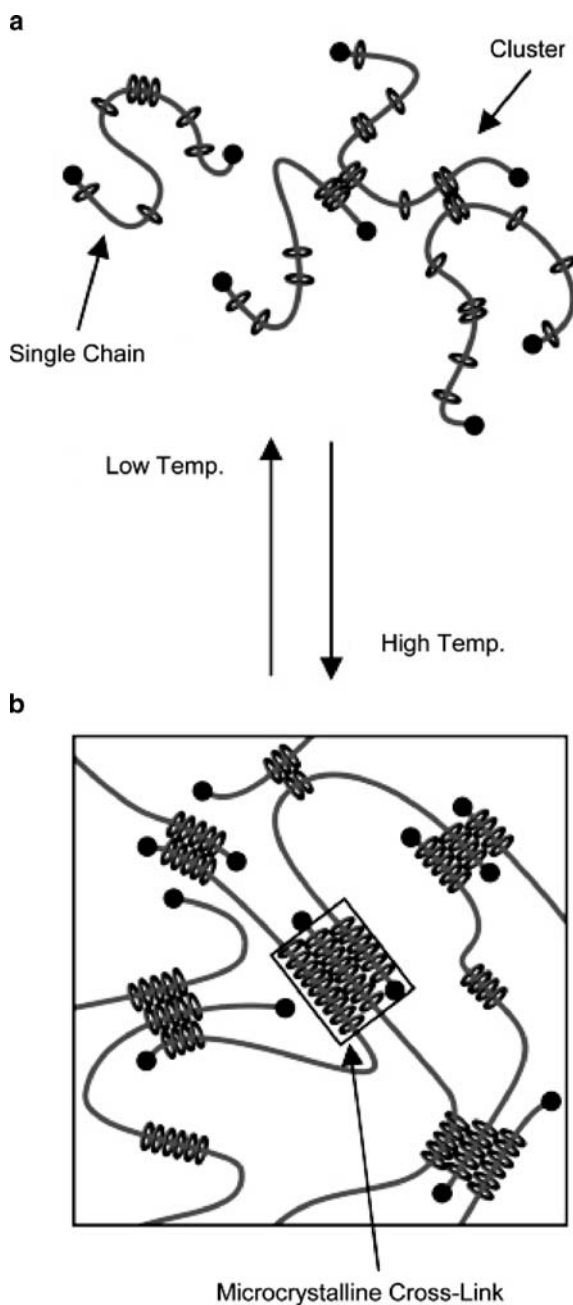
Fig. 18 a, b Schematic illustration of the sol–gel transition of the polyrotaxane of methylated α-CD in Water. There are isolated chains and only limited clusters of polyrotaxane in the solution at lower temperature **a** and large number of crosslinks consisting of crystal-like aggregates among localized methylated CDs in the gel at higher temperatures **b** [87]
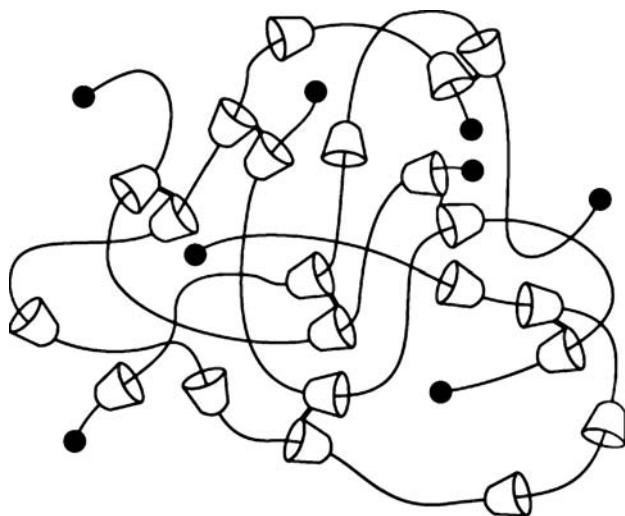
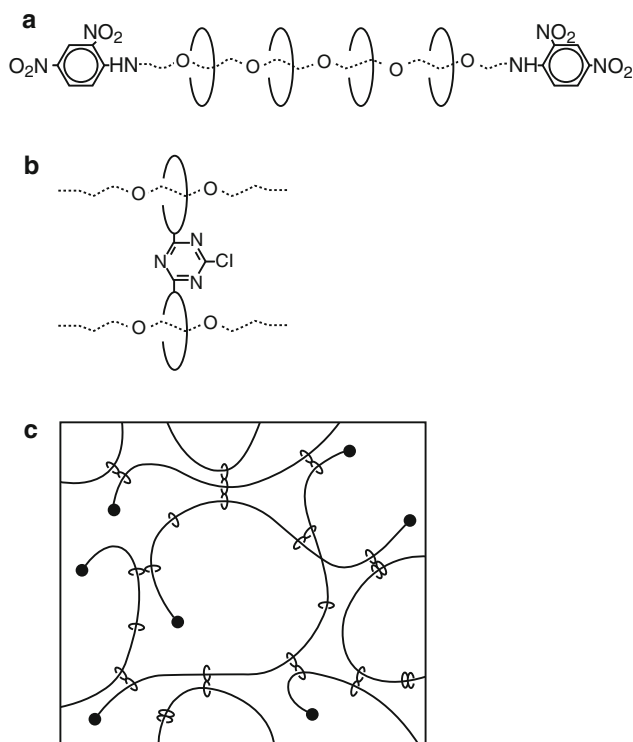**Fig. 19** Schematic illustration of the sliding gel [88]

Fig. 20 a The polyrotaxane formed by α-CD and PEO with 2,4-dinitro-phenyl end caps. **b** The figure-of-eight cross-link: covalently cross-linked cyclodextrins. **c** Schematic diagram of the polyrotaxane gel prepared from the sparse polyrotaxane by covalently cross-linking cyclodextrins using cyanuric chloride as crosslinking agent [89]
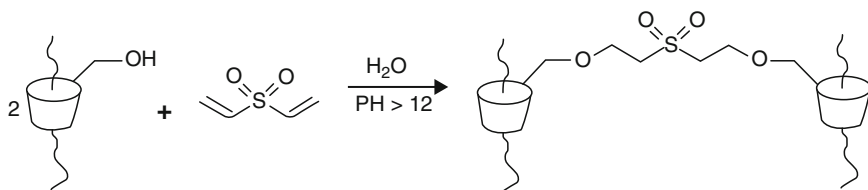
Fig. 21 General scheme for chemically crosslinking α-CD molecules in a polyrotaxane formed by α-CD and PEO with 2,4-dinitro-phenyl end caps by divinyl-sulfone as crosslinking agent [88]
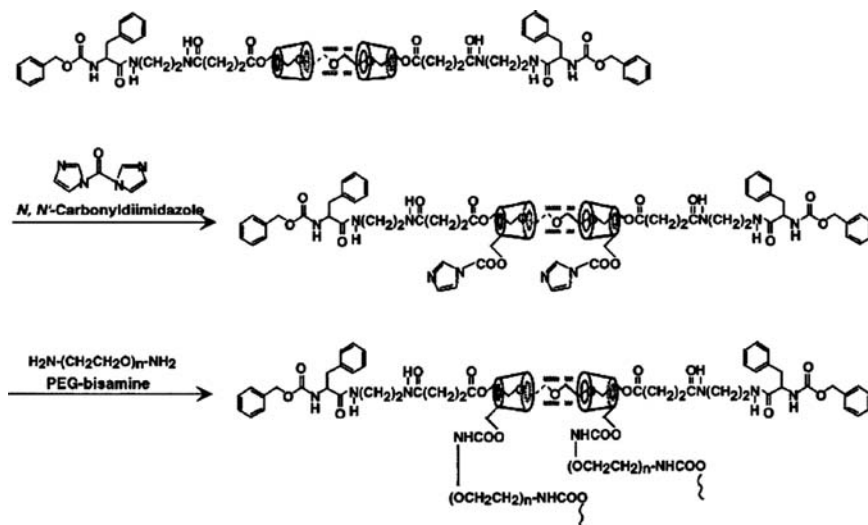

Fig. 22 Schematic illustration for the preparation of polyrotaxane hydrogels by chemically crosslinking α-CD molecules in the polyrotaxane with hydrolyzable end caps, using PEO-bisamine as the crosslinking agent [92]

Yui's lab prepared hydrogels by chemically crosslinking α-CD molecules in the polyrotaxanes using bifunctional PEO as the crosslinking agent (Fig. 22) [92–95]. In this design, a polyrotaxane with hydrolyzable end caps was used in order to obtain a biodegradable hydrogel. In addition, PEO is also a popularly used biocompatible polymer in biomaterials, therefore, the polyrotaxane hydrogels crosslinked PEO may be of interest in biomedical applications.

A series of polyrotaxane hydrogels crosslinked by PEO was prepared and their hydrolytic erosion behavior was studied [92–95]. Because of the interlocked supramolecular structure, the hydrogel degradation in a physiological condition followed a bulk mechanism. This characteristic may be useful for a biodegradable polymer hydrogel scaffold for tissue engineering application. The control of the gel erosion time with bulk mechanism can allow the scaffold to maintain its structures and properties during the tissue regeneration, and then rapidly decompose and disappear by the bulk erosion after the tissue regeneration has completed.

From the result of the erosion study, the time to reach complete gel erosion was found to be prolonged by increasing the PEO/α-CD ratio, the number of PEO chains per one α-CD molecule in the hydrogels. These results indicate the enhanced stability of ester hydrolysis in the hydrogels with highly water swollen state. The erosion profile of the hydrogels can be controlled by the molecular weight of the PEO-bisamine used, in addition to the PEO/α-CD ratio [93]. The fibroblast adhesion and proliferation on the polyrotaxane hydrogels were also studied [94].

3.2 Gelation Induced by Chemical Crosslinking of Threading Polymers

A class of supramolecular hydrogels was developed by Feng's group through chemically crosslinking the threading polymers in the polypseudorotaxane hydrogels [96–99]. Basically, polypseudorotaxanes were prepared from α-CD and photopolymerizable PEO copolymers bearing acrylate terminals. Since the PEO block has large molecular weight, the polypseudorotaxanes formed physical hydrogels as described in Sect. 2.1. The chemically crosslinked supramolecular hydrogels were prepared from the polypseudorotaxane hydrogels in a mixed solvent of water and dimethyl sulfoxide via in situ photopolymerization under UV irradiation using 2,2-dimethoxy-2-phenyl acetophenone as the photoinitiator. In the resultant chemical hydrogels, multiple α-CD rings are threaded and immobilized onto the network chains with the crosslinking junctions as topological stoppers to prevent the dethreading of the α-CD rings, forming permanent supramolecular hydrogels (Fig. 23) [96, 97].

The threading acrylate-terminated PEO copolymers used in these hydrogels preparation include PCL–PEO–PCL triblock polymer [96], PLA–PEO–PLA triblock polymer [97], 4-arm PEO star polymer [98], and PCL–Pluronic–PCL block polymer [100]. Particularly for those formed from biodegradable block copolymers as the threading polymers, the hydrogels may be of interest in biomaterials applications because of their potential biodegradability.
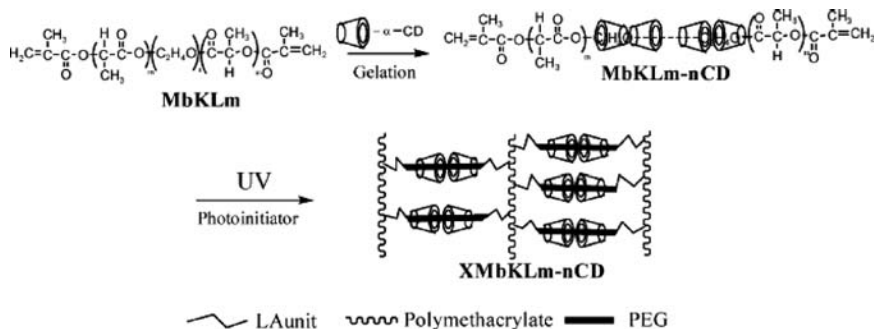

Fig. 23 Schematic illustration of the preparation of chemically crosslinked polyrotaxane hydrogels through crosslinking the ends of the threading polymers via UV photopolymerization [97]

Thermosensitive supramolecular hydrogels of this type were synthesized via copolymerization of *N*-isopropylacrylamide (NIPA) with photocurable and biodegradable polypseudorotaxanes as crosslinkers under UV irradiation, where the polypseudorotaxane precursors were prepared by α-CD and amphiphilic PLA–PEO–PLA copolymers end-capped with methacryloyl groups [99]. It was reported that the crosslinked hydrogel made of only the macromer guest shows also thermosensitive. However, this stimuliresponsive property disappears when α-CD rings are threaded onto the PLA–PEO–PLA polymeric backbone and reappears when PNIPA segments are introduced. The thermosensitivity of these hydrogels could be modulated by changing the PNIPA content as well as the α-CD to macromer ratio.

Most recently, three-dimensional crosslinked networks based on the α-CD polypseudorotaxane hydrogels formed from thiolated 4-arm PEO were prepared by thiol-disulfide interchange reaction using a three-step oxidation (Fig. 24) [101]. The channel-type crystalline structure of inclusion complexes is still maintained after the oxidation processes. The hydrogels may undergo a reversible gelation–decomposition transition through the oxidation and reduction processes because of the disulfide crosslinks. The swelling behaviors and degradation properties can be readily regulated by tuning the feed compositions of α-CD and PEO-thiolated prepolymer.
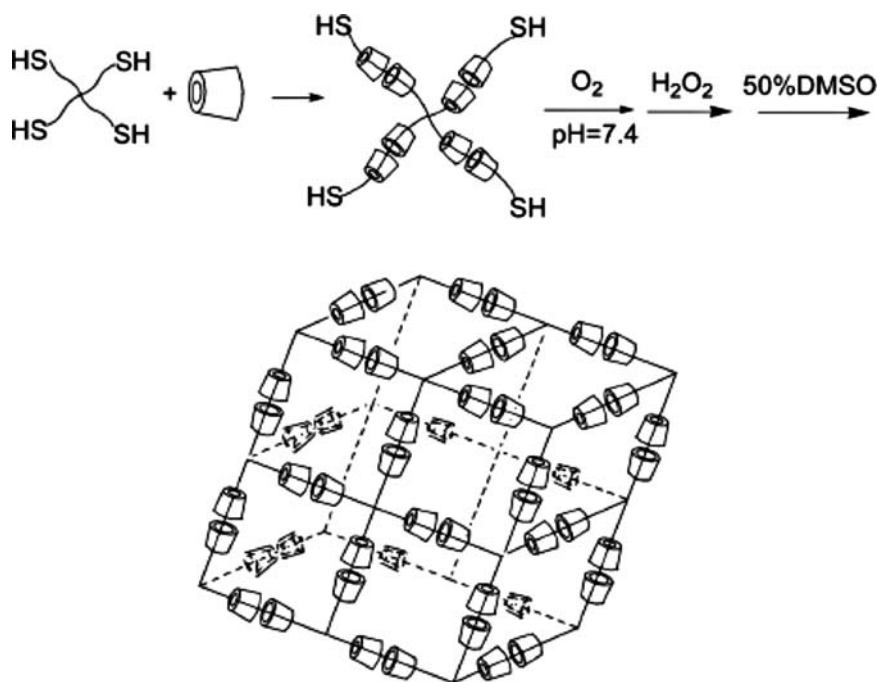

Fig. 24 Schematic illustration of the preparation of chemically crosslinked polyrotaxane hydrogels through crosslinking the ends of the threading polymers via oxidation crosslinking processes [101]

4 Concluding Remarks

The advances in the studies on the inclusion complexes of CDs threading onto polymer chains have led to interesting development of supramolecular hydrogels with many different molecular and supramolecular structures. Both physical and chemical hydrogels of many different types were developed based on the CD-based polypseudorotaxanes and polyrotaxanes.

Physical hydrogels were formed induced by self-assembled water-insoluble and crystalline polypseudorotaxane domains which act as physical crosslinking points. Such physical hydrogels include the polypseudorotaxane systems of α-CD threading on PEO or its copolymers, α-CD threaded on PEI, PL, or their copolymers, and even β-CD or γ-CD threaded PPO or PEI copolymers. The thermo-reversible and thixotropic properties of these supramolecular hydrogels have inspired their applications as injectable drug delivery systems. Physical hydrogels induced by physical interaction of threaded CD molecules in polyrotaxanes were also developed.

Chemical hydrogels formed from polypseudorotaxanes and polyrotaxanes were based on the chemical crosslinking of either CD molecules or the threading polymer chains. Polyrotaxane hydrogels with chemically crosslinked CD rings are also called sliding gels. A number of different crosslinking agents including PEO and small molecules were used for the crosslinking. Photopolymerizable or oxidative crosslinkable threading copolymers were used to form polypseudorotaxane hydrogels followed by chemical crosslinking. Such processes resulted in formation of another type of supramolecular chemical hydrogels. Notably, the chemical hydrogels formed from polypseudorotaxanes and polyrotaxanes were often made biodegradable through incorporation of hydrolyzable threading polymers, end caps, or crosslinkers, for their potential applications as biomaterials.

The hydrogels based on CD-based polypseudorotaxanes and polyrotaxanes will continue to be a hot topic because of the tremendous possibility of the different properties and functionalities induced by the supramolecular structures.

References

1. Peppas NA (1987) Hydrogels in medicine and pharmacy, vol. 1. CRC, Florida
2. Park K, Shalaby WSW, Park H (1993) Biodegradable hydrogels for drug delivery. Technomic, Lancaster
3. Kishida A, Ikada Y (2002) Hydrogels for biomedical and pharmaceutical applications. In: Dumitriu S (ed) Polymeric biomaterials. Marcel Dekker, New York
4. Li J (2004) Polymeric hydrogels. In: Teoh SH (ed) Biomaterials engineering and processing series, vol. 1. Engineering materials for biomedical applications. World Scientific, New Jersey
5. Park H, Park K (1996) Pharm Res 13:1770–1776

6. Kim S, Bae Y, Okano T (1992) Pharm Res 9:283–290
7. Heller J (1993) Adv Drug Deliv Rev 10:163–204
8. Kamath KR, Park K (1993) Adv Drug Deliv Rev 11:59–84
9. Graham NB (1987) Poly(ethylene oxide) and related hydrogels. In: Peppas NA (ed) Hydrogels in medicine and pharmacy, vol. 2. CRC, Boca Raton
10. Harris JM (1992) Poly(ethylene glycol) chemistry: biotechnical and biomedical applications. Plenum, New York
11. Apicella A, Capello B, Del Nobile MA, La Rotonda MI, Mensitieri GL, Nicolais S, Seccia S (1994) Poly(ethylene oxide)-based delivery systems. In: Ottenbrite M (ed) Polymeric drugs and drug administration. American Chemical Society, Washington DC
12. Dimitrov I, Trzebicka B, Muller AHE, Dworak A, Tsvetanov CB (2007) Prog Polym Sci 32:1275–1343
13. Bender ML, Komiyama M (1978) Cyclodextrin chemistry. Springer, Berlin Heidelberg New York
14. Szejtli J (1982) Cyclodextrins and their inclusion complexes. Akademiai Kiado, Budapest
15. Szejtli J (1998) Chem Rev 98:1743–1753
16. Harada A, Kamachi M (1990) Macromolecules 23:2821–2823
17. Harada A, Li J, Kamachi M (1992) Nature 356:325–327
18. Wenz G, Keller B (1992) Angew Chem Int Ed Engl 31:197–199
19. Wenz G (1994) Angew Chem Int Ed Engl 33:803–822
20. Wenz G, Han BH, Muller A (2006) Chem Rev 106:782–817
21. Harada A, Li J, Kamachi M (1993) Macromolecules 26:5698–5703
22. Harada A, Li J, Kamachi M (1994) Nature 370:126–128
23. Li J, Harada A, Kamachi M (1994) Bull Chem Soc Jpn 67:2808–2818
24. Li J, Uzawa J, Doi Y (1998) Bull Chem Soc Jpn 71:1953–1957
25. Fujita H, Ooya T, Yui N (1999) Macromolecules 32:2534–2541
26. Li J, Li X, Toh KC, Ni XP, Zhou ZH, Leong KW (2001) Macromolecules 34:8829–8831
27. Li J, Toh KC (2002) J Chem Soc Perkin Trans 2:35–40
28. Jiao H, Goh SH, Valiyaveettil S (2002) Macromolecules 35:1980–1983
29. Li J, Ni XP, Leong K (2003) Angew Chem Int Ed 42:69–72
30. Li X, Li J, Leong KW (2003) Macromolecules 36:1209–1214
31. Li J, Ni XP, Zhou ZH, Leong KW (2003) J Am Chem Soc 125:1788–1795
32. Jiao H, Goh SH, Valiyaveettil S, Zheng JW (2003) Macromolecules 36:4241–4243
33. Shuai XT, Porbeni FE, Wei M, Shin ID, Tonelli AE (2001) Macromolecules 34:7355–7361
34. Lu J, Mirau PA, Shin ID, Nojima S, Tonelli AE (2002) Macromol Chem Phys 203:71–79
35. Zhao TJ, Beckham HW (2003) Macromolecules 36:9859–9865
36. Li J, Chen B, Wang X, Goh SH (2004) Polymer 45:1777–1785
37. Li X, Li J, Leong KW (2004) Polymer 45:6845–6851
38. Girardeau TE, Zhao TJ, Leisen J, Beckham HW, Bucknall DG (2005) Macromolecules 38:2261–2270
39. Liu Y, Liang P, Chen Y, Zhang YM, Zheng JY, Yue H (2005) Macromolecules 38:9095–9099
40. Liu Y, Yang YW, Chen Y, Zou HX (2005) Macromolecules 38:5838–5840
41. Huang JC, Li X, Lin TT, He CB, Mya KY, Xiao Y, Li J (2004) J Polym Sci B Polym Phys 42:1173–1180
42. Huang FH, Gibson HW (2005) Prog Polym Sci 30:982–1018
43. Choi HS, Yui N (2006) Prog Polym Sci 31:121–144
44. Nepogodiev SA, Stoddart JF (1998) Chem Rev 98:1959–1976
45. Raymo FM, Stoddart JF (1999) Chem Rev 99:1643–1663
46. Rusa CC, Tonelli AE (2000) Macromolecules 33:1813–1818
47. Rusa CC, Rusa M, Gomez M, Shin ID, Fox JD, Tonelli AE (2004) Macromolecules 37:7992–7999
48. Hernandez R, Rusa M, Rusa CC, Lopez D, Mijangos C, Tonelli AE (2004) Macromolecules 37:9620–9625
49. Liu KL, Goh SH, Li J (2008) Macromolecules 41:6027–6034
50. Li J, Loh XJ (2008) Adv Drug Deliv Rev 60:1000–1017

51. Yui N, Ooya T (2006) Chem Eur J 12:6730–6737
52. Yui N, Ooya T, Kumeno T (1998) Bioconjugate Chem 9:118–125
53. Ooya T, Yui N (1999) J Control Release 58:251–269
54. Li J, Yang C, Li HZ, Wang X, Goh SH, Ding JL, Wang DY, Leong KW (2006) Adv Mater 18:2969–2974
55. Yang C, Wang X, Li HZ, Goh SH, Li J (2007) Biomacromolecules 8:3365–3374
56. Yang C, Li H, Wang X, Li J (2009) J Biomed Mater Res A: DOI: 10.1002/jbm.a.31976
57. Shuai XT, Merdan T, Unger F, Wittmar M, Kissel T (2003) Macromolecules 36:5751–5759
58. Loethen S, Kim JM, Thompson DH (2007) Polym Rev 47:383–418
59. Li J, Harada A, Kamachi M (1994) Polym J 26:1019–1026
60. Deng W, Yamaguchi H, Takashima Y, Harada A (2007) Angew Chem Int Ed 46:5144–5147
61. Amiel C, Sebille B (1999) Adv Colloid Interf Sci 79:105–122
62. Weickenmeier M, Wenz G, Huff J (1997) Macromol Rapid Commun 18:1117–1123
63. Wenz G, Weickenmeier M, Huff J (2000) ACS Symp Ser 765:271
64. Guo XH, Abdala AA, May BL, Lincoln SF, Khan SA, Prud'homme RK (2005) Macromolecules 38:3037–3040
65. Kretschmann O, Choi SW, Miyauchi M, Tomatsu I, Harada A, Ritter H (2006) Angew Chem Int Ed 45:4361–4365
66. Zhang ZX, Liu X, Xu FJ, Loh XJ, Kang ET, Neoh KG, Li J (2008) Macromolecules 41:5967–5970
67. Li J, Ni XP, Leong KW (2003) J Biomed Mater Res A 65A:196–202
68. Li J, Li X, Zhou ZH, Ni XP, Leong KW (2001) Macromolecules 34:7236–7237
69. Li J, Li X, Ni XP, Wang X, Li HZ, Zhou ZH (2005) Key Eng Mater 288–289:117–120
70. Ni X, Cheng A, Li J (2009) J Biomed Mater Res A: DOI: 10.1002/jbm.a.31906
71. Li J, Li X, Ni XP, Wang X, Li HZ, Leong KW (2006) Biomaterials 27:4132–4140
72. Li X, Li J (2008) J Biomed Mater Res A 86A:1055–1061
73. Li J, Li X, Ni XP, Leong KW (2003) Macromolecules 36:2661–2667
74. Li J, Ni XP, Li X, Tan NK, Lim CT, Ramakrishna S, Leong KW (2005) Langmuir 21:8681–8685
75. Li X, Mya KY, Ni XP, He CB, Leong KW, Li J (2006) J Phys Chem B 110:5920–5926
76. Jongpaiboonkit L, Zhou ZH, Ni XP, Wang YZ, Li J (2006) J Biomater Sci Polym Ed 17:747–763
77. Huh KM, Ooya T, Lee WK, Sasaki S, Kwon IC, Jeong SY, Yui N (2001) Macromolecules 34:8657–8662
78. Huh KM, Cho YW, Chung H, Kwon IC, Jeong SY, Ooya T, Lee WK, Sasaki S, Yui N (2004) Macromol Biosci 4:92–99
79. He LH, Huang J, Chen YM, Xu XJ, Liu LP (2005) Macromolecules 38:3845–3851
80. Wang ZM, Chen YM (2007) Macromolecules 40:3402–3407
81. Choi HS, Ooya T, Sasaki S, Yui N, Kurisawa M, Uyama H, Kobayashi S (2004) ChemPhysChem 5:1431–1434
82. Choi HS, Yamamoto K, Ooya T, Yui N (2005) ChemPhysChem 6:1081–1086
83. Choi HS, Kontani K, Huh KM, Sasaki S, Ooya T, Lee WK, Yui N (2002) Macromol Biosci 2:298–303
84. Joung YK, Ooya T, Yamaguchi M, Yui N (2007) Adv Mater 19:396
85. Jeong B, Bae YH, Lee DS, Kim SW (1997) Nature 388:860–862
86. Jeong B, Bae YH, Kim SW (2000) J Control Release 63:155–163
87. Kataoka T, Kidowaki M, Zhao CM, Minamikawa H, Shimizu T, Ito K (2006) J Phys Chem B 110:24377–24383
88. Fleury G, Schlatter G, Brochon C, Hadziioannou G (2005) Polymer 46:8494–8501
89. Okumura Y, Ito K (2001) Adv Mater 13:485–487
90. Takata T (2006) Polym J 38:1–20
91. Ito K (2007) Polym J 39:489–499
92. Watanabe J, Ooya T, Park KD, Kim YH, Yui N (2000) J Biomater Sci Polym Ed 11:1333–1345
93. Ichi T, Watanabe J, Ooya T, Yui N (2001) Biomacromolecules 2:204–210

94. Watanabe J, Ooya T, Nitta KH, Park KD, Kim YH, Yui N (2002) Biomaterials 23:4041–4048
95. Ichi T, Ooya T, Yui N (2003) Macromol Biosci 3:373–380
96. Feng ZG, Zhao SP (2003) Polymer 44:5177–5186
97. Wei HL, He JY, Sun LG, Zhu KQ, Feng ZG (2005) Eur Polym J 41:948–957
98. Wei HL, Zhang AY, Qian LJ, Yu HQ, Hou DD, Qiu RX, Feng ZG (2005) J Polym Sci Pol Chem 43:2941–2949
99. Wei HL, Yu HQ, Zhang AY, Sun LG, Hou DD, Feng ZG (2005) Macromolecules 38: 8833–8839
100. Zhao SP, Zhang LM, Ma D, Yang C, Yan L (2006) J Phys Chem B 110:16503–16507
101. Yu HQ, Feng ZG, Zhang AY, Sun LG, Qian LJ (2006) Soft Matter 2:343–349

Molecular Processing of Polymers with Cyclodextrins

Alan E. Tonelli

Abstract We summarize our recent studies employing the cyclic starch derivatives called cyclodextrins (CDs) to both nanostructure and functionalize polymers. Two important structural characteristics of CDs are taken advantage of to achieve these goals. First the ability of CDs to form noncovalent inclusion complexes (ICs) with a variety of guest molecules, including many polymers, by threading and inclusion into their relatively hydrophobic interior cavities, which are roughly cylindrical with diameters of $\sim 0.5 - 1.0$ nm. α-, β-, and γ-CD contain six, seven, and eight α-1,4-linked glucose units, respectively. Warm water washing of polymer-CD–ICs containing polymer guests insoluble in water or treatment with amylase enzymes serves to remove the host CDs and results in the coalescence of the guest polymers into solid samples. When guest polymers are coalesced from the CD–ICs by removing their host CDs, they are observed to solidify with structures, morphologies, and even conformations that are distinct from bulk samples made from their solutions and melts. Molecularly mixed, intimate blends of two or more polymers that are normally immiscible can be obtained from their common CD–ICs, and the phase segregation of incompatible blocks can be controlled (suppressed or increased) in CD–IC coalesced block copolymers. In addition, additives may be more effectively delivered to polymers in the form of their crystalline CD–ICs or soluble CD–rotaxanes. Secondly, the many hydroxyl groups attached to the exterior rims of CDs, in addition to conferring water solubility, provide an opportunity to covalently bond them to polymers either during their syntheses or via postpolymerization reactions. Polymers containing CDs in their backbones or attached to their side chains are observed to more readily accept and retain additives, such as dyes and fragrances. Processing with CDs can serve to both nanostructure and functionalize polymers, leading to greater understanding of their behaviors and to new properties and applications.

A.E. Tonelli (✉)
Fiber & Polymer Science Program, North Carolina State University, Campus Box 8301,
Raleigh, NC 27695-8302, USA
e-mail: alan_tonelli@ncsu.edu

Keywords Additives, Blends, Complexation processing, Cyclodextrins, Polymers, Threading

Contents

1   Introduction

Though cyclodextrins (CDs) had long been known to form both soluble and crystalline inclusion compounds (ICs) with a variety of small molecule guests, Harada and Kamachi first demonstrated in 1990 [1], using poly(ethylene oxide) (PEO) oligomers, that noncovalent bonded crystalline ICs could be formed between guest polymers and host CDs as well. This is accomplished by threading of the guest polymers through the CD cavities to form polymer threaded crystalline stacks, as illustrated in Fig. 1f. CDs are cyclic molecules formed by six (α-CD), seven (β-CD), and eight (γ-CD) α-1,4-linked glucose units, with internal hydrophobic cavities of $\sim$0.5 $-$ 1.0 nm in diameter (Fig. 1a). Their 18–24 hydroxyl groups are located on the CD rims making them soluble in water.

Since the middle of the 1990s our research group has formed a large number of crystalline CD–ICs [2–70] containing either high molecular weight guest polymers or small-molecule guests that can serve as polymer additives (Fig. 1c–f). The motivation for our studies is threefold. First, polymer chains included in CD–ICs are necessarily both highly extended and isolated from neighboring chains, because they are threaded through and confined in the narrow CD channel cavities (see Fig. 1a, f). As suggested in Fig. 2, if the host CDs in polymer-CD–ICs are carefully removed and the guest polymer chains are permitted to coalesce into a bulk solid sample, then
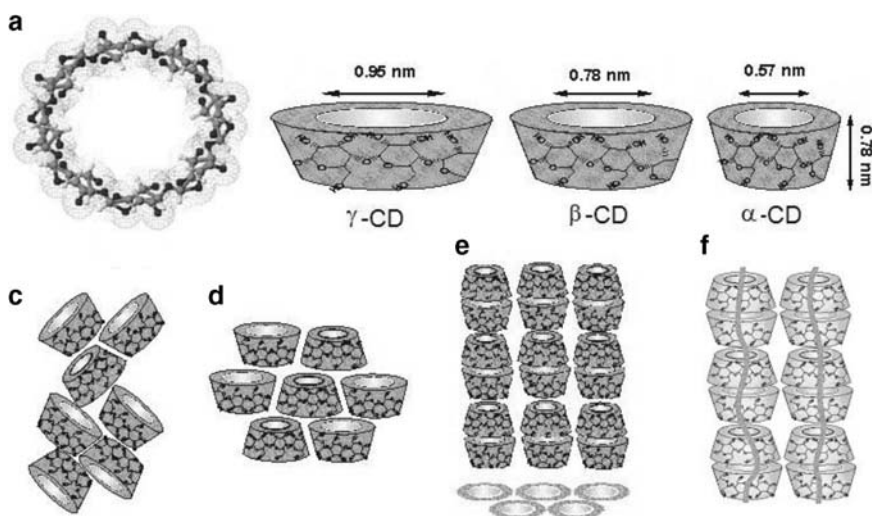
Fig. 1 (**a**) γ-CD chemical structure and approximate dimensions of α-, β-, and γ- CDs; schematic representation of packing structures of (**c**) cage-type, (**d**) layer-type, and (**e**) head-to-tail channel-type CD crystals; and (**f**) CD–IC channels containing included polymer guests
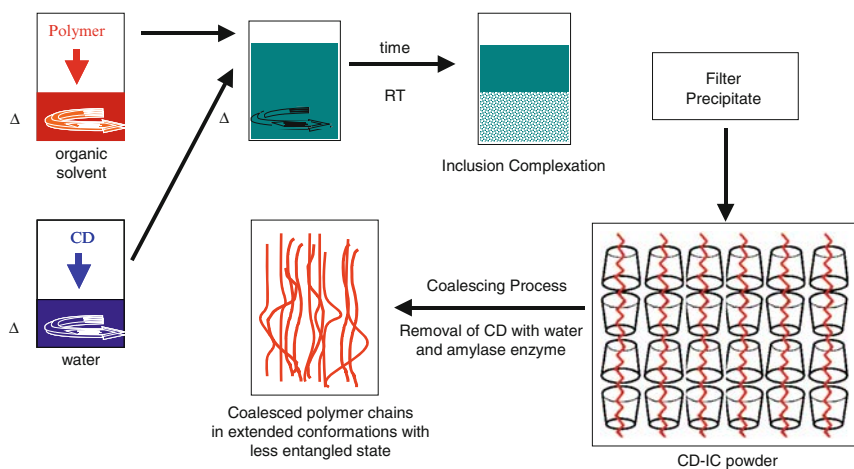

Fig. 2 Schematic representation of polymer-CD IC formation, the coalescence process, and the coalesced polymer

it can be reasonably expected that the arrangement of chains, or their packing, might be significantly different from those normally produced from their randomly coiling and entangled solutions or melts. This expectation has been confirmed numerous times in our laboratory.

Processing with CDs can serve to both nanostructure and functionalize polymers, leading to greater understanding of their behaviors and to new properties and

applications. In fact, we generally observe upon coalescence from their CD–ICs that (1) crystallizable homopolymers evidence increased levels of crystallinity, unusual polymorphs, and higher melting, crystallization, and decomposition temperatures, while amorphous homopolymers exhibit higher glass-transition temperatures, than samples consolidated from their disordered solutions and melts; (2) molecularly mixed, intimate blends of two or more polymers that are normally believed to be immiscible can be obtained from their common CD–ICs, (3) the phase segregation of incompatible blocks can be controlled (suppressed or increased) in coalesced block copolymers, and (4) the thermal and temporal stabilities of the coalesced and well-mixed homopolymer blends and block copolymers appear to be substantial, thereby suggesting retention of their as-coalesced structures and morphologies under normal thermal processing conditions.

Because crystalline CD–ICs are high-melting and thermally stable, even when containing small-molecule guests that are volatile liquids or even gases in the bulk, delivery of additives to polymer materials can be improved by using additive-CD–ICs, which may often be conveniently melt-processed into polymers. If we begin with appropriate soluble CD–ICs formed with polymer additives and then react the free ends of the included additive with capping groups that prevent it from unthreading, we create CD–rotaxanated additives. One advantage of additive-CD–rotaxanes is the protection (thermal, chemical, UV–Vis, etc.) afforded by their CD coats. Another is the ability to utilize the many hydroxyl groups on the CD coat to target the delivery of the CD-additive–rotaxane to a particular polymer substrate.

Our second motivation for utilizing CDs with polymers is to alter their functionalities through incorporation of CDs into their backbones during polymerization or to attach them to polymer side chains via postpolymerization reactions. The presence of covalently bonded CDs in polymers serves to increase their acceptance and retention of additives, such as dyes, fragrances, antibacterials, etc. They may also be further reacted or treated through their covalently bonded CDs to cross-link and form networks or to form blends with other polymers having a propensity to thread through their attached CD cavities.

Thirdly, CDs are nontoxic, biodegradable, and bioabsorbable, and, as such, may be used in medical applications and as materials more friendly to the environment.

As indicated above, in this report we summarize our recent studies employing cyclodextrins (CDs) to both nanostructure and functionalize polymer materials.

2 Experimental

2.1 Polymer-CD–ICs

CD–ICs formed with polymer guests are crystalline solids (see Fig. 1f), which may be formed by mixing host CD solutions (usually aqueous) with guest polymer solutions (usually nonaqueous and organic) with the aid of heating, stirring, and

sonication [6]. Solid CDs may also be suspended in polymer solutions [24, 41, 71] or neat bulk liquid polymers [45, 72] to form polymer-CD–ICs. Because native CDs with only water of hydration included in their cavities assume herringbone or brick-type crystal structures illustrated in Fig. 1c, d, while polymer-CD–ICs assume the very different columnar, channel structure shown in Fig. 1e, f, X-ray diffraction is utilized to test for successful polymer-CD–IC formation. This is supplemented by DSC, FTIR, and solid-state ^{13}C-NMR observations to confirm that polymer is present and included in the CD–ICs formed.

Warm water washing of polymer-CD–ICs containing polymer guests insoluble in water or treatment with amylase enzymes serves to remove the host CDs and results in the coalescence of the guest polymers into solid samples. X-ray diffraction, DSC, TGA, and FTIR and NMR spectroscopies are typically used to characterize the coalesced polymer samples.

2.2 Additive-CD–ICs and –Rotaxanes

Crystalline CD–ICs with low molecular weight additive guests, both soluble and crystalline, may be prepared [7, 9, 13, 17, 52, 53, 65, 68–70] by virtually the same means as polymer-CD–ICs. Corresponding soluble CD–rotaxanes can be obtained from soluble CD–ICs, by attaching bulky end-groups to both ends of the included additive or by extending the CD cavity, thereby preventing the unthreading of the additive. An example of the synthetic route for obtaining an azo-dye-α-CD–rotaxane will be subsequently discussed.

3 Nanostructuring/Functionalizing Polymers via CD–IC Formation and Coalescence and Additive Delivery with Additive-CD–ICs and –Rotaxanes

3.1 Nanothreading of Polymers [55, 73, 74]

Before presenting and discussing our results concerning the processing of polymers with CDs, it seems appropriate to discuss several experiments designed to determine those factors important to the nanothreading of polymers with CDs during the process of forming polymer-CD–ICs, and which were recently summarized [55, 73, 74]. These include (1) the competitive CD threading of polymers with different chemical structures and molecular weights from their solutions containing suspended solid or dissolved CDs, (2) the threading and insertion of undiluted liquid polymers into solid CDs, and (3) suspension of IC crystals containing polymer A or B in a solution of polymer B or A and observation of the exchange of polymers between the solution

and the CD–IC crystals, without dissolution of the CD–ICs. The reader is also referred to the recent work of Gerhard Wenz [75].

3.1.1 Competitive Threading

Two studies were conducted to probe the potential for using the complexation of polymers with CDs as a means to separate them according to their molecular weight (MW) or chain lengths [11, 15]. In the first investigation two poly(ethylene glycol) (PEG) samples, with MW = 600 (PEG600) and 20,000 (PEG20000) and narrow MW distributions of 1.1 and 1.34, respectively, were dissolved in water and added to an aqueous solution of α-CD to form PEG-α-CD–ICs. α-CD–ICs were separately formed with PEG600, PEG20000, and with various mixtures of the two PEG samples. By comparing the viscosities of their solutions after filtering off the PEG-α-CD–ICs formed, it was found that the PEG-α-CD–IC formed from an equimolar PEG600/PEG20000 solution, using enough α-CD to complex either all of one or half of each PEG, contained 80% of the higher molecular weight PEG20000.

The second study compared the α-CD–ICs formed in solution with poly(ε-caprolactone) (PCL) and hexanoic acid (HA), which closely mimics the PCL repeat unit [15]. FT–IR observations of the α-CD–ICs formed with PCL, HA, and PCL/HA mixtures were used to determine the presence of PCL and HA guests (PCL and HA C = O stretching bands at 1,734 and 1,714 cm^{-1}, respectively). Both guests were observed to be equally present in the α-CD–ICs when equal amounts of PCL and HA were mixed with enough α-CD to complex both guests. However, when half the amount of α-CD was used, i.e., enough to complex all of the PCL, or all of the HA, or half of each, PCL was observed to be predominantly included.

Thus, both studies showed a preference for the inclusion of the longer, higher MW guest polymer, irrespective of their very different chemical natures: PEGs are hydrophilic and soluble in water, while PCL and HA are not. This suggests that the formation of α-CD–ICs in solution with both PEG and PCL guests may be dominated by the kinetics of the process, which favors higher MW, longer guests. It was suggested that longer polymer chains partially threaded with CDs would nucleate the growth of polymer-CD–IC crystals more readily than partially threaded shorter chains, because the unthreading of CDs from the longer chains would be slower or retarded compared with the unthreading of CDs from the shorter chains.

The dependence of CD–IC formation from solution for polymers with different stereosequences was investigated for isotactic (i) and atactic (a) poly(3-hydroxy-butyrates) (i-PHB and a-PHB) [26]. i-PHB was found to form an IC with α-CD, but not with β- or γ-CDs, while only γ-CD formed an IC with a-PHB. From these observations it was concluded that extended conformations available to i-PHB were too narrow, thin for a tight-packing fit with β- or γ-CDs, while the much wider, thicker extended conformations available to a-PHB chains precluded their inclusion in the narrower α- and β-CDs, but fit tightly in the more spacious channels of its IC formed with γ-CD.

The solution complexation of PCL and the related aliphatic polyester poly(L-lactic acid) (PLLA) with CDs was studied [29]. PCL was observed to be able to form ICs with both α- and γ-CDs, with the latter containing two PCL chains in each γ-CD channel, while only α-CD formed an IC with PLLA. When a solution containing equivalent amounts of PCL and PLLA was added to an aqueous solution containing enough α-CD to complex with all of the PCL, or all of the PLLA, or half of each, only PCL-α-CD–IC was formed. Furthermore, when a PCL solution was added to an aqueous solution containing the same molar quantities of α- and γ-CDs, each sufficient to fully complex with the added PCL, only PCL-α-CD–IC was formed. These observations led to the following tentative conclusions: (1) interactions between extended and included PCL chains and α-CD may be more favorable than the average of the interactions between the two parallel side-by-side PCL chains included in PCL-γ-CD–IC and the two included PCL chains with γ-CD, or the double-threading of PCL chains required to form the PCL-γ-CD–IC might retard the kinetics of its formation, (2) interactions between included PCL chains and α-CD channels are more favorable than those involving PLLA, (3) differences in PCL/solvent and PLLA/solvent interactions are not important, and (4) the preference of PCL over PLLA inclusion by α-CD is not a consequence of a difference in the cross-sections of their extended conformations nor a difference in the kinetics of their threading by α-CD, because the PLLA sample consisted of longer chains than the PCL sample.

3.1.2   Threading of Polymers into Solid CDs

We have discovered a simple precipitation method for forming solid CDs in an empty channel structure, CD_{CS} (see Fig. 1e), containing no complexed guest aside from water of hydration [24, 71]. When propionic acid (PA), which in solution forms a cage structure α-CD–IC (see Fig. 1c) with dissolved α-CD, is dissolved in a nonsolvent for α-CD and $α$-CD_{CS} is suspended therein, PA entered $α$-CD_{CS} and transformed it to a cage structure PA-α-CD–IC. However, when $α$-CD_{CS} was vacuum-dried before suspension in the same PA solution, a columnar structure PA-α-CD–IC was formed. Clearly the role of water, some of which is displaced from the air-dried $α$-CD_{CS} channels upon inclusion of PA, is important in the formation of CD–ICs, as well as the packing interactions between host α-CDs. Apparently the vacuum drying of a-CD_{CS} stabilizes the packing of α-CDs in the columnar structure, because as PA is included, the solid state transformation to a cage structure PA-α-CD–IC is prevented. α- and γ-CD–ICs formed with PCL were suspended in acetone and aqueous solutions of γ- and α-CDs, respectively [29]. In the first case nothing happened, but in the second case the PCL chains in suspended PCL-γ-CD–IC dissociated, unthreaded, and were instead complexed with α-CD to form PCL-α-CD–IC.

In another set of experiments [29], PCL- and PLLA-α-CD–ICs were suspended in dioxane solutions initially containing dissolved PLLA and PCL, respectively. After several days the suspended α-CD–ICs crystals were filtered out and observed by FT–IR (distinct C = O absorption bands of PCL and PLLA) to determine whether

PCL, PLLA, or both were included. The α-CD–IC resulting from the suspension of PLLA-α-CD–IC in the PCL solution was found to contain only PCL guest chains, while the α-CD–IC resulting from the suspension of PCL-α-CD–IC in the PLLA solution contained only a very small amount of PLLA guest chains. The above results were interpreted to signify the importance of both guest polymer hydrophobicity and guest/host steric compatibility in the formation of polymer-CD–ICs.

The ability of poly(N-acylethylenimine) (PNAI) to be complexed from its solutions containing suspended cage and columnar structure γ-CDs was investigated [41]. PNAIs with two different MWs were synthesized and two different PNAI solvents (acetone and chloroform) were employed. Complexation of the PNAIs from solutions containing suspended γ-CDs was directly monitored by ^{1}H NMR, as shown in Fig. 3. The time-dependent intensities of PNAI and water ^{1}H resonances were observed and permitted an evaluation of the kinetics of the PNAI inclusion.

In the acetone solutions the inclusion of PNAIs by columnar γ-CD$_{CS}$ was greater in both quantity and speed than for cage γ-CD (Fig. 4). In both cases PNAI inclusion was accomplished without any dissolution of the suspended γ-CDs, because
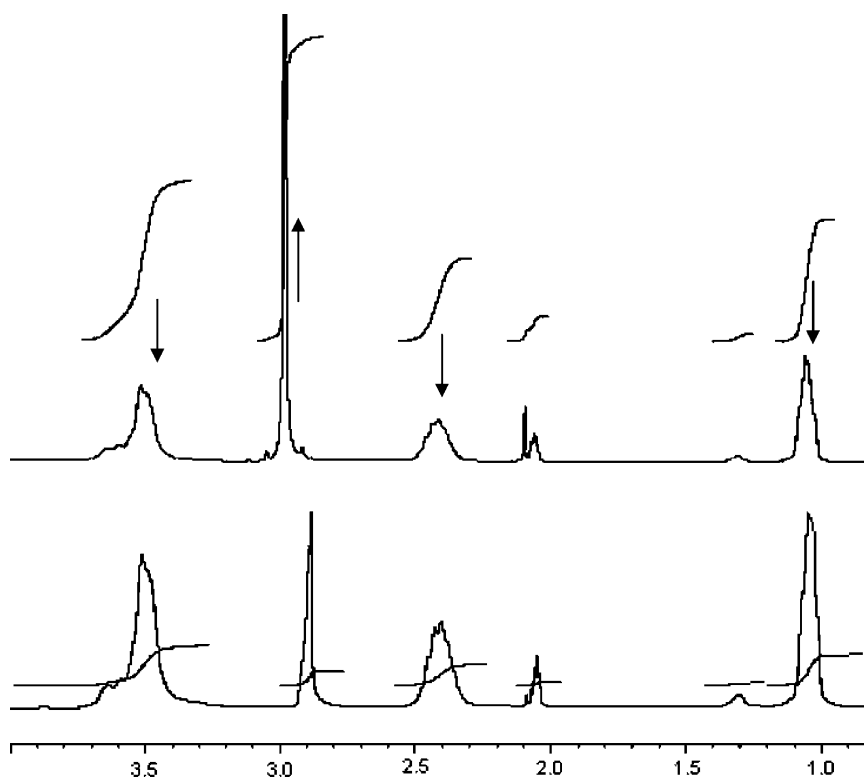

Fig. 3 Time-dependent ^{1}H-NMR spectra of PNAI-1 in acetone solution containing settled, initially cage structure γ-CD: *bottom* (initial); *top* (after 90 h). *downward arrow*, *upward arrow* = decreasing, increasing PNAI, H$_2$O peak intensities
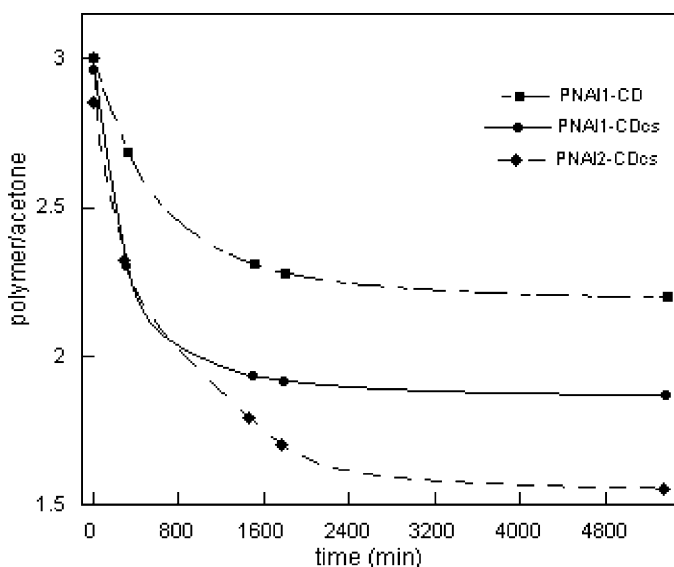
Fig. 4 Decrease of polymer peak intensities with time as a result of inclusion in cage γ-CD or in columnar $\gamma - CD_{CS}$. PNAI2 has a higher molecular weight than PNAI1

[1]H resonances were never observed for dissolved γ-CDs. In comparison to the lower MW sample, more of the higher MW PNAI was included in γ-CD_{CS}, but the rate of PNAI inclusion was the same for both samples. Of the six water molecules residing in the channels of each γ-CD_{CS} [24,71], only two were observed to be removed upon inclusion of the PNAI guest chains. Furthermore, when the γ-CDs were suspended in chloroform solutions of the PNAIs, no ejection of hydration water nor inclusion of PNAI chains was observed.

Thus, the inclusion of PNAIs in suspended γ-CDs was both thermodynamically and kinetically preferred in the case of γ-CD_{CS}, while the inclusion of high MW PNAI is apparently thermodynamically favored. Using chloroform as a solvent for PNAI and as a suspension medium for the γ-CDs prevented PNAI inclusion, presumably because of the unfavorable environment provided by chloroform for the potentially displaced and ejected water. By comparison to the estimated increase in conformational free energy experienced by randomly coiling polymers as they are extended and confined in γ-CD channels [76], which is mainly entropic in origin, it could be estimated that each water molecule ejected during PNAI inclusion in γ-CD_{CS} must lower its free energy by at least $\sim 1 \, \text{kcal mol}^{-1}$ to offset the loss of conformational entropy of the included polymer.

PEG oligomers (MWs = 200 and 400), which are liquids at room temperature, were mixed with solid, native cage structure α-CD and observed by X-ray diffraction to convert to columnar structure PEG-α-CD_{CS} [45,72]. An example is presented in Fig. 5, where the scattering peaks at 2θ $\sim$ 12 and $\sim 20°$, characteristic [6] of cage α-CD and columnar α-CD_{CS}, respectively, are observed to decrease and increase
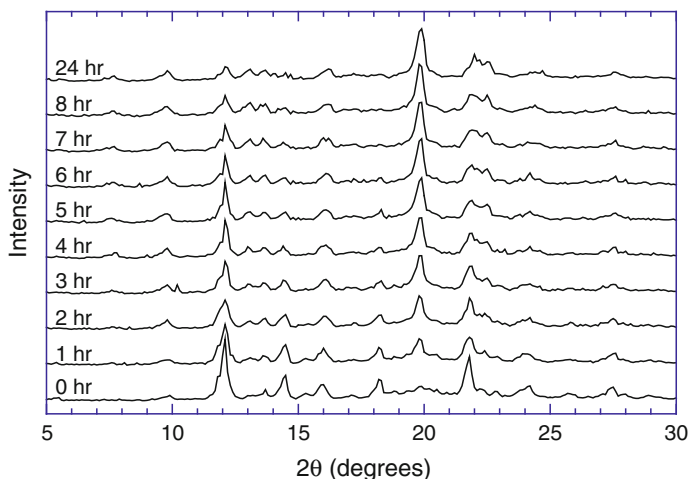
Fig. 5 Time-dependent diffractometer scans for a 2:1 mixture of PEG200:α-CD obtained at 20°C [45, 72]

over time as the liquid PEG threads into the solid α-CD crystals. Both the time and temperature dependences of the solid-state conversion of cage to columnar structure α-CD through inclusion of bulk liquid PEG oligomers were investigated. An activation energy of $8.3\,kcal\,mol^{-1}$ of α-CD was determined from the observed temperature dependence of inclusion kinetics. Increasing the PEG/α-CD ratio increased the rate of PEG inclusion, while increasing the MW of PEG slowed the inclusion. Drying the as-received cage structure α-CD before mixing with the PEG oligomers had little effect on the rate of PEG inclusion. More recent observations indicate that the rate and extent of PEG inclusion may be affected by the degree of α-CD hydration [77].

In addition, native cage α-CD was suspended in acetone solutions of the PEGs, and its solid-state conversion to channel structure as PEG chains were included and formed PEG-α-CD–IC crystals was observed by solution ^{1}H NMR. The rate of PEG inclusion from solution was ∼10-times faster than the rate observed for the neat PEGs, even though the PEG concentration in solution was only ∼1% that of neat PEG.

These observations may be generally summarized as follows: as the mobility of PEG increases, i.e., moving from neat to dissolved PEG and/or from higher to lower MW, so does the rate of inclusion of PEG into suspended cage α-CD via the solid–solid cage-to-columnar crystal structure transition. Since drying the as-received cage structure α-CD did not affect the rate of its transition to columnar α-CD, α-CD$_{CS}$, by the inclusion of neat PEG, apparently this process is not sensitive to the internal hydration level of the suspended cage structure α-CD. However, the water vapor content in the atmosphere surrounding the solid α-CD and liquid PEG was recently shown [77] to have a significant effect.

The inclusion of neat and dissolved PEG oligomers into suspended columnar α-CD$_{CS}$, was preliminarily observed by DSC and solution ^{1}H NMR [45, 72] to proceed at much faster rates than inclusion by suspended cage structure α-CD, because of the absence of the need to transform the solid-state packing of α-CDs upon inclusion of PEG. As a consequence, analysis of the temperature-dependent kinetics of PEG oligomer inclusion in α-CD$_{CS}$ enabled [76] an experimental assessment of the free energy change experienced by randomly coiling PEG oligomers as they are extended and thread into the narrow α-CD$_{CS}$ channels.

Extension of the investigations summarized here should eventually permit a more complete answer to the question "Why do randomly coiling polymer chains in solution or the neat melt become threaded or thread into the nano-pores of dissolved or solid CDs, where they are highly extended and segregated from other polymer chains?" However, we can currently conclude that electrostatic, van der Waals, and hydrogen-bonding interactions and relief of conformational strain in CDs are not important, while hydrophobic interactions, exclusion of high energy, cavity-bound water, and crystalline packing of host CDs are important in the formation of polymer-CD–ICs.

4 Polymers Coalesced from their CD–ICs

4.1 Homopolymers Coalesced from their CD–ICs

4.1.1 Poly(ethylene terephthalate) [21, 33, 59]

When PET chains are included in the ∼1.0 nm channels of its γ-CD–IC [21] they adopt kink conformations, as drawn in Fig. 6, which are nearly as extended, but are narrower in cross-section than the crystalline all trans PET conformation also shown. Upon coalescence from its γ-CD–IC, PET rapidly crystallizes, achieving
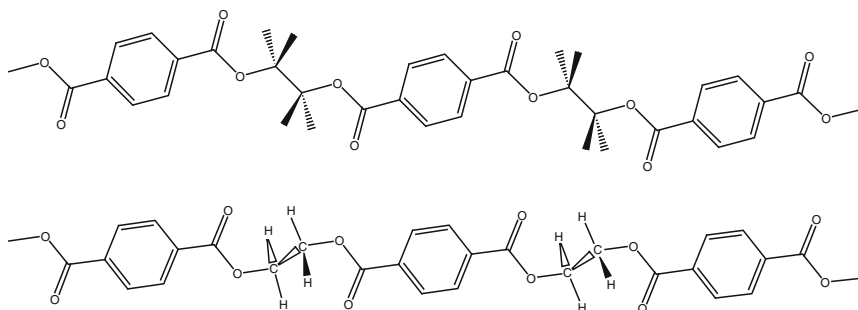

Fig. 6 All trans (*top*) and g±tg∓ kink (*bottom*) conformations of crystalline and IC-included PET chains, respectively

Table 1 PET Film Densities [59]

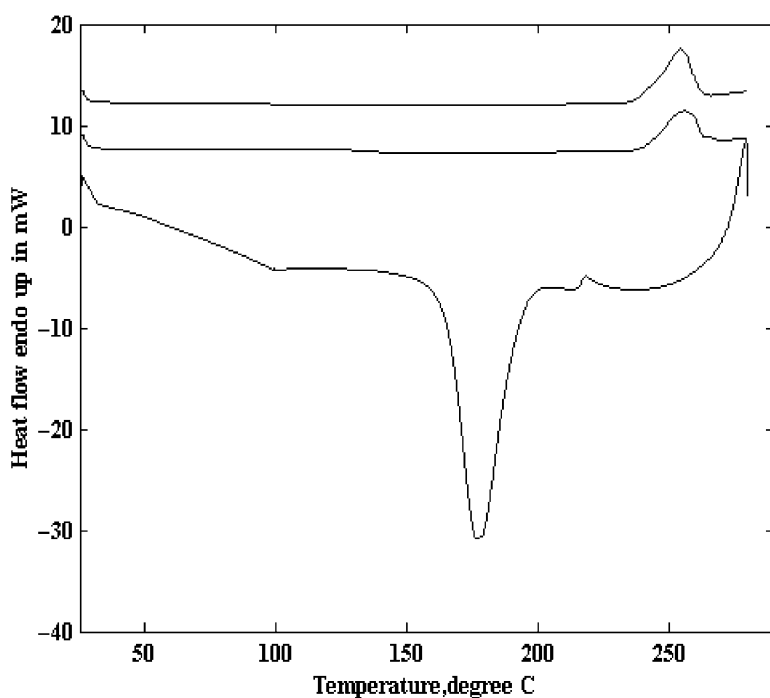| Sample	Density $(\rho)[\mathrm{g\,cm^{-3}}]$	Crystallinity from DSC	Crystallinity from X-ray
Coalesced PET	1.3670	0.39	0.32
Annealed as-received PET	1.3497	0.39	0.31
As-received PET	1.3497	0.10	0.06

Fig. 7 DSC thermogram of coalesced PET. First (*upper*), second (*middle*) heating and (*lower*) interim cooling scans. (Note that the heat flow units on the ordinate are only appropriate for the cooling scan and that the magnitudes of the melting endotherms and crystallization exotherm obtained from them are actually nearly identical.) PETs normally processed from their solutions and melts, on the other hand, do not evidence recrystallization upon rapid cooling ($-200°\mathrm{C\,min^{-1}}$) from their melts [33]

∼40% crystallinity (see Table 1, for typical levels of crystallinity in PET), while solid-state FTIR and NMR observations presented later [21, 33] indicate that the PET chains in the noncrystalline regions of coalesced PET largely retain their included kink conformations.

The reorganized morphology of the coalesced PET is manifested in its thermal behavior, as presented in the DSC scans shown in Fig. 7. Note that no glass-transition or crystallization is observed in either heating scan, with the former observation receiving support from temperature-dependent solid-state NMR relaxation

observations discussed below [33]. Instead, both heating scans simply evidence a large melting endotherm, indicating substantial crystallinity for the coalesced PET both after coalescence and subsequent to rapid cooling from the melt. In summary, including PET chains in and coalescing them from its γ-CD–IC has reorganized them into a sample that is repeatedly and rapidly crystallizable from its melt, with noncrystalline regions that do not show a T_g, behavior that is normally very uncharacteristic of usually amorphous and slow to crystallize PET.

This contrasting thermal behavior for coalesced and normal PETs is further emphasized in the density results presented in Table 1. There the densities measured for as-received PET before and after high temperature annealing (110°C for 30 min) are compared with the density of the coalesced sample. Not surprisingly the densities of both the annealed and coalesced samples are higher than that of the as-received PET, because the former samples are more crystalline than the latter one. What is initially surprising, however, is even though the annealed and coalesced PET samples have closely similar levels of crystallinity, the density of the coalesced sample is much higher. Thus, it appears that the PET chains in the noncrystalline regions of the coalesced PET film are more densely packed (by ∼1.4%) than in the amorphous regions of the annealed PET film, even though each film is ∼65% noncrystalline. The coalesced PET film has a higher density noncrystalline phase, because there the chains are more extended and tightly packed, and possibly more oriented, with a higher trans conformer content for the -CH_2–CH_2- bonds (FTIR results presented below [21]). In fact, the density estimated for the noncrystalline regions in coalesced PET ($\rho_{nc} = 1.354\,\mathrm{g\,cm^{-3}}$) exceeds slightly the overall density of the annealed PET film ($1.3497\,\mathrm{g\,cm^{-3}}$).

In Fig. 6 both the all trans crystalline conformation of PET and noncrystalline, though also highly extended, kink conformation of PET are drawn. PET chains in the narrow channels of its γ-CD–IC crystals adopt the kink conformations, which after coalescence were also demonstrated to persist in the noncrystalline regions [21, 33, 59]. PET kink conformers have been suggested to occupy only ∼2/3 of the volume occupied by the all trans crystalline PET conformation [78]. If the kink conformers also dominate the noncrystalline regions of coalesced PET, then the observation that $\rho_{nc} = 1.354\,\mathrm{g\,cm^{-3}}$ exceeds the overall density of annealed PET, $\rho_{anneal} = 1.3497\,\mathrm{g\,cm^{-3}}$, may be understood. In addition, the kink conformations adopted by PET included in its γ-CD–IC may upon coalescence be easily and rapidly converted into the crystalline all trans conformation solely by facile counter rotations about the -O–CH_2- and -CH_2–O- bonds, a conformational transformation producing little swept out volume and resulting in a highly crystalline sample. Largely amorphous as-received PET, on the other hand, is slow to crystallize, because its largely gauche -CH_2–CH_2- bonds must be rotated to the trans conformation during crystallization, a conformational transformation that must sweep out a large volume [21].

The FTIR spectra (Fig. 8) of as-received and solution-cast PET samples, although very similar, are clearly distinct from the spectrum of coalesced PET. The most noticeable difference is the much improved resolution observed in the spectrum of PET coalesced from its γ-CD–IC, in which nearly every vibrational absorption,
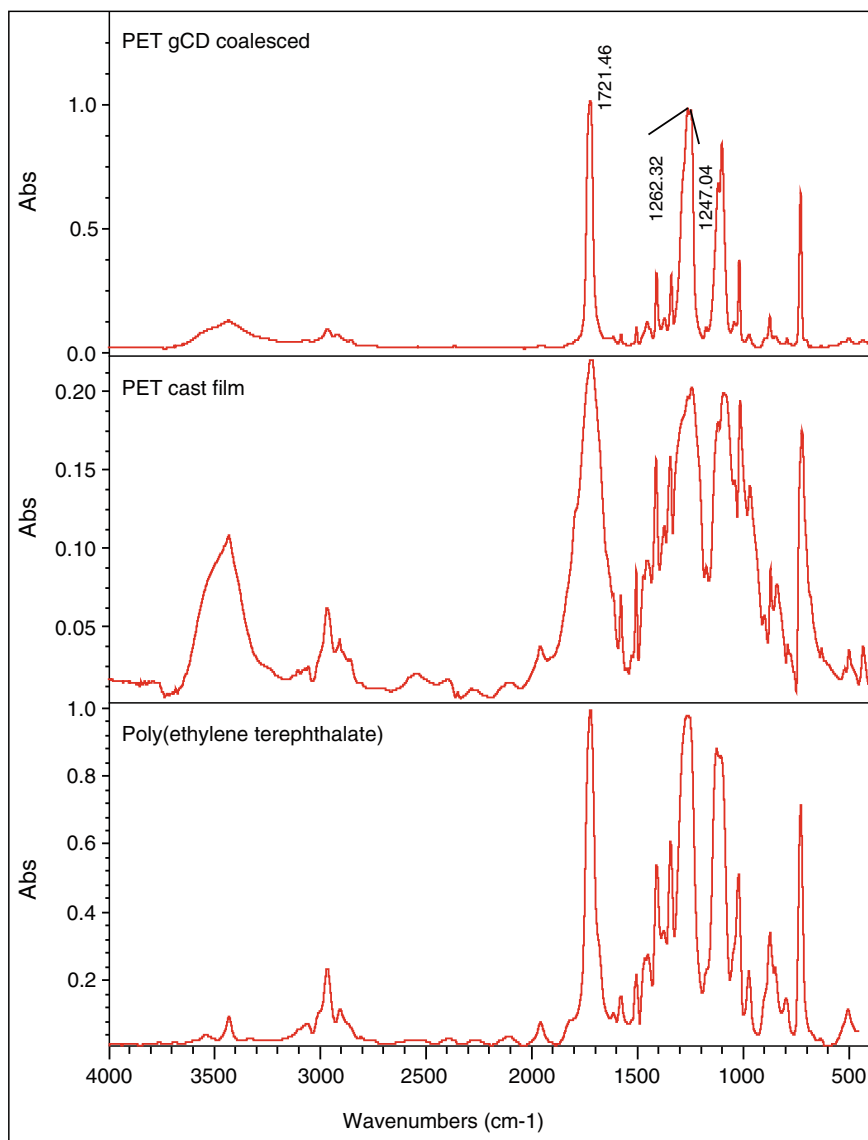
Fig. 8 FTIR spectra of as-received PET (melt-extruded pellets [21]), solution-cast PET, and IC-coalesced PET samples, from *bottom* to *top*, respectively [21]

except those likely contributed by residual γ-CD or H$_2$O above 3,200 cm^{-1}, is resolved to the baseline. This improved resolution may be a result of the already suggested improved order in the noncrystalline regions of the sample; the chains are not as nearly randomly coiling or interpenetrating as those in the noncrystalline regions of the as-received and solution-cast samples and, as a result, do not exhibit

a glass transition (DSC and solid-state NMR [33] below). The generally broad IR bands observed in polymer samples are undoubtedly due to the large variety of polymer conformations and chain-packing environments surrounding each vibrating molecular bond or group. Because of the improved order in the noncrystalline regions of the coalesced PET, vibrating molecular bonds and groups are subjected to smaller variations in their local conformational and packing environments.

For example, a clear doublet band can be seen at 1,247 and 1,262 cm^{-1} in the coalesced PET spectrum, possibly reflecting crystal or correlation field splitting generally produced by short-range interchain interactions [79, 80] between closely packed molecules in their crystals. Because both X-ray (not shown [21]) and DSC observations indicate very similar crystal structures for the solution-cast and coalesced PET samples, this vibrational band splitting may instead be occurring in the noncrystalline regions of the coalesced sample, as a result of distinct short-range interactions between pairs of PET chains adopting the highly extended narrow and noncrystalline kink conformations, which may permit PET chains to be in closer contact than the all-trans chains in their crystals. In fact, these vibrations have been associated [81] with the terephthaloyl residues of PET in the amorphous sample portions [82], with the 1,247 cm^{-1} vibration appearing as a shoulder on the 1,262 cm^{-1} band. Because these bands appear as a distinct doublet in the coalesced PET spectrum, a more homogeneous population of conformations is suggested for the noncrystalline chains, which are also apparently quite tightly packed with the terephthaloyl residues of neighboring chains in close proximity. The distinct morphologies of melt-crystallized as-received and coalesced PETs are made clear in Fig. 9, where their polarized micrographs are presented. Though both samples were crystallized from their melts, more uniformly distributed much smaller crystallites are evident in the coalesced PET sample. The as-received PET formed typical large spherulites after crystallization from the melt, which have spherical shapes and dark crosses through their centers when viewed with polarized light. The average size of the as-received PET spherulites is about 25 µm. In contrast, the morphology of PET coalesced from its γ-CD inclusion complex and subsequently crystallized from its melt shows a distinct crystal pattern without clear spherical shapes. Under polarized light, the coalesced, melt-crystallized PET shows much less dark areas than the as-received PET, although both samples were crystallized from their melts under the same conditions.

Because the crystallization of polymers from their melts is related to their microstructural properties, such as chain conformations and entanglements [83], the polarized light microscopy results suggests a molecular-level difference between the coalesced and as-received PETs even in their melts.

In Fig. 10 the high-resolution ^{13}C-NMR spectra observed for various solid PET samples are presented [33]. Consistent with our molecular modeling [78, 84] and FTIR [21] results, the solid-state NMR spectra indicate that as-received PET has predominantly g± -CH$_2$–CH$_2$- bonds and substantial amounts of t -CH$_2$–O- and -O–CH$_2$- bonds, while coalesced, included, and precipitated PETs have preponderantly t -CH$_2$–CH$_2$- and g± -CH$_2$–O- and -O–CH$_2$- bonds. (Details are presented as part of [33]).
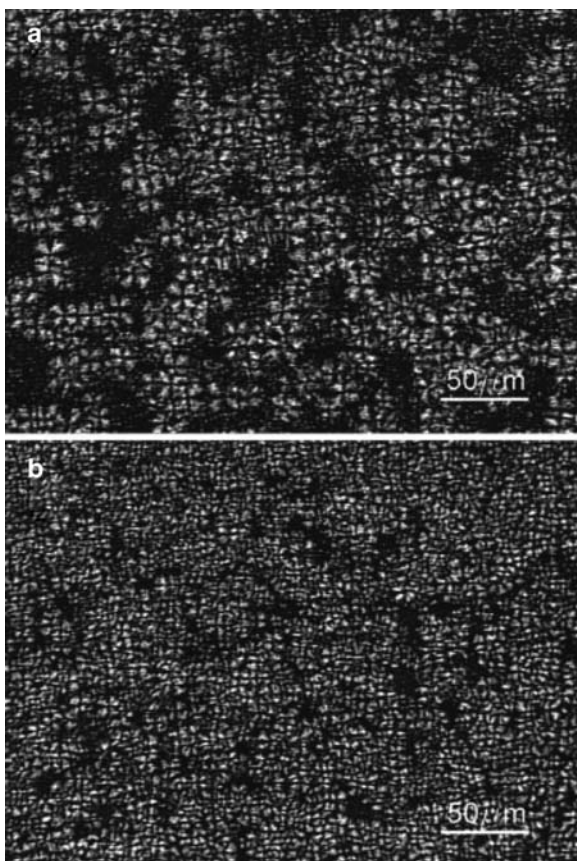
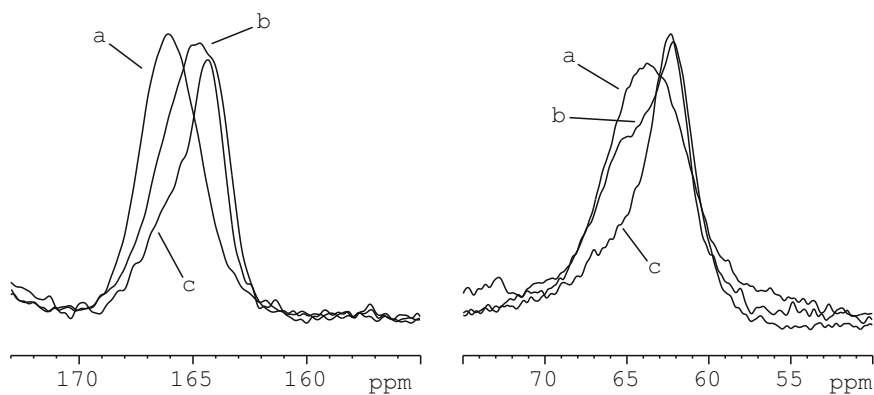**Fig. 9** Polarized light micrographs of melt-crystallized (**a**) as-received PET and (**b**) coalesced PET [33]

Fig. 10 Methylene carbon ($\sim$60–65 ppm vs. TMS) and carbonyl carbon ($\sim$163–168 ppm vs. TMS) resonance peaks for PETs: (**a**) as received PET; (**b**) precipitated PET; (**c**) coalesced PET or PET-γ-CD–IC [33]
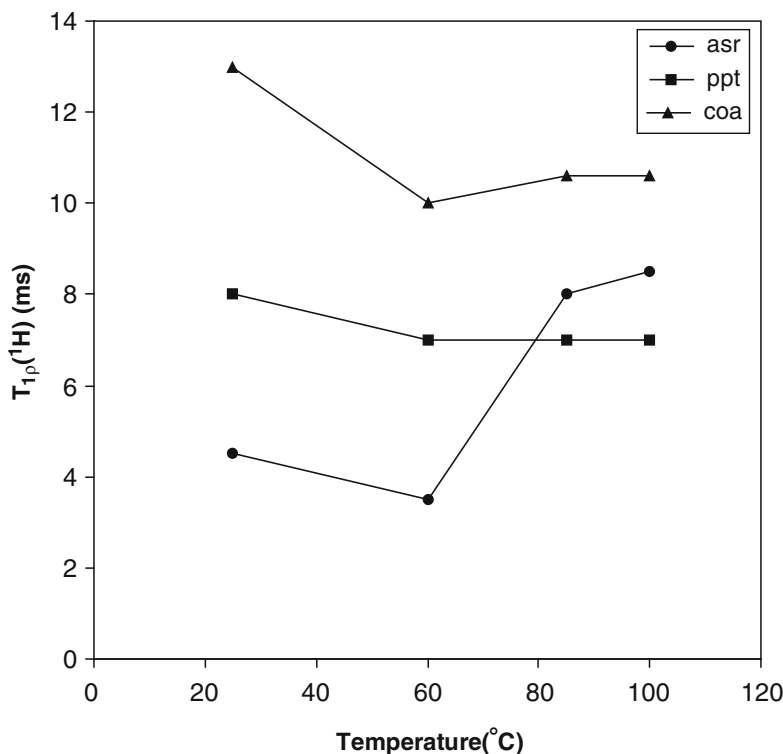
Fig. 11 Dependence of ^{1}H rotating-frame relaxation times $T^1_{1\rho}(H)$ on temperature for asr = as-received; ppt = precipitated; coa = coalesced PETs [33]

The ^{13}C-observed ^{1}H spin-lattice relaxation times observed in the rotating frame $[T_{1\rho}{}^1(H)]$, which reflect motions in the kHz frequency regime, are presented as a function of temperature for our PET samples in Fig. 11. The results are consistent with the presence and absence of a glass transition observed in the DSC scans of as-received and coalesced (see Fig. 7) or precipitated [59] PETs, respectively. Thus, both macroscopic (DSC) and microscopic (NMR) observations point to the absence of a glass transition in the noncrystalline regions of coalesced or precipitated PETs. (Again details are presented as part of [33].)

In summary, microscopic and thermal observations of PET samples coalesced from their crystalline γ-CD–IC suggest crystalline characters and melt-crystallized morphologies that are different from normal samples. After coalescence of their segregated, extended chains from the narrow channels of the crystalline inclusion complex formed with host γ-CD, PET chains are much more readily crystallizable, and, locally, quickly form small, possibly chain-extended crystals. In addition, the noncrystalline regions of coalesced PET exhibit conformational and motional

behavior quite distinct from as-received PET. The extended kink conformations adopted by guest PET chains included in the PET-γ-CD–IC crystals are largely retained upon coalescence, and as such, are not only readily crystallizable, but result in the absence of normal glassy behavior for those coalesced PET chains that do not crystallize. What remains puzzling is the apparent retention of the extended kink PET conformers in the coalesced melt, even after holding it at $T > T_m$ for extended periods, and which still results in their rapid crystallization upon cooling to a distinct, possibly chain-extended crystalline morphology.

4.1.2   Polyolefins

Coalesced i-PP [42, 85–91]

Wide-angle X-ray diffractograms of as-received, precipitated, and coalesced isotactic polypropylene (i-PP), though not presented here [42], clearly indicated that only the α-form polymorph is present in the as-received and coalesced samples and a very poor α-form or almost a smectic form is obtained in the precipitated one [85–87]. Careful analysis of all diffractograms and DSC observations revealed that the γ-CD inclusion/coalescence process does not modify the crystalline form nor the melting temperature of the coalesced i-PP, but does yield a higher crystallinity for the coalesced i-PP, with an increase of about 27% in comparison with that of as-received i-PP. A significant increase in the crystallization rate from the melt was also observed for coalesced i-PP, which crystallized at 130°C compared with melt-crystallization temperatures of 117°C for as-received i-PP or 121°C for precipitated i-PP. Holding the coalesced i-PP sample in the melt at 200°C for an extended period did not alter its recrystallization behavior. Similar behavior has been observed in other semicrystalline coalesced polymers, such as PET, and can be explained by considering that the included polymer chains retain a certain degree of their extended and untangled natures even after coalescence, which facilitates their rapid crystallization.

Coalesced i-PB [42, 85–91]

X-ray diffractograms of as-received, precipitated, and coalesced isotactic poly(1-butene) (i-PB) are presented in Fig. 12. The diffractograms of both as-received and precipitated i-PB show clearly the form I polymorph (3_1 helical conformation) with the (110) reflection at 9.9°, the (300) at 17.3°, and the (220) at 20.2°(2θ). In contrast, the coalesced i-PB predominantly adopts the form II polymorph (11_3 helical conformation), along with some form III, which are normally obtained from the melt or by solution casting, respectively. The characteristic diffraction peaks of form II appear at $2\theta = 11.8°$(200), 16.8° (220), and 18.1° (213). Form III has a strong reflection (110) at $2\theta = 11.8°$ and three weak (200), (111), and (120) reflections at $2\theta = 13.8, 16.8,$ and 20.7°, respectively. Although very noisy, the peak at 13.8°
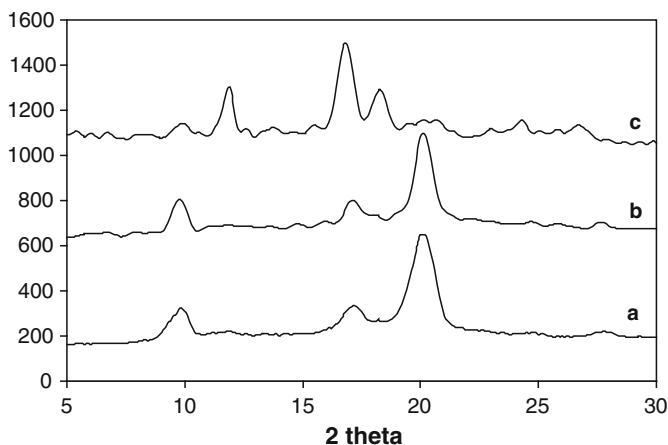
Fig. 12 WAXD patterns of as-received (**a**), precipitated (**b**), and coalesced (**c**) high molecular weight i-PB

indicates the presence of form III. The diffraction peak of form III at $2\theta = 20.7°$ overlaps with a diffraction peak belonging to form I′. However, the weak peak at $2\theta = 10.0°$ reveals a (110) reflection from form I or form I′. Forms I and I′ cannot be distinguished by X-rays, but exhibit different melting points in the DSC. First heating scans revealed distinct single and multiple melting peaks for the as-received and coalesced and precipitated i-PB samples, reflecting the presence of distinct crystalline polymorphs.

Interestingly, after quiescent storage for 6 months at room temperature, the coalesced i-PB, with a high molecular weight of 380,000, shows exactly the same diffraction pattern. It is very well known that the form II (tetragonal) polymorph is metastable and transforms to form I (hexagonal) at atmospheric pressure and room temperature with a half-life in the range 250–1,600 min [90]. We did not observe the same stability of the initial form II crystals when low molecular weight i-PB was coalesced from its γ-CD–IC.

As previously mentioned, CD–IC formation forces the included polymer chains to adopt an extended conformation in the host narrow channels, which in the case of i-PB might favor the formation of form I, with a more extended 3_1 helical conformation, from among its polymorphs. However, an investigation of the phase transformations in i-PB upon drawing has demonstrated [91] the formation of form II (11_3 helical conformation) upon tensile drawing and a strong dependence of the deformation process on the crystal form of the initial starting sample. Because it is likely that both form I and II helices can be accommodated in the ∼1 nm γ-CD–IC channels, these observations suggest further study of the polymorphic transformations of coalesced i-PB samples.

It is also noteworthy to mention the observation of a similar, yet even more significant, increase in the recrystallization kinetics from the melt of coalesced i-PBs

(crystallizes at 71°C upon cooling), compared with as-received or precipitated i-PBs (both crystallize at 42°C upon cooling from their melts).

4.1.3 PCL and PLLA [27]

When the biodegradable/bioabsorbable aliphatic polyesters PCL and PLLA were coalesced from their α-CD–ICs, they were observed [27] to have higher crystallinities (60 and 69% and 74 and 82% for as-synthesized and coalesced PCL and PLLA, respectively), elevated T_ms (65 and 69°C and 162 and 164°C for as-synthesized and coalesced PCL and PLLA, respectively), and, upon cooling from their melts, faster rates of crystallization and higher crystallization temperatures, T_c, than their as-synthesized counterparts. Coalescence from their α-CD–ICs is so rapid that the guest polymer chains crystallize almost at the same time they are consolidated, without losing the extended conformations required of them by the α-CD–IC channels [21]. Therefore, CD–IC formation/coalescence may be an effective way to modify the crystallinities and properties of biomedical polymers. (In this regard, see subsequent discussion of PCL-b-PLLA block copolymer behavior [20, 27], following coalescence from its α-CD–IC.)

The melting and crystallization behaviors observed for PCL and PLLA enzymatically coalesced with the alpha-amylase enzyme from *Bacillus licheniformis*, indicate that they might lead to superior drug carriers when coalesced from common CD–ICs also containing drugs (see Fig. 13). The rapid solidification of PCL
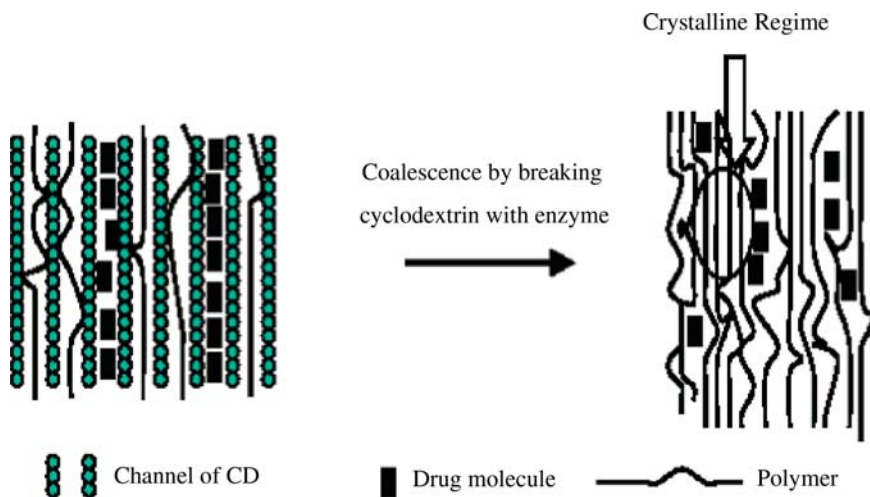

Fig. 13 Scheme of a polymeric drug delivery system formed by the simultaneous coalescence of matrix polymer and drug molecules from their common inclusion complex

and PLLA upon coalescence [12] implies a potentially improved dispersion of the drug in the PCL and PLLA matrices, which likely will critically impact their ability to deliver drugs.

4.1.4   Nylon [23, 37, 92–94]

We successfully formed an inclusion complex between nylon-6 and α-CD, and attempted to use the formation and subsequent disassociation of the nylon-6-α-CD–IC to manipulate the polymorphic crystal structures, crystallinity, and orientation of nylon-6 chains in the coalesced sample. Examination of as-received and IC-coalesced nylon-6 samples showed that the α-form crystalline phase of nylon-6 is the dominant crystalline component in the coalesced sample. X-ray diffraction patterns (Fig. 14) demonstrate that the γ-form is significantly suppressed in the coalesced sample. Along with the change in crystal form, an increase in crystallinity of ∼80% was revealed by DSC, and elevated melting and melt-recrystallization temperatures were also observed for the coalesced nylon-6 sample, in comparison to the as-received nylon-6 pellets. Thermogravimetric analysis indicated that nylon-6 has an ∼30°C higher thermal degradation temperature after modification by threading into and being coalesced from its α-CD–IC.

FTIR spectroscopy revealed a significant degree of orientation for the nylon-6 chains coalesced from their α-CD–IC crystals. In the FTIR spectrum of the IC-coalesced sample (Fig. 15), there is a very strong $1,030\,\mathrm{cm}^{-1}$ peak compared to
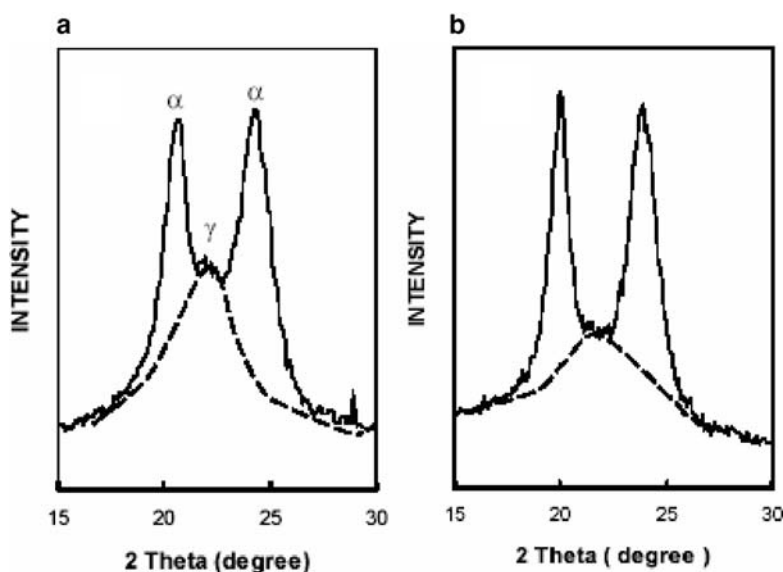

Fig. 14 Wide Angle X-ray Diffraction Patterns of (**a**) as-received and (**b**) IC coalesced nylon-6 [23, 92–94]
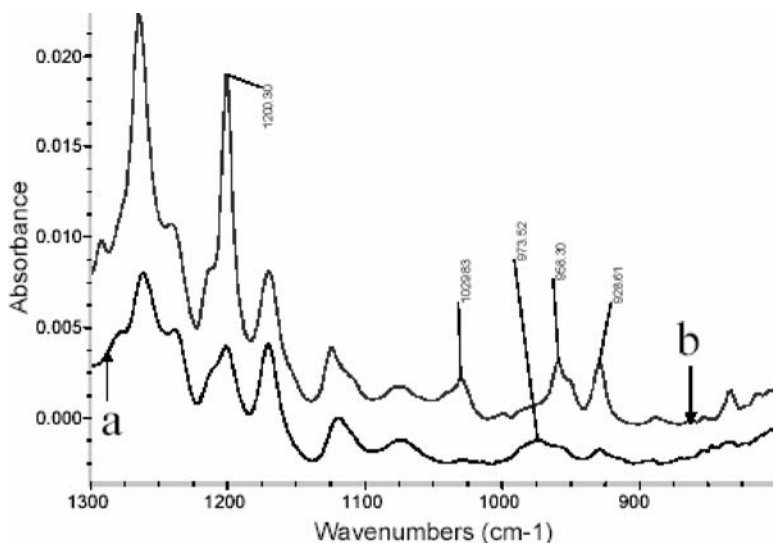
Fig. 15 Expanded FTIR spectra of (**a**) as-received and (**b**) IC coalesced nylon-6 [23, 92–94]

as-received nylon-6. According to FTIR studies of nylon 6-yarns, it is clear that the intensity of this peak increases with increasing draw ratio [95]. This may demonstrate that the extended, planar conformation that must be adopted by nylon-6 chains in the narrow channels of its α-CD–IC crystals are substantially retained after coalescence.

4.1.5 PEI [58]

The glass transition temperature of poly(ethylene isophthalate) (PEI) coalesced from its γ-CD–IC is ∼15–20°C higher (∼70°C) than that of the as-synthesized PEI, though both appear completely amorphous [58]. Typically polymer chains in amorphous regions start to move at the glass transition temperature. The coalesced PEI chains only begin to move at a temperature significantly higher than as-synthesized PEI chains, probably because the coalesced PEI chains are extended and their packing is more orderly than in the as-synthesized totally amorphous PEI with its randomly coiling chains. The greater extension and tighter packing of coalesced PEI chains apparently remains even after heating well above T_g to 260°C, because nearly identical elevated T_gs are observed during the first and second DSC heating scans. These observations somewhat parallel those observed previously for coalesced PET [21, 33], where in the noncrystalline sample regions chains were also more tightly packed.

The process of coalescing PEI from its inclusion compound with γ-CD has resulted in the extension and parallelization of PEI chains during the formation of the inclusion compound, which do not completely disappear after the removal of

random coil polymer chain   polymer/CD   coalesced polymer
                                inclusion compound
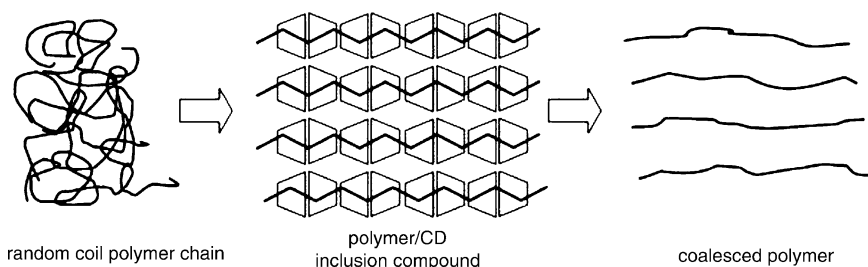
Scheme 1 Representation of polymer chain packing in PEI controlled by the formation of and subsequent coalescence from its γ-CD-inclusion compound

γ-CD by washing with hot water and coalescence of the PEI chains. A schematic representation of our view of the formation of and coalescence from PEI-g-CD–IC is shown in Scheme 1. The 15–20°C elevation in T_g of amorphous PEI produced by inclusion in and coalescence from its γ-CD–IC is significant, the more so because the coalesced amorphous PEI with tighter chain-packing does not disorder even after heating above its T_g to 260°C.

4.1.6 PVA Gels [43]

We prepared and characterized poly(vinyl alcohol) (PVA) hydrogels formed during freeze–thaw (F–T) cycles of their aqueous solutions, which also contained γ-CD [43]. Crystalline inclusion compound (IC) formation was observed between PVA and γ-CD in these gels at low concentrations of γ-CD (γ-CD:PVA molar ratios <1 : 25). Confirmation of the existence of the channel structure for γ-CD was achieved by characterizing the dried PVA/γ-CD hydrogels with solid-state DSC, TGA, WAXD, and ^{13}C-NMR. Some aspects of the mechanism of formation and structures of PVA gels obtained via F–T cycles in the presence/absence of γ-CD were presented based on UV–Vis, swelling, solution ^{1}H-NMR, and rheological observations. It was observed that the swelling and rheological responses [96–98] of the aqueous PVA gels formed during F–T cycles in the presence of γ-CD can be controlled by adjustment of the γ-CD:PVA molar ratio employed during their gelation.

Rheological observations of PVA hydrogels with γ-CD formed during five F–T cycles evidenced lower elastic moduli, G', than pure PVA hydrogels subjected to the same treatment. The magnitude of G' was a function of the quantity of γ-CD present in the hydrogels. When the concentration of γ-CD increased, G' decreased. Similarly in Fig. 16 the swelling ratio, $Q_r = \frac{W_s - W_r}{W_r}$, where the swollen and nascent sample weights W_s and W_r, respectively, of the various PVA and PVA/γ-CD gels are presented, and they are shown to increase with the increased presence of γ-CD during the F–T cycles. Both observations strongly imply that the threading of PVA chains by γ-CD, thereby isolating them and preventing their cooperative hydrogen
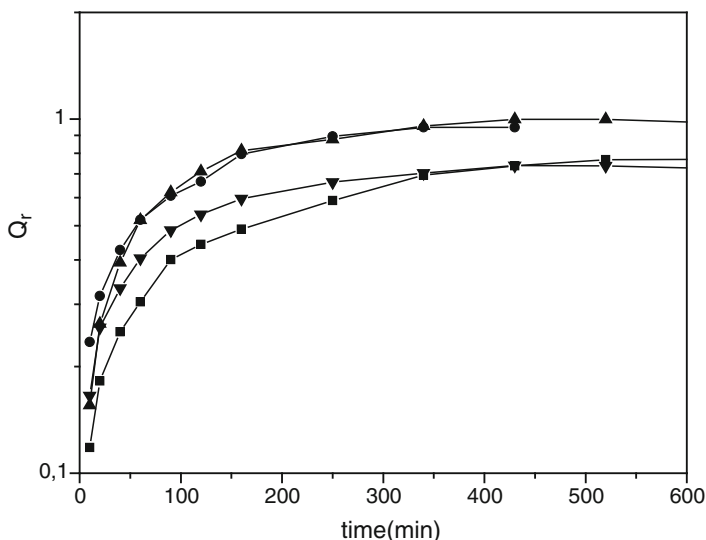
Fig. 16 Swelling measurements of PVA-γ-CD hydrogels subjected to five freezing–thawing cycles as a function of time for different PVA:γ-CD molar ratios: (*filled box*) PVA 10% (g ml^{-1}); (*filled circle*) PVA/γ-CD (26:1); (*filled triangle*) PVA/γ-CD (39.5:1); and (*filled inverted triangle*) PVA/γ-CD (53.4:1)

bonding and crystallization, limits the primary source of PVA physical cross-links in these gels [99].

According to these and other experimental results, we have proposed structures for PVA gels formed in the presence of γ-CD, which are shown in Fig. 17. As can be seen there, some small portions of the PVA polymer chains may be covered by γ-CD. Unlike the nascent and swollen gels observed as films after drying, WAXD observation of the PVA-γ-CD hydrogels show no evidence of crystallinity, so the γ-CD remaining after swelling the nascent PVA/γ-CD gels is only threaded on the PVA chains, as illustrated, or it is dissolved in the water and is removed from the gel upon swelling. In fact, ^{1}H-NMR observations of the PVA/γ-CD hydrogels performed upon dissolution in D$_2$O indicated that most ($\sim$70%) of the γ-CD present in the nascent gels remains after swelling. The portions of the PVA chains that are not covered by γ-CD can presumably interact through PVA hydrogen bonds leading to the formation of the PVA/γ-CD hydrogels via freeze–thaw cycling and subsequent swelling.

Whether nascent or swollen, all of our PVA and PVA/γ-CD hydrogels were found to be soluble in D$_2$O indicating an absence of the formation of chemical cross-links produced by the scission of PVA chains during their F–T preparation, which had been reported previously [98]. It is clear that the elasticities of the PVA and PVA/γ-CD hydrogels studied here are a result of the physical cross-linking of PVA chains.
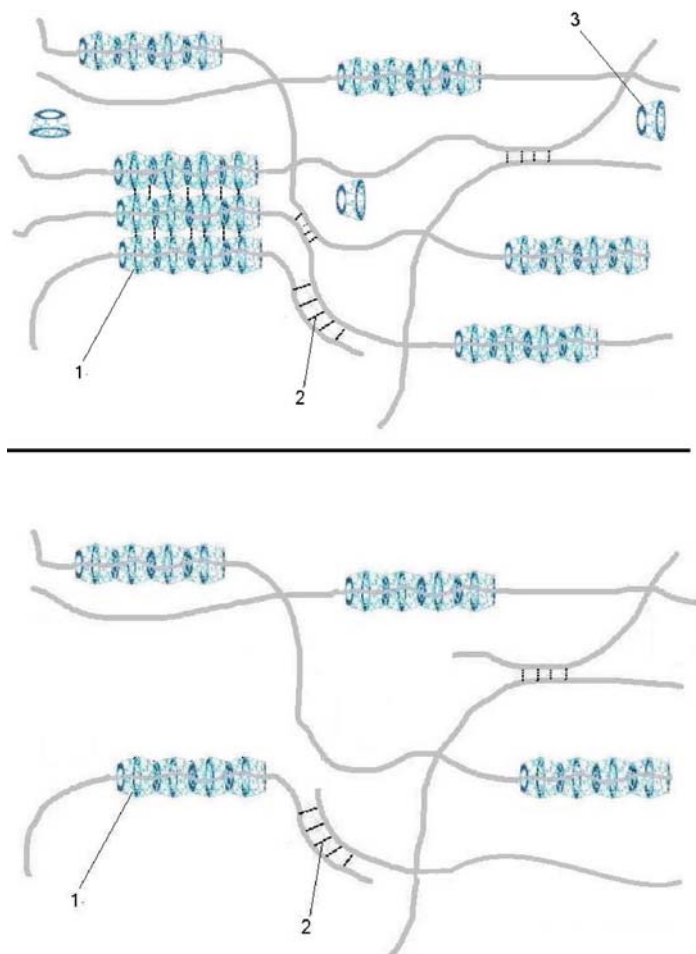
Fig. 17 Schematic illustrations of the proposed structures of PVA/γ-CD dried films (*upper*) and swollen gels (*lower*) produced by F–T cycling. **1** channel structure of PVA-γ-CD–IC, **2** hydrogen-bonded interactions/crystals/cross-links between PVA chains, and **3** free γ-CD molecules

4.1.7 Silk Protein [48]

Recently, and for the first time, we reported the formation of a CD–IC with a guest protein, silk fibroin from the *Bombyx mori* silk worm (SF) [48]. Formation of the crystalline SF-γ-CD–IC was verified by wide-angle X-ray diffraction, solid-state NMR, and infrared spectroscopy to have the host γ-CD molecules arranged in a channel structure (see Fig. 1e, f), with the extended and isolated silk chains included, at least in *large part*, in their internal cavities. Coalescence of the SF chains, by washing the γ-CD molecules away with warm water, led to suppression of the silk I and/or randomly coiling entangled conformations in the resulting solid SF sample,
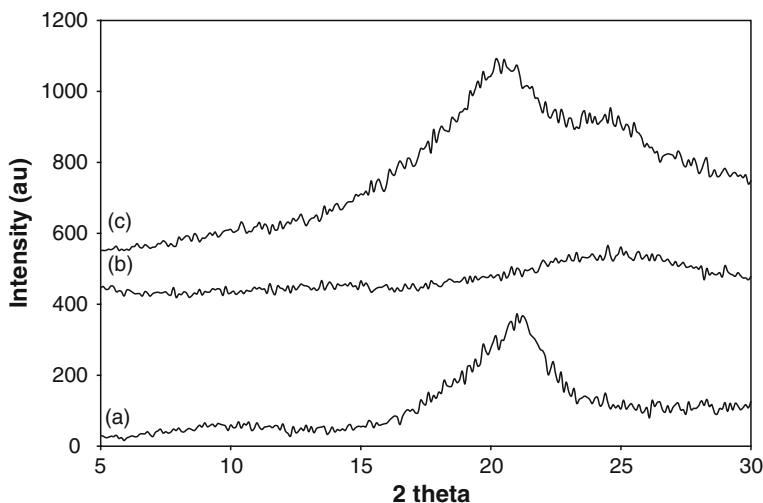
Fig. 18 Powder X-ray patterns of degummed native silk fibroin (SF) fibers from the *Bombyx mori* silk worm (**a**), SF precipitated from a $Ca(NO_3)_2 \cdot 4H_2O/2MeOH$ solution (**b**), and SF coalesced from its γ-CD–IC (**c**)

which instead contained a much higher quantity of silk-II β-sheet conformation. FTIR, WAXD, and solid-state ^{13}C NMR analyses indicated a higher degree of crystallinity and more orientated chains for the coalesced SF in comparison with the precipitated SF sample, as may be seen in Fig. 18, much like the initial degummed SF fibers. Note the preponderance of silk-II (scattering peak at $2\theta = 21°$ from the β-sheet structure) in both the degummed native fiber and coalesced SF samples, while scattering at $2\theta = 25°$ from silk-I preponderant in the precipitated sample is minimal in the coalesced sample. These modifications may have a substantial impact on the overall physical properties of γ-CD-processed silk. As a consequence, γ-CD–IC formation/coalescence processing has proved to be an effective method of manipulating both the polymorphic structures and the final level of crystallinity in the SF protein, mimicking the actual spinning behavior of the silk worm.

Though ∼85% of the amino acid residues in the SF protein are compact with small side chains (glycine, alanine, and serine), near both the N- and C-termini of the SF chain, several quite bulky amino acid residues (proline, histidine, trypthophan) are present in the SF primary structure [100]. At first glance, the possibility that γ-CDs (9–10Å channel diameter) have completely threaded over SF protein chains to form the SF-γ-CD IC seems unlikely. However, there is precedence for such an observation in the study of the complexation of propylene oxide-*b*-ethylene oxide-*b*-propylene oxide (PPO–PEO–PPO) block copolymer with α-CD [101]. As pointed out in this study, PPO and PEO homopolymers are known to form CD–ICs only with β- and α-CDs, respectively. Nevertheless, it was observed there that α-CDs are able to thread over the bulkier PPO end-blocks and complex with the central PEO

block. In an analogous manner, γ-CDs are apparently able to thread over the bulky amino acid residues in the SF protein chains and form a SF-γ-CD–IC [75].

4.2 Nonstoichiometric Polymer-CD–ICs as Nucleating Agents for the Crystallization of Polymers [103–106]

Formation of polymer-CD–ICs with amounts of host CDs insufficient to completely thread and confine the guest polymers, results in polymer-CD–IC crystals with portions of the guest polymer chains emerging from the host CD crystalline surfaces [102]. When a nonstoichiometric (*n-s*) polymer-CD–IC, with only partially included chains, is added in small quantities to a bulk sample of the same polymer, which can crystallize and has a T_m below the decomposition temperature of CD–ICs ($\sim$ 250–300°C), it has been observed that its crystallization from the melt is enhanced [103–106]. Melt crystallized polymers nucleated with *n-s* polymer-CD–ICs crystallize more rapidly, evidence greater levels of crystallinity, higher melt crystallization temperatures, and semicrystalline morphologies characterized by crystals which are smaller and more uniformly distributed than in un-nucleated pure bulk samples.

The effectiveness/efficiency of nucleation with (*n-s*) polymer-CD–ICs was observed to be at least comparable or superior to that produced by more traditional nucleation agents, such as talc, and for that matter pure CDs. The alteration of crystalline morphology achievable by using *n-s* polymer-CD–ICs as nucleants in melt-crystallization is demonstrated in Fig. 19. It is very clear that the morphology of PCL melt-crystallized in the presence of a small amount of (*n-s*) α-PCL-C–IC is very distinct from the pure melt-crystallized PCL. Crystal sizes are drastically reduced and more homogeneously distributed for the nucleated PCL.

The distinct changes in morphology achieved by melt-crystallization of polymers in the presence of small amounts of their (*n-s*) polymer-CD–ICs results in changes in other physical properties as well. For example, in Table 2 a comparison of the properties of poly(3-hydroxy butyrate) (PHB) melt-spun with and without the presence of (*n-s*) PHB-α-CD–IC are compared [104]. The mechanical properties of the PHB/(*n-s*) PHB-α-CD–IC fibers are superior. In fact, their lower elongation at break likely contributes to the removal of the stickiness normally observed between melt-spun PBH fibers [104].

There is an important additional advantage of using (*n-s*) polymer-CD–ICs to nucleate the melt-crystallization of polymers. Because CDs are nontoxic, biocompatible, and biodegradable, they may be safely utilized in (*n-s*) polymer-CD–IC nucleants to fabricate both permanent and biodegradable/bioabsorbable implants that are also nontoxic.
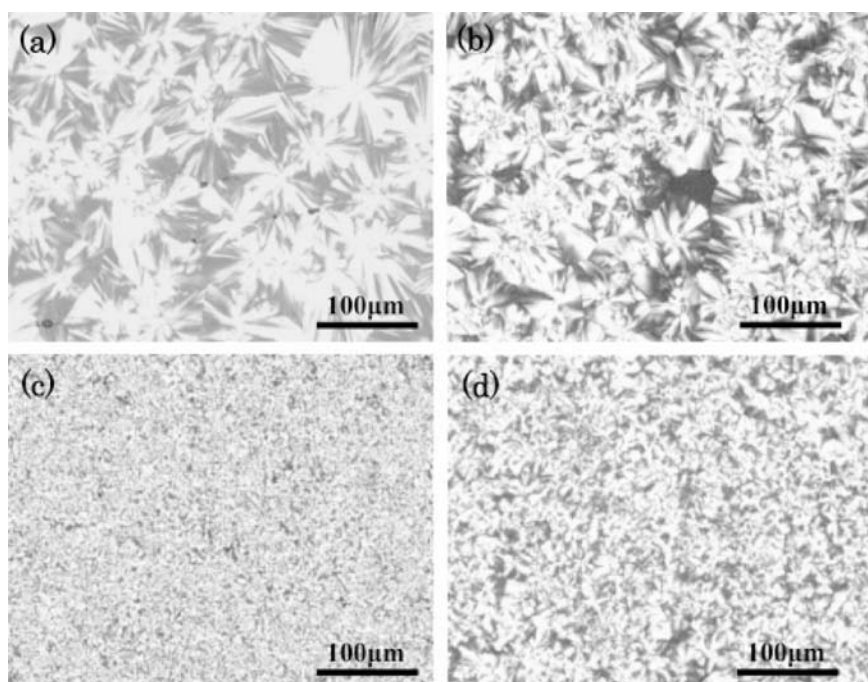
Fig. 19 Polarized optical micrographs of PCL (**a**), and PCL containing 2 wt% α-CD (**b**), talc (**c**), and (n-s) PCL-α-CD–IC (**d**) [105]

Table 2 Young's modulus, E_t, tensile stress at break, ς_H, and elongation at break, ε_H, of PHB fiber samples [104]

Fiber sample	E_t [Gpa]	$\sigma_H[N-mm^{-2}]$	ε_H [%]
PHB (DR 3)*	4.45	116.64	50.02
PHB (DR 4)	4.44	164.38	52.82
PHB + 0.5% IC	4.94	161.33	18.51

*Draw ratio

4.3 Homopolymer Blends Coalesced from their Common CD–ICs

By combination of a solution containing two chemically distinct dissolved polymers with a CD solution, it is possible to form a common CD–IC containing both guest polymers. Assuming that each of the guest polymers is randomly included or "mixed" in the CD channels of their common CD–IC (see Figs. 1f, 2), we may anticipate that upon coalescence an intimate blend would result. The intimate blending of normally incompatible polymers, both binary and ternary blends, by coalescence from their common CD–ICs has in fact been demonstrated [40].
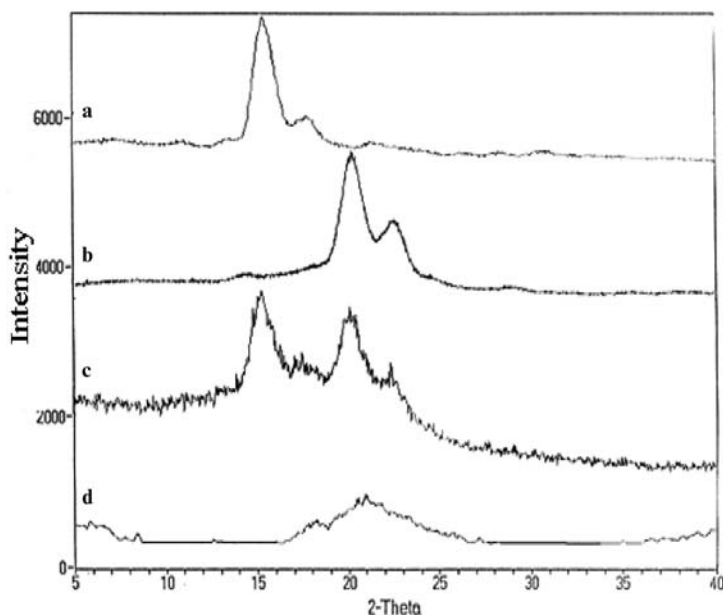
Fig. 20 X-ray diffractograms of pure PCL (**a**) and PLLA (**b**) and PCL/PLLA blends obtained by casting from dioxane solution (**c**) and hot water coalescence from PCL/PLLA-α-CD–IC (**d**) [12]

4.3.1 PCL/PLLA Blends [12, 27, 46]

In Fig. 20 the X-ray diffractograms of the biodegradable/bioabsorbable polyesters PCL, PLLA, and their blends, either cast from dioxane solution or coalesced from a common α-CD–IC containing both PCL and PLLA as guests, are presented. Their solution-cast blend shows extensive crystallinities for both phase-segregated components, while the PCL/PLLA blend coalesced from their common α-CD–IC crystals shows virtually none and very little PCL and PLLA crystallinities, respectively. Unlike the solution-cast blend, the mainly amorphous coalesced blend strongly suggests intimate mixing of PCL and PLLA chains, which prevents their separate crystallization. In fact detailed analyses of two-dimensional HETCOR NMR spin-diffusion experiments [46] revealed that the length scale of mixing in the coalesced PCL/PLLA blend is smaller than the radii of gyration of both components and the mobility of PLLA chains in this blend is greater than in the amorphous regions of pure PLLA. Both observations confirm that PCL and PLLA chains are indeed intimately mixed in the blend coalesced from their common α-CD–IC crystals.

4.3.2 PVAc/PMMA Blends [40, 47, 49, 51]

Direct insertion probe mass spectrometry (DIP–MAS) analyses of poly(methyl methacrylate) (PMMA), poly(vinyl acetate) (PVAc), and their coalesced and precipitated blends were performed [51] (see Fig. 21). The fact that the pyrolysis mass
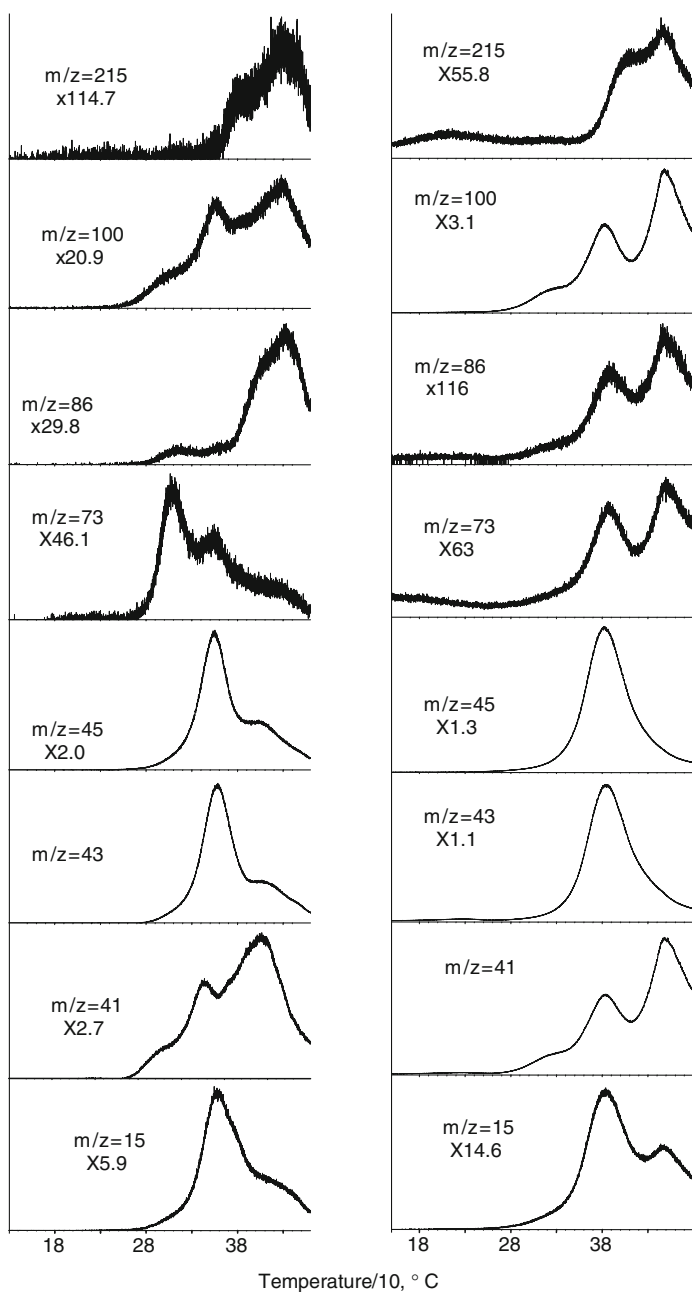
Fig. 21 Evolution profiles of some characteristic products recorded during the pyrolysis of the coalesced (*left*) and solution-cast (*right*) PMMA/PVAc blends

spectra of all the samples were dominated by peaks having the same m/z values, though they were due to different thermal degradation products, caused some additional difficulty in the analyses of PMMA/PVAc physical and coalesced blends. To reach reliable conclusions more emphasis was given to the trends in the evolution profiles of their thermal degradation products.

PVAc degrades in two stages, around 360 and 440°C, corresponding to deacetylation and disintegration of the polyolefinic backbone, respectively. For PMMA the low temperature weight losses were attributed to evolution of dimer, low molecular weight oligomers, scission of head-to-head linkages, and loss of unsaturated end groups. At elevated temperatures (380–420°C), however, initiation of weight loss was thought to be a mixture of chain end and chain scission processes, followed by depropagation to the end of the polymer chain. It is known that the probability of cleaving a particular bond during thermal degradation depends not only upon its inherent strength, but also on the stability of products formed.

It is clear that the thermal degradation behaviors of both PVAc and PMMA have been changed in the coalesced blend. The decrease in MMA monomer yield may be associated with inhibition of PMMA depolymerization. Depolymerization of PMMA can be inhibited if the loss of side chains is favored, which implies that proton-transfer to the $C = O$ groups of PMMA occurs. So, for the coalesced PMMA/PVAc blend, PMMA depolymerization was likely inhibited as a result of proton-transfer to the $C = O$ groups of the MMA units. Because both coalesced and as-received PMMA degrade mainly by depolymerization reactions, the source for the depolymerization inhibiting proton transfer in the coalesced blend could only be PVAc. However, it is clear that the simple presence of PVAc was not sufficient for proton-transfer, as depolymerization of PMMA was also recorded for the phase-segregated PMMA/PVAc physical blend. Instead, it may be suggested that such a proton-transfer can only be possible if the separation between PMMA and PVAc chains is comparable to the distance between γ-H and $C = O$ groups within a single PMMA molecule.

It seems likely that PVAc containing $CH_3–C = O$ groups, with more acidic protons, should be more effective in McLafferty-type rearrangement reactions and intermolecular proton-transfer to PMMA chains, even if the distances between PVAc–PMMA and PMMA–PMMA are comparable, i.e., PMMA and PVAc chains in the coalesced blend are very intimately mixed. Making use of the above proposal permits the approximate reaction scheme shown in Scheme 2 to be written.

As a result of such an intermolecular proton-transfer from PVAc to PMMA, the thermal degradation of PVAc should shift to the high temperature ranges. Furthermore, thermal degradation products of poly(methyacrylic acid) (PMA) should appear in the pyrolysis mass spectra. Because of the similarities in the structures of PMMA and PMA, a depolymerization reaction yielding mainly CH_2CCH_3COOH, CH_2CCH_3, and COOH fragment peaks at m/z $= 86, 43$, and 45 Da, respectively, can be expected. The pyrolysis data indicating an increase in relative intensities of the 15 Da peak (due to CH_3), in the temperature range where PVAc degrades, and the 45 and 86 Da peaks (due to COOH and CH_2CCH_3COOH, respectively), in the temperature region where PMMA degradation occurs, support the proposed

intermolecular proton-transfer from PVAc to PMMA in the coalesced blend. The relative intensity ratios of the above-mentioned peaks in the pyrolysis mass spectra are summarized in Table 3.
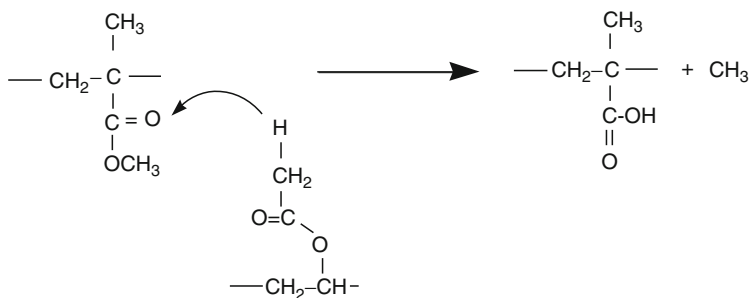
Scheme 2 Proposed McLafferty-type rearrangement via intermolecular proton transfer from the CH$_3$ of PVAc to the ester group of PMMA in the well-mixed coalesced PVAc/PMMA blend. Note that only the conversion of PMMA to PMA is depicted in the proton-transfer from PVAc

Table 3 The assignments and intensities (relative to the weakest peak) of the characteristic and intense peaks in the pyrolysis mass spectra of physical and coalesced PMMA/PVAc blends at temperatures corresponding to maxima in the TIC curves (Fig. 21) [51]

m/z, Da	PMMA/PVAc 360°C	Physical mixture 430°C	Coalesced 310°C	PMMA/PVAc 360°C	PMMA/PVAc 430°C	Assignments
15	75	46	80	152	151	CH$_3$
41	585	1,000	1,000	276	1,000	CH$_2$ CCH$_3$
43	1,000	207	979	1,000	725	CH$_2$ CHO, CH$_3$ CO
45	769	115	505	509	352	COOH, CHOO
60	690	85	566	300	195	CH$_3$ COOH
69	546	924	649	141	544	CH$_2$ CCH$_3$
73	13	17	241	16	20	C$_3$ H$_5$O$_2$
78	103	14	22	63	49	C$_6$ H$_6$
86	6	8	37	3	77	C$_4$ H$_6$O$_{2,}$ VAc
91	46	51	73	26	164	C$_7$ H$_7$
100	215	351	140	39	116	MMA
128	51	42	36	24	83	C$_{10}$ H$_8$
141	25	37	26	8	58	C$_{12}$ H$_9$
179	15	38	25	7	31	C$_{14}$ H$_{11}$
180	13	13	5	6	21	C$_{14}$ H$_{12}$
215	6	16	21	3	24	C$_{14}$ H$_{12}$
232	3	5	4	2	8	C$_{18}$ H$_{16}$
284	1	2		1	4	C$_{22}$ H$_{20}$
315	1	3		1	7	C$_{24}$ H$_{27}$

4.3.3 PC/PMMA/PVAc Ternary Blends [35]

We reported the formation of an intimate polycarbonate (PC)/PMMA/PVAc ternary blend by coalescence of these polymers from their common IC formed between γ-CD hosts and PC, PMMA, and PVAc guests [35]. Figure 22 shows the MDSC thermograms of the ∼1:1:1 molar coalesced PC/PMMA/PVAc ternary blend. The total signal of heat flow may be separated into reversing and nonreversing heat flows, as a result of the temperature modulation employed. Thermal transitions in the reversing signal arise from thermodynamic phenomena, such as the T_g and melting. The nonreversing signal exhibits kinetic phenomena, including evaporation and recrystallization. By plotting the reversing heat flow versus temperature, the effect of the solvent release, as well as enthalpic recovery (an endothermic peak that occurs just above the T_g), are eliminated, revealing a clear, single glass transition.

In both the first and second MDSC heating scans, only a single glass transition can be observed at 57°C, which is different from the glass transition temperatures observed for pure PC (133°C), PMMA (82°C), and PVAc (39°C) by DSC in Fig. 23 for the phase-segregated PC/PMMA/PVAc blend coprecipitated from their common solution. This result indicates the presence of a single homogeneous amorphous phase in the coalesced ternary blend of PC/PMMA/PVAc, where the three component polymer chains are intimately mixed with each other. The appearance of one glass transition in the second scan also confirms the stability and molecular degree of mixing of the PC, PMMA, and PVAc chains in their coalesced blend. The
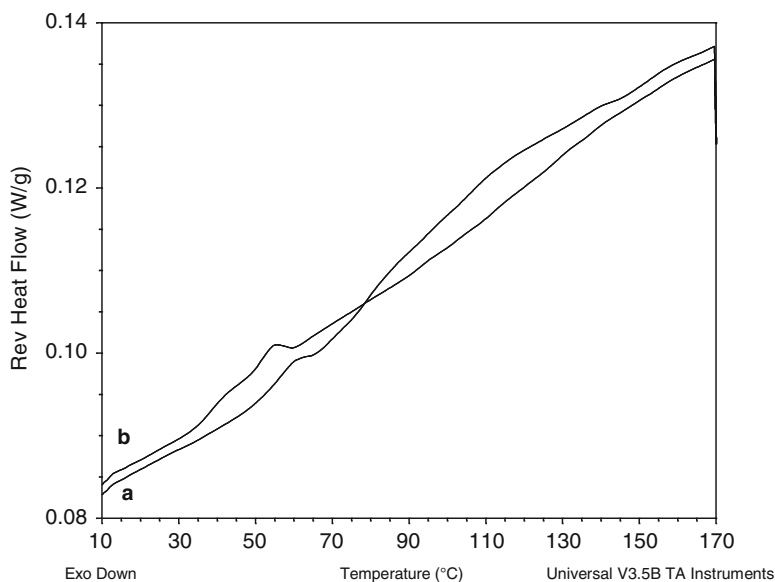
Fig. 22 MDSC scans of the (**a**) first, and (**b**) second heating runs recorded for the ∼1:1:1 molar PC/PMMA/PVAc coalesced blend. The sample was held for 3 min at 170°C after the first heating [35]
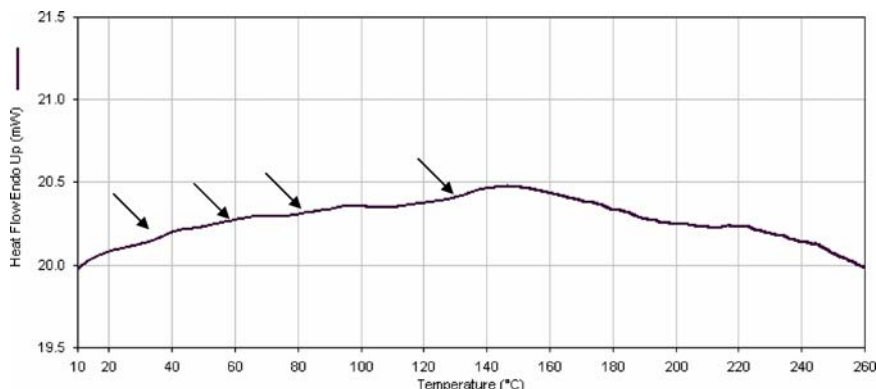
Fig. 23 DSC thermogram of the coprecipitated PC/PMMA/PVAc blend, first heating scan

DSC scans recorded for PC/PMMA/PVAc blends obtained by solvent-casting and coprecipitation evidenced four distinct glass-transitions, one for each component polymer and one indicating that some of the PMMA and PVAc chains were mixing (see Fig. 23).

We also observed that the PC chains possess a preferred ability to form inclusion compounds with γ-CD in solution, when competing with PMMA and PVAc. From the ^{1}H NMR spectrum of the coalesced ∼1:1:1 PC/PMMA/PVAc blend (not shown), the molar ratio of PC:PMMA:PVAc was determined to actually be 1.6:1:1.4 compared to the initial molar ratio of 1:24:24, respectively, used in solution to form their common γ-CD–IC. Despite the initial 1:24:24 PC:PMMA:PVAc molar ratio in solution, the PC component in the coalesced PC/PMMA/PVAc blend is still prevalent over the PMMA and PVAc components, which indicates that there may be additional factors that govern the inclusion process from a multiguest system. We believe that this very strong preference of the host γ-CD molecules for PC chains, rather than the other two possible guests, is due to their different hydrophobicities. Although the final molar ratio of the coalesced ternary blend can be somewhat controlled by modifying the initial molar ratio of polymers in their common solution, our eventual aim is to be able to adjust, as desired, the constituent polymer ratios in coalesced ternary blends.

4.4 Coalescence of Block Copolymers from their CD–ICs

Inherently incompatible blocks in block copolymers normally segregate into separate phases in the bulk. However, if block copolymers are included in and then subsequently coalesced from their CD–ICs, the phase segregation of their incompatible blocks may be controlled. For example, if all blocks of a block copolymer are included in its CD–IC, then, similar to the case for common CD–ICs containing two or more homopolymers, upon coalescence we would expect a reduction in the phase segregation of their blocks. On the other hand, if some blocks are included

in their CD–ICs, while others are not, then we might anticipate an increased phase segregation of their constituent blocks upon coalescence.

4.4.1 PCL-b-PLLA [18, 20, 27]

When melt-pressed films of as-synthesized PCL-b-PLLA and PCL-b-PLLA that had been included in and then coalesced from its α-CD–IC are observed by X-ray diffraction (see Fig. 24) [20], it is clear that the coalesced film is predominantly amorphous, as a consequence of the mixing of PCL and PLLA blocks, while the as-synthesized PCL-b-PLLA film shows substantial crystallinity for both the PCL and PLLA blocks (compare with Fig. 20), indicating a phase segregation of blocks. These PCL-b-PPLA films were then subjected to enzymatic degradation and their structures monitored with X-ray diffraction. From Fig. 24 we can see that the phase segregated as-synthesized block copolymer film underwent only limited degradation even after 2 weeks of enzymatic digestion. The coalesced PCL-b-PLLA film on the other hand experienced much more extensive degradation, as evidenced by the transition of its X-ray diffraction pattern from that of a largely amorphous material initially to one that is highly crystalline after 14 days of degradation. Clearly the enzyme almost exclusively attacked the abundant amorphous sample regions of the coalesced film, where the PCL and PLLA blocks are well mixed. Thus, the bio-degradation of block copolymers, and by extension, homopolymer blends can be controlled by processing them with CDs.
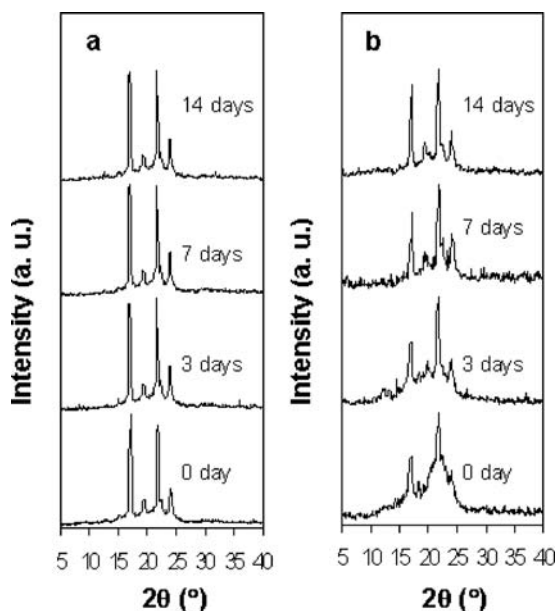
Fig. 24 X-ray diffraction patterns of as-synthesized (**a**) and coalesced (**b**) PCL-b-PLLA melt-pressed films observed following various enzymatic degradation times [20]

Table 4 Thermal properties and crystallinities, χ_c, of various PCL–PPG–PCL triblock copolymer samples revealed by DSC [25]

Sample	T_m [°C]	ΔH_m [J/g]	χ_c [%]
As-synthesized copolymer	57.3	58.6	56.5
Coalesced from α-CD–IC	63.8	76.8	74.1
Coalesced from γ-CD–IC	63.0	51.3	49.5

4.4.2 PCL–PPG–PCL [25]

When ICs are formed between guest PCL-poly(propylene glycol) (PPG)-PCL triblock copolymer and α- and γ-CD hosts [25], in the first case only the PCL blocks are included, while in the PCL–PPG–PCL-γ-CD–IC entire triblock copolymer chains are included. As a result, in comparison to the as-synthesized triblock copolymer, we would expect that upon coalescence from the PCL–PPG–PCL-α- and γ-CD–ICs an increase and a decrease in the phase segregation of PCL and PPG blocks would occur, respectively. As can be seen in Table 4, these expectations are in fact realized as indicated by the increased, decreased level of PCL block crystallinity in PCL–PPG–PCL coalesced from its α-,γ-CD–ICs. Because two side-by-side PCL blocks may be included in the channels of the γ-CD– IC [107,108], while only single PPG blocks may be included, the less than expected minor reduction in the phase segregation achieved upon coalescence from the PCL–PPG–PCL-γ-CD–IC can be understood.

It should also be mentioned that block copolymers, such as PCL–PPG–PCL, may be utilized to form polymer-CD–ICs [102–104] that are effective as nucleating agents. For example, if β-CD is used to form an IC with PCL–PPG–PCL, only the central PPG blocks will be included [101], and the unincluded terminal PCL blocks will extend from the surfaces of the b-PPG-β-CD–IC crystals. By altering the PCL block lengths we may be able to tailor their ability to control the melt-crystallization of PCL. In comparison to (*n-s*) PCL-α-CD–ICs, or (*n-s*) polymer-CD–ICs in general, block copolymer-CD–ICs with some blocks able to be included, while other blocks are excluded, may potentially be superior nucleating agents.

5 Additive CD complexes

It is possible to more effectively deliver small-molecule additives to polymers by employing either crystalline additive-CD–ICs or additives that are permanently complexed/rotaxanated with CDs and that remain soluble. Additive-CD–IC complexes may be delivered by melt-processing up to temperatures of $\sim 300°$C, while the permanently threaded and soluble additive-CD–rotaxanes can be delivered from their solutions.

5.1 Additive-CD–ICs [7, 9, 13, 17, 52, 53, 65, 69, 70]

5.1.1 Antibacterial-CD–ICs

Because crystalline CD–ICs are high-melting and thermally stable, even when containing small-molecule guests that are volatile liquids [52, 53] or even gases in the bulk, delivery of additives to polymer materials can be improved by using additive-CD–ICs, which may often be conveniently melt-processed into polymers. An example of CD–IC delivery of a polymer additive is provided by the commercial antibacterial triclosan [17].
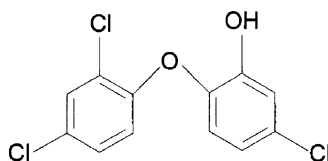
The triclosan-β-CD–IC was formed and small amounts were mixed with PCL powder, which was sprinkled onto cotton fabric and then covered with another piece of cotton fabric. The cotton-PCL/triclosan-β-CD–IC-cotton was ironed into a laminate, placed on an Agar plate, and then tested against the growth of *E. coli* bacteria. As can be seen from the test results in Table 5, *E. coli* bacteria were unable to grow upon the laminated cotton fabric containing triclosan-β-CD–IC. In fact the laminated fabric was just as effective as films of PCL containing triclosan-β-CD–IC or pure triclosan.

The use of triclosan-β-CD–IC to deliver the antibacterial properties of triclosan has an important advantage over the pure antibacterial agent. Triclosan is crystalline, but melts in the range of 55–60°C. Though it is possible to blend pure triclosan with low melting polymers like PCL ($T_m \sim 60°C$), this would not be the case for polymers with higher melting or softening temperatures. On the other hand,

Table 5 *E. coli* test results for cotton fabric laminated with PCL films embedded with Triclosan or Triclosan-β-CD–IC [17]

Sample	Zone of inhibition (diameter in mm)
PCL (between pieces of fabric) (1 g of PCL)	0
PCL (1 g of PCL)	0
PCL + triclosan (between pieces of fabric) (1 g of PCL and 0.1 g of triclosan)	15
PCL + triclosan (1 g of PCL and 0.1 g of triclosan)	15
PCL + triclosan-β-CD–IC (between pieces of fabric) (1 g of PCL and 0.1 g of triclosan-β-CD–IC)	12–15
PCL + triclosan-β-CD–IC (1 g of PCL and 0.1 g of triclosan-β-CD–IC)	14–17

triclosan-β-CD–IC is thermally stable and solid well above 250°C [53, 69, 70], and so may be melt-processed into many polymeric materials. The thermal stabilities [53, 69, 70] of small-molecule-CD–IC crystals has permitted us to more conveniently and effectively deliver [7, 9, 13, 17, 52, 53, 65, 69, 70] several additives to polymer materials, including antibacterials, flame retardants, spermicidals, and insect repellants.

5.1.2 Spermicide-CD–IC [69, 70]

A crystalline IC has been formed with α-CD and the liquid spermicide Nonoxynol-9 (N-9). Testing of siloxane rubbers embedded with small amounts of N-9-α-CD−IC
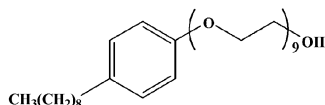
crystals against bovine sperm has begun with initially promising results (see Table 6) [69, 70]. The siloxane networks swollen with neat nonoxynol-9 and embedded with N-9- α-CD–IC crystals with similar N-9 concentrations appear to be equally effective in killing bovine sperm. However, the delivery of N-9 by embedding the rubber network with N-9-α-CD− IC crystals has two advantages over swelling the network with neat N-9: (1) more convenient and longer lasting delivery and (2) less potential for human contact with N-9. Both of these advantages are a result of the inclusion of N-9 in the crystalline matrix of its IC formed with α–CD.

Table 6 Bovine sperm motility on various silicone rubber films swollen or embedded with pure N-9 or N-9-α-CD–IC

Treatment group	wt% N-9	Sperm motility (% motile) at time [min]			
		0	10	30	60
1. Silicone rubber with N-9	0.37	26.67	2.33	0.00	0.00
2. Silicone rubber	0	41.67	40.00	21.67	8.67
3. Silicone rubber with N-9-α-CD–IC	0.44	26.67	1.67	0.00	0.00
4. Silicone runner with N-9-α-CD–IC	0.83	28.33	4.00	0.00	0.00
5. Silicone rubber with N-9	0.73	38.33	10.67	0.33	0.00
6. Silicone rubber with N-9	4.35	0.00	0.00	0.00	0.00
7. Blank well with a parafilm circle inserted	-	46.67	17.32	18.33	8.67
Untreated	-	46.67	40.00	41.67	31.67
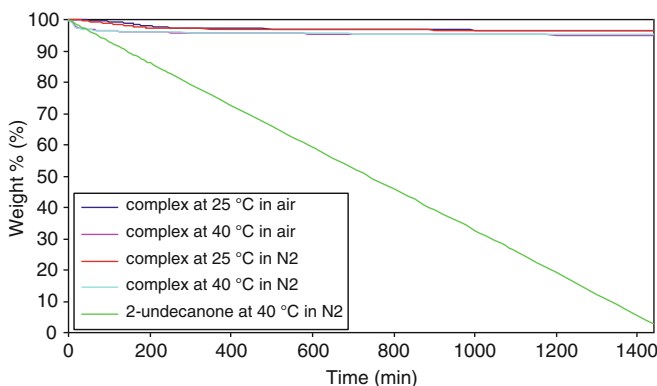
Fig. 25 Time-dependent, constant-temperature TGA scans of pure and α-CD complexed 2-undecanone

5.1.3 Insect Repellant-CD–IC [69, 70]

2-Undecanone (methyl nonyl ketone), a natural nontoxic insect repellant compound, was recently isolated from the trichomes of wild tomatoes, and is currently being introduced as a replacement for insect repellants containing N,N-diethyl-meta-toluamide or DEET, which are permitted for use only on children older than 2 months. In an effort to improve the delivery of the somewhat volatile liquid 2-undecanone, we have successfully formed the crystalline inclusion compound (IC) between 2-undecanone and α-CD, using a coprecipitation method [69, 70].

The release characteristics of 2-undecanone insect repellant from its α-CD–IC were studied using TGA either at a heating rate of 20°C/min in nitrogen and air atmospheres or at constant temperatures of 25 and 40°C over a period of 24 h (see Fig. 25). By integrating and comparing the areas of resonance peaks contributed by 2-undecanone and α-CD in the ^{1}H NMR spectrum of 2-undecanone-α-CD–IC, it was found that α-CD forms a 2:1 inclusion complex with 2-undecanone. This translates to 8 wt% 2-undecanone and 92 wt% α-CD in the stoichiometric 2-undecanone-α-CD–IC, which can be used to analyze TGA results to determine 2-undecanone weight loss.

The release/loss of 2-undecanone insect repellant from its α-CD–IC was ∼60% after 24 h at 40°C. By comparison, ∼97% of pure 2-undecanone was volatilized and lost over 24 h at 40°C. These results suggests that the gradual, long-term delivery of the insect repellant 2-undecanone can be significantly improved through employment of its crystalline α-CD–IC, as was recently demonstrated [69, 70].

5.1.4 Flame Retardant-CD–IC [13]

We successfully formed an inclusion compound (IC) between a commercial flame retardant (FR = Antblaze RD-1) [13], which is shown below in its protonated form, and β-cyclodextrin (CD). The FR-β-CD–IC was melt-processed into PET films which were tested for flammability. The flammabilities of pure PET films, PET

$$
\begin{array}{c}
\text{O} \\
\| \\
\text{H}_4\text{NO - PH}_2\text{C} \quad\quad \text{N} \quad\quad \text{CH}_2\text{P - ONH}_4 \\
| \quad\quad\quad |\quad\quad\quad\quad \| \\
\text{ONH}_4 \quad\quad\quad | \quad\quad\quad \text{ONH}_4 \\
\quad\quad \text{O} \\
\quad\quad \| \\
\text{CH}_2\text{P - ONH}_4 \\
| \\
\text{ONH}_4
\end{array}
$$
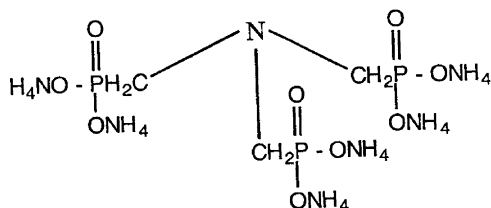
Table 7 Flammability of PET Films

Film/Trial	Char Length (cm)			Burning Time (s)		
	1	2	3	1	2	3
PET	BEL*	BEL	BEL	26.0	28.0	25.0
PET/FR	5.3	BEL	BEL	14.0	16.0	16.0
PET/β-CD	BEL	BEL	BEL	15.0	19.0	15.0
PET/FR IC	1.0	0.8	1.0	6.0	4.0	6.0

*BEL, burned entire length

films containing pure CD, and PET films containing FR applied from a bath and then oven-cured, were also observed. Flammability was measured using a modified AATCC Test Method 34, and the results are presented in Table 7. It is apparent that all but the PET films embedded with FR-β-CD–IC were either completely or substantially consumed when ignited on a single edge with a 3.8 cm flame applied for 3 s. To our knowledge, this is the only reported demonstration of flame retardance achieved by means of delivering a FR to a polymer in the form of its CD–IC.

When embedded in thin PET films at levels (10 wt%) comparable to those achieved in cotton/polyester blend fabrics via bath padding and oven-curing ($\sim$ 4–12 $wt\%$), substantial flame retardancy is imparted to the PET films. This despite the fact that the molecular weights of FR and β-CD are 401 and 1,135, respectively, which suggests that the FR is actually present at much reduced levels in the FR-β-CD–IC embedded PET films.

The temperature stability of the FR-β-CD–IC crystals makes them suitable for embedding in a variety of polymers that melt below $\sim$300°C. Our results suggest that incorporation of FR-CD–ICs directly into polymer films or fibers during their melt-processing may be a means to protect them from burning that is superior to postfabrication application of FRs. In addition, liquid FRs and other additives, which are difficult to incorporate and retain in solid polymers, may be included in their high-melting ICs formed with CDs and embedded directly into polymer samples, because the guest additive is protected both from the environment and its processing into polymers by the thermally stable crystalline lattice provided by the host CD.

These results give further impetus to our belief that a variety of additives may be more effectively delivered to polymer films and fibers as high melting inclusion compounds formed with CDs. In this connection for flame retardants, which can be toxic and mutagenic on contact, their confinement in CD–ICs not only protects them from the environment, but protects the wearer of fabrics containing embedded FR-CD–ICs from direct contact with the FR. Thus, one can envision the use of the most effective FRs with little regard to issues of FR toxicity, if they are delivered in the form of their CD–ICs.

5.2 Additive-CD–Rotaxanes

5.2.1 Dyeing with an Azo-Dye-CD–Rotaxane

Soluble additive-CD–rotaxanes can be obtained by first forming a soluble additive-CD–IC, and then attaching bulky groups to both ends of the included guest additive nearest to or extending from the host CD, thereby preventing the unthreading of the additive. Scheme 3 illustrates an example of the synthetic route for obtaining an azo-dye-α-CD–rotaxane [64, 109–111]. The azo-dye-α-CD–rotaxane is water soluble, which is not the case for the original azo-dye. Polyolefin yarns, which are normally pigmented due to their unreactive and hydrophobic surfaces, cannot be dyed without chemical or plasma pretreatments or the introduction of a comonomer. Because it has been demonstrated that CDs have a strong affinity to bind with TiO_2 films [110, 111], when i-PP fibers, containing small amounts of particulate TiO_2 as a delusterant, are heated in aqueous solution of the azo-dye-α-CD–rotaxane, they are quickly dyed.

The characteristics of dyeing i-PP with the azo-dye-α-CD–rotaxane are presented in Fig. 26. Not shown in the figure, however, is that the dyed i-PP yarns are both light and wash fast.

The general procedure of delivering additives in the form of their CD–rotaxanes appears to offer improved solutions to a wide-range of polymer-additive and textile-finishing problems, because of two factors. First, CD–rotaxanation of an additive permits control of its solubility and offers protection (UV and chemical) to the threaded additive. Second, chemical modification of the hydroxyl groups on the
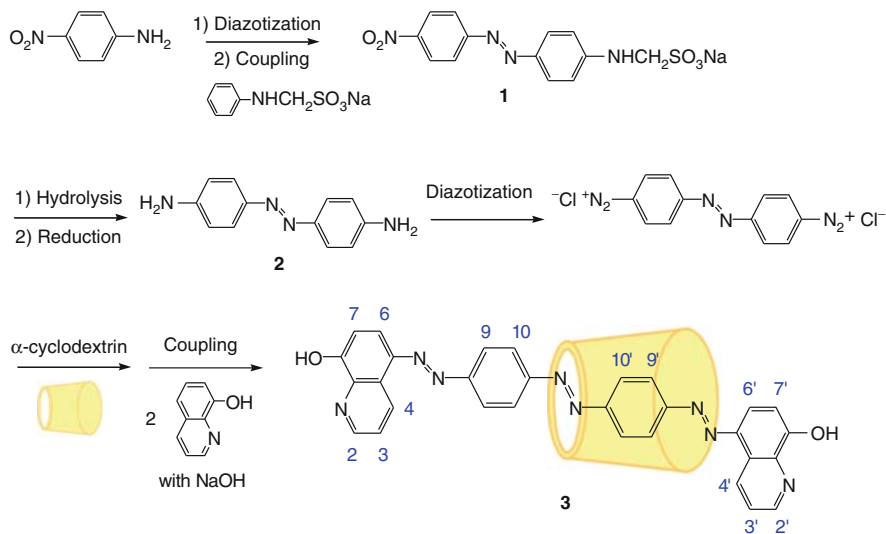
Scheme 3 Synthesis of an azo-dye rotaxane 3 (RD) with 8-hydroxyquinoline as coupling components
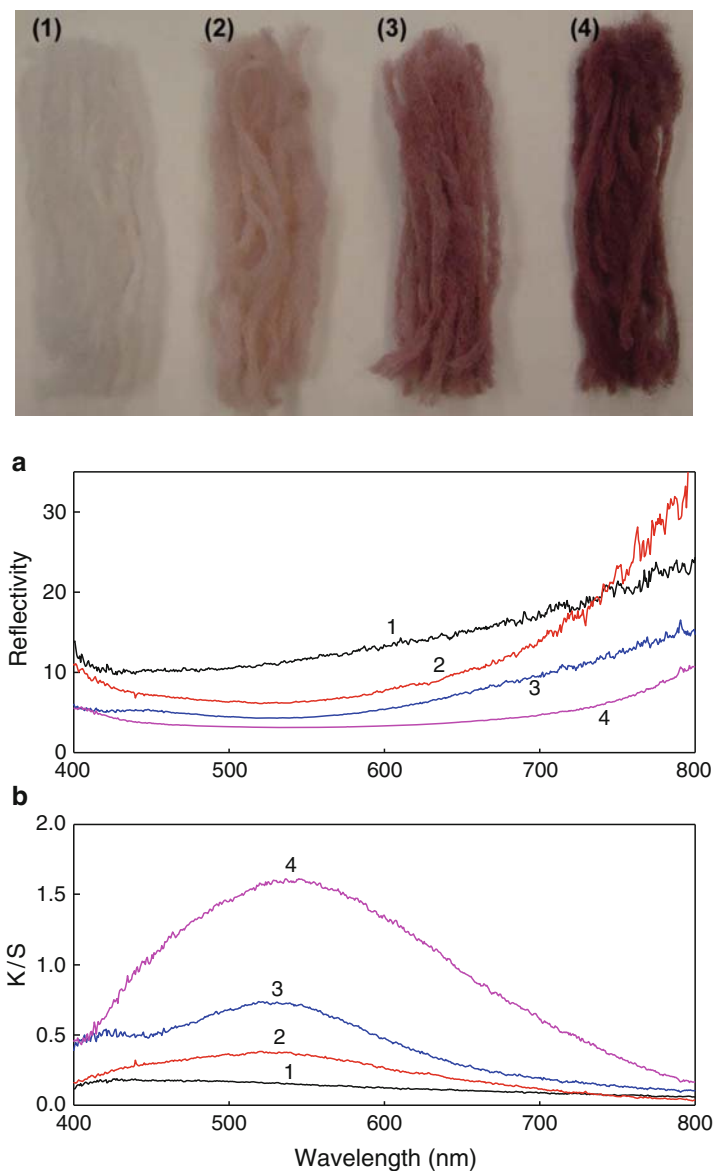
Fig. 26 **1** Reflectivity and **2** K/S curves of PP fibers $K/S = (1-R)^2/2R$, where R = fractional reflectivity, and is a measure of the strength or depth of shade of dyeing. **1** PP before dyeing, **2** after dyed with AzoxFD (free dye), **3** after dyeing with AzoxRD (rotaxanated dye), and **4** after dyeing with AzoxRD complexed with Cu^{2+}. (*Note also photos of the corresponding PP yarns in the top panel*)

CD-coat permits specific substrate targeting of the additive-CD–rotaxane, without the need to modify the chemistry of the additive itself. Together these advantages should soon lead to a new class of polymer and textile additives in the form of their CD–rotaxanes.

5.2.2 Detection of Ni^{+2} with an Azo-Dye-CD–Rotaxane

In fact, recently it has been shown [109] that this same rotaxanated azo-dye is a very sensitive and selective colorimetric and spectrophotometric sensor for nickel(II) salts dissolved in water, showing a submicromolar sensitivity that is highly selective, with a detection range between that of a traditional spectrophotometer and the ion selective electrode (see Figs. 27–29). The effects of anionic species were also studied by adding millimolar amounts of F$^-$, Cl$^-$, and HSO$_4^{2-}$ (as their tetrabutylammonium salts) to the Ni^{2+} solution containing the azodye–rotaxane. No interference in the presence of these anionic species for the detection of Ni^{2+} was observed (see Fig. 29).

From elemental analysis, the stoichiometric ratio between Ni^{2+} and the rotaxanated-azo-Dye was 1:1, which shows that the Ni–Dye complex forms linear chains via the hydroxyquinolone ligands. A possible structure of the Ni^{2+}–Dye complex is shown in Scheme 4.
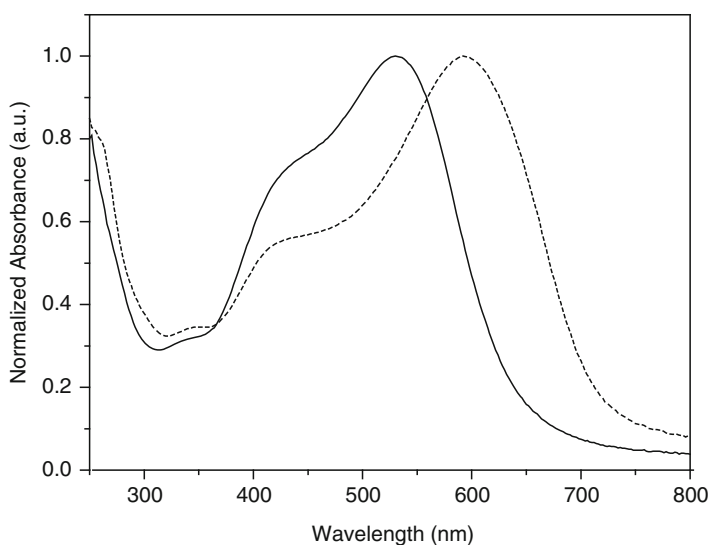
Fig. 27 Normalized UV–Vis absorption spectra in the absence (*solid line*) and presence (*dashed line*) of Ni^{2+} ions added to 3 ml of 20-µM rotaxanated-azo-Dye solution
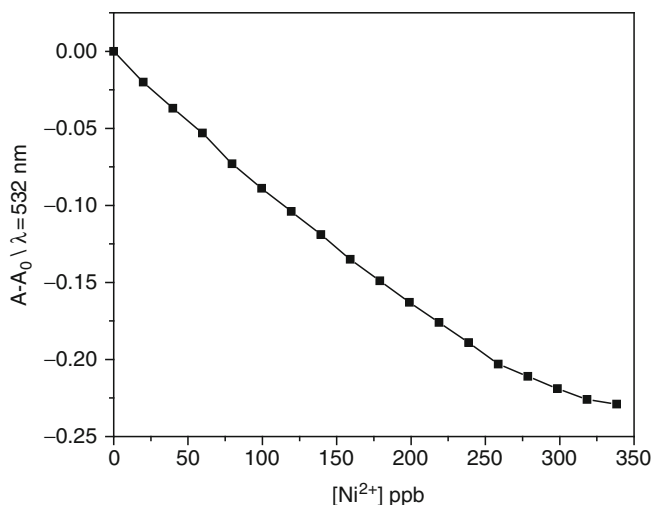
Fig. 28 Titration of the change in the absorption of a rotaxanated-azo-Dye solution measured at ~532 nm vs. the concentration of added Ni^{2+} ions
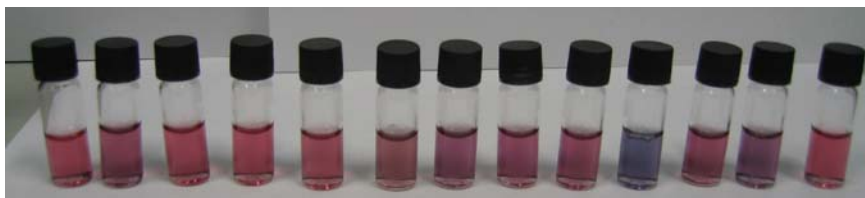
Fig. 29 Color changes observed by "Naked Eye" at very low amounts of M^+ added (for Ni^{2+} 240 ppb) to 1 ml of the azodye rotaxane solution. From left to right: No metal, $+Hg^{2+}$, $+Ca^{2+}$, $+Mg^{2+}$, $+Fe^{3+}$, $+Fe^{2+}$, $+Cd^{2+}$, $+Cu^{2+}$, $+Co^{2+}$, $+Ni^{2+}$, $+Pb^{2+}$, $+Zn^{2+}$, $+Li^+$
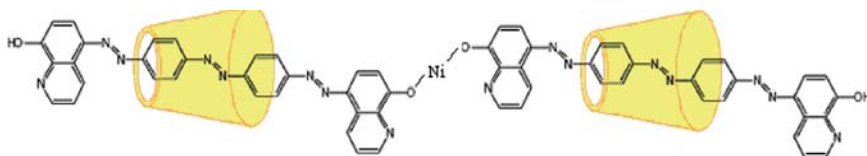
Scheme 4 Possible structure of the 1:1 complex of Ni^{2+} with the rotaxanated-Azo Dye

6 Polymers Functionalized via Covalent Attachment of CDs [112–118]

6.1 Polymers with CDs in their Backbones and as Side Chains

To provide new functionalities to polymer materials, CDs have been chemically bonded to polymers. For example, Sebille et al. [112] grafted β-CD onto

poly-ethyleneimine for the purpose of binding guest drugs. Weickenmeier and Wenz [113] similarly attached β-CDs to the maleic anhydride units in a N-vinyl-2-pyrrolidone/maleic anhydride copolymer, and measured its ability to bind various guest molecules. Here we present several more recent attempts to chemically modify polymers with CDs via covalent bonding.

6.1.1 Step-Growth Polymers

The many hydroxyl groups attached to CDs enable them to be covalently bonded to polymers, either directly to their backbones during, or attached to their side chains subsequent to polymerization. In a modified interfacial polymerization, nylon-6,10 containing various amounts of covalently bonded methyl-β-CDs have been obtained (in methyl-β-CDs two of the three –OHs on each glucose ring are –OCH$_3$) (see Fig. 30) [114–118]. These methyl-β-CD-nylon-6,10 polymers show thermal degradation characteristics very similar to pure nylon-6,10, and are more rapidly dyed to higher dye levels than pure nylon-6,10, as indicated in Fig. 31. Likewise, methyl-β-CD-nylon 6,6 fibers have been synthesized in a similar fashion. DSC data collected for all methyl-β-CD/nylon-6,6 compositions show a characteristic T_m for nylon-6,6 at 255°C, and all are fully soluble in *m*-cresol.

Thus, it is reasonable to assume that the inherent chain mobility of nylon-6,6 is retained in the methyl-β-CD-nylon-6,6s, suggesting that they can be traditionally processed.

6.1.2 Chain-Growth Polymers

Thionyl chloride converts the carboxyl side groups of poly(acrylic acid) to acid chlorides, which will then react with the hydroxyl groups of CD. The degree of CD modification can be varied by controlling the stoichiometry of the CD reaction. Alternatively, the starting material can be a copolymer of acrylic acid or acryloyl chloride with a nonCD-containing comonomer. Incorporation of CD is again achieved by converting the side-groups of the acrylic monomer to CD esters. The CD content of this copolymer can be controlled by varying the initial composition of the copolymer.

Copolymers of acryloyl chloride with methyl methacrylate and styrene have been synthesized, compositional control has been achieved, and the acid chloride side groups have been successfully esterified with methyl-β-CD. One caveat to this method is the difficultly controlling the attachment of just one methyl-β-CD on the reactive side-group, since there are still many hydroxyl groups present on the methyl-β-CD. This then causes methyl-β-CD to act as a crosslinker reacting with several acid chlorides on the copolymer, thereby preventing the methyl-β-CD-incorporated material to be further processed via solution or thermal means.

Mixing low molecular weight PEG with polymers containing CD side groups could lead to a new class of polymer blends in which the polymer A (with CD side
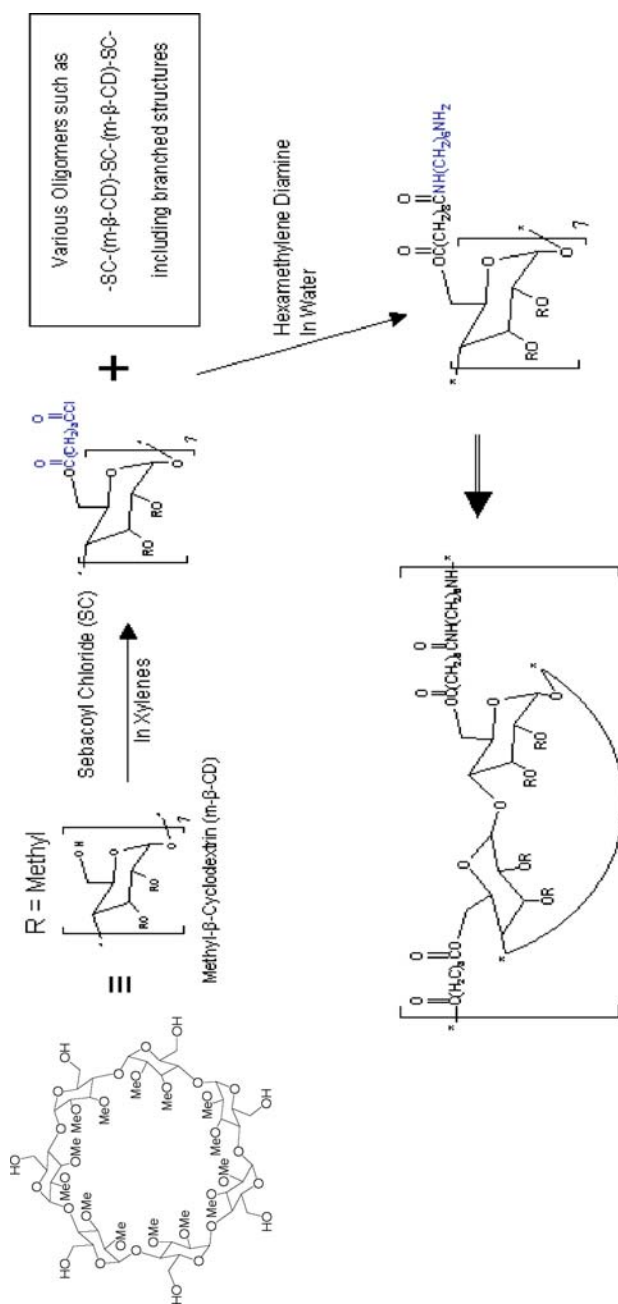
Fig. 30 Synthesis of methyl-β-CD-nylon-6,10 via condensation polymerization using sebacoyl chloride modified methyl-β-CD
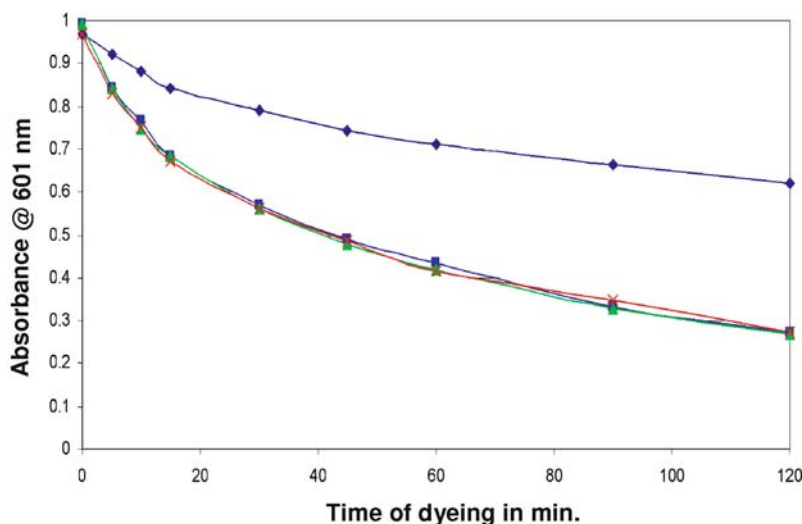
Fig. 31 Disappearance of blue-29 dye from dye bath upon introduction of nylon-6,10 fibers without (*upper curve*) and with (*lower curves*) various contents of covalently bonded methylated-β-CDs in their backbones

groups) is physically crosslinked by polymer B (PEG) through the IC links formed between the CD side groups and PEG. The degree of crosslinking and crosslink length can be controlled simply by varying the amount of PEG added and the PEG chain length, respectively. Using this approach, it may be possible to create a new class of materials which exhibit controllable elastomeric properties.

6.1.3 CD-Star Polymers [114–118]

CDs have several reactive hydroxyl groups, which can be chemically modified and then functionalized with vinyl monomers, such as *t*-butyl acrylate, methyl methacrylate, styrene or acrylonitrile, producing star polymers with CD at their centers (see Fig. 32). One way to control the length of the star arms is through use of atom-transfer radical polymerization (ATRP), which is known to produce highly controlled and uniform polymer molecular weights [119]. This synthetic scheme is applicable to a wide variety of vinyl monomers, and it could become a general method for preparing CD-containing star polymers of differing chemical compositions. Table 8 shows characterization data from our recent work synthesizing stars with a γ-CD core and polystyrene arms [114, 115]. These stars are currently being evaluated for compatibilizing immiscible polymer blends for the purpose of making a more intimately blended system. The theory behind using these CD-stars for compatibilization will be discussed later in this section.

One advantage γ-cyclodextrin has demonstrated is its ability to thread many types of homopolymers into its interior cavity due to its larger inner core dimension of
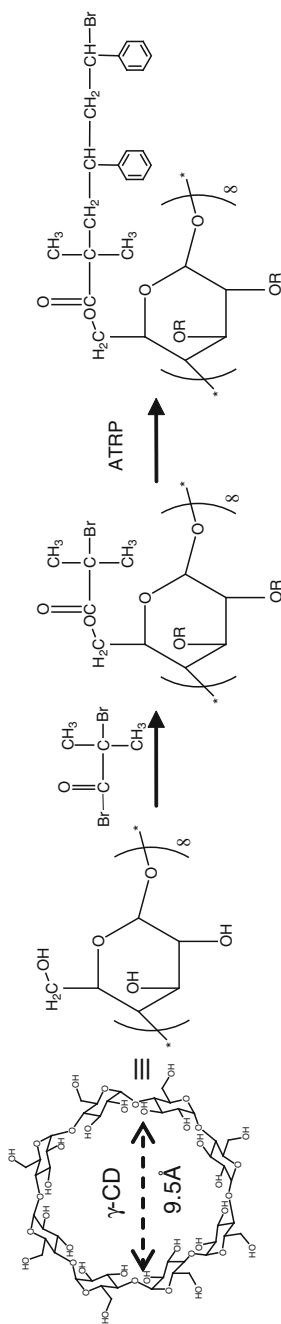
Fig. 32 ATRP synthesis of PS stars with γ-CD core

Table 8 Tabulated characterization results for the PS-γCD-stars [114, 115]

PS$_x$-gCD[a]	gCD[b] [wt%/mole%]	Mw$^b_{(actual)}$ [g mol^{-1}]	Tg[c] [°C]	Mw[d] [g mol^{-1}]	Mn[d] [g mol^{-1}]	Mw/Mn[d]
PS$_0$-gCD (initiator)	41.69/7.69	3,085	–	2,060	2047	1.01
PS$_{3.4}$-gCD	17.53/2.39	7,334	87.5	5,465	5,023	1.09
PS$_{32}$-gCD	2.99/0.26	43,079	96.5	28,826	25,229	1.14
PS$_{52}$-gCD	1.89/0.16	68,075	99.8	42,317	36,115	1.17
PS$_{90}$-gCD	1.11/0.09	115,567	109.0	102,035	85,545	1.19

[a] "x" denotes the degree of polymerization per PS arm (average of 12 arms on each γ-CD);
[b] Calculated from ^{1}H-NMR data. MW of modified γ-CD is noted to be *1,286 g mol^{-1}* [= 1,298 g mol^{-1} − 12 (H's)] which accounts for the attachment of 12 initiator/arm sites;
[c] Measured with Perkin–Elmer DSC-7 at a heating and cooling rate of 40°/min under air, values represent second heating cycle from 20 to 120°C;
[d] Relative measurements based on SEC linear polystyrene standards in THF

9.5 Å, whereas α- and β-CDs have diameters of 5.7 and 7.8 Å, respectively. A general exception to γ-CD threading has been observed for polystyrene, although this may depend on its tacticity [34, 56]. Isotactic sequences of PS (i-PS) have been modeled [34] to show that threading is possible with a cross-sectional area of 8.9 Å. On the other hand, the cross-sectional diameter of 10.2 Å for syndiotactic PS (s-PS) sequences has been modeled to be too large for threading into the γ-CD cavity [34]. Therefore, an atactic PS (a-PS) containing isotactic sequences on the polymer chain end will have some tendency for inclusion, but full threading of the chain is unlikely. Thus, in theory, using PS for growing arms from the γ-CD core will inherently help to reduce self-threading and thus self-gelation leaving the γ-CD cavity open for other molecular guests.

These star polymers with γ-CD cores have the ability to complex with a variety of additives via formation of CD–ICs. They may also be able to be blended with a second normally incompatible polymer, such as PDMS, with a strong propensity to thread through and complex with their γ-CD cores [14]. Both of these potential applications are illustrated schematically in Fig. 33.

In order to encourage mixing of γ-CD into a given polymer matrix, γ-CD needs to be chemically modified with the same chemical make-up as the matrix polymer to not only make it more compatible with the matrix, but also to break-up and discourage hydrogen bonding between γ-CD hydroxyl groups, which will help to reduce precipitation of crystalline γ-CD and to reduce the heterogeneity of the mixture. Ideally, individual molecules of modified γ-CD will be isolated homogeneously within the matrix (polymer A), where the second homopolymer (polymer B) would be threaded through the γ-CDs, resulting in a homogeneously blended sample. Figure 33 illustrates this concept, where the matrix polymer (polymer A is shown in red, the blended polymer (polymer B) in blue, and the γ-CD in black.

As can be seen, polymer B now has a second possibility for lowering its overall energy, which is accomplished by threading through the cyclodextrin rather than
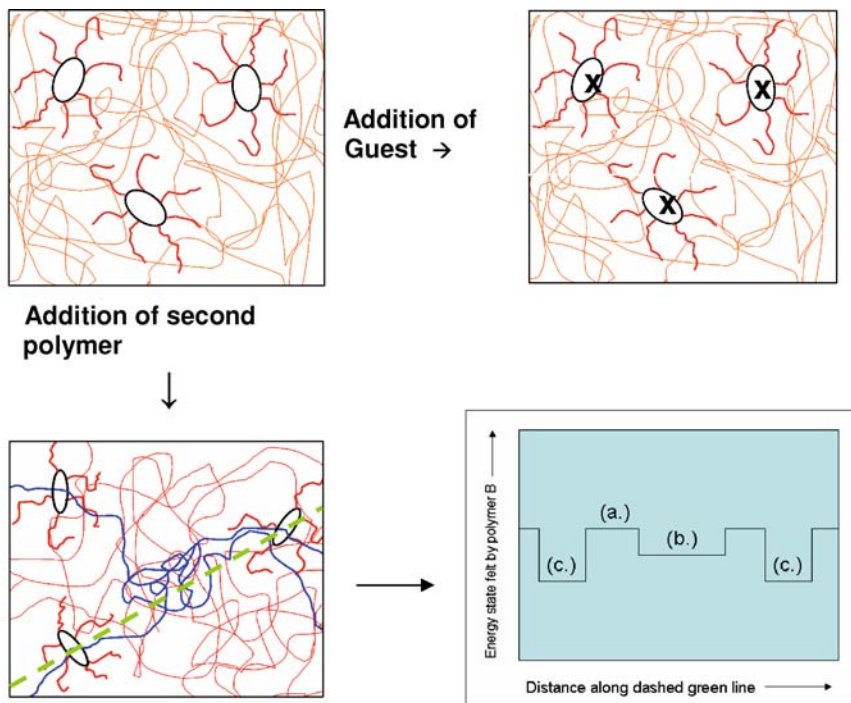
Fig. 33 Complexing small-molecule additive and polymer guests in CD-star polymers. The hypothetical graph in the bottom right corner suggests the relative energy states that may be experienced by polymer B along the *dashed line* in the reference schematic, where (**a**) refers to the A–B energy state, (**b**) to the B–B energy state, and (**c**) is the B–CD energy

coiling into its own phase to maximize B–B interactions. In fact in some polymer cases, if γ-CD is mixed neat into a bulk polymer liquid, an inclusion compound will spontaneously form, indicating that the polymer's environment in the inclusion compound is more energetically favorable than interchain interactions in its bulk [45, 72]. In the lower right corner of Fig. 33, a hypothetical graph of the relative energy states that may be experienced by polymer B along the green dashed line in the schematic shown just to its left in Fig. 33 is suggested. Point (a.) refers to the A–B energy state, (b.) to the B–B energy state, and (c.) is the B–CD energy state.

A point to consider is the physical entrapment of polymer B in the polymer A matrix by the CD "handcuff." If the modified CD is truly dispersed in the matrix polymer, then the polymer-A-modified-CD will be anchored to the polymer A matrix through "like-chain" polymer A–polymer A interactions. So when the blended polymer, polymer B, threads through the CD at that point in the matrix, then the chain motions will be reduced forcing the chain to be channeled through that particular point. This will then lead to kinetic entrapment, which can be viewed as a physical "crosslink," when the temperature is below the glass transition temperature (T_g) of polymer B. For the case when the temperature is above the T_g of polymer

B, it might have enough kinetic energy to wiggle free of the CD handcuff, due to reptilian-like motions, thus becoming able to migrate to another B-chain, where it could possibly lower its overall energy state through B–B interactions, resulting in phase segregation.

Additionally, if both polymers A and B have an affinity for inclusion into cyclodextrin, then the kinetics of IC complexation and competitive lower energy states might need to be carefully considered. To a degree, inclusion may potentially be controlled by molecular weight (MW). Harada et. al. [1] suggested, based on noncompetitive CD–IC formation studies, that there is a much lower probability of CD to find a chain-end for threading higher molecular weight polymers, than for lower MW polymers, thus causing the threading time to be drastically increased [1,55,73,74]. However, in competitive CD–IC formation with polymers of low and high MWs it was found that the CD–ICs formed contained predominantly the high MW polymer. [11,15,41]

In Figs. 34 and 35 we present films formed with PS-γ-CD stars and linear PS (MW = 280 k) and chloroform solutions containing PS-γ-CD stars, linear PS, and poly(dimethyl siloxane) (PDMS), respectively. The synthesized stars were blended with PS homopolymer to give a 1 wt% γ-CD (7.7 μmols γ-CD core per 1 g) incorporation. The components were initially dissolved in chloroform. After the solvent was removed by evaporation under vacuum and heat, the solid was collected, compression molded under 6 kpsi at 125°C, and quenched to room temperature. The resultant films were clear with a slight yellow tinge. This color is thought to be due to the bromine group capping the end of the PS arms on the stars. These clear and transparent films point to miscibility of the PS-γ-CD-stars in linear PS.

Blending experiments with PS-γ-CD stars were conducted using PDMS, a polymer normally immiscible with PS. The synthesized stars were blended with PS homopolymer (MW = 280 kg mol^{-1}) at a level of 1 wt% γ-CD (7.7 μmols per 1 g)
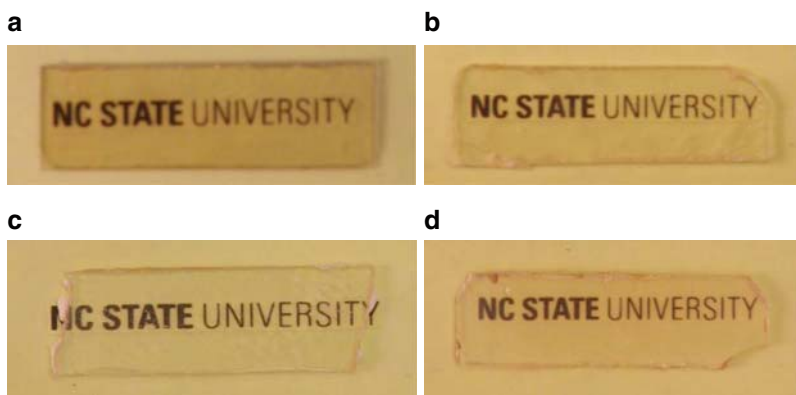
Fig. 34 Images of clear compression molded films made with linear PS (MW = 280 kg mol^{-1}) blended with PS-γ-CD 12-arm star molecules. (**a**) PS3.4-γ-CD, (**b**) PS32-γ-CD, (**c**) PS52-γ-CD, and (**d**) PS90-γ-CD
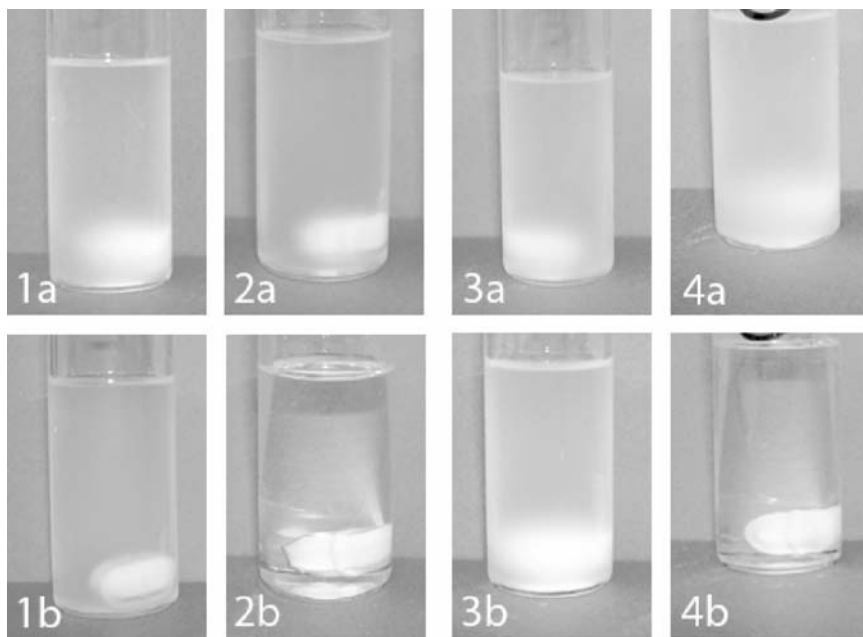
Fig. 35 Before (**a**) and after heating (**b**) solutions to 60°C containing 5 wt% PDMS, where the respective mixtures are made up of (1) PDMS (MW = 62 kg/mol) + PS, (2) PS19γCD star + PDMS (MW = 62 kg mol^{-1}) + PS, (3) PDMS (MW = 308 kg mol^{-1}) + PS, and (4) PS10γCD star + PDMS + PS. Samples containing stars used 1 wt% γ-CD incorporation, where PS (MW = 280 = kg mol^{-1}) made up the remainder of the mass. All solutions had total concentrations of 1 g/10 ml CHCl$_3$. The white masses on the bottom of the vials are PTFE-coated stir bars which can be used to judge the clarity of the solutions

incorporation and 5 wt% PDMS. The degree of polymerization of each star arm (or length) is denoted by the number following the PS designation (e.g., PS90-γ-CD), whereas every star contains 12 arms. Upon mixing the components in chloroform, the solutions were turbid and hazy and remained so after 2 weeks at room temperature. Conversely, heating of these solutions to 60°C for 20–40 h just after preparation resulted in clear solutions. Figure 35 shows images of nonstar and star incorporated solutions before and after heating to 60°C. These solutions were clear and stable for several days after cooling back to room temperature. The stirbar at the bottom of the vials can be used to gauge the clarity of the solutions. Clearing of the solutions containing the stars, illustrated in Fig. 35, provides evidence pointing to threading of PDMS though the γ-CD cores.

Figure 36 shows differential scanning calorimetry heating traces comparing films processed identically from select solutions in Fig. 35. It can be observed that the sample containing only PDMS + PS shows evidence of a T_m at −39°C due to the PDMS, whereas the sample containing star + PDMS + PS does not show a T_m in this region due to the PDMS. This leads to the notion that the PDMS is molecularly dispersed and not able to crystallize, which is a result of the PDMS being
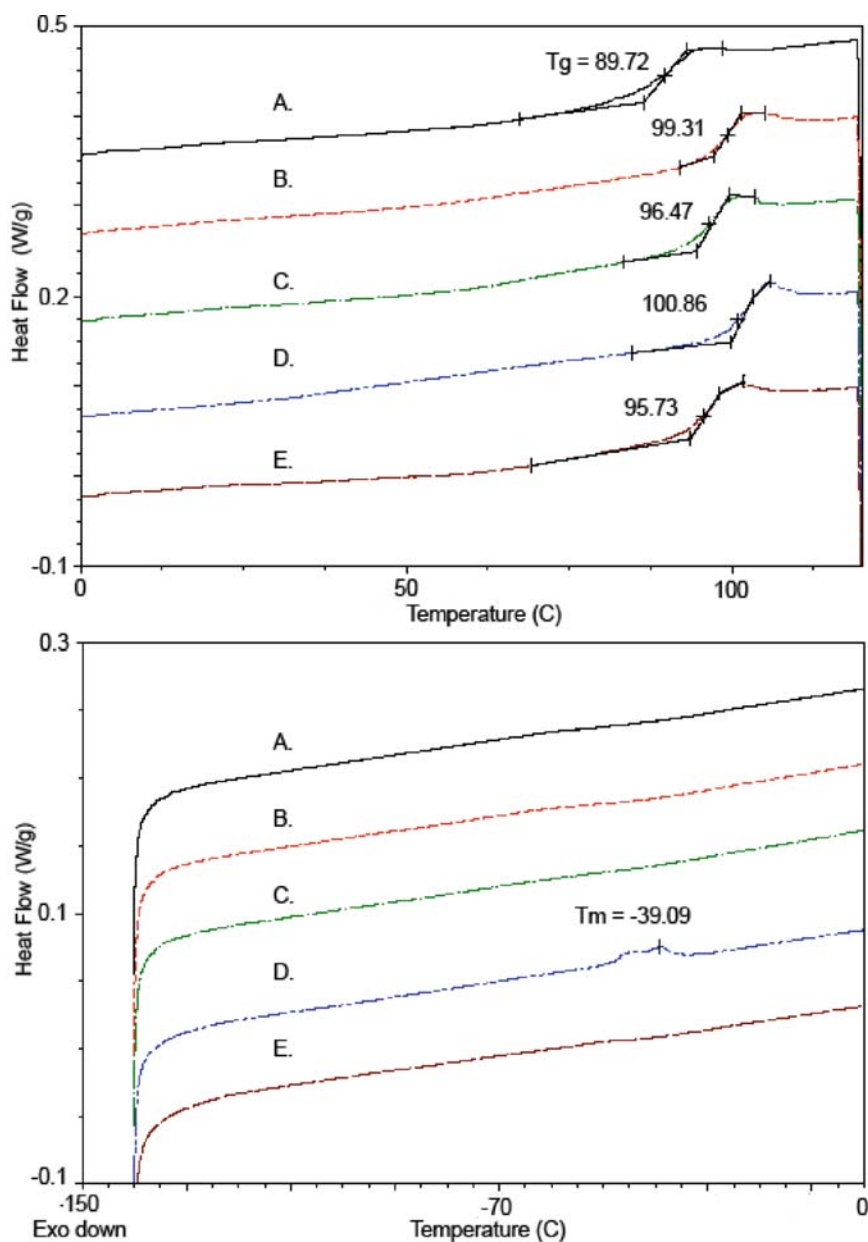
Fig. 36 Differential Scanning Calorimeter traces of (**a**) PS10-γ-CD star, (**b**) PS, (**c**) PS10-γ-CD star + PS, (**d**) PDMS + PS, and (**e**) PS10-γ-CD star + PDMS + PS. The star containing sample incorporated 1 wt% γ-CD, whereas samples containing PDMS (MW = 308 kg mol^{-1}) incorporated 5 wt%, while with the remainder of the mass was composed of PS (MW = 280 kg mol^{-1}). All DSC curves present the second heating cycle for each sample at a heating rate of 10°C min^{-1} under helium purge gas

physically handcuffed into the PS matrix by the cyclodextrin star leading to reduced molecular interactions and motions. Further evidence of molecular mixing is the PS glass transition (T_g) region for the star + PDMS + PS sample. In this region the T_g of the star + PDMS + PS sample is slightly reduced to 95.7°C when compared to only star + PS, which has a T_g of 96.5°C. Overall the DSC data suggests that at least partial intimate blending is occurring.

7   Summary and Conclusions

We have demonstrated that the structures, morphologies, and even chain conformations of solid polymer samples may be altered by including them in and then coalescing them from their CD–ICs. In addition to altering their physical behaviors, coalescence of guest polymers from their CD–ICs permits us to obtain solid polymer samples that are distinct from bulk samples made from their solutions and melts. Clearly study of such reorganized coalesced polymer samples can contribute to our ability to understand and develop improved structure–property relations for them.

Additionally, because crystalline CD–ICs are high-melting and thermally stable, even when containing small-molecule guests that are volatile liquids or even gases in the bulk, delivery of additives to polymer materials can be improved by using additive-CD–ICs, which may often be conveniently melt-processed into polymers. If we begin with appropriate soluble additive-CD–IC and then react the unincluded ends of the guest additive with capping groups that prevent it from unthreading, we create a CD-additive-rotaxane. One advantage of CD-additive-rotaxanes is the protection (thermal, chemical, UV–Vis, etc.) afforded by their CD coats. Another is the ability to utilize the many –OH groups on the CD coat to target the delivery of the CD-additive-rotaxane to a particular polymer substrate.

CDs may also be covalently bonded to polymers to alter their functionalities through incorporation of CDs into their backbones during polymerization or attachment to their side-chains via postpolymerization reactions. The presence of covalently bonded CDs in polymers serves to increase their acceptance and retention of additives, such as dyes, fragrances, antibacterials, etc. They may also be further reacted or treated through their covalently bonded CDs to cross-link and form networks or to form blends with other polymers having a propensity to thread through their attached CD cavities.

Because CDs are nontoxic, biodegradable, and bioabsorbable, they may be used in medical applications, as well as providing for the fabrication of more environmentally responsible polymer materials. In this report we have summarized almost exclusively our own recent studies employing the cyclic starch derivatives called cyclodextrins to both nanostructure and functionalize polymer materials. Lest the reader gets the erroneous impression that our studies have been carried out in isolation, we refer to a recent review [120], and a summary [121], describing related

research that also attempts to utilize CDs and polymers to create materials with improved and new properties for advanced applications.

References

1. Harada A, Kamachi M (1990) Macromolecules 23:2821
2. Huang L, Vasanthan N, Tonelli AE (1997) J Appl Polym Sci 64:281
3. Tonelli AE (1997) Polym Int 43:295
4. Huang L, Allen EJ, Tonelli AE (1997) In: Pandalai SG (ed) Recent research developments in macromolecular research, Vol. 2. Research Signpost, Trivandrum, India, p 175
5. Huang L, Allen E, Tonelli AE (1998) Polymer 39:4857
6. Huang L, Tonelli AE (1998) J Macromol Sci Revs Macromol Chem Phys C38(4):781
7. Huang L, Tonelli AE (1999) In: Dinh SM, DeNuzzio JD, Comfort AR (eds) Intelligent materials for controlled release technologies, Chap.10. ACS Symposium Series No. 728. ACS, Washington, DC
8. Huang L, Allen E, Tonelli AE (1999) Polymer 40:3211
9. Huang L, Taylor H, Gerber M, Orndorff P, Horton J, Tonelli AE (1999) J Appl Polym Sci 74:937
10. Lu J, Shin ID, Nojima S, Tonelli AE (2000) Polymer 41:5871
11. Rusa CC, Tonelli AE (2000) Macromolecules 33:1813
12. Rusa CC, Tonelli AE (2000) Macromolecules 33:5321
13. Huang L, Gerber M, Lu J, Tonelli AE (2001) Polym Degrad Stabil 71:279
14. Porbeni FE, Edeki EM, Shin ID, Tonelli AE (2001) Polymer 42(16):6907
15. Rusa CC, Luca C (2001) Macromolecules 34:1318
16. Wei M, Tonelli AE (2001) Macromolecules 34:4061
17. Lu J, Hill M, Hood M, Greeson DF Jr, Horton IR, Orndorff PE, Herndon SA, Tonelli AE (2001) J Appl Polym Sci 82:300
18. Shuai X, Porbeni FE, Wei M, Shin ID, Tonelli AE (2001) Macromolecules 34:7355
19. Huang L, Gerber M, Taylor H, Lu J, Tapazsi E, Wutkowski M, Hill M, Harvey A, Rusa CC, Wei M, Porbeni FE, Lewis CS, Tonelli AE (2001) Macromol Chem Macromol Sympos 176:129
20. Shuai X, Wei M, Porbeni FE, Bullions TA, Tonelli AE (2002) Biomacromolecules 3:201
21. Bullions TA, Wei M, Porbeni FE, Gerber MJ, Peet J, Balik M, Tonelli AE (2002) J Polym Sci Polym Phys Ed 40:992
22. Shuai X, Porbeni FE, Wei M, Bullions TA, Tonelli AE (2002) Macromolecules 35:3126
23. Wei M, Davis W, Urban B, Song Y, Porbeni FE, Wang X, White JL, Balik CM, Rusa CC, Fox J, Tonelli AE (2002) Macromolecules 35:8039
24. Rusa CC, Bullions TA, Fox J, Porbeni FE, Wang X, Tonelli AE (2002) Langmuir 18:10016
25. Shuai X, Porbeni FE, Wei M, Bullions TA, Tonelli AE (2002) Macromolecules 35:2401
26. Shuai X, Porbeni FE, Wei M, Bullions TA, Tonelli AE (2002) Macromolecules 35:3778
27. Wei M, Shuai X, Tonelli AE (2003) Biomacromolecules 4:783
28. Bullions TA, Edeki EM, Porbeni FE, Wei M, Shuai X, Tonelli AE (2003) J Polym Sci Polym Phys Ed 41:139
29. Rusa CC, Fox J, Tonelli AE (2003) Macromolecules 36:2742

30. Abdala AA, Khan S, Tonelli AE (2003) Macromolecules 36:7833
31. Tonelli AE (2003) J Tex. Appar Tech Manage 3(2):1
32. Tonelli AE (2003) Macromol Sympos 203:71
33. Wei M, Bullions TA, Rusa CC, Wang X, Tonelli AE (2003) J Polym Sci B Polym Phys Ed 42:386

As seen in Fig. 10 in both non-aromatic carbon spectral regions the least shielded, downfield resonance belongs to as-received PET, the most shielded, upfield resonance comes from coalesced or included PETs, and the precipitated PET [59] seems to contain ~30 and ~70% material resonating at the frequencies of these downfield and upfield, as-received, and coalesced or included PET peaks, respectively. We expect [122] carbonyl carbons terminating ethylene glycol fragments whose -CH$_2$–O- and -O–CH$_2$- bonds have g± conformations to resonate upfield from those with t conformations. This is consistent with conclusions drawn previously from modeling the conformations of included PET chains [78, 84] and the FTIR analysis [21] of as-received and coalesced PET conformations.

We would normally expect the methylene carbon resonances of these PET samples to exhibit the same order of resonance frequencies, because they are γ to the carbonyl carbons and are either t or g± to them conformationally across the same -CH$_2$–O- and -O–CH$_2$-bonds. This is, in fact, what we observe in Fig. 10. However, a recent solid-state ^{13}C-NMR study of PETs by Kaji and Schmidt-Rohr [123] has convincingly established that the resonance frequencies of methylene carbons in PETs are insensitive to the conformations of the -CH$_2$–O- and -O–CH$_2$- bonds, and instead seem to depend only upon the conformations of the -CH$_2$–CH$_2$- bond connecting them. On highly crystalline and predominantly amorphous PET samples with ^{13}C-enriched methylene carbons they were able to separately observe methylene carbon resonances belonging to t and to g ± -CH$_2$–CH$_2$- bonds. They found that in both PET samples the methylene carbons belonging to t -CH$_2$–CH$_2$- bonds resonated ~2 ppm upfield from those methylene carbons with g ± -CH$_2$–CH$_2$- bonds, even though the -CH$_2$–O- and -O–CH$_2$- bonds are predominantly t in the highly crystalline PET and significantly g± in the nearly completely amorphous PET sample. As a consequence, we can conclude that our coalesced and included PETs have predominantly t -CH$_2$–CH$_2$- bonds, as-received PET predominantly g±, and our precipitated PET [59] sample seems to have about 30% g± and 70% t -CH$_2$–CH$_2$ bonds. Again, this is consistent with our molecular modeling [78, 84] and FTIR [21] results, so as-received PET has predominantly g ± -CH$_2$–CH$_2$- bonds and substantial amounts of t -CH$_2$–O- and -O–CH$_2$- bonds, while coalesced, included, and precipitated PETs have preponderantly t -CH$_2$–CH$_2$- and g ± -CH$_2$–O- and -O–CH$_2$- bonds.

The ^{13}C-observed ^{1}H spin-lattice relaxation times in the rotating frame [$T_{1\rho}(^1H)$], which reflect motions in the kHz frequency regime, are presented as a function of temperature for our PET samples in Fig. 11. Generally the coalesced sample has the longest and the as-received sample the shortest $T_{1\rho}(^1H)$, indicating an increasing kHz mobility for PET chains in the coalesced, precipitated, and as-received samples, respectively. Also note that the $T_{1\rho}(^1H)$s of as-received PET show a marked sensitivity to temperature at $T \sim T_g$, which is largely unobserved in the coalesced and precipitated samples. Initially, the molecular motion increases with temperature resulting in shorter $T_{1\rho}(^1H)$s for all the PET samples. However, the $T_{1\rho}(^1H)$ of the as-received PET reaches a minimum near T_g, and further heating results in molecular motions that are too rapid for efficient nuclear spin energy transfer, so $T_{1\rho}(^1H)$ increases for $T > T_g$. This is consistent with the presence and absence of a glass transition observed in the DSC scans of as-received and coalesced (see Fig. 7) or precipitated [59] PETs, respectively. Thus, both macroscopic (DSC) and microscopic (NMR) observations point to the absence of a glass transition in the noncrystalline regions of coalesced or precipitated PETs.

At room temperature, the ^{13}C spin-lattice relaxation times, $T_1(^{13}C)$ in seconds, for the as-received (asr), precipitated (ppt), and coalesced (coa) PETS are $C = O \rightarrow 31.8\,s$ (asr) and $36.2\,s$ (coa, ppt); nonprotonated aromatic $\rightarrow 28.6\,s$ (asr) and 36.2 (coa, ppt); protonated aromatic $\rightarrow 14.4\,s$ (asr) and $21.0\,s$ (coa, ppt); and $CH_2 \rightarrow 7.1\,s$ (asr) and $9.6\,s$ (coa, ppt).

Coalesced and precipitated PETs have longer $T_1(^{13}C)$s than as received PET. Thus, motions in the MHz frequency regime are also more restricted in the coalesced and

precipitated PETs, compared with as-received PET, possibly because of both their higher crystallinities and the tighter packing of kink conformers in their noncrystalline regions. Temperature dependencies similar to those observed in the rotating frame for ^1Hs, $T_{1\rho}(^1H)s$, are also observed for the $T_1(^{13}C)s$. This behavior implies that the noncrystalline regions of coalesced and precipitated PETs are distinct from the amorphous regions in as-received PET, because only in as-received PET are the kHz, MHz motions important to $T_{1\rho}(^1H)$ and $T_1(^{13}C)$ relaxations sensitive to whether or not the sample is below or above its T_g. This is again consistent with the failure to observe a glass transition by DSC for coalesced [21] and precipitated [33, 59] PETs.

34. Hunt MA, Uyar T, Shamsheer R, Tonelli AE (2004) Polymer 45:1345
35. Rusa CC, Uyar T, Rusa M, Hunt MA, Wang X, Tonelli AE (2004) J Polym Sci B Polym Phys Ed 42:4182
36. Abdala AA, Wu W, Olesen K, Jenkins RD, Tonelli AE, Khan S (2004) J Rheol 48:979
37. Wei M, Shin ID, Urban B, Tonelli AE (2004) J Polym Sci B Polym Phys Ed 42:1369
38. Rusa CC, Shuai X, Bullions TA, Wei M, Porbeni FE, J. Lu, L. Huang, J. Fox, Tonelli AE (2004) J Polym Environ 12(3):157
39. Rusa CC, Wei M, Bullions TA, Rusa M, Gomez MA, Porbeni FE, Wang X, Shin ID, Balik CM, White JL, Tonelli AE (2004) Cryst Growth Design 4:1431
40. Rusa CC, Wei M, Shuai X, Bullions TA, Wang X, Rusa M, Uyar T, Tonelli AE (2004) J Polym Sci B Polym Phys Ed 42:4207
41. Rusa M, Wang X, Tonelli AE (2004) Macromolecules 37:6898
42. Rusa CC, Rusa M, Gomez MA, Shin ID, Fox JD, Tonelli AE (2004) Macromolecules 37:7992
43. Hernandez R, Rusa M, Rusa CC, Lopez D, Mijanos C, Tonelli AE (2004) Macromolecules 37:9620
44. Rusa CC, Wei M, Bullions TA, Shuai X, Uyar T, Tonelli AE (2005) Polym Adv Technol 16:269
45. Peet J, Rusa CC, Hunt MA, Tonelli AE, Balik CM (2005) Macromolecules 38:537
46. Jia X, Wang X, Tonelli AE, White JL (2005) Macromolecules 38:2775
47. Uyar T, Rusa CC, Wang X, Rusa M, Hacaloglu J, Tonelli AE (2005) J Polym Sci B Polym Phys Ed 43:2578
48. Rusa CC, Bridges C, Ha S-W, Tonelli AE (2005) Macromolecules 38:5640
49. Uyar T, Rusa CC, Hunt MA, Aslan E, Hacaloglu J, Tonelli AE (2005) Polymer 46:4762
50. Porbeni FE, Shin ID, Shuai X, Wang X, White JL, Jia X, Tonelli AE (2005) J Polym Sci B Polym Phys 43:2086
51. Uyar T, Aslan E, Tonelli AE, Hacaloglu J (2006) Polym Degrad Stabil 91(1):1
52. Uyar T, El-Shafei A, Hacaloglu J, Tonelli AE (2006) J Inclus Phenom Macrocyc Chem 55:109
53. Uyar T, Hunt MA, Gracz HS, Tonelli AE (2006) Cryst Growth Design 6:1113
54. Uyar T, Oguz G, Tonelli AE, Hacaloglu J (2006) Polym Degrad Stabil 91:2471
55. Rusa CC, Rusa M, Peet J, Uyar T, Fox J, Hunt MA, Wang X, Balik CM, Tonelli AE (2006) J Inclus Phenom Macrocyc Chem 55:185
56. Uyar T, Gracz HS, Rusa M, Shin ID, El-Shafei A, Tonelli AE (2006) Polymer 47:6948
57. Uyar T, Tonelli AE, J. Hacaloglu (2006) Polym Degrad Stabil 91:2960
58. Pang K, Schmidt B, Kotek R, Tonelli AE (2006) J Appl Polym Sci 102(6):6049
59. Vedula J, Tonelli AE (2007) J Polym Sci B Polym Phys Ed 45:735 (Here the slow addition of a heated trifluoroacetic acid solution of PET into rapidly stirred acetone resulted in a precipitated PET sample (p-PET) whose physical behaviors closely parallel those of PET coalesced from its γ-CD-IC.)
60. Tonelli AE (2007) In: Brown P, Stevens K (eds) Handbook of nanofiber & nanotechnology in textiles. Woodhead, Cambridge, UK
61. Paik Y, Poliks B, Rusa CC, Tonelli AE, Schaefer J (2007) J Polym Sci Part B Polym Phys Ed 45:1271
62. Uyar T, Rusa CC, Tonelli AE, Hacaloglu J (2007) Polym Degrad Stabil 92:32
63. Martinez G, Gomez MA, Villar S, Garrido L, Tonelli AE, Balik CM (2007) J Polym Sci A Polym Chem 45:2503
64. Park JS, Tonelli AE, Srinivasaro M (2009) Adv Mater YY:xxxx

65. Whang H-S, Medlin E, Wrench N, Hockney J, Farin CE, Tonelli AE (2007) J Appl Polym Sci 106:4104
66. Yang H, El-Shafei A, Schilling FC, Tonelli AE (2007) Macromol Theor Simul 16:797
67. Tonelli AE (2008) J Inclus Phenom Macrocyc Chem 60:197
68. Whang H-S, Vendeix FAP, Gracz HS, Gadsby J, Tonelli AE (2008) Pharm Res 25:1142
69. Whang H-S, Hunt MA, Medlin E, Wrench N, Hockney J, Farin CE, Tonelli AE (2007) J Appl Polym Sci 106:4104
70. Whang H-S, Tonelli AE (2008) J Inclus Phenom Macrocyc Chem 62:127
71. Steinbrunn MB, Wenz G (1997) DE 19707855.9, PCT/DE 98/0056
72. Harada A, Okada M, Kawaguchi Y (2007) Chem Lett 34:542
73. Wenz G, Han BH, Muller A (2006) Chem Revs 106(3):782
74. Harada A, Hashidzume A, Takashima Y (2006) Adv Polym Sci 201:1
75. Wenz G (2008) Molecular Recognition of Polymers by Cyclodextrins. Adv Polym Sci
76. Tonelli AE (1991) Theor Comput Polym Sci 1:22
77. Hunt MA, Tonelli AE, Balik CM (2007) J Phys Chem 111:3853
78. Tonelli AE (1992) Comp Theor Polym Sci 2:80
79. Koenig JL (1992) Spectroscopy of polymers, Chap. 4. American Chemical Society, Washington, DC
80. Zerbi G (1999) Modern polymer spectroscopy, Chap. 3. Wiley, New York
81. Miyake A (1959) J Polym Sci 38:479
82. D'Esposito L, Koenig JL (1976) J Polym Sci Polym B Polym Phys Ed 14:1731
83. Psarski M, Piorkowska E, Galeski A (2000) Macromolecules 33:916
84. Tonelli AE (2002) Polymer 43:637
85. Natta G, Corradini P (1960) Nuovo Cim Suppl 15:40
86. Turner-Jones A, Aizlewood JM, Beckett DR (1964) Makromol Chem 75:134
87. Gomez MA, Tanaka H, Tonelli AE (1987) Polymer 28:2227
88. Tonelli AE (1991) Macromolecules 24:3069
89. Eaton P, Vasanthan N, Tonelli AE (1995) Macromolecules 28:2531
90. Belfiore LA, Schilling FC, Tonelli AE, Lovinger AJ, Bovey FA (1984) Macromolecules 17:2561
91. Nakamura K, Aioke K, Usaka K, Kanamoto T (1999) Macromolecules 32:4975
92. Wenz G, Steinbrunn MB (1997) (University of Karlsruhe (TH), Germany). De 19608354 Chem Abstr:623641
93. Steinbrunn MB, Wenz G (1996) Angew Chem Int Ed 35:2139
94. Wenz G, Steinbrunn MB, Landfester K (1997) Tetrahedron 53:15575 (for inclusion and coalescence of nylon-11 from α-CD)
95. Vashanthan N, Salem D (2001) J Polym Sci Polym B Phys Ed 39:536
96. Willcox PJ, Howie DW, Schmidt-Rohr K, Hoagland DA, Gido SP (1999) J Polym Sci Pol Phys 37:3438
97. Hassan CM, Peppas NA (2000) Adv Polym Sci 153:37
98. Hernández R, López D, Mijangos C, Guenet JM (2002) Polymer 43:5661
99. Hernandez R, Sarafian A, López D, Mijangos C (2004) Polymer 45:5543
100. http://www.gl.iit.edu/frame/genbank.htm, Fibroin heavy chain precursor (Fib-H) (H- fibroin), gij9087216jspjP05790j FBOH_BOMMO[9087216], Gene Bank
101. Li J, Ni X, Zhou Z, Leong KW (2003) J Am Chem Soc 125:1788
102. Girardeau TE, Zhao T, Leisen J, Beckham HW (2005) Macromolecules 38:2261
103. He Y, Inoue Y (2003) Biomacromolecules 4:1865
104. Vogel R, Tandler B, Haussler L, Jehnichen D, Brunig H (2006) Macromol Biosci 6:730
105. Dong T, He Y, Zhu B, Shin K, Inoue Y (2005) Macromolecules 38:7736
106. Dong T, Shin K, Zhu B, Inoue Y (2006) Macromolecules 39:2427
107. Kawaguchi Y, Nishiyama T, Okada M, Kamachi M, Harada A (2000) Macromolecules 33:4427
108. Lu J, Mirau PA, Tonelli AE (2001) Macromolecules 34:3276
109. Park JSK, Srinivasaro M (2009) Macromolecules YY:xxxx
110. Haque SA, Park JS, Srinivasarao M, Durrant JR (2004) Adv Mater 16(14):1177

111. Craig MR, Claridge TDW, Hutchings MG, Anderson HL (1999) Chem Commun 1537
112. Sebille B, Thuaud N, Behar N, Piquion J (1987) J Chromatogr 409:61
113. Weickenmeier M, Wenz G (1996) Macromol Rapid Commun 17:731
114. Busche BJ, Balik CM (2006) Abstr Pap Am Chem Soc 231:2
115. Busche BJ, Tonelli AE, Balik CM (2007) Abstr Pap Am Chem Soc 232:2
116. Miura Y, Narumi A, Matsuya S, Satoh T, Duan Q, Kaga H, Kakuchi T (2005) J Polym Sci A Polym Chem 43:4271
117. Xiao H, Li J (2005) Tetrahedron Lett 46:2227
118. Plamper FA, Becker H, Lanzendorfer M, Patel M, Wittemann A, Ballauf M, Muller AHE (2005) Macromol Chem Phys 206:1813
119. Odian G (2004) Principles of polymerization, Chap. 3, 4th edn. Wiley, New York
120. Wenz G, Han BH, Muller A (2006) Chem Rev 106(3):782
121. Volume 57 of J. Inclusion Phenom Macrocyclic Chem 2007, is devoted to papers presented at the XIII International Cyclodextrin Symposium held May, 2006 in Turin, Italy.
122. Tonelli AE (1989) NMR spectroscopy and polymer microstructure: the conformational connection. VCH, New York
123. Kaji H, Schmidt-Rohr K (2002) Macromolecules 35:7993

Polymerization of Included Monomers and Behaviour of Resulting Polymers

SooWhan Choi, Sadik Amajjahe, and Helmut Ritter

Abstract Cyclodextrins (CDs) are of interest to synthetic chemists because of their chemical stability and the possibility to modify these molecules in a regioselective manner. For supramolecular chemistry CDs are of great importance, since they represent a homologous series of water-soluble and chiral host molecules which can be used as models for studying weak interactions. In addition, their low price provides motivation for the discovery of new applications. Thus, CDs are used for the solubilization and encapsulation of drugs, perfumes, and flavourings. These applications are due to their low toxicity and their biodegradablity. Finally, they are of general interest because they are obtained from a renewable resource, starch (Eggersdorfer, M., Warwel, S., Wulff, G.: Nachwachsende Rohstoffe Perspektiven für die Chemie. VCH, Weinheim (1993).

Contents

S. Choi, S. Amajjahe, and H. Ritter (✉)
Institute of Organic Chemistry and Polymer Chemistry, Heinrich-Heine-University of Duesseldorf, Universitaetsstr. 1 40225 Duesseldorf, Germany
e-mail: H.Ritter@uni-duesseldorf.de

Abbreviations

AIBN	$2,2'$-Azobis(2-methylpropionitrile)
AMPS	2-Acrylamido-2-methylpropansulfonate
ANS	8-Anilino-1-naphthalinsulfonacid ammonium
CD	Cyclodextrin
2D-ROESY	Two-dimensional rotating-frame overhauser spectroscopy
DEF	Diethyl fumarate
DEM	Diethyl maleate
DMF	N,N-Dimethyl formaldehyde
DSC	Differential scanning calorimetry
MDAA	N,N-Dimethylacrylamide
EDT	3,4-Ethylenedioxythiophene
FT-IR	Fourier transformations infra red
GPC	Gel Permeation Chromatography
HPLC	High pressure liquid chromatography
LCST	Lower critical solution temperature
MALDI-TOF MS	Matrix assisted laser desorption ionization time of flight mass spectroscopy
Me	Methylated
M_w/M_n	Polydispersities
NIPAAM	N-Isopropylacrylamide
NMR	Nuclear magnetic resonance spectroscopy
r	Copolymerization parameters
RAFT	Reversible addition–fragmentation chain transfer
R_f	Retention factor
T_{crit}	Critical solution temperature
T_g	Glass transition temperature
t	Transparency
TLC	Thin layer chromatography
TTC	Thiocarbonylsulfanylpropionic acid
UV	Ultra violet spectroscopy
V50	2-Methylpropionamidine dihydrochloride
VA44	$2,2'$-Azobis[2-(2-imidazolin-2-yl)propane]dihydrochloride

1   Cyclodextrins as Hydrophilic Hosts

A supramolecular structure results from defined non-covalent interactions between several individual molecules. [1–9]. Host–guest complexes [10–13] are important examples of this type of structure. The host molecule offers the guest molecule a suitable environment, generally a cavity (Scheme 1). The driving forces for complexation can arise from coulombic, dipole–dipole, van der Waals, hydrophobic, solvatophobic, or hydrogen bonding interactions between host and guest [14, 15]. The outer sphere of the host should be compatible with the required solvent in order to avoid aggregation or insolubility problems.
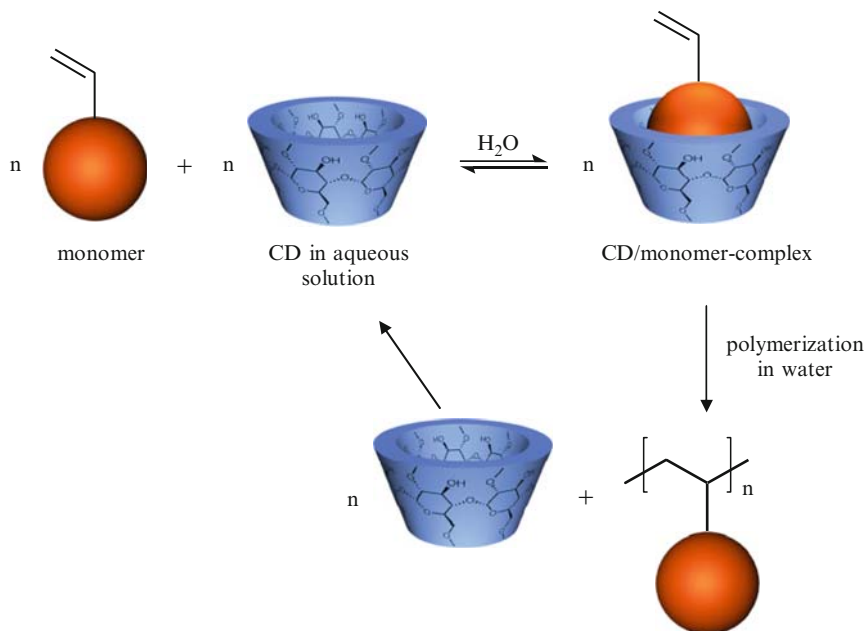
Scheme 1 Schematic illustration of complexation and polymerization of β-CD-complexed monomers

The formation of the complexes leads to significant changes of the solubility and reactivity of the guest molecules without any chemical modification. Thus, water insoluble molecules may become completely water soluble simply by mixing with an aqueous solution of native CD and CD derivatives, e.g. methylated (Me) or hydroxypropylated CD. The water solubility of these inclusion compounds enables detection of complex formation in solution by spectroscopic methods, such as NMR [16], UV, fluorescence, or circular dichroism spectroscopy, as well as by thermodynamic methods, e.g. microcalorimetry [17] or density [18, 19], or by solubility measurements. Likewise, mass spectrometry was used [20].

A crystal of the complexes suitable for X-ray diffraction analysis shows an orthorhombic structure, in which the guest molecule is complexed by the CD cavity (Fig. 1) [21, 22]. It is interesting to note that the complexes are packed in columns, and the CD toruses are tilted in an alternatively oriented way, wherein the orientation of the entire column can be either upwards or downwards. The guest molecules are located almost perpendicularly to the host.

2D–ROESY measurements can be evaluated along with the constitution of the complexes (Fig. 2) [23]. Cross peaks can be detected between the protons of the guest molecule and the inner protons of the Me-β-CD torus.

A further important and easy method to prove the formation of a complex is thin layer chromatography. For example, the R_f-values of methylated β-CD (Me-β-CD, $R_f = 0.69$) and uncomplexed phenyl methacrylate ($R_f = 0.92$) in methanol are significantly different from the values of the complex ($R_f = 0.54$) [24].

a

b
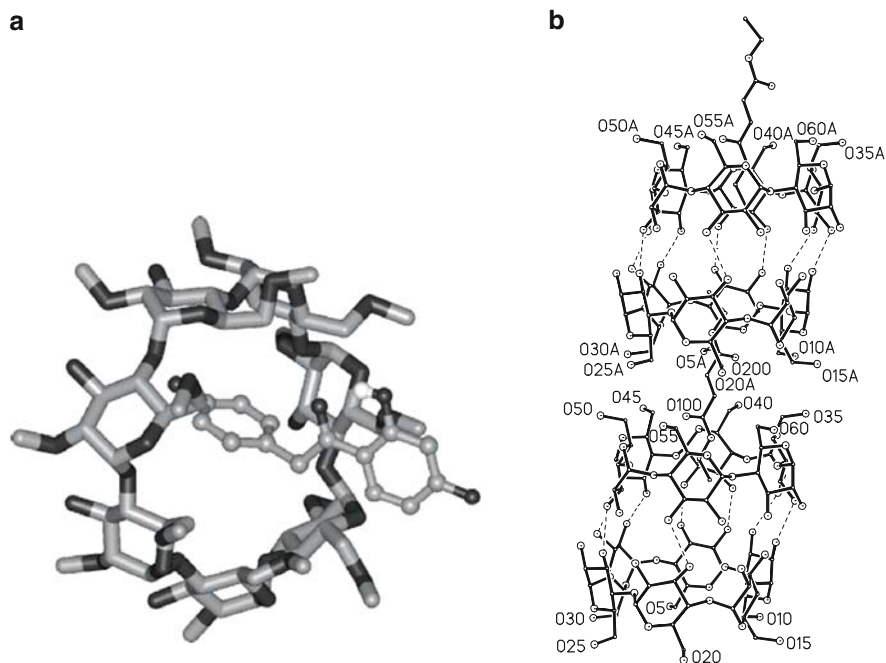
Fig. 1 **a** X-ray structure of 2,4-dihydroxyphenyl-4′-hydroxybenzylketone/Me-β-CD [21]. **b** Arrangement of α-CD dimers and diethyl fumarate molecules to columns along [001] in the crystal (note: packing of host/guest columns) [22]
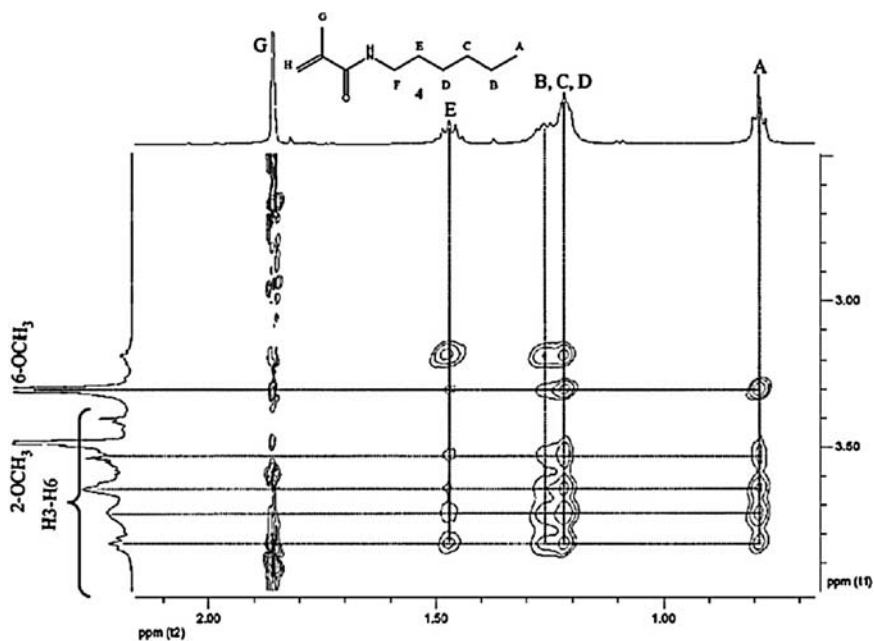
Fig. 2 2D-ROESY-NMR-spectrum of *N*-methacryloyl-1-aminohexane/Me-β-CD [23]

The FT–IR spectra of the complexed and uncomplexed guest molecules 11-(methacryloylamino)-undecanoic acid showed that the carbonyl bonds of the complexed monomer are shifted to higher frequencies from 1,708 to $1,712\,cm^{-1}$. This clearly indicates the influence of the host ring molecule on the carbonyl vibration [25].

2 Influences of CDs on Co- and Homopolymerization

We applied CDs to solubilize various types of vinyl monomers which are otherwise water insoluble. This unique behaviour of CD allows it to copolymerize hydrophobic monomers complexed in CDs with water soluble comonomers.

2.1 Polymerization of CD Complexed Monomers

In earlier works we reported on the preparation and structural analysis of 1:1 host–guest compounds of several types of CDs with pyrrole or 3,4-ethylenedioxythiophene (EDT), and their oxidative polymerization in water. These complexes were prepared simply by adding one equivalent of monomer to one equivalent of CD in water (Fig. 3) [26].

From some of these complexes, i.e. pyrrole/α-CD, EDT/α-CD, and EDT/β-CD, we were able to obtain single crystals that were studied by X-ray analysis. These show the herringbone fashioned cage-type crystal structure of pyrrole/α-CD, proving that it is a 1:1 complex with the pyrrole molecule located within the CD-cavity. The solid host–guest complexes are very stable under ambient conditions [21, 22]. After several weeks, the crystals remain unchanged while the unmodified monomers

: α-CD, β-CD, γ-CD, Me-α-CD, Me-β-CD, Me-γ-CD
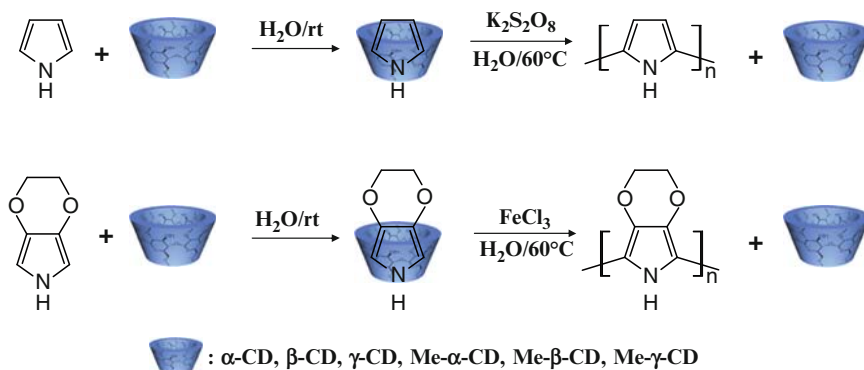
Fig. 3 Pyrrole or 3,4-ethylenedioxythiophene (EDT)/CD complex formation in water and oxidative polymerization of CD complexes

themselves change colour after a short time under the same conditions due to partial oxidation. Surprisingly, in the case of the EDT/α-CD, X-ray analysis showed the formation of a 1:1 non-inclusion channel-type packed supramolecular complex based on multiple hydrogen bonds. These colourless, crystalline pyrrole/CD and EDT/CD complexes that are barely soluble at room temperature were polymerized in water at 60°C under oxidative conditions.

All experiments showed that the corresponding polymers precipitated from solution. After filtration and washing with hot water, polypyrrole and poly(EDT) were obtained as dark powders in their oxidized state. Conductivity measurements showed that these materials have the same electrical properties $(10–100\,\mathrm{S\,cm^{-1}})$ as conventionally prepared polypyrrole or poly(EDT) [27, 28].

We also reported on the first examples of the free radical polymerization and copolymerization of a fluorinated 2-vinylcyclopropane monomer in aqueous solution via the host–guest complexation with Me-β-CD using a water-soluble initiator [29]. 2-Vinylcyclopropanes containing electron-withdrawing and radical-stabilizing groups are known to undergo radical ring-opening polymerization leading to polymers consisting predominantly, but not solely, of 1,5-linear olefin structures. The fluorinated vinylcyclopropane was homopolymerized in the presence of 7 mol equivalent of random Me-β-CD in aqueous medium at 60°C by the water-soluble azo initiator V50 within 2 h, in 50% yield (Fig. 4).

Fluorinated vinylcyclopropane was copolymerized with different ratios of hexyl substituted vinylcyclopropane via their respective complexes in Me-β-CD in
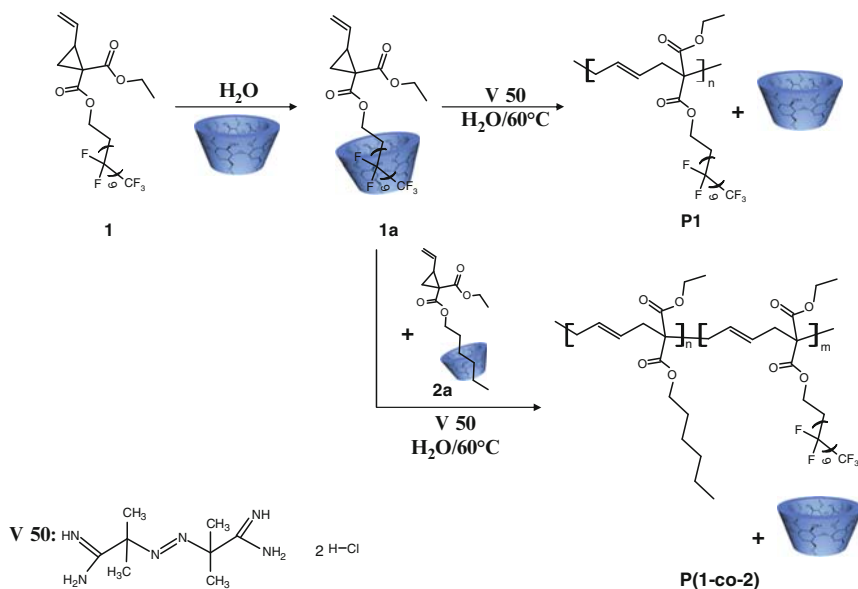
Fig. 4 Complexation of fluorinated vinylcyclopropane monomer with Me-β-CD and its homopolymerization and copolymerization with hexyl substituted vinylcyclopropane in aqueous solution

Table 1 Phase transition temperatures of fluorinated copolyvinylcyclopropanes (by DSC, scan rate 10°C min^{-1})

Polymer	1 in copol. [mol%]	T_g [°C]	T_i[a] [°C]	ΔH_i[a] [J g^{-1}]
P(1-*co*-2)a	29	19	173	0.7
P(1-*co*-2)b	55	18	182	14.6
P(1-*co*-2)c	77	30	184	15.3
P1	100	35	188	14.1

[a]Smectic-isotropic or isotropization temperature and enthalpy

aqueous solution in an analogous manner (Table 1). The prepared polymers exhibited liquid crystal behaviour. No crystallinity was detected by our DSC analyses of the fluorinated copolymers and the thermotropic mesophases occurred above the glass transition temperature. The fluorinated homopolymer is known to form smectic phases [30], and we assume that consistently the copolymers poly(1-*co*-2) also formed a smectic mesophase. This was generated by the self-assembly of the fluorinated side groups into an ordered registry of smectic layers. The degree of order of the mesophase could vary with copolymer composition according to the different isotropization enthalpies measured.

It is noteworthy that the formation of a mesophase was sustained in the copolymers even incorporating low proportions of mesogenic fluorinated side groups. Moreover, the introduction of repeat co-units with hexyl substituents lowered T_g by internal plasticization and resulted in a somewhat broader mesophase range for the copolymers relative to the fluorinated homopoymer (e.g. $T_i - T_g = 164$°C for copolymer).

Furthermore, we have reported on the first examples of free radical homopolymerization and copolymerization of 2,3,4,5,6-pentafluorostyrene (**3**) with styrene (**5**) and its derivative 4-(*N*-adamantylamino)-2,3,5,6-tetrafluorostyrene (**4**) in aqueous solution via the host–guest complexation with Me-β-CD using water-soluble initiators (Fig. 5) [31]. The fluorinated monomers (**3** and **4**) and styrene (**5**) were complexed by Me-β-CD in water. The stoichiometries of the host-guest complexes were determined by NMR spectroscopy according to the Job method [32–34]. It was clearly shown that styrene (**5**) forms a defined 1:1 complex while the fluorinated monomers (**3** and **4**) are encapsulated by two Me-β-CD molecules. In the case of fluorinated monomer (**3**) this result was not expected since **3** and **5** have the same molecular scaffold and molecular modelling showed that the fluorinated styrene derivative **3** is only slightly bigger than styrene itself (Fig. 6) [35].

The Me-β-CD/monomer complexes **3a** and **4a** were homopolymerized in water at room temperature using the redox initiator system K$_2$S$_2$O$_8$/Na$_2$S$_2$O$_5$ (Figs. 6 and 7). To compare our technique with traditional polymerization methods, all polymerizations were also carried out starting from the free monomers **3**, **4**, and **5** in organic solvents (toluene or benzene) at 80°C using AIBN as initiator (Table 2).

In all cases almost quantitative yields of the homo and copolymers from complexed monomers were obtained. Poly(pentafluorostyrene) (**P3a**) and polymer
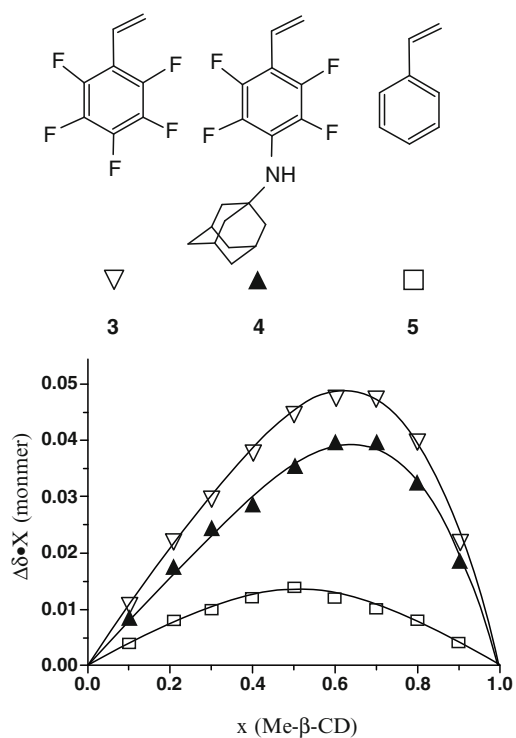
Fig. 5 Job plots by considering the shifts of protons of three kinds of monomers in the presence of Me-β-CD
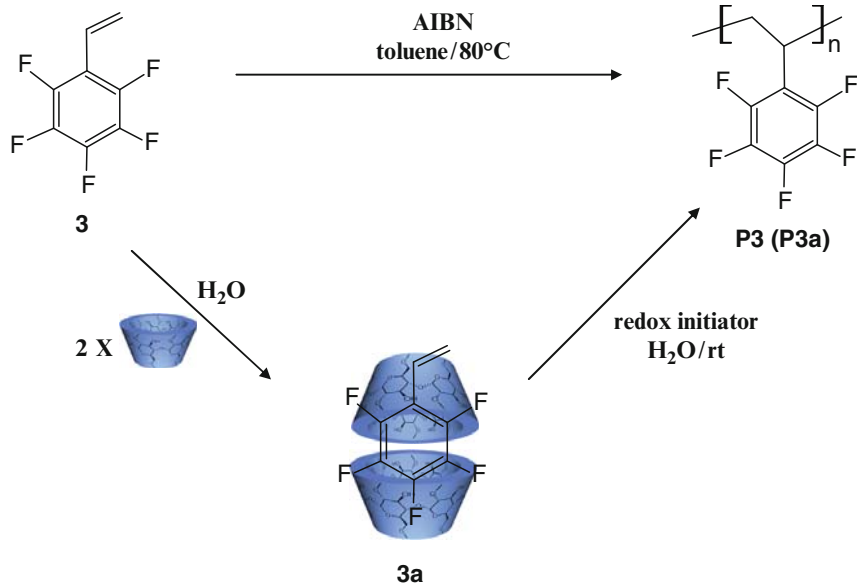
Fig. 6 Homopolymerization of pentafluorostyrene in toluene and water by CD-complexation of the monomer respectively
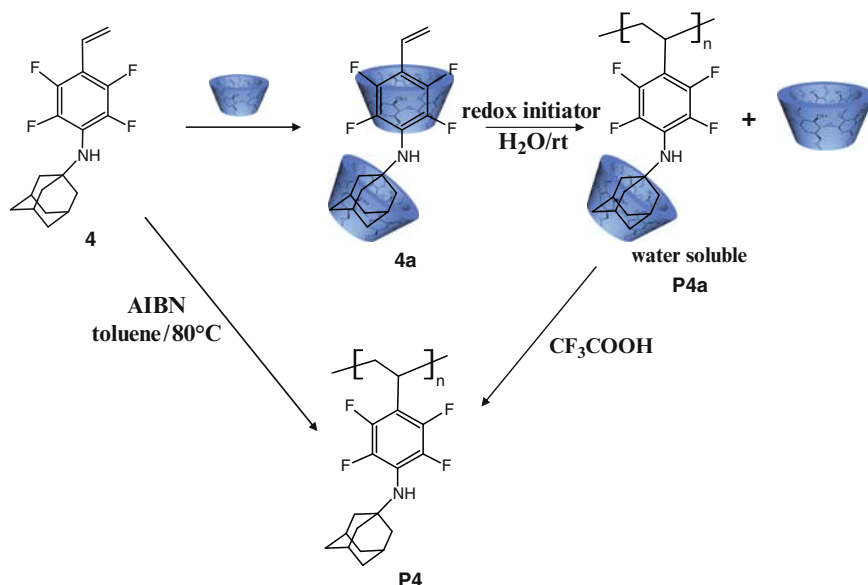
Fig. 7 Homopolymerization of free monomer in toluene and with Me-β-CD in water followed by degradation of Me-β-CD with trifluoroacetic acid

Table 2 Characterization of obtained polymers

Polymer	Monomer	Solvent	T [°C]	M_n	PD	T_g
P3a	**3a**	CD/water[a]	25	5,600	2.1	100
P3	**3**	Toluene[b]	80	4,500	1.5	90
P4a	**4a**	CD/water[a]	25	11,900	3.2	
P4	**4**	Toluene[b]	80	12,300	3.1	
P(3a-*co*-4a)	**3a,4a**	CD/water[a]	25	11,400	3.0	103
P(3-*co*-4)	**3,4**	Toluene[b]	80	4,500	1.5	90
P3-1	**3**	CD/water[a]	80	10,900	2.0	104
P3-2	**3**	Water[c]	80	38,500	3.2	106

[a]Redox initiator
[b]AIBN
[c]$K_2S_2O_8$, semibatch polymerization

P(3a-*co*-4a) could be isolated via simple filtration (Table 2). Polymer **P4a** was completely water-soluble due to the presence of non-covalently attached Me-β-CD. After treatment with trifluoroacetic acid to decompose the Me-β-CD ring, polymer **P4** precipitated after some hours and could be isolated by filtration (Fig. 7).

As an example, myrcene, an isoprene dimer, is found in many natural oils. Most of the polymerizations of myrcene were affected by a metal catalyst in organic solvents [36–39]. We tried to synthesize copolymers containing myrcene, styrene and diethyl fumarate (DEF) by using Me-β-CD in water (Fig. 8) [40].
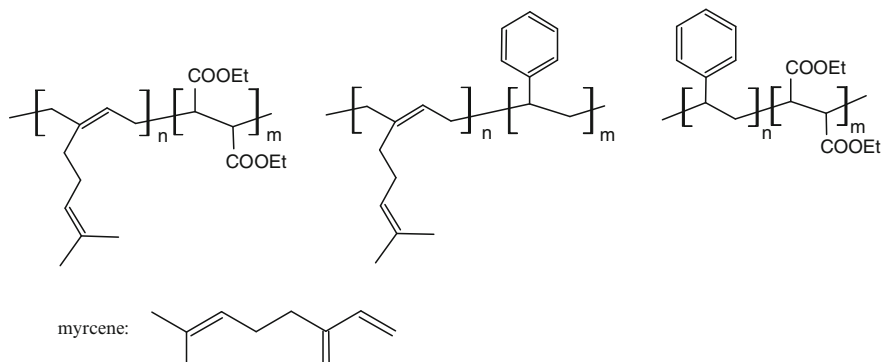
Fig. 8 Copolymers containing myrcene, styrene and diethyl fumarate (DEF) after Me-β-CD mediated copolymerization using redox initiator in aqueous media
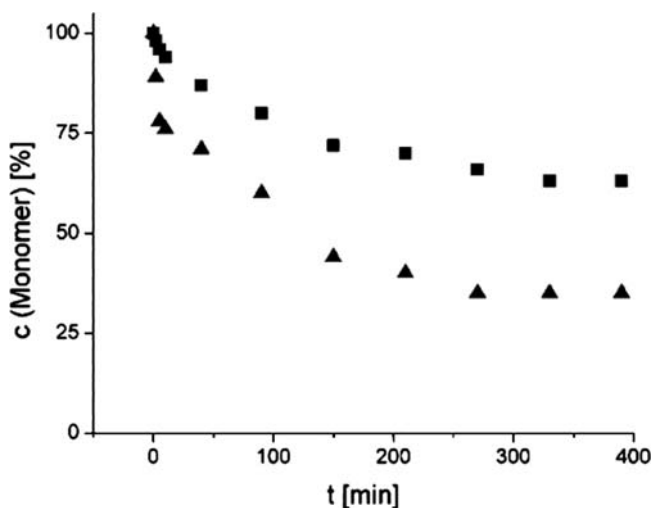
Fig. 9 Kinetic plots of the radical copolymerization of a 1:1 molar mixture of CD-complexed styrene (*filled triangles*) and diethyl fumarate (*filled squares*) in water at room temperature (using 2.5 mol% redox initiator $K_2S_2O_8/Na_2S_2O_5$)

We have found that the polymerization in homogenous, aqueous CD solution is normally much faster and ends up with higher yields and molecular weights than polymerization under similar conditions in an organic solvent [41, 42]. The polydispersities (M_w/M_n) of polymers were similar in all cases. Only the M_w/M_n values of the polymer containing styrene monomer units showed higher values.

The copolymerization of CD-complexed styrene and DEF led to a precipitation of the corresponding water-insoluble copolymers [43]. The reactivity of the styrene complex is higher than that of complexed DEF. The conversions of both monomers were finished after about 6 h at room temperature. The lower reactivity of DEF in comparison to styrene can be explained by the fact that the double bond is sterically hindered by the two ester groups in the *trans*-1,2 position (Fig. 9).
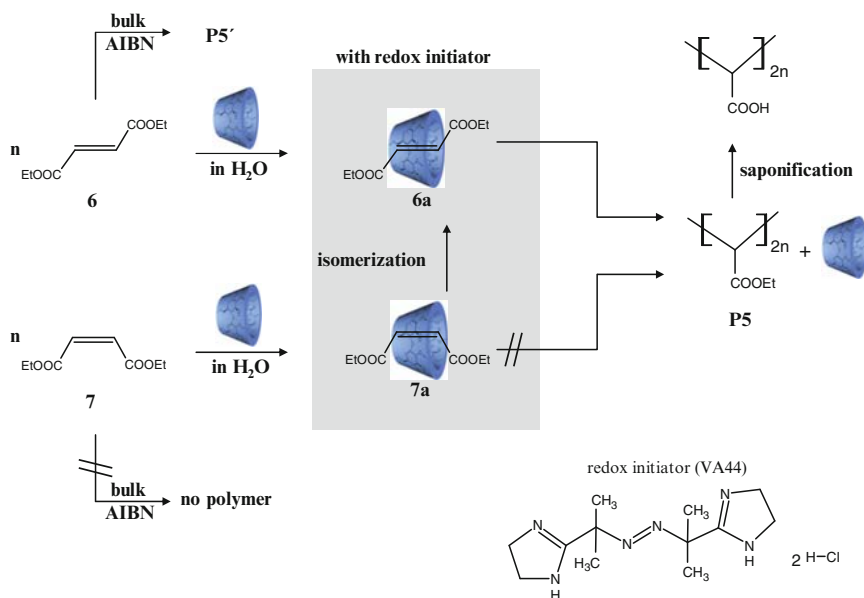
Fig. 10 Preparation of poly(ethoxycarbonylmethylene) from **6** and **7** with/without Me β-CD

Additionally, the double bond is preferentially covered by the CD ring. In contrast, the double bond of styrene is located more or less out of the CD centre, which allows easy access of the growing radicals. Furthermore, copolymerization parameters indicate that styrene is incorporated preferentially into the copolymer chain ($r_{styrene} = 1.95 \pm 0.02$ and $r_{DEF} = 0.97 \pm 0.01$). The reduced rate of copolymerization of DEF with styrene-rich compositions remains constant up to a fairly high conversion. It can be shown from the $r_{styrene}$ and r_{DEF} values that the monomer composition changes during the progress of the reaction. Thus, the consumption of the DEF monomer is slower than that of styrene, leading to polymer compositions with an increased amount of homo segments. The strong influence of CD on the copolymerization parameters becomes obvious when comparing the values given in the literature for polymerization in an organic solvent ($r_{styrene} = 0.36 \pm 0.04$ and $r_{DEF} = 0.10 \pm 0.02$) giving rise to almost alternating copolymers [44]. In contrast to this, the CD-complexed monomers copolymerize in a completely different manner, as discussed above.

DEF (**6**) and diethyl maleate (DEM, **7**) were complexed with equimolar amount of Me-β-CD and polymerized with redox initiator ($K_2S_2O_8/Na_2S_2O_5$) at room temperature and with VA44 at 50°C in aqueous media (Fig. 10) [22]. The homopolymerization of CD complexed monomers **6a** and **7a** with redox initiator led to a precipitation of the corresponding water-insoluble polymer **P6**, which was separated by centrifugation.

Normally, the maleic ester *cis*-isomers do to not give any homopolymer under similar condition as applied in the case of *trans*-isomers [45–47]. Surprisingly, in
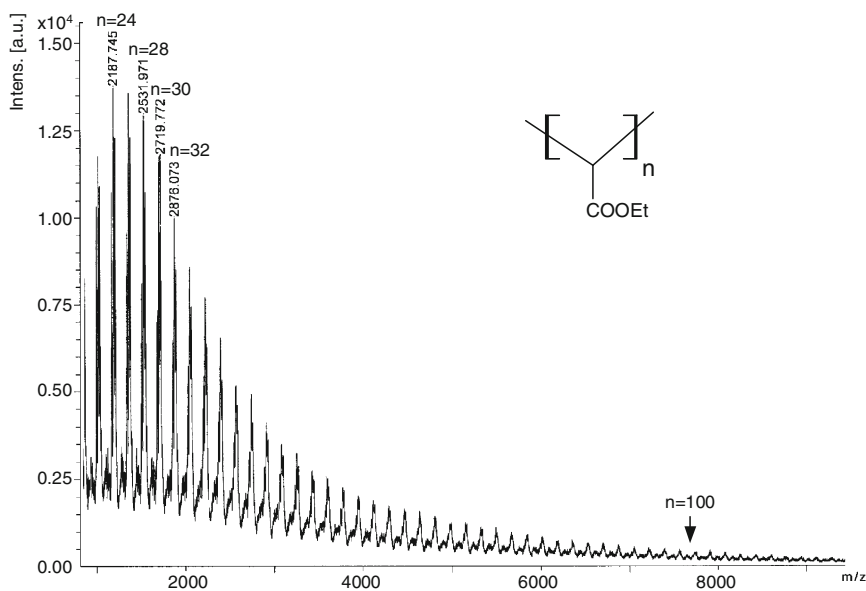
Fig. 11 MALDI-TOF spectrum of polymer **P5**

the presence of both Me-β-CD and redox initiator **7** undergoes homopolymerization via complexation with CD to give poly(ethoxycarbonylmethylene) **P5**. We evaluated the independent potential influence of CD and redox initiator on observed isomerization. It was shown that in the presence of only one of the components no isomerization takes place. Since **7** can be radically polymerized via a *cis-trans*-isomerization of the monomer, this reaction obviously needs both redox initiator and CD (Fig. 10).

The molecular weight of polymer was estimated by MALD-TOF MS (Fig. 11). The peaks show exactly the molecular masses of the polymers. The glass transition temperature (T_g) of the polymers obtained from DEF **6** and DEM **7** are almost identical. The effective CD-mediated homopolymerization reactivity of **6a** and **7a** are visualized in Fig. 12. The uncomplexed monomers **6** and **7** did not polymerize under the same conditions.

The unreacted residual *trans*-monomer was found to consist of only fumarate after polymerization of the complex **6a** by means of HPLC. In contrast, the residual **7a** was detected to consist of *cis*- and *trans*-isomer during the polymerization. This means that the complexed *cis*-isomer **7a** isomerized to *trans* configuration in the presence of radicals. Figure 13 shows the chromatograms of monomers obtained during the polymerization of complex **7a** with redox initiator. It indicates that the peak of *trans*-monomer increased with increasing reaction time. Therefore, it was clear that the polymerization of *cis*-olefin monomers **7** in the presence of both CD and redox initiator takes place via an isomerization radical polymerization

Fig. 12 Kinetic plot of homopolymerization of methylated β-CD-complexed monomer **6a** (*filled triangles*) and **7a** (*filled inverted triangles*) and CD-uncomplexed monomer **6** (*open squares*) and **7** (*open circles*) using redox initiator in aqueous media at room temperature
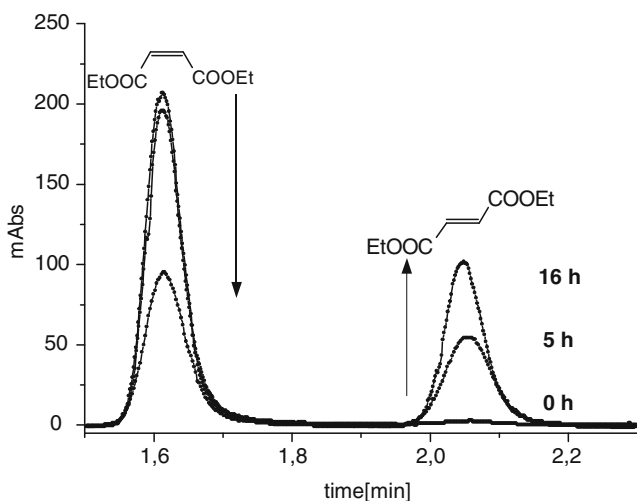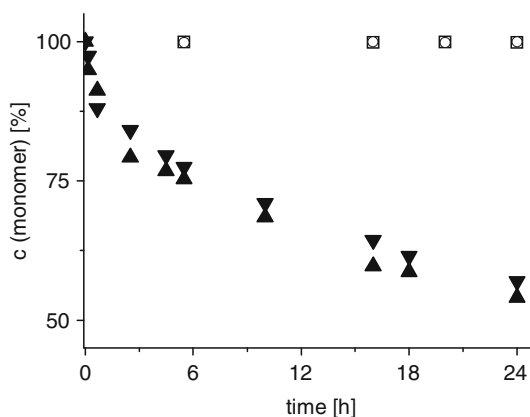
Fig. 13 HPLC Chromatograms of **7a** showing *cis/trans* isomerization during the polymerization with redox initiator ($R_{f(DEM)} = 1.63$ and $R_{f(DEF)} = 2.50$)

mechanism, i.e. maleates radicals isomerize first into fumarates and then these fumarates undergo radical polymerization.

Copolymerization of the CD-complexed macromonomer **8a** with hydrophilic comonomers 2-acrylamido-2-methylpropansulfonate (AMPS) and *N*,*N*-dimethylacrylamide (DMAA) leads to formation of hydrophobically associative polymers (Fig. 14) [48].

To study the aggregation of the synthesized polymers, 8-anilino-1-naphthalinsulfonacid ammonium (ANS) was used as the fluorescence probe. ANS has a minimum solubility of $28\,g\,L^{-1}$ in water but a higher solubility in hydrophobic media. With increasing polarity of the media its fluorescence intensity increases sensitively, and a simultaneous blue shift of the fluorescence band was also
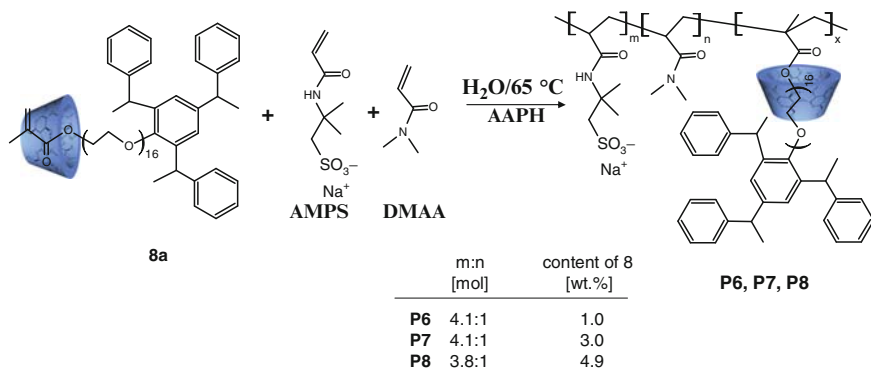
Fig. 14 Synthesis of hydrophobically associative polymers **P6**, **P7** and **P8**
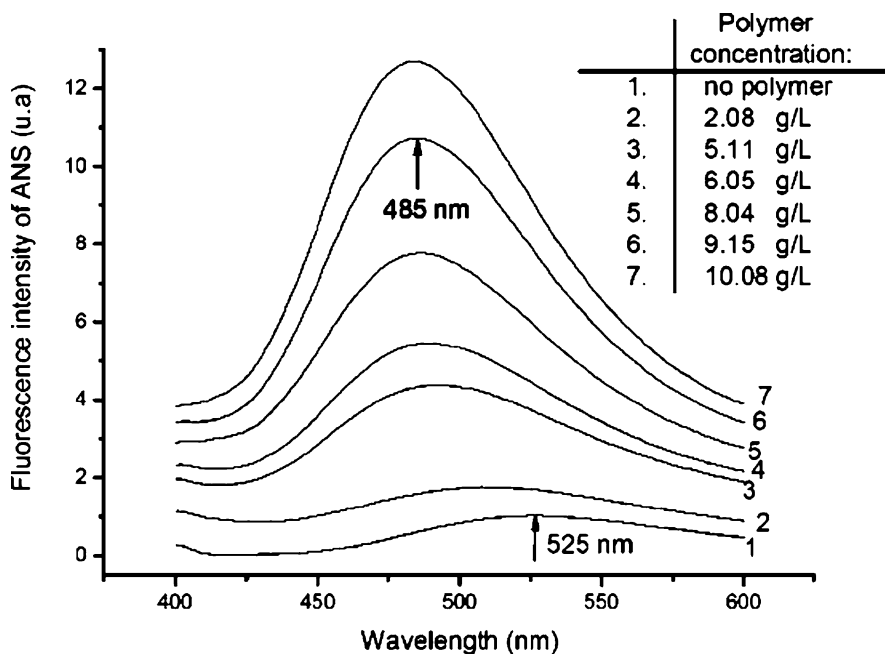
Fig. 15 Fluorescence spectra of ANS in differently concentrated aqueous solution of polymers at RT (**P8**:contains 5 wt% of the macromonomer)

observed. Its fluorescence is independent on pH value for pH > 6. Therefore, ANS is a suitable fluorescence probe to study the aggregation of the polymers (**P6–P8**) [49]. According to Fig. 15 the fluorescence spectra of ANS in differently concentrated aqueous solutions of polymer **P8** indicate the potential aggregation. It is interesting to note that the copolymer is a sidechain polyrotaxane. The content of CD was proved by GPC equipped with a chiral detector.
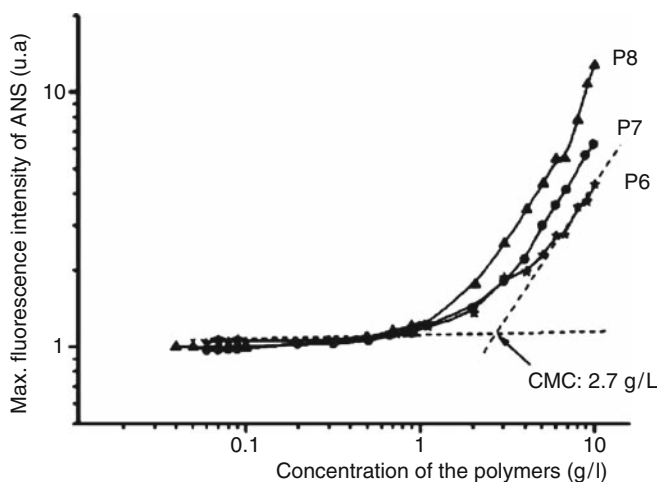
Fig. 16 Plots of the maximum fluorescence intensity as a function of polymer concentration at RT (**P6**: 1.0 wt% of 8; **P7**: 3.0 wt% of 8; **P8**: 4.9 wt% of 8)

In Fig. 16 the maximum fluorescence intensity of ANS was plotted against the concentration of the polymers with different content of associative macromonomer (**P6–P8**). In diluted polymer solutions, the maximum fluorescence intensity increased gradually with increasing polymer concentration. At the same polymer concentration, ANS showed higher fluorescence intensity in a solution of polymer that contains more of the associative macromonomer **8**.

The monomers N-methacryloyl-1-aminopropane (**9**), N-methacryloyl-1-aminobutane (**10**), N-methacryl-oyl-1-aminopentane (**11**), and N-methacryloyl-1-aminohexane (**12**) are synthesized directly from the corresponding amine and methacrylic acid by microwave irradiation [50], or classically by the treatment of amines with methacryloyl chloride (Fig. 17).

^{1}H–NMR spectroscopic measurements were carried out to investigate the stoichiometry of the CD complexes [51]. D_2O is used as the solvent at pH 7.3 and different mole fractions are considered ranging from 0.1 to 1.0 at increments of 0.1 with Me-β -CD as the host. The plot of $-\Delta\delta^* \bullet X_{CD}$ vs the mole fraction X_4 for the Me-β -CD-complexed hexyl methacrylamide (**12a**) shows a maximum at $X_4 = 0.50$. This is a strong hint that a 1:1 complex was formed (Fig. 18).

The hydrodynamic volumes of both Me-β-CD and the Me-β-CD complexes were measured by use of dynamic light scattering to prove the existence of molecularly dispersed complexes. Interestingly, results indicate that no aggregates are formed. However, because of guest monomer incorporation the hydrodynamic volume of the complex increases slightly in comparison to Me-β-CD (Fig. 19).

To evaluate the effect of Me-β-CD on polymerization kinetics, the free uncomplexed monomers **9–12** and the corresponding Me-β-CD complexes (**9a–12a**) are homopolymerized in water by a free radical mechanism under identical conditions. In the case of the aqueous polymerization of the free monomers **9–12** the initial
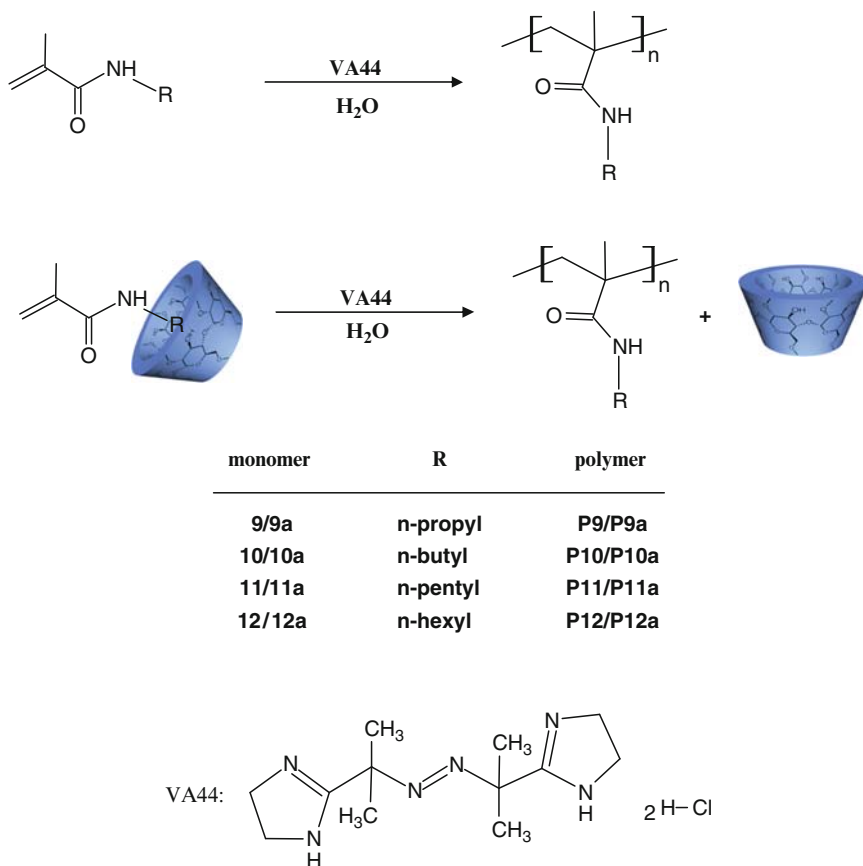
Fig. 17 Structures of the complexed Me-β-CD monomers and subsequent polymerization

polymerization rate increases with increasing water solubility. The opposite effect is observed in the case of the polymerization of the Me-β-CD complexed methacrylamide monomers **9a–12a**. The polymerization rates are increased with increasing alkyl chain length of the complexed monomers **9a–12a** and the decreasing water solubility of the free monomers **9–12** (Fig. 20).

2.2 Polymerization of a CD Complexed Photoinitiator and a Water Soluble Monomer

For evaluating the influence of CD on the photoinitiated polymerization process, the polymerization of a water soluble monomer, *N*-isopropylacrylamide (NIPAAM), using complex of Me-β-CD and 2-hydroxy-2-methyl-1-phenylpropan-1-one (**13**) as
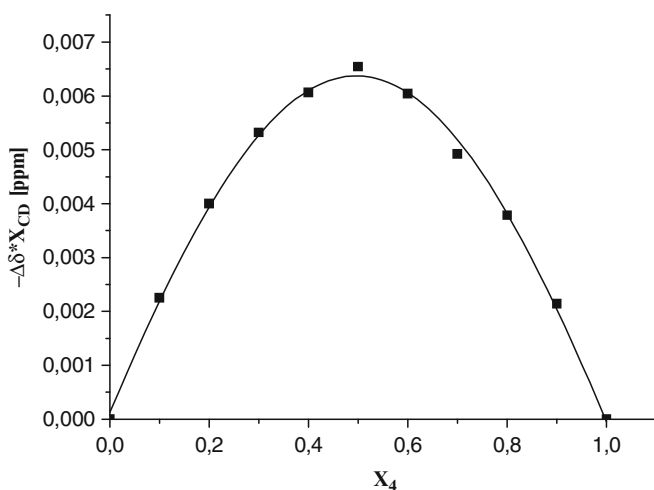
Fig. 18 Job plot of the complex of monomer **12a** in D_2O with Me-β-CD (pH 7.3), the maximum is at $X_4 = 0.50$
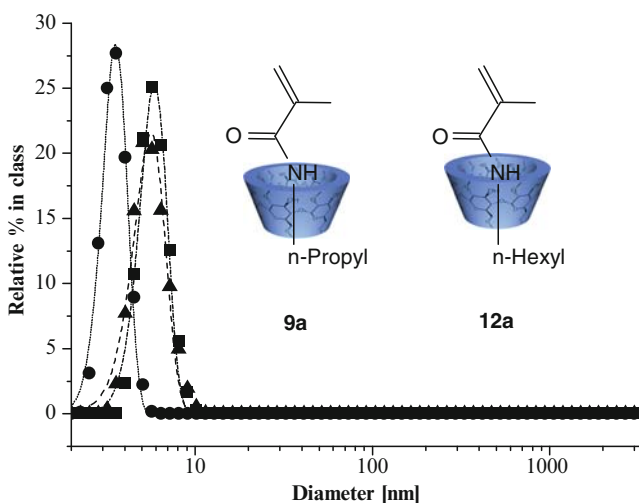
Fig. 19 Particle size distribution by dynamic light scattering of free Me-β-CD (*filled circles*) and Me-β-CD complexes **9a** (*filled squares*) and **12a** (*filled triangles*) in water at 50°C

the initiator, was performed in aqueous medium [52]. After the addition of 2 mol% of photoinitiator or CD-complexed photoinitiator the mixtures were irradiated simultaneously at constant temperature (20°C) with a high-pressure mercury lamp as the light source. In accordance with TLC measurements the photo initiator stays in the complexed form also in the presence of NIPAAM monomer, indicating that the equilibrium between free monomer and CD-monomer complex can be neglected.
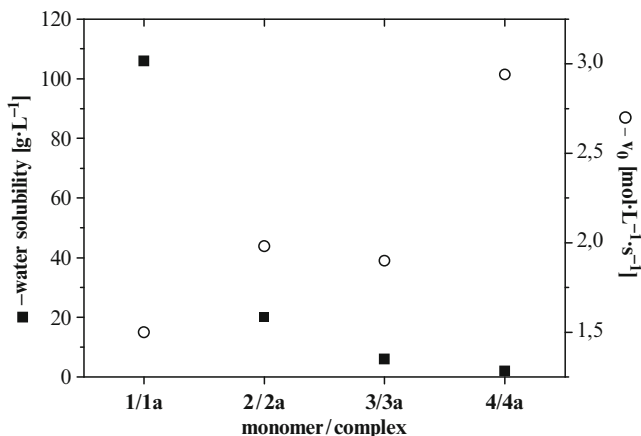
Fig. 20 Initial polymerization rate v_0 of CD complexed monomers **9a–12a** (*open circles*) vs water solubilities of monomers **9–12** (*filled squares*)
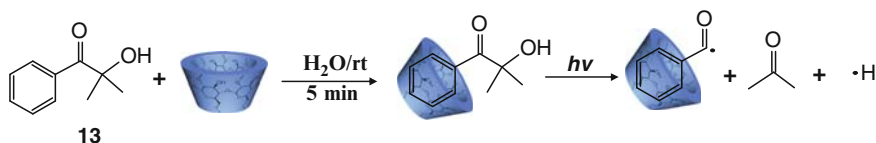
Fig. 21 Preparation of the CD-photoinitiator complex in water and proposed decomposition mechanism of the complex

UV spectroscopic measurements revealed that the polymerization reaction initiated with CD-complexed photo initiator is faster and, thus, ends up with higher yields than the polymerization reaction initiated with the same molar concentration of uncomplexed photo initiator. Radical photo polymerization is achieved by the homolytic fragmentation of carbon–carbon bonds of a photo-excited molecule as illustrated in Fig. 21.

2.3 Polymerization of CD Complexed Monomer and Water Soluble Monomer

Copolymerization of CD complexed myrcene (**14**) and NIPAAM was carried out (Fig. 22). The obtained polymer **P13** was water soluble and little amounts of CD still remained in the polymers as detected by ^{1}H NMR spectroscopy. The thermosensitive properties of aqueous solutions of copolymers were investigated by monitoring the changes of turbidity as a function of temperature. Surprisingly, **P13** shows exceptional high LCST transition temperature of 80°C. Thus, the turbidity points of copolymers is significantly higher than of poly(NIPAAM) itself (32°C) because of the existence of hydrophilic CD complexes of the side groups.
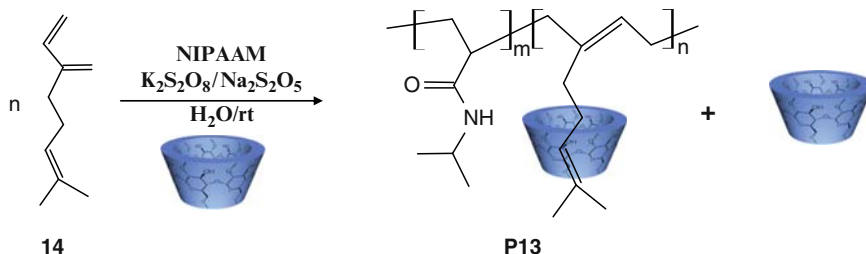
Fig. 22 Polymerization of CD-complexed myrcene with NIPAAM in H_2O using redox initiator
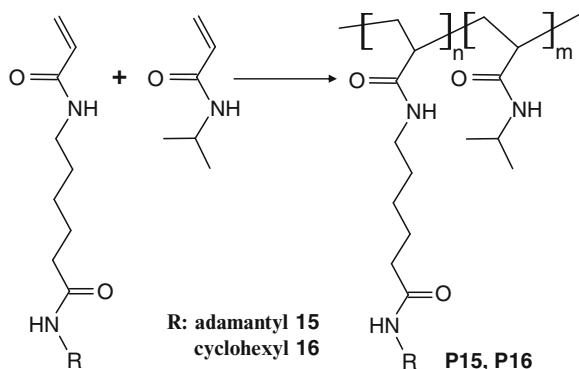
Fig. 23 Radical copolymerization of acrylamide with R = adamantyl (**15**) or cyclohexyl (**16**) and NIPAAM in DMF without any host compound; n/m = 1 : 20

The LCST value can be influenced, for example, by copolymerization of NIPAAM or by chemical modification of the acrylamide polymer itself. The slightly cross-linked LCST polymers, so-called hydrogels, find potential application in the medical and biochemical fields, for controlled drug delivery [53] and as materials for bioreactors [54]. One general explanation of the LCST effect is that strong hydrogen bonds exist between water molecules and the hydrophilic groups of the polymer at low temperature [55]. With increasing temperature, intramolecular interactions between hydrophobic chain components of the polymer increase.

For the investigation of the LCST behaviour further NIPAAM containing copolymers containing hydrophobic adamantine or cyclohexayl groups were synthesized (Fig. 23) [56–59].

Optical turbidity measurements showed a LCST for aqueous solutions of **P14** up to 17°C. On the other hand, solutions of copolymer with cyclohexyl **P15** have a transition at 31°C, which is 4°C lower than that of pure NIPAAM polymer **P16** (Table 3). The lower LCST for **P15** compared to **P16** is attributed to the hydrophobic effect [60], which is the decrease of the LCST with increasing numbers of hydrophobic side-chain groups.

In addition, the thermosensitive properties of aqueous solutions of copolymers **P17**–**P19** and of their supramolecular non-covalent cross-linked networks were

Table 3 The properties of the synthesized copolymers

Polymer	LCST [°C]	n/m	M_n [g mol^{-1}]	PD
P14	17	1:20	17,400	2.90
P15	31	1:20	16,100	3.58
P16	35	–	71,000	6.18
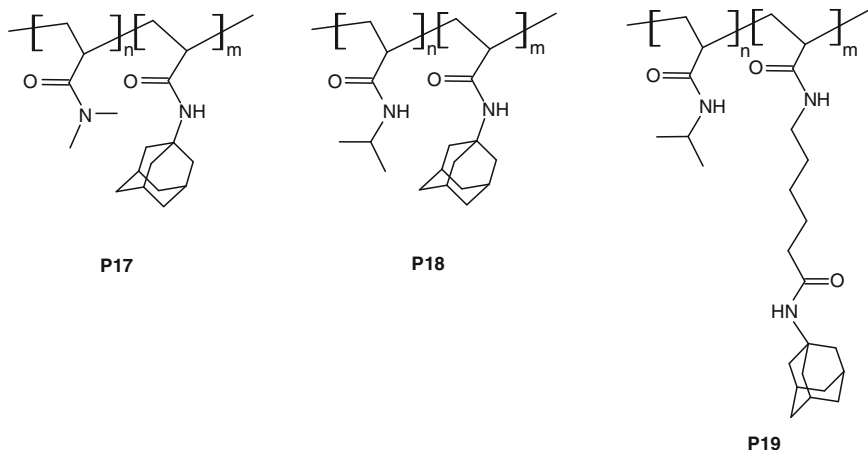
Fig. 24 NIPAAM and N,N-dimethylacrylamide containing copolymers (n : m = 20 : 1)

investigated by monitoring the changes of turbidity as a function of temperature [61,62]. The N,N-dimethylacrylamide-containing copolymer **P17** shows no turbidity point at temperatures between 10°C and 90°C in water. For copolymer **P18** we obtained the LCST transition at 23°C; for copolymer **P19** we found a cloud point of 21°C (Fig. 24). Both copolymers showed a sharp phase transition in response to a small temperature change. The fact that the turbidity points of copolymers **P18** and **P19** are significantly lower than that of poly(NIPAAM) itself (32°C) is caused by the hydrophobic adamantyl units in the copolymers; copolymers **P18** and **P19** are less soluble in water than a homopolymer of NIPAAM.

To investigate the effect of adding monomeric and dimeric CD on the change of phase transition temperature of the polymers **P18** and **P19**, we performed turbidity measurements at the same polymer concentration as above in the presence of a defined amount of Me-β-CD and CD dimer, respectively (Fig. **25 a,**b) [61,62]. As reported previously [56–59], we found that addition of Me-β-CD led to cloud points of polymers **P18** and **P19** of 32°C, which correlates to the LCST of pure poly(NIPAAM). This increase of the cloud points relative to the cloud points of pure **P18** and **P19** results from the inclusion of the hydrophobic adamantyl units by Me-β-CD.

When a CD dimer was added to the aqueous polymer solutions at half the molar ratio (relative to the amount of Me-β-CD), the cloud points decreased significantly. This observed effect again can be explained by the supramolecular
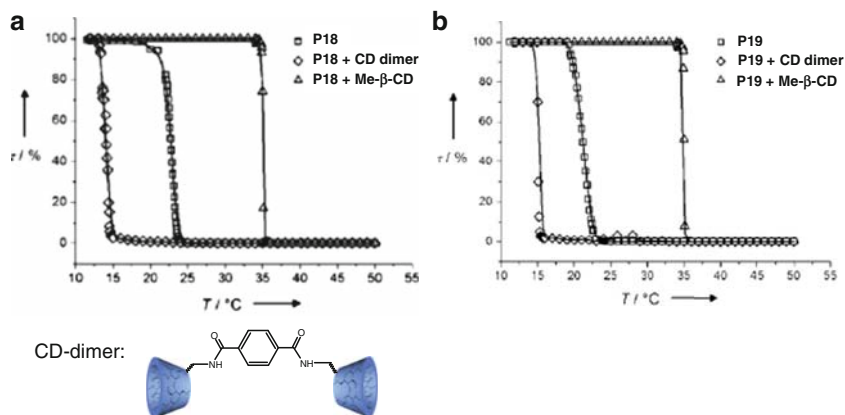
Fig. 25 a,b Turbidity measurements of aqueous solutions of the polymers **P18 a** and **P19 b** without addition of host molecules and measurements of the supramolecular complexes of the polymers with CD dimer and Me-β-CD respectively. $C_P = 10\,\mathrm{g\,L^{-1}}$, $C_{\text{Me-β-CD}} = 10\,\mathrm{g\,L^{-1}}$, and $C_{\text{CD dimer}} = 5\,\mathrm{g\,L^{-1}}$, $10°\mathrm{C}$

cross-linkage of single polymer chains upon complexation of the CD dimer. The resulting supramolecular structures are restricted in their mobility and solubility, which is reflected in cloud points of $14.0°\mathrm{C}$ for polymer **P18** and $15.7°\mathrm{C}$ for polymer **P19**. As a result of the LCST behaviour of the polymer/CD dimer mixtures the obtained hydrogels show different transparencies. The gel formed from copolymer **P17** is transparent at room temperature, whereas those from polymers **P18** and **P19** are turbid at room temperature and transparent below their cloud points of $14.0°\mathrm{C}$ and $15.7°\mathrm{C}$, respectively.

As another example, when the transparent solutions of the complexed polymers **P20a** were heated above $70°\mathrm{C}$, a sudden turbidity was observed [63, 64]. Surprisingly, when the solution was cooled, transparency was completely restored. Exact turbidity measurements were performed to evaluate the solubility as a function of temperature. We found that the complexed monomer **17a** is completely soluble in the temperature range $10–85°\mathrm{C}$. This means that the monomer complex is stable enough to keep the monomer in solution independent of temperature. In contrast, the polymer complex **P20a** showed a definite clouding point at a temperature of $54°\mathrm{C}$ for the heating run (Fig. **27 a,b**a) and a clearing point of about $50°\mathrm{C}$ for the cooling run (Fig. **27 a,b**b).

These temperatures were found to be a function of the molecular mass of the β-CD-free polymers. Figure 26 shows the reversible decomplexation–complexation process of polymer **P20** in water. The transmittance change of a solution of **P20a** is plotted as a function of temperature in Fig. **27 a,b**. The decrease in the transmittance of the complexed polymer to 0% occurs within a temperature interval of roughly $5°\mathrm{C}$. In the subsequent cooling step the polymer returns to solution by new formation of polymer/β-CD complex. In contrast, the β-CD free polymer is not soluble in water at any temperature in this range.
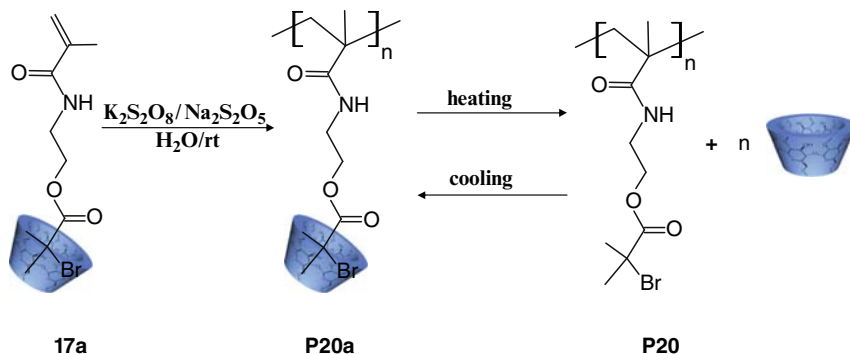
Fig. 26 Temperature-dependent reversible unthreading of CD from the bulky side group of **P20a** during the heating procedure
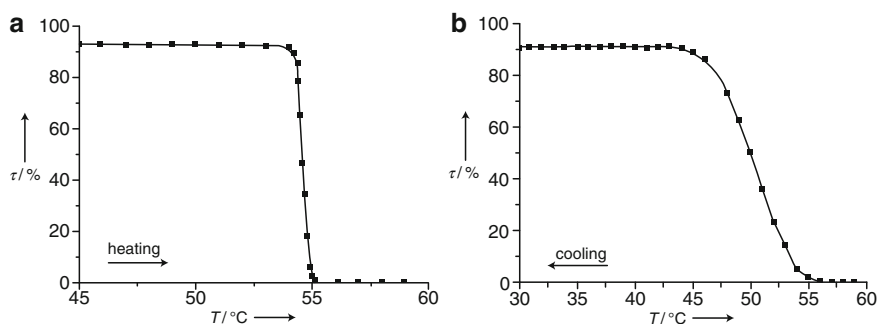
Fig. 27 a,b Transmittance of a solution of complexed polymer **P20a** vs temperature during heating **a** and cooling **b**

The interesting polymer-solubility behaviour led us to compare this phenomenon with classical LCST effects. In our case, because of the reversible complex formation between the polymer **P20** and CD, the optical effect is based on supramolecular interactions. This means that the discovered pseudo-LCST behaviour is a result of non-covalent interactions between the CD host and polymer guest. Furthermore, in this system competitive inhibition or control of the LCST is possible by addition of other suitable guest molecules of low molecular weight, for example, potassium 1-adamantylcarboxylate. CD complexes these molecules preferably and the polymer precipitates. This special effect cannot be observed in regular LCST systems.

A further important application of CD is the preparation of relatively low polydispersity polystyrenes (compared to radical CD polymerization) using the water-soluble RAFT reagent 3-benzylsulfanyl thiocarbonylsulfanylpropionic acid (TTC) complexed in aqueous Me-β-CD solution (Fig. 28) [65]. This method also allows the direct synthesis of amphiphilic block copolymers in aqueous solution without compatibility issues.
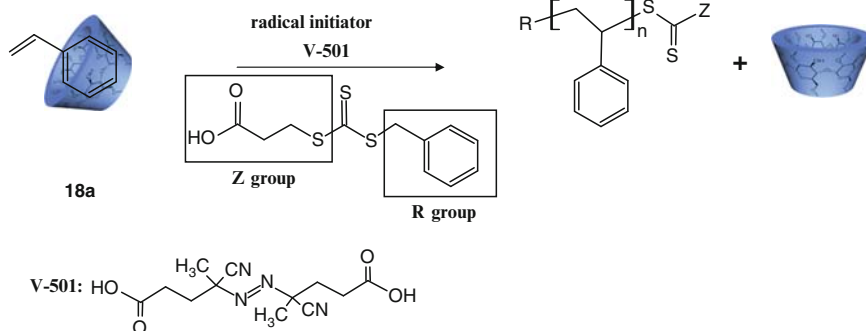
Fig. 28 Schematic presentation of complexation and RAFT polymerization of Me-β-CD complexed styrene **18a** with 3-benzylsulfanylthiocarbonylsulfanylpropionic acid (TTC) as RAFT agent
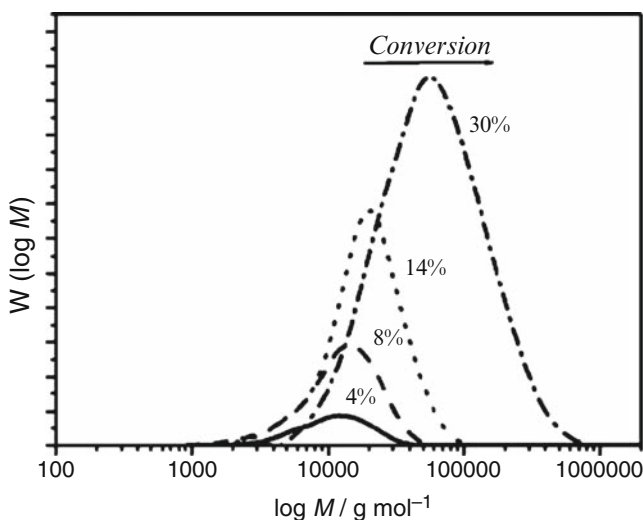
Fig. 29 Evolution of the full molecular weight distributions in the CD-mediated styrene RAFT polymerization in aqueous solution at 70°C. RAFT agent/initiator to 10:1. Samples were taken after 75, 180, 300 and 420 min, respectively. The individual conversions to polystyrene are given within the figure

Controlled living radical polymerization of CD-complexed styrene in water can be conducted via the RAFT process, especially at low conversion ($<20\%$). The molecular weight of PS can be controlled by variation of the RAFT agent concentration and the number-average molecular weight increases linearly with conversion (Fig. 29).

The polymers produced with the CD-RAFT system exhibited narrower polydispersities ($1.23 < M_w/M_n < 2.36$) than those without RAFT agent ($5.24 < M_w/M_n < 9.21$). However, the polydispersities in the CD-RAFT system are considerably higher (especially at increased conversions) than those in conventional (bulk or
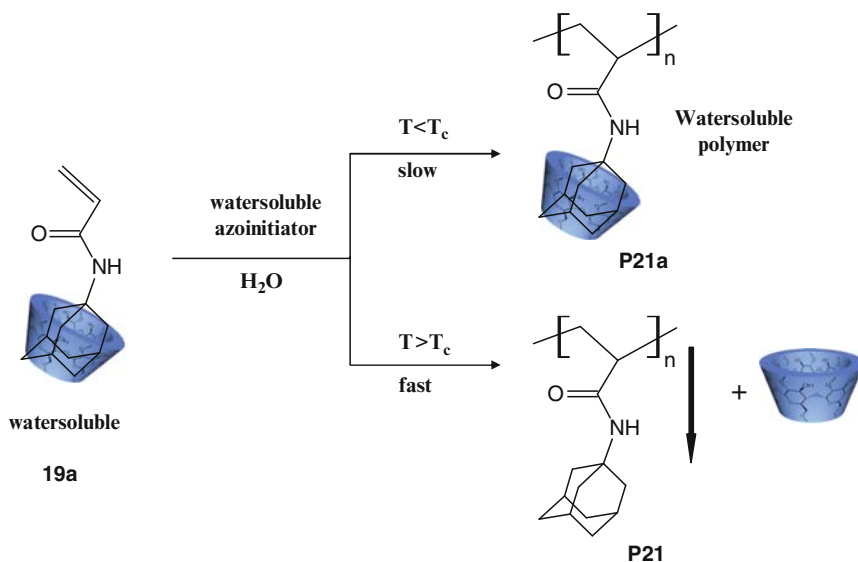
Fig. 30 Schematic illustration of the polymerization of **19a** using 1 mol% water-soluble azo initiator (VA044) at different temperatures in water

solution) RAFT systems and the molecular weight evolution deviates considerably from the theoretically expected one. We attribute these effects to the continuous precipitation of the polymer with increasing conversion, which effectively leads to a hybrid system between conventional and controlled living free radical polymerization.

Furthermore, we investigated temperature-dependent solution behaviour of Me-β-CD with poly(meth)acrylamides bearing bulky hydrophobic side groups (Fig. 30) [66].

The free radical polymerization of complexed monomer **19a** was carried out at different temperatures in water in the presence of 1 mol% water-soluble azoinitiator. The temperature range of interest was 50–90°C, to determine v_0 below and above the T_{crit} of 65°C of the given CD-polymer system (**P21a**).

In Fig. 31, the transparency τ of an aqueous solution of **P21a** is plotted against the temperature. While heating, it can be observed that the transparency of the solution of **P21a** decreases from almost 100% to 0% around 65°C (± 3°C). We would like to emphasize that the point of turbidity certainly depends on the sample concentration. With increasing concentration of CD, the LCST shifts to higher values [67,68]. During the cooling phase, the water insoluble polymer **P21** remains insoluble. However, the reformation of the complex **P21a** takes place within 12 h of stirring at room temperature or below. We suspect that, once precipitated, the bulky adamantyl-side group of polymer **P21** is hardly accessible by the Me-β-CD, so that reconstitution of the complex **P21a** takes hours (Figs. 30 and 31).

The complexation–decomplexation equilibrium of the polymer is strongly entropy driven. The monomer complex **19a** (Fig. 30) is stable up to 100°C, since it
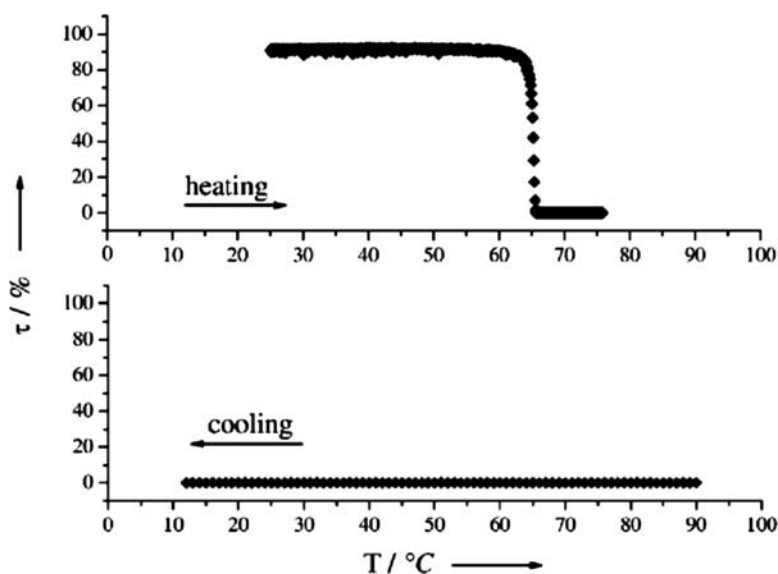
Fig. 31 Transparency t of an aqueous solution of **P21a** ($c = 30\,\mathrm{g\,L^{-1}}$) against the temperature during heating and cooling

has a high mobility in solution. However, in contrast, a strong increase in total mobility of the polymer system takes place above T_{crit} because the CD rings are released from the polymer.

The incorporation of a flexible spacer between the polymer backbone and the adamantyl groups strongly affects the thermosensitive properties of the supramolecular complex [67,68]. In Fig. 32, the turbidity measurement of a $100\,\mathrm{g\,L^{-1}}$ aqueous solution of polymer/Me-β-CD-complex **P22a** is presented. The heating run indicates the cloud point of **P22a** at 38.6°C, which is 6°C lower than that of **P21a** (Fig. 32). In the cooling run the transparency recovers from 0% to almost 100% at about the same temperature as in the heating run. Apparently recomplexation of the spacer-containing polymer **P22** is significantly faster than that of polymer **P21a**, which contains directly attached adamantyl groups. These results correlate with the degree of mobility of the adamantyl groups attached to the polymer.

In addition, we reported about the behaviour of an LCST copolymer **P23** bearing a covalently attached solvatochromic 4-azastilbene dye and investigated the solvatochromism of this polymer in the presence of Me-β-CD [69].

A characteristic bathochromic shift from orange to dark red could be observed when the aqueous polymer solution at basic pH is heated above the LCST value of about 31°C (Figs. 33 and 34). This means that, during precipitation of the polymer due to heating above the LCST value, most of the polar water molecules are pushed out of the polymer coil. This causes a negative change of polarity next to the dye moiety, which results in a colour change. This temperature-dependent colour change
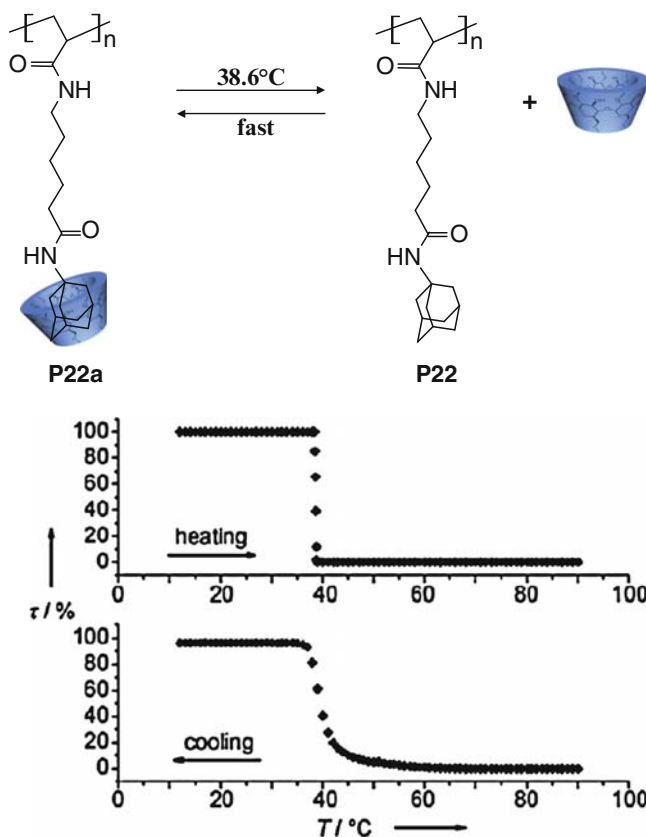
Fig. 32 Rapid complexation of **P22** by Me-β-CD. Transmittance as a function of temperature for an aqueous solution of polymer/Me-β-CD complex **P22a** at a heating/cooling rate of $1°C$ min^{-1}. [**P22a**] = $100 g$ L^{-1} ($13.75 g$ L^{-1} polymer, $86.25 g$ L^{-1} Me-β-CD)
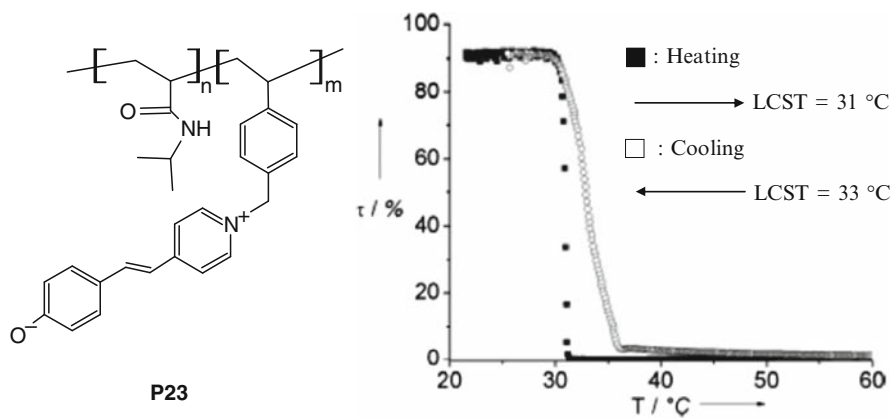
Fig. 33 Transmittance (τ) of a solution of polymer **P23** in water ($5 mg$ mL^{-1}) at pH 10 vs temperature during heating and cooling
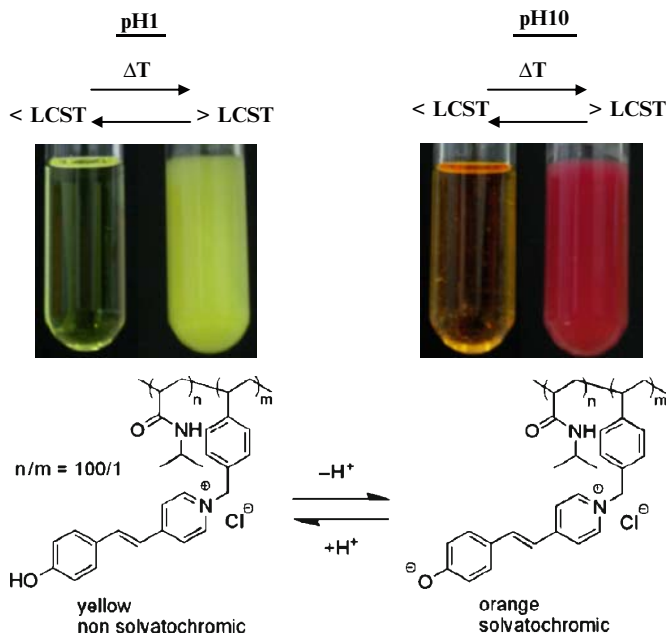
Fig. 34 Colour effects of copolymer **P23** at pH 1 (no shift) and at pH 10 (bathochromic shift)

is fully reversible. However, the protonated copolymer showed no colour change effect due to the solubility change at its LCST.

We clearly found that the bathochromic shift due to negative polarity change was also visible after excessive CD addition to the aqueous polymer solution below its LCST. This means that the complexation of the copolymer **P23** by CD could also be recognized simply by the naked eye.

The unpolar cavity of CD creates an unpolar environment around the dye moiety. The colour change due to CD threading is nearly identical compared to the colour change caused by phase transition. This proves that the dye–dye interaction plays a minor role. As mentioned above, this effect influenced only the deprotonated polymer at high pH. Addition of CD to the polymer solution with the protonated dye (pH 1) showed only a small effect on the visible spectrum. UV measurements started directly after acid addition. Thus, decomposition of CD is not to be expected. This small effect might be due to weak interaction of CD with the protonated dye. In measurements of an aqueous solution of **P23** without CD, glucose was excessively added to this solution to verify the host–guest interactions. As it was expected, no colour change could be detected (Fig. **35 a,**b).

In conclusion, CDs constitute excellent hosts for homo- and copolymerizations. This important property has encouraged the use of CDs in a range of applications related to polymers, as described in this review. These investigations demonstrate the successful application of CDs in polymer synthesis in aqueous medium via free radical polymerization or via a oxidative recombination mechanism. CDs as

a

b
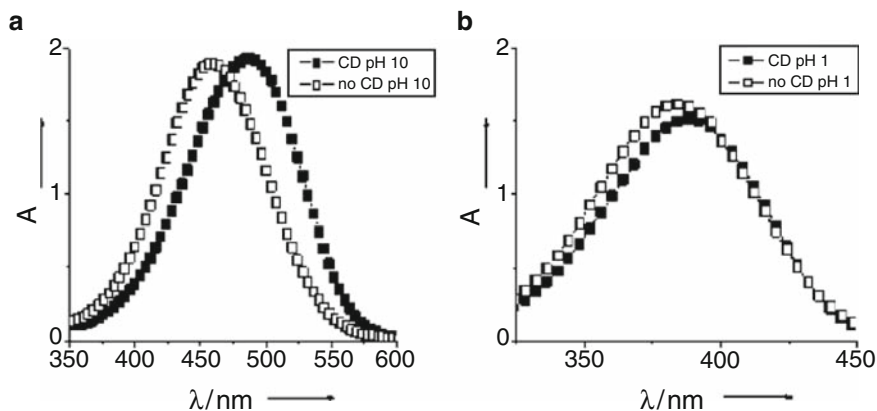
Fig. 35 a,b Visible spectra of a 1.25 g L^{-1} aqueous solution of **P23** with (*filled squares*) (addition of 60 mg of CD) or without (*open squares*) (addition of 60 mg of glucose) at pH 10 **a** and at pH 1 **b**

reaction media are useful to alter both polymerization kinetics and copolymerization-parameters. New aqueous LCST systems can be designed with switchable physical properties.

As expected, within only a few decades an important revolution in the polymer chemistry through CD-mediated reactions might change the current production processes in chemical industry. Undoubtedly, the unique host properties of CDs should be taken into account when novel polymerization processes are created.

References

1. Lehn J-M (1985) Science 227:849
2. Lehn J-M (1988) Angew Chem 100:91
3. Lehn J-M (1988) Angew Chem Int Ed Engl 27:89
4. Lehn J-M (1990) Angew Chem Int Ed Engl 102:1347
5. Lehn J-M (1990) Angew Chem Int Ed Engl 29:1304
6. Rebek J Jr (1990) Angew Chem Int Ed Engl 102:245
7. Rebek J Jr (1990) Angew Chem Int Ed Engl 29:261
8. Vogtle F (1992) Supramolekulare Chemie. Teubner, Stuttgart
9. Vogtle F (1991) Supramolecular chemistry. Wiley, New York
10. Cram DJ, Cram JM (1974) Science 183:803
11. Cram DJ, Cram JM (1978) Arch Chrom Res 11:8
12. Ritter H, Tabatabi M (2002) Prog Polym Sci 27:1713
13. Ritter H, Tabatabi M (2003) Adv Macromol Supramol Mater Prog 41
14. Schneider HJ (1991) Angew Chem 103:1419
15. Schneider HJ (1991) Angew Chem Int Ed Engl 30:1417
16. Funasaki N, Ishikawa S, Neya SJ (2004) Phys Chem B 108:9593
17. Höfler T, Wenz G (1996) J Inclusion Phenom 25:81
18. Isaacs NS, Young DJ (1999) Tetrahedron Lett 40:3953
19. Abou-Hamdan A, Bugnon P, Saudan C, Lye PG, Merbach AE (2000) J Am Chem Soc 122:592
20. Hori K, Hamai S (1999) J Inclusion Phenom Macrocyclic Chem 34:245

21. Mejias L, Schollmeyer D, Sepulveda-Boza S, Ritter H (2003) Macromol Biosci 3(8):395
22. Choi SW, Frank W, Ritter H (2006) React Funct Polym 66:149–156
23. Steffens C, Choi SW, Ritter H (2006) Macromol Rapid Commun 27:542–547
24. Jeromin J, Ritter H (1998) Macromol Rapid Commun 19:377
25. Jeromin J, Ritter H (1999) Macromolecules 32:5236
26. torsberg J, Ritter H, Peilatzik H, Groenendaal L (2000) Adv Mater 12:567
27. Rodriguez J, Grande H-J, Otero TF (1997) Handbook of organic conductive molecules and polymers, vol. 2. Wiley, Chichester, pp 417
28. Heywang G, Jonas F (1992) Adv Mater 4:116
29. Choi SW, Kretschmann O, Ritter H, Ragnoli M, Galli G (2003) Macromol Chem Phys 204:1475
30. Galli G, Gasperetti S, Bertolucci M, Gallot B, Chiellini (2002) Macromol Rapid Commun 23:814
31. Cinar H, Kretschmann O, Ritter H (2005) Macromolecules 38:5078–5082
32. Blanda T, Horner JH, Newcomb M (1989) J Org Chem 54:4626–4636
33. Job P (1928) Ann. Chimica 9:113
34. Connors A (1987) Binding constants, the measurement of molecular complex stability. Wiley, New York
35. Wenz G, Han A (2006) Chem Rev 106:782
36. Frank RL, Adams CL, Blegen JR, Deanin R, Smith PV (1947) Ind Eng Chem 39:887
37. Marvel CS, Williams JLR, Baumgarten HE (1949) J Polym Sci 4:583
38. Clabaugh WS, Leslie RT, Gilchrist RJ (1955) Res Natl Bur Stand 55:261
39. Marvel CS, Hwa CCL (1960) J Polym Sci 28:25
40. Choi SW, Ritter H (2007) e-Polymers 045
41. Storsberg J, Ritter H (2000) Macromol Rapid Commun 21:236
42. Storsberg J, Aert H van, Roost C van, Ritter H (2003) Macromolecules 36:50
43. Choi SW, Ritter H (2004) Macromol Rapid Commun 25:716
44. Mayo FR, Lewis FM (1944) J Am Chem Soc 66:1594
45. Otsu T, Toyoda N (1981) Macromol Chem Rapid Commun 2:79
46. Toyoda N, Yoshida M, Otsu T (1983) Polym J 15:255
47. Otsu T, Shiraishi K (1985) Macromolecules 18:1795
48. Pang Y, Ritter (2006) Macromol Chem Phys 207:201
49. Yusa S-I, Shimada Y, Mitsukami Y, Yamamoto T, Morishima Y (2003) Macromolecules 36:4208
50. Goretzki C, Krlej A, Steffens C, Ritter H (2004) Macromol Rapid Commun 25:513
51. Steffens C, Choi SW, Ritter H (2006) Macromol Rapid Commun 27:542
52. Alupei IC, Alupei V, Ritter H (2002) Macromol Rapid Commun 23:55
53. Han JH, Krochta JM, Kurth MJ, Hsieh Y-L (2000) J Agric Food Chem 48:5278–5282
54. Heo J, Thomas KJ, Seong G, Crooks RM (2003) Anal Chem 75:22–26
55. Feil HY, Bae H, Feijen J, Kim SW (1993) Macromolecules 26:2496–2500
56. Ritter H, Sadowski O, Tepper E (2003) Angew Chem 115:3279
57. Ritter H, Sadowski O, Tepper E (2003) Angew Chem Int Ed 42:3171
58. Ritter H, Sadowski O, Tepper E (2005) Angew Chem 117:6253 (Corrigendum)
59. Ritter H, Sadowski O, Tepper E (2005) Angew Chem Int Ed 44:6099
60. Heskins M, Guilett JE (1969) J Macromol Sci Chem 2:1441
61. Kretschmann O, Choi SW, Miyauchi M, Tomatsu I, Harada A, Ritter H (2006) Angew Chem 118:4468–4472
62. Schmitz S, Ritter H (2006) Angew Chem Int Ed 45:4361–4365
63. Schmitz S, Ritter H (2005) Angew Chem 117:3000–3006
64. Schmitz S, Ritter H (2005) Angew Chem Int Ed 44:5658–5661
65. Köllisch H, Barner-Kowollik Ch, Ritter H (2006) Macromol. Rapid Commun 27:848
66. Steffens C, Kretschmann O, Ritter H (2007) Macromol. Rapid Commun 28:623
67. Kretschmann O, Steffens C, Ritter H (2007) Angew Chem 119:1–5
68. Kretschmann O, Steffens C, Ritter H (2007) Angew Chem Int Ed 46:2708
69. Koopmans C, Ritter H (2007) J Am Chem Soc 129(12):3502
70. Eggersdorfer M, Warwel S, Wulff CT (1993) Nachwachsende Rohstoffe Perspektiven für die Chemie. VCH, Weinheim

Cucurbituril and Cyclodextrin Complexes of Dendrimers

Wei Wang and Angel E. Kaifer[*]

Abstract This chapter reviews the growing body of data on the binding interactions between dendrimers and two types of well-established molecular hosts: cyclodextrins and cucurbit[*n*]urils. Dendrimers are highly branched macromolecules to which functional groups can be attached in spatially defined locations. The attachment of guest functional groups to dendrimers allows the investigation of their binding interactions with freely diffusing hosts/receptors. The effect of dendrimer size on the thermodynamics of these host–guest reactions varies widely depending on factors described here. In optimum cases, it is possible to use these binding interactions to exert redox control on dendrimer self-assembly and even control the size of the resulting assemblies.

Keywords Cobaltocenium, Cucurbit[*n*]urils, Cyclodextrins, Dendrimers, Ferrocene, Host–guest complexation, Inclusion complexes, Viologens

Contents

W. Wang and A.E. Kaifer (✉)
Center for Supramolecular Science and Department of Chemistry, University of Miami, Coral Gables, FL 33124–0431, USA
e-mail: akaifer@miami.edu

1   Introduction

Dendrimers [1–6] are highly branched macromolecules spanning from a central core and containing a series of structurally and synthetically different layers, which are usually referred to as "generations." Thus, a first-generation dendrimer is a small-to-medium size molecule, while a fifth-generation dendrimer is a high molecular weight species with a diameter of several nanometers. The generational growth of dendrimers gives rise to large macromolecules, which constitute some of the most important building blocks in soft nanotechnology. Dendrimers are usually considered polymers, because their structure can be described by the repetitive connection of one or two building blocks. However, the hyperbranched character of dendrimers results –in just a few generations of growth– in macromolecules with roughly spherical or globular shapes. In contrast, most polymers are based on the concatenation of monomers into approximately linear chain arrangements. The different morphologies of linear polymers and dendrimers give rise to pronounced differences in the properties of these two types of macromolecules. For instance, linear polymer solutions tend to be highly viscous, while dendrimer solutions at similar concentration levels are much less viscous. Dendrimers are usually noncrystalline materials, while linear polymers exhibit varying degrees of crystallinity. Low generation dendrimers are truly monodisperse, have a perfectly defined molecular weight and can be treated as molecules. On the other hand, linear polymers are polydisperse materials, with a certain degree of variability in their chain lengths and molecular weights.

The globular shape and size of dendrimers allow us to establish some analogies with proteins, and this realization is responsible for some of the substantial research interest attracted by dendrimers in the last two decades or so. With dendrimers it is possible to place functional groups in relatively well-defined molecular locations and control to some extent the distances separating two or more residues in the same macromolecule, which represents another important reason to explain the extraordinary research interest on dendrimers. While dendrimer research was initially dominated by the development of synthetic methodology and characterization issues, the last decade has seen an increased interest in the functionalization of dendrimer structures with metal complexes, redox centers, and groups exhibiting catalytic or light absorption/emission properties, to name a few examples. In simple terms, there are two general ways to approach dendrimer functionalization:

(1) Attachment of multiple copies of the same functional residue to the dendrimer surface (peripheral functionalization).
(2) Attachment of dendritic mass branching out from a central functional group (core functionalization).
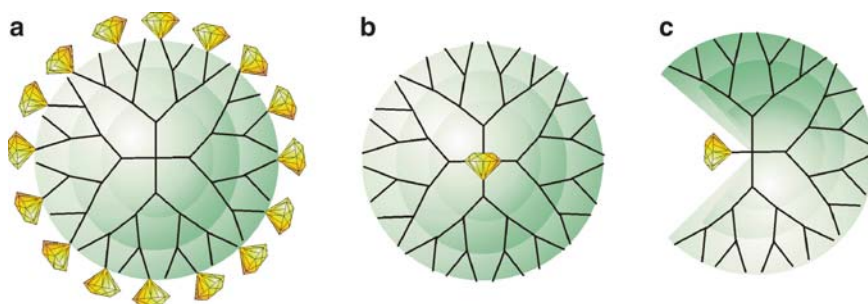
Fig. 1 Schematic renderings of **a** peripheral, **b** core, and **c** open core functionalized dendrimers

Both functionalization approaches (see Fig. 1 for schematic drawings) have different advantages and target different purposes. Peripheral functionalization is normally used when developing systems capable of multivalent interactions or to achieve chemical amplification, taking advantage of the multiple identical residues attached to the dendrimer surface. In clear contrast to this, core functionalization leads to pronounced changes on the microenvironment of the active residue and brings about the possibility of site isolation and/or encapsulation, which may result in considerable changes of the core residue's properties.

Our group has been interested in peripheral and core functionalization methods [7]. However, we have introduced a slight twist on the latter method. We have focused on the functionalization of an active (typically redox active or fluorescent) residue by covalent attachment of dendritic mass to a single point of the residue (see Fig. 1c). This open core functionalization approach yields macromolecules in which the microenvironment of the active residue may be affected by dendron growth, while maintaining the ability of the residue to interact directly with other species in solution, as long as the growth of the dendrimer mass is kept within reasonable limits. Open core functionalized dendrimers are thus of substantial interest because of the considerable differences in reactivity that are expected depending on the direction of reactant approach. If the reactant approaches on the side of the dendrimer containing the active residue, a fast reaction will result. On the other hand, reactant approach on the opposite side of the dendrimer may give rise to a much slower reaction. This type of orientation effect on reactivity is well known in redox proteins, which engage in faster or slower electron transfer depending on the relative orientation of the protein with the reaction partner (or electrode surface, in the case of heterogeneous electron transfer reactions).

Both peripheral and open core functionalized dendrimers can be regarded as possible guests in host–guest molecular recognition phenomena. Functionalization of the dendrimer periphery with multiple copies of a suitable guest residue and exposure to an appropriate host molecule in the same solution may lead to the formation of multiple host–guest complexes on the dendrimer surface. Similarly, open core functionalized dendrimers can be regarded as "dendronized" guests. If the dendron

attached to the guest residue is not large enough to completely engulf it –in other words, if complete encapsulation does not take place– it should be possible for the host molecule to find its way, bind the guest and form an interesting type of host–guest complex. Binding events including multiple guest dendrimers or dendronized guests are of particular interest because they allow us to investigate molecular recognition phenomena that may be strongly affected by multivalency issues or by the microenvironment of the guest itself. In this regard, these noncovalent association reactions borrow some characteristics from biological binding events, in which the receptor–substrate interaction may be strongly affected by nearby components (as in a receptor protruding from a biological membrane) [8].

In this review we will examine the body of research work in which dendrimers have been employed as guests in host–guest complexation reactions. By design, we will not address the possibility of using dendrimers as hosts, which may result from the natural presence of cavities in these macromolecules or from the specific design of receptors within their frameworks.

2   Cyclodextrins and Cucurbit[*n*]urils

Most of the molecular recognition work performed with dendrimer guests has been done using either cyclodextrins or cucurbit[*n*]urils as host molecules. Therefore, it seems appropriate to provide here a brief description of both host families, emphasizing their relative advantages and disadvantages. Both cyclodextrins (CD's) and cucurbit[*n*]urils (CB's) are relatively water-soluble molecules that contain a rather rigid, well-defined cavity whose inner surface is best described as hydrophobic. Both host families are capable of forming inclusion complexes in aqueous solution with a variety of guests. Although the guests are not restricted to those containing hydrophobic moieties, the most stable inclusion complexes are usually formed by guests with a hydrophobic residue that fits well inside the host cavity. In spite of these general similarities between CD's and CB's, it is also important to establish clearly some of their most salient differences. The CD's are natural compounds made by the action of enzymes on starch [9]. They are macrocyclic glucopyranose oligomers, having at least six units linked together by α-(1,4) linkages (see Table 1 for structures). The three most important unmodified (natural) CD's are α-cyclodextrin (α-CD), β-cyclodextrin (β-CD), and γ-cyclodextrin (γ-CD), composed of six, seven, and eight sugar units, respectively. The CB's are synthetic compounds prepared by the condensation of glycoluril with formaldehyde in acidic media [10, 11]. This reaction produces a complex mixture of macrocyclic and acyclic oligomers from which the cyclic pentameric (CB5), hexameric (CB6), heptameric (CB7), octameric (CB8), and decameric (CB10) receptors can be separated in small-to-reasonable yields. Very small amounts of other related compounds with less interesting binding properties can also be isolated from these reaction mixtures, but we will not attempt to provide an exhaustive account of these phenomena here. Because of their range of applications as molecular container hosts and ease of

Table 1 General structures of cyclodextrin (left) and cucurbit[*n*]uril (right) receptors and relevant parameters for the most representative members of both host families

n = 6, α CD
n = 7, β CD
n = 8, γ CD

n = 6, CB6
n = 7, CB7
n = 8, CB8
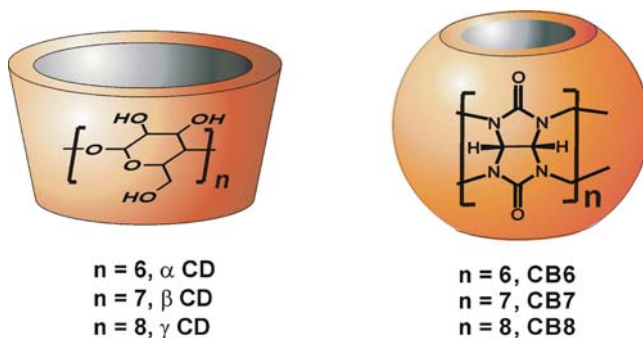
Host	*n*	M.W.	Cavity dia. [Å]	Aq. Sol. [mM]
α−CD	6	972	4.7–5.3	149
β−CD	7	1,135	6.0–6.5	16
γ−CD	8	1,297	7.5–8.3	178
CB6	6	996	3.9–5.8	0.02
CB7	7	1,163	5.4–7.3	20
CB8	8	1,329	6.9–8.8	<0.01

isolation, we will focus our attention on the hosts CB6, CB7, and CB8 (see Table 1). While the cyclodextrins are chiral, the cucurbit[*n*]urils are not, as they exhibit a well-defined equatorial plane of symmetry and both cavity openings (or portals, as they are usually referred to in the literature) are identical. In CD's the two cavity openings are different in size and chemical nature, with primary hydroxyls lining up the narrower cavity openings and secondary hydroxyls around the wider portal. The cavity openings in the CB hosts are lined by the carbonyl oxygen atoms from the glycoluril units.

The cavity of the CD's has the shape of a truncated cone, reaching its maximum diameter at the wider opening. In contrast to this, the cavity of the CBn's has the shape of a barrel and its maximum diameter is located at the molecular equator. The inner surface of the cavity has hydrophobic character in both host families, but the cavity portals are lined up by negative charge density (from the carbonyl oxygen atoms) in the CB's [12]. The hydroxyl groups on the CD portals are believed to be extensively hydrogen bonded, and electrostatic surface potential calculations show little net charge density accumulated on the CD cavity openings. This also constitutes an important difference between both types of hosts.

The CD's form stable inclusion complexes in aqueous solution with guests containing hydrophobic residues that fit well inside the host cavity [13]. The stability of the inclusion complex is the result of hydrophobic interactions and is usually enthalpically driven. Typically, the equilibrium association constant (*K*) between

an excellent guest and the β-CD host is in the range 10^3–$10^5\,\mathrm{M}^{-1}$, with very few CD inclusion complexes exceeding this level of binding affinity. However, the formation of highly stable CB inclusion complexes is usually driven by a combination of hydrophobic forces and ion–dipole interactions between strategically located positive charges on the guest and the rim of carbonyl oxygen atoms on the cavity portals. As a result, CB inclusion complexes in aqueous solution may reach equilibrium association constants as high as $10^{15}\mathrm{M}^{-1}$ (equivalent to that of the avidin–biotin host–guest pair) [14]. Some reported examples suggest that CB hosts are much more sensitive to the presence and nature of charges near the hydrophobic residue [12], giving rise to considerably more pronounced binding selectivities.

The functionalization chemistry of the CD's has been extensively developed at this time [15, 16]. Synthetic methodology is available to either mono-functionalize or perfunctionalize either the primary or secondary hydroxyl portal of these hosts. Derivatization is still a pending subject in the chemistry of cucurbit[n]uril hosts. Kim and coworkers have reported a procedure that allows the equatorial functionalization of the periphery of CB6 [17], but the same procedure is highly inefficient with either CB7 or CB8. Further developments in this area may be of great significance to extend the range of applications of these compounds.

3   Cyclodextrin-Containing Dendrimers

Although this work does not focus on the host properties of dendrimers, it is interesting to mention briefly some work that has been done on the covalent functionalization of cyclodextrins with dendritic structures, to yield what can be appropriately described as dendritic cyclodextrins. Early work on this area was reported by Ahern et al. [18], which prepared β-CD derivatives per-functionalized with hydroxyethylamino chains on the 6-deoxy position (primary face). These CDs, considered as dendrimer precursors, showed a modest degree of binding selectivity with fluorescent guests.

In 1997, Suh, Hah, and Lee [19] reported the covalent attachment of β-CD to poly(ethyleneimine) dendrimers, yielding new compounds that can be viewed as dendrimers with well-defined binding sites on the surface of cyclodextrins with multiple amino groups around the cavity. One year later, Newkome and coworkers [20] reported the per-functionalization of the primary face of β-CD with seven dendrons, giving rise to the dendronized cyclodextrins **1** and **2**. The CD cavity of these compounds remains open and active for inclusion complexation of suitable guests, as was demonstrated with experiments using the competing guests phenolphthalein and aminoadamantane.
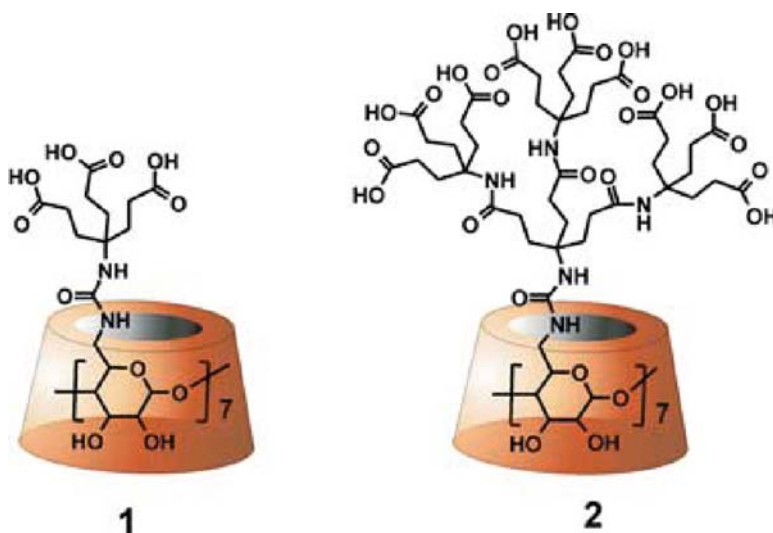
The use of cyclodextrins as a scaffold for the preparation of dendrimers has been explored further by other groups [21–25], but this is beyond the scope of this work.

4 Binding Interactions of Dendrimers with Cyclodextrins

In this section we will focus on the utilization of dendrimers as cyclodextrin guests. Given the solubility limitations of the cyclodextrins and their optimal operation as molecular receptors in aqueous solution, the dendrimers must have significant solubility in water in order to make these studies possible. This constitutes a more serious problem, as we will see, when dealing with dendrimers functionalized with multiple guest units on their surfaces. In general terms, we can divide the work done in this area into two categories, depending on the structure of the dendrimer guests. First, we will review the research work done with dendrimers containing multiple copies of a guest residue on their surfaces (Fig. 1a). Since the guest residue in core dendrimers (Fig. 1b) is shielded from access by freely diffusing hosts, we are left with open core dendrimers (Fig. 1c) as the only other type of dendritic guests available for the investigation of their binding interactions with cyclodextrin hosts.

4.1 Multiple Site Dendrimer Guests

The subject of host–guest binding interactions between water-soluble ferrocene derivatives and CD hosts constitutes a long-standing topic of research interest in our group [26, 27]. Therefore, the preparation of dendrimers containing multiple

ferrocenyl centers on their peripheries attracted our attention pretty quickly. The group of Isabel Cuadrado and the late Moisés Morán (Madrid) started their work on these compounds in the mid 1990s [28, 29]. A little later my group initiated collaborative work with them and we started to investigate the binding interactions between multi-ferrocene dendrimers and CD hosts. Initially, we encountered serious problems related to the lack of solubility of some of these dendrimers in aqueous media. Eventually, we overcame some of these difficulties with the set of dendrimers shown below (**4** and **5**). Compound **3** was used as a model compound.
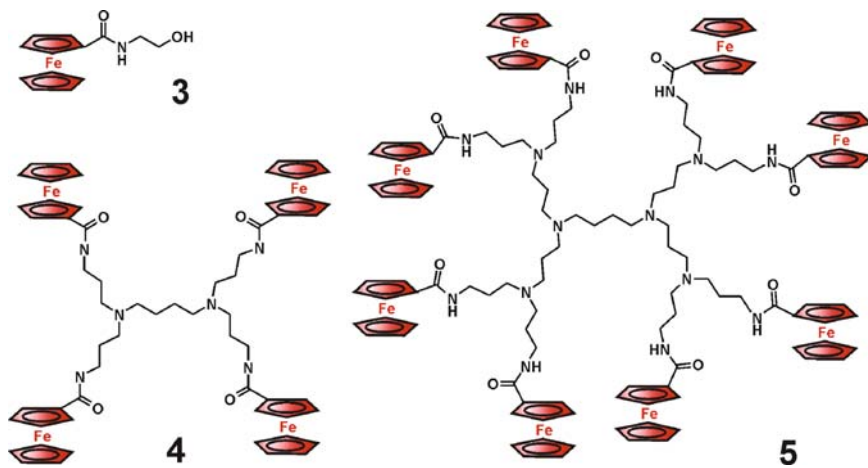
The binding interactions between β-CD and model compound **3** can be investigated by voltammetric techniques or ^{1}H NMR spectroscopy. The latter technique is more convenient to determine the equilibrium constant, K, for the association process:

$$3 + \text{β-CD} \rightleftharpoons 3 \bullet \text{β-CD}$$
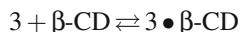
In $0.1\,\text{M NaCl/D}_2\text{O}$, using the variation of the chemical shift of the ferrocene protons as a function of the concentration of CD host, K was found to be $1,230\,\text{M}^{-1}$. The case of dendrimers **4** and **5** is more complicated because their solubility in aqueous media is extremely low. However, two-phase experiments were possible and showed that both dendrimers are effectively extracted from dichloromethane into aqueous solutions containing $6.0\,\text{mM}$ β-CD [30]. From the increased solubility of these dendrimers, we concluded that a minimum number of ferrocene residues in the macromolecule must be CD-bound for solubilization in the aqueous medium to take place. Competition experiments with a second guest (2-naphthalenesulfonate) and voltammetric measurements in the aqueous phase revealed that all ferrocene residues in **4** and **5** are accessible for complexation by β-CD. This is a reflection of the lack of crowding on the surface of these relatively small dendrimers. However, a larger dendrimer containing 16 ferrocenyl units on the surface behaved differently under these conditions, and our experimental results showed that not all 16 ferrocene centers were accessible for binding by the CD host [30]. This is a dendritic effect opposite from that observed by Astruc and coworkers (Bordeaux) with structurally

related multi-ferrocene dendrimers, which serve as voltammetric anion sensors [31]. In their case, increasing the size of the dendrimer and the number of peripheral ferrocenyl units creates more surface anion binding sites and leads to increased binding efficiency, probably as a result of multivalency. In our system, binding of each ferrocenyl residue to β-CD requires some free space around the organometallic center. Therefore, dendrimer growth increases surface crowding and some of the ferrocene units become unavailable to interact with the CD hosts.

From a conceptual point of view, these binding interactions have another supramolecular dimension that should be mentioned here. The dendrimer can be considered as a template that organizes the interacting CD hosts in a defined spatial arrangement [30]. The overall supramolecular complexes reach relatively high molecular weights. For instance, the complex formed by eight β-CD hosts interacting with dendrimer **5**, has a molecular weight over 11 kDa. Furthermore, the redox activity of the templating dendrimer allows the controlled dissociation of these large complexes. It is well known that ferrocene oxidation decreases substantially its binding affinity with β-CD. With small, water-soluble ferrocene derivatives the K value decreases from the 10^3 to $10^4\,M^{-1}$ range to less than $50\,M^{-1}$ upon one-electron oxidation [32]. The latter K value is insufficient to guarantee significant complexation at millimolar concentration levels. Therefore, oxidation of the eight ferrocenyl centers on the surface of dendrimer **5** leads to the dissociation of its complex with β-CD (Fig. 2). This constitutes a remarkable example of redox control on supramolecular structure. It is important to state here that the oxidation of the eight ferrocene residues in **5** takes place in a single voltammetric wave. In other words, the range of half-wave potentials for the individual one-electron oxidations is relatively narrow, reflecting the lack of effective electronic communication between the ferrocene centers. Somewhat surprisingly, a similar situation is found in all reported multiferrocene dendrimers, regardless of their relative degree of surface steric crowding (Fig. 2).

After completing this work with multiferrocene dendrimers, we planned to continue our research work with dendritic macromolecules containing multiple cobaltocenium centers on their surfaces. In analogy to ferrocene, cobaltocenium is also an 18-electron sandwich complex, formally composed of two cyclopentadienyl anions and a Co(III) ion. Overall, it has a positive charge and undergoes one-electron, reversible reduction to the neutral compound cobaltocene. Before the beginning of our work with cobaltocenium dendrimers, we investigated the electrochemical reduction of cobaltocenium to cobaltocene in the presence of β-CD in aqueous solution [33]. Our findings indicate that, while the interaction between cobaltocenium and β-CD is very weak, the reduced form, cobaltocene, forms a stable inclusion complex with β-CD ($K \sim 2 \times 10^3\,M^{-1}$). In the absence of β-CD, cyclic voltammograms for the reduction of cobaltocenium in aqueous media show distorted, very sharp anodic peaks, which result from the precipitation of the uncharged, hydrophobic cobaltocene on the electrode surface. Addition of β-CD removes these precipitation effects, because the inclusion complex between cobaltocene and β-CD is water-soluble [33].
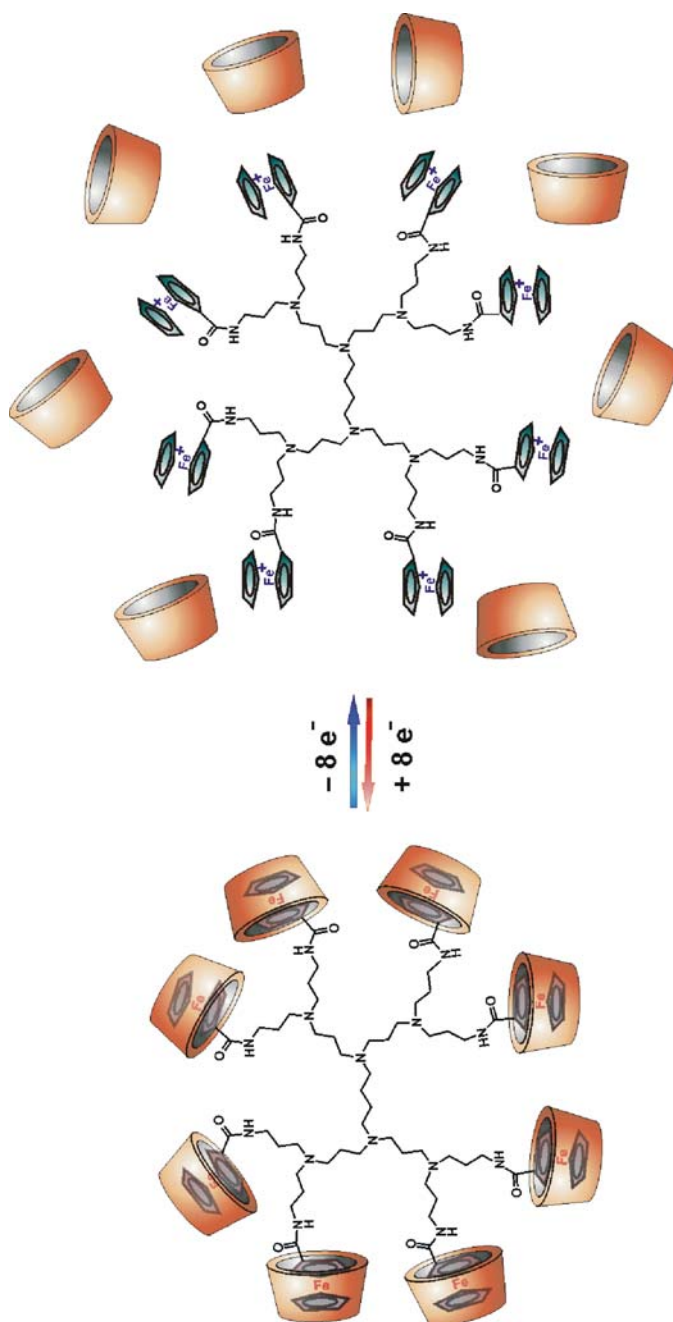
Fig. 2 Redox-induced dissociation of the complex formed between eight β-CD hosts and dendrimer 5

The cobaltocenium dendrimers were also prepared by the Cuadrado–Morán group. These dendritic macromolecules have multiple positive charges on their surfaces and are, thus, water-soluble, which facilitates the investigation of their binding interactions with CD hosts. We investigated dendrimers with a similar poly(propyleneimine) skeleton to those of the multiferrocene dendrimers. Compounds **6** and **7** are typical examples of these macromolecules. Cyclic voltammetry turned out to be a very powerful technique to monitor the binding interactions between these dendrimers and β-CD. As is the case with simple, underivatized cobaltocenium, compounds **6** and **7** show little interaction with this host [34]. The lack of binding interactions between β-CD and the cobaltocenium forms of **6** and **7** was verified by ^{1}H NMR spectroscopy. The voltammetric behavior, however, is highly dependent on the presence of β-CD. Electrochemical reduction of either dendrimer in the absence of the host leads to a sharp, distorted peak for the reoxidation of the dendrimer from its insoluble cobaltocene form [34]. The presence of excess β-CD removes these precipitation effects, strongly suggesting that the same binding mechanism operates with them and with simple cobaltocenium.
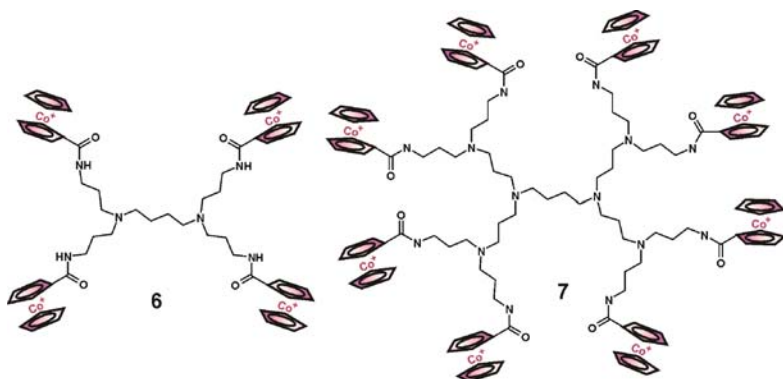
Overall, dendrimers **6** and **7** require *electrochemical activation* (one-electron reduction of each of the cobaltocenium centers) to trigger strong binding interactions with freely diffusing β-CD hosts. Conversely, the ferrocene analogues (**4** and **5**) interact strongly with β-CD in their initial redox states, but a different electrochemical stimulus (one-electron oxidation of each of the ferrocene residues) leads to the breakup of their supramolecular complexes. In both cases, the β-CD hosts form supramolecular complexes with dendrimers containing hydrophobic, uncharged organometallic centers (ferrocene, cobaltocene) on their surfaces, while rejecting the redox forms of the dendrimers decorated with positively charged organometallic residues (ferrocenium, cobaltocenium). We have actually combined both types of stable organometallic centers in a compound containing terminal ferrocene and cobaltocenium residues and shown that the three possible oxidation states of this compound (ferrocenium–cobaltocenium, ferrocene–cobaltocenium, and ferrocene–cobaltocene) can interact with zero, one, or two β-CD hosts, respectively [35]. Cuadrado, Morán and coworkers successfully incorporated

both types of organometallic centers (ferrocene and cobaltocenium) on the surface of poly(propyleneimine) dendrimers, although they did not investigate their binding interactions with β-CD [36].

These poly(propyleneimine) dendrimers (**4**–**7**), as well as their higher analogues containing 16, 32, and more ferrocene or cobaltocenium surface units, provide an excellent illustration of peripheral functionalization. We noted quite early that dendrimers with multiple copies of a functional group expressed on their surfaces could be of interest in applications exploiting chemical amplification [30], but we did not explore these phenomena. The group of Reinhoudt (Twente) started to investigate the interactions between dendrimers having multiple adamantyl residues and β-CD hosts [37]. Like ferrocene, adamantane is one of the best substrate moieties for inclusion complexation by β-CD [27], and its hydrophobic character is also quite pronounced. By lowering the pH of the solution and presumably achieving the protonation of some of the internal amine nitrogen atoms in the dendrimer framework, Reinhoudt and coworkers were able to solubilize these dendrimers in aqueous media, which facilitated the study of their interactions with β-CD [37]. This was the beginning of a very successful and exciting research program that this group has developed during the last decade. The highlight of this program is the effective use of multivalent binding interactions [38]. If one considers the binding interactions between a multiferrocene dendrimer, similar to compound **5**, with a planar surface covered with a self-assembled monolayer of complementary receptors, such as β-CD, it is easy to see that several ferrocene-CD binding interactions may take place simultaneously. While a single binding interaction of this type is worth ca. $-4.5\,\text{kcal mol}^{-1}$ in free energy ($K \sim 2,000\,\text{M}^{-1}$), the multiple presence of several contact points between the dendrimer and the monolayer leads to a much deeper stabilization of the complex, which constitutes a nice example of multivalent binding. We can easily calculate that three simultaneous binding interactions, each with $\Delta G^o = -4.5\,\text{kcal mol}^{-1}$, lead to an effective K value approaching $10^{10}\,\text{M}^{-1}$. Therefore, these multivalent dendrimers are very strongly adsorbed on surfaces containing multiple, organized copies of suitable receptors. This is the fundamental idea behind the concept of the *molecular printboard*, which has led to the elegant development of a new class of soft nanolithographic patterning methods [39].

4.2 Single Site Dendrimer Guests

While our initial interest in dendrimers was concerned with macromolecules containing multiple copies of organometallic centers on their surfaces, we became quickly interested in the idea of using the dendritic framework to partially or fully encapsulate a redox active center, with the main purpose of investigating the effects on the thermodynamics and kinetics of the corresponding electron transfer reactions. In this regard, core functionalization of dendrimers with redox active groups results in macromolecules in which growth of the dendritic components quickly attenuates the rates of most electrochemical reactions [40]. Furthermore,

core functionalization usually affords structures in which the redox center is essentially located in the approximate center of the macromolecule (Fig. 1b), while the active center of many redox proteins is partially buried within the polypeptide framework, but often located away from the center of the protein structure. Therefore, we realized that open core functionalization (Fig. 1c) would offer properties of considerable interest to us, as we tried to design macromolecules that resemble biological molecules [41]. We thus prepared the series of dendrimers **8–10**, which can be succinctly described as dendronized ferrocenes. Full synthetic details for these molecules have been reported elsewhere [42]. Very briefly, their preparation relies on the reaction between chlorocarbonylferrocene and the corresponding amine dendron, which were originally developed by Newkome and coworkers [43]. We fully characterized the structures of these dendrimers by ^{1}H and ^{13}C NMR, IR and UV–Visible spectroscopic data, as well as MALDI–TOF mass spectrometric and electrochemical data [42].
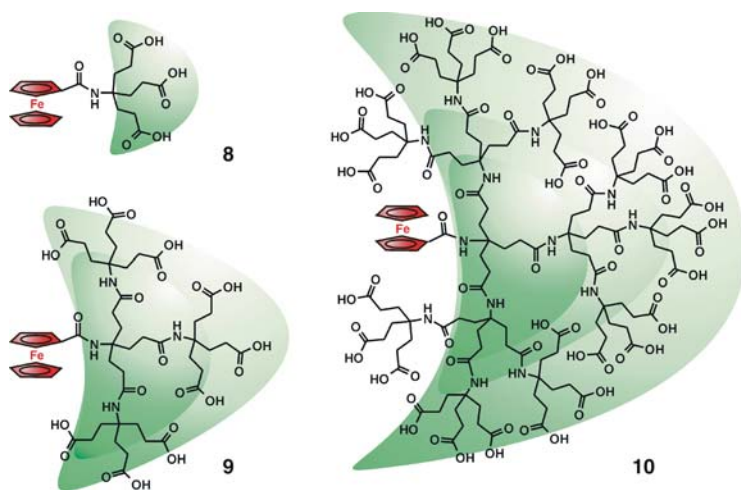
As anticipated, the electrochemical behavior of these dendrimers in aqueous solution is dominated by the reversible, one-electron oxidation of the ferrocene center [41,42]. Although the rate of this electrochemical process decreases with dendrimer size, the voltammetric behavior remains in the quasi-reversible regime even for the largest dendrimer. Dendrimers **9** and **10** evidenced strong pH-controlled orientation effects on their electrochemical reaction rates on gold electrodes modified with a positively charged monolayer of cystamine [44]. More importantly, although dendrimer growth from **8** to **10** affects the half-wave potential for ferrocene oxidation, the small magnitude of this potential variation suggests that the ferrocene is far from being fully encapsulated by the dendron. This is in perfect agreement with molecular modeling of these dendrimers. We reasoned that the ferrocene center must then be still accessible as a substrate for inclusion complexation by β-CD. In fact, cyclic voltammetric experiments readily verified this hypothesis [42]. Addition of β-CD

has two effects on the recorded current-potential curves. First, a general decrease in
the current levels of the ferrocene/ferrocenium wave compared to those measured
in the absence of CD host is observed in all cases. Second, a β-CD-induced half-
wave potential shift to more positive values is also clearly detected. Both effects on
the voltammetric data are well established for ferrocene derivatives interacting with
β-CD [26]. The current decrease is associated to the larger size of the CD complex,
which has lower diffusivity than the free ferrocene derivative, thus leading to smaller
currents. The potential shift reflects the preferential stabilization by the CD of the
ferrocene center (compared to ferrocenium). In this series of dendrimers, the rela-
tive magnitude of both CD-induced effects decreases as we move from compound **8**
to compound **10**. Clearly, increasing the dendron size diminishes the strength of the
ferrocene-CD interaction. In order to quantify this dendrimer size effect, we ana-
lyzed the cyclic voltammetric data using digital simulations. From the optimization
of the fit between digitally simulated and experimental voltammetric data, we ob-
tained reliable values for the equilibrium association constants between all three
dendrimers and β-CD [42]. The corresponding K values (Fig. 3) are 950 ± 140,
250 ± 50, and $50 \pm 10 \, M^{-1}$ for **8**, **9**, and **10**, respectively, at 25°C in 0.1 M NaCl
buffered at pH 7 with 0.05 M Tris.

The K value for the complexation of the first-generation dendrimer (**8**) is at the
low end of the usual range for complexation of water-soluble ferrocene derivatives.
The K values decrease very quickly with dendronized guests **9** and **10**. With the
latter the binding affinity is so low that only a small fraction (ca. 5%) of complex
is formed when millimolar concentrations of dendrimer and host are mixed in so-
lution. We ascribe this drastic loss of binding affinity primarily to steric effects, as
the growth of the dendron hinders the approach of β-CD to the ferrocene center.
However, later investigations (vide infra) of binding affinities between other den-
dronized guests and freely diffusing hosts led us to believe that additional factors
may be at play [8]. Perhaps dendrimer growth increases the hydrophobic character
of the microenvironment around the ferrocene, thus decreasing the strength of the
host–guest hydrophobic interactions that stabilize the inclusion complex.

Our data with β-CD and dendrimers **8–10** opened a number of interesting ques-
tions. Therefore, we decided to investigate binding interactions between various
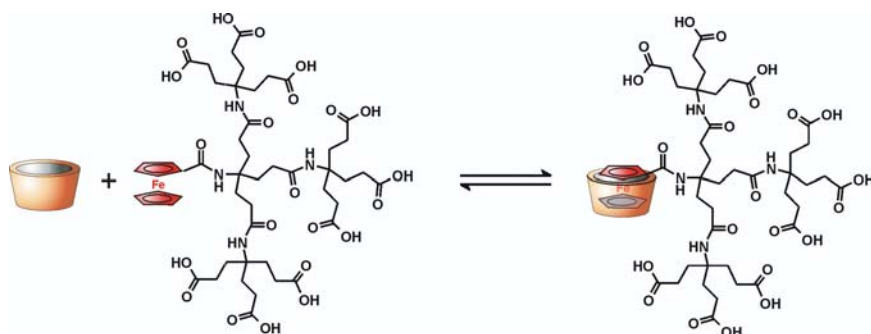
Fig. 3 Binding equilibrium between β-CD and dendrimer 9

types of dendronized guests and CDs, as well as other molecular hosts. Driven by our interest in the microenvironmental changes that may result from dendron growth around a functional group, we synthesized the dansyl-containing dendrimers, **11–13**, using similar methodology [45]. The photophysical properties associated with the fluorescent emission of these compounds were investigated in collaboration with the group of Frank Bright (Buffalo). From their data, obtained in pH 7 buffered aqueous solution, we concluded that dendron growth partially protects the excited state of the dansyl subunit, while decreasing the effective polarity of its microenvironment [45].
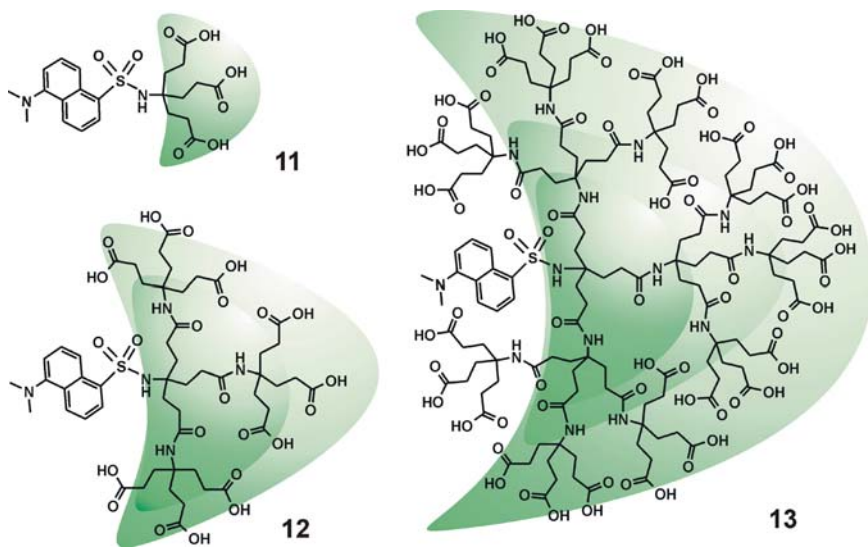
Since dansyl is also a well-known substrate for inclusion complexation by β-CD, we measured the corresponding binding constants for complexation of these dendrimers. As an interesting comparison, the K values for complexation by a selective antidansyl antibody were also determined using fluorescence anisotropy measurements [45]. The results are given in Table 2. Dansyl amine (DA) is included in the table as a model compound, which lacks any dendron component covalently attached to the fluorescent group. The data clearly show that the binding affinity with β-CD is quickly eliminated by dendron growth [45]. In stark contrast to this, the binding affinities with the antibody are not only much higher, as anticipated, but the corresponding K values decrease only slightly in going from dendrimer **11** to **13**. This specific host–guest interaction suffers only minor effects from the growth of the dendron component. The contrast between these two sets of data can be understood by considering the intrinsic binding affinities (measured with the model compound DA) with both receptors. The K value with β-CD is five orders of magnitude lower than that for the antibody. Therefore, since complexation with the antibody releases much more free energy, it seems that any required conformational rearrangements on the dendrimer take place, as needed, to allow complex formation with the dansyl

Table 2 Equilibrium association constants (M^{-1}) between dansyl guests and the indicated receptor in aqueous buffer solution (pH = 7) at 22°C

Guest	β – CD Host	Antibody
DA	307 ± 35	$4.97 \pm 0.23 \times 10^7$
11	136 ± 23	$4.07 \pm 0.20 \times 10^6$
12	<1	$1.91 \pm 0.12 \times 10^6$
13	~ 0	$.46 \pm 0.10 \times 10^6$

group. In the case of the β-CD host, the free energy released upon complexation is modest, which prevents complexation when the dendron is sufficiently large (2nd and 3rd generation). In fact, the binding affinity with β-CD decreases so quickly in this series (compared to the series of dendronized ferrocenes) probably because the intrinsic K value (measured for DA-β-CD) is lower than that observed between simple ferrocene derivatives, such as compound **3**, and the same host.

Credi, Raymo and coworkers reported in 2002, the preparation of a new type of carbohydrate-coated, dendronized ferrocenes [46]. The structures of these dendrimers are illustrated by compounds **14** and **15**. Binding interactions with β-CD were investigated by liquid secondary ion mass spectrometry, ^{1}H NMR spectroscopy, voltammetry and circular dichroism. Upon addition of β-CD, cyclic voltammetric experiments showed data similar to those obtained with our dendronized ferrocenes, that is, a CD-induced current level decrease and anodic half-wave potential shift. At 22°C, these authors obtained K values of $2,000 \pm 200$ and $1,300 \pm 200 \, M^{-1}$ for the complexation of **14** and **15**, respectively, by β-CD in $0.1 \, M \, NaClO_4$. Similar dendrimers in which carbohydrate branches are covalently attached to both cyclopentadienyl rings of the ferrocene residue were not bound at all by β-CD, reflecting the shielding of the core ferrocene center in these more symmetric compounds.
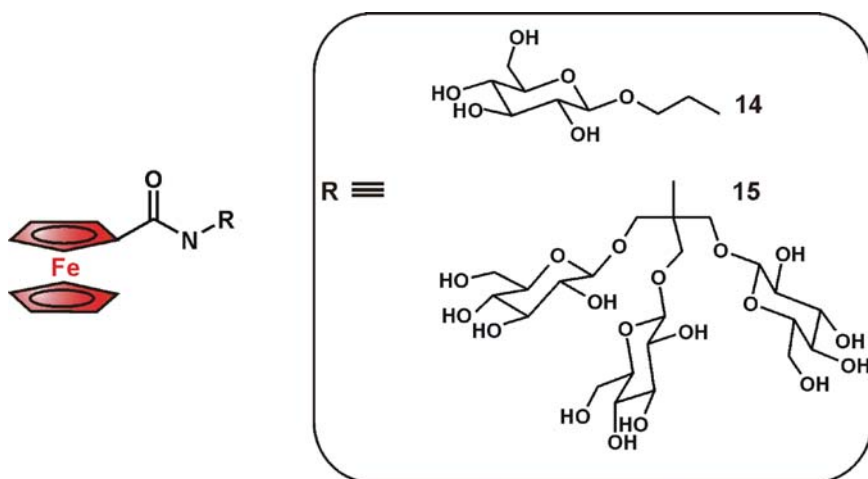
In related work, Newkome and coworkers have prepared conifer-shaped dendrimers or dendronized adamantyl derivatives with structures similar to those of compounds **11–13**. In this case the adamantyl group is connected to the dendron by a five-methylene aliphatic tether. The inclusion of the adamantyl group inside the β-CD cavity was demonstrated by NMR spectroscopy but no binding constants were reported [47]. An interesting variation on this general idea has been reported by Ionita and Chechik, who labeled β-CD with a paramagnetic TEMPO subunit and used Electron Paramagnetic Resonance (EPR) spectroscopy to detect binding to sizable guests, such as dendronized adamantyl derivatives [48].

5 Binding Interactions of Dendrimers with Cucurbit[*n*]urils

Interest in the host binding properties of the cucurbit[*n*]urils (CBs) is increasing very quickly. As a result of this growing interest, several reports on the binding interactions between CB hosts and dendrimers are available. However, although very promising, the chemistry of CBs is still less developed than that of CDs and the body of work is much smaller in the former case. Furthermore, the lack of practical synthetic methods for CB functionalization limits the possibilities of structural elaboration around CB hosts. While the CDs have been used as scaffolds for the construction of dendrimers or covalently attached to dendritic structures, similar research work with CBs is still in its infancy.

5.1 Multiple Site Dendrimer Guests

A very interesting multisite guest for the CB6 host was reported by Kim and coworkers in 2001 [49]. This group prepared a series of poly(propyleneimine) dendrimers with 4, 8, 16, and 32 protonated diaminobutane terminal units on their surface. These dendrimers are very soluble in aqueous media, due to their polycationic nature. The terminal diaminobutane subunit that decorates the surfaces of these macromolecules is known to be an excellent guest for CB6, especially in acidic medium, where both amine nitrogen atoms are protonated and, thus, positively charged. These authors verified using ^{1}H NMR spectroscopic data that exposure of the protonated dendrimers to excess CB6 in aqueous solution leads to threading of the CB receptors around the diaminobutane termini, forming pseudorotaxane-terminated dendrimers (Fig. 4). While the uncomplexed dendrimers afford good quality electrospray mass spectrometric data, the authors could not obtain reasonable mass spectrometric data for the CB6-complexed dendrimers [49]. The only exception was the smaller dendrimer, which has only four diaminobutane termini and is capable of binding four CB6 hosts. Molecular dynamic simulations and ^{1}H NMR relaxation time measurements indicate that multiple CB6 complexation of the peripheral diaminobutane units leads to a very rigid dendrimer shell. The authors suggested that this shell may be useful to trap small molecules in the dendrimer inner phase. In fact, these
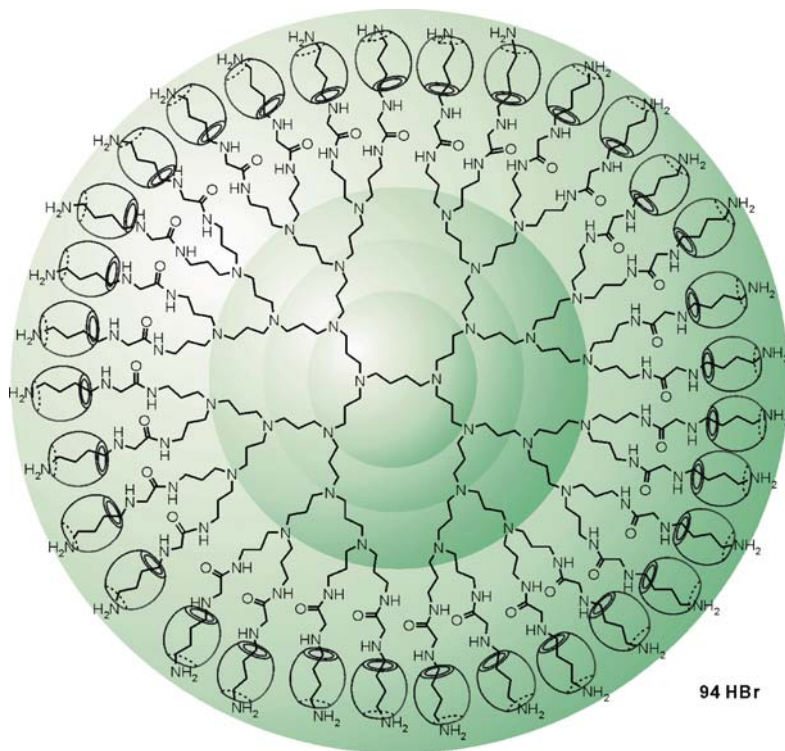
Fig. 4 Illustrative structure of the pseudo-rotaxane complex formed between Kim's diaminobutane dendrimer and 32 CB6 hosts

dendrimers can be viewed as cargo delivery vehicles under pH control, since increasing the solution pH to basic values deprotonates the amine nitrogen atoms and triggers the dissociation of the CB6 hosts, which may in turn release the cargo molecules from the dendrimer interior.

We have also performed a number of experiments with multiferrocene dendrimers and discovered that we can extract these hydrophobic macromolecules from dichloromethane into CB7-containing aqueous solutions. The binding interactions between the ferrocenyl residues and the CB7 hosts drive the phase transfer of the dendrimers, in a similar way to our reported findings with β-CD. However, these results have not been published yet and further work needs to be performed in this area.

5.2 Single Site Dendrimer Guests

Most of the research work done in this topic deals with the CB7 host because its cavity has the right size to bind aromatic molecules, such as bipyridinium derivatives,

or even organometallic sandwich compounds, such as ferrocene and cobaltocenium. Given the importance of viologens (4,4'-bipyridinium salts) in electron transfer reactions and molecular devices, the first report on the isolation of CB7 prompted us to consider the possible formation of inclusion complexes between this host and methylviologen and related compounds. In 2002, we reported the formation of a stable inclusion complex in aqueous media between CB7 and methylviologen [50]. The corresponding K value at 25°C was found to be $1.03 \pm 0.03 \times 10^5 \, M^{-1}$ in 0.2 M NaCl. Later on, we reported that the apparent K value is very sensitive to the concentration of NaCl and other alkali and alkaline-earth metal salts in the medium [51]. This complex is primarily stabilized by (1) hydrophobic interactions between the cavity of CB7 and the biphenyl core of the viologen, and (2) ion–dipole interactions between the positively charged nitrogen atoms on the guest and the rims of carbonyl oxygen atoms on the corresponding cavity portals. Of course, the N–N distance in any viologen is very similar to the distance between the two cavity openings in CB7, which allows the simultaneous development of favorable ion–dipole interactions at both ends of the complex (see Fig. 5).

Around the time in which we completed this research we had prepared in our group a series of dendronized viologens, **16**–**18**, with a molecular design very similar to those of compounds **8**–**10** or **11**–**13**. A unique aspect of this dendrimer series, however, is the five-methylene tether connecting the viologen (4,4'-bipyridinium) group to the focal amide from which the dendron spreads out. The length of this tether was dictated by reasons of molecular stability, as we realized that shorter aliphatic tethers lead to unstable compounds. As usual, these compounds were
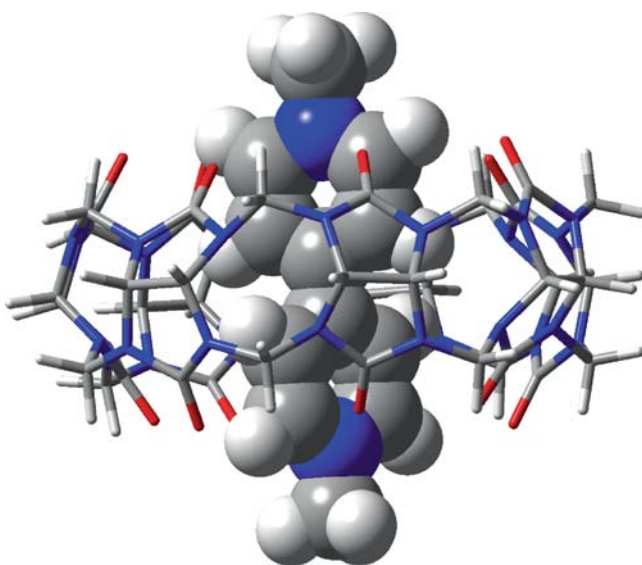
Fig. 5 Energy-minimized (PM3 method) structure of the methylviologen-CB7 inclusion complex

characterized by UV–Vis, ^{1}H and ^{13}C NMR spectroscopies, electrochemical techniques, and MALDI–TOF mass spectrometry [52]. Their open functional core structure may allow the binding of the viologen residue by freely diffusing CB7.
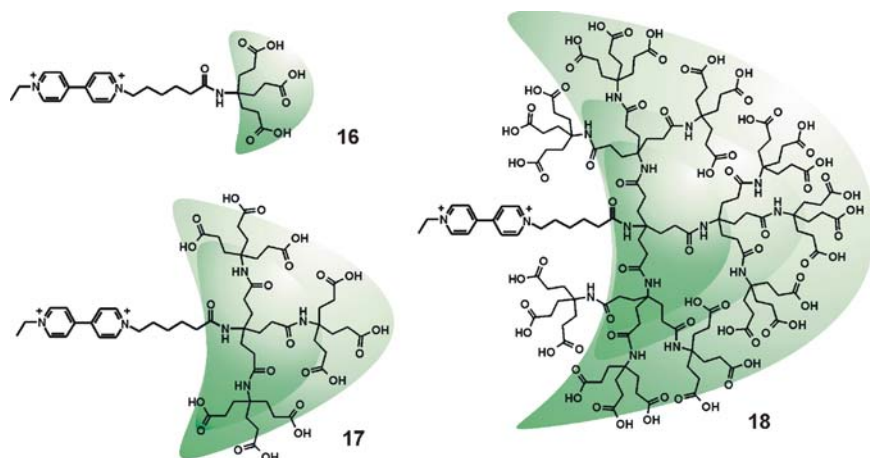
^{1}H NMR experiments show that the viologen residue interacts effectively with the CB7 host [53]. Voltammetric and mass spectrometric data are also consistent with the formation of inclusion complexes between the dendronized viologens and CB7. As was the case with methylviologen, complexation by CB7 depresses the molar absorptivity coefficient for the viologen UV absorption band and this effect can be conveniently utilized to fit the absorbance data in titration experiments to 1:1 binding isotherms. From the optimization of these fittings we obtained the corresponding equilibrium association constants (Table 3).

The K values in the table reveal some interesting trends. First, the binding affinities are higher at pH 3.2, where the carboxylic acid groups on the dendron periphery are protonated and, thus, uncharged. At neutral pH, the negatively charged, ionized

Table 3 Equilibrium association constants[a] (M^{-1}) at 25°C for the complexation of dendronized viologens **16–18** by the CB7 host in aqueous solution buffered at the indicated pH values

Solution pH	Dendrimer		
	16	**17**	**18**
3.2[b]	5.9×10^5	6.2×10^5	3.4×10^5
7.3[c]	5.5×10^4	5.7×10^4	1.3×10^4

[a] Error margin: $\pm 12\%$; [b] $0.2 - M$ formic acid buffer; [c] $0.03 - M$ Tris buffer

carboxylates may induce the dicationic viologen unit to fold, decreasing its accessibility for complexation by the host. At either pH value, however, the binding constants show a very slight decrease in going from the first-generation (**16**) to the third-generation dendrimer (**18**). In fact, the observed trend in the binding affinities is similar to that found between the dendronized dansyl guests and the antidansyl antibody (Table 2) and very different from those observed with the β-CD host. This suggests once again that a relatively high intrinsic binding affinity, as measured between the undendronized guest and the host, is usually maintained as the attached dendron increases in size from first to third generation. In addition to this factor, we have also speculated before [8] that the host approach (host-to-guest residue) might be less disturbed by dendron growth in the case of CB7 binding a viologen unit than in the case of β-CD binding either a ferrocenyl or a dansyl residue.

At the end of the previous section we mentioned that the ferrocene-CB7 binding interaction is quite strong. For the sake of clarity, it is convenient to describe the binding between this host and several simple, water-soluble ferrocene derivatives before addressing the binding interactions between dendronized ferrocenes **8**–**10** and CB7. Our group first reported that ferrocene and its oxidized form, ferrocenium, both form stable inclusion complexes with CB7 [54]. However, in order to determine binding constants, one must do experiments with more water-soluble ferrocene derivatives, such as ferrocenemethanol (**19**), ferrocenecarboxylate (**20**), and the two positively charged derivatives containing one (**21**) or two (**22**) trimethylammonium termini. ^{1}H NMR spectroscopic, mass spectrometric and voltammetric data provide strong evidence for the formation of highly stable CB7 inclusion complexes with **19**, **21**, and **22** [12]. In contrast to this, anionic **20** is not bound at all by CB7, a finding which is attributed to the strong electrostatic repulsion between the negative charge on the guest's carboxylate and the negative charge density on the carbonyl oxygen atoms on the host's cavity opening. These results highlight an important difference between β-CD and CB7, as the former host forms stable inclusion complexes ($K \sim 10^3$–$10^4\,\mathrm{M}^{-1}$) with all these ferrocene derivatives, including ferrocenecarboxylate [13]. The larger selectivity of CB7 is not only evidenced by its complete lack of binding affinity to anionic **20**, but also by the wide range of K values measured with the other derivatives. Thus, isothermal titration calorimetry experiments performed in the presence of competing guests yielded the following K values: $3.0 \pm 0.5 \times 10^9$, $2 \pm 1 \times 10^{12}$, and $3 \pm 1 \times 10^{15}\,\mathrm{M}^{-1}$ for **19**, **21**, and **22**, respectively [12, 14]. These binding affinities are extremely high. In fact, the **22** · CB7 complex exhibits a binding affinity similar to that of the biotin–avidin combination, which constitutes an extremely interesting result in its own right [14]. These binding data allow us to establish a nice comparison between the receptor properties of CD and CB hosts and emphasize that the latter are capable of reaching much higher affinities with suitable guests, while maintaining more selectivity, based on the functional groups directly attached to the main binding site (the ferrocene moiety is included very tightly in the CB7 cavity in all these complexes).
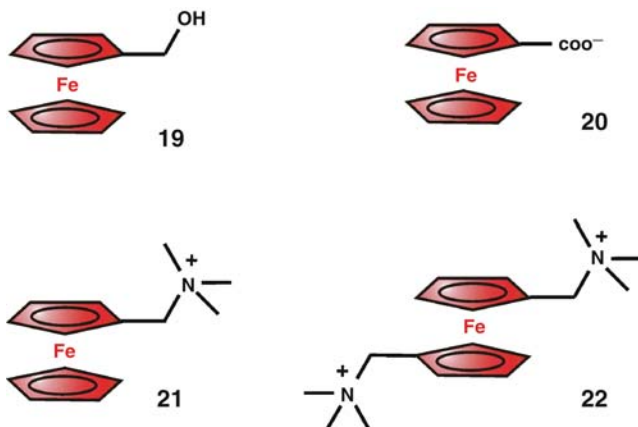
As a result of these findings and given the availability of the dendronized ferrocenes **8–10** in our group, we decided to investigate their binding interactions with CB7. We also prepared a new series of dendronized cobaltocenium guests (**23–25**), following similar synthetic methodology and characterization techniques [55]. The binding constant in aqueous media between simple cobaltocenium and CB7 was measured in our group using UV–Vis measurements in the presence of a competing, reference guest (1,6-hexanediamine), whose binding constant had been accurately measured by Isaacs and coworkers [56]. At 25°C the obtained K value for cobaltocenium–CB7 association was $5.7 \pm 0.6 \times 10^9 M^{-1}$ [55]. This finding led us to add compounds **23–25** to the list of substrates for inclusion complexation by CB7. All the binding constants were measured using ^{1}H NMR spectroscopic experiments in which the guest of interest was set to compete for a limited amount of CB7 with a second, reference guest, whose binding constant was previously known. The binding results for the dendronized ferrocene and cobaltocenium derivatives are given in Table 4 [55, 57].
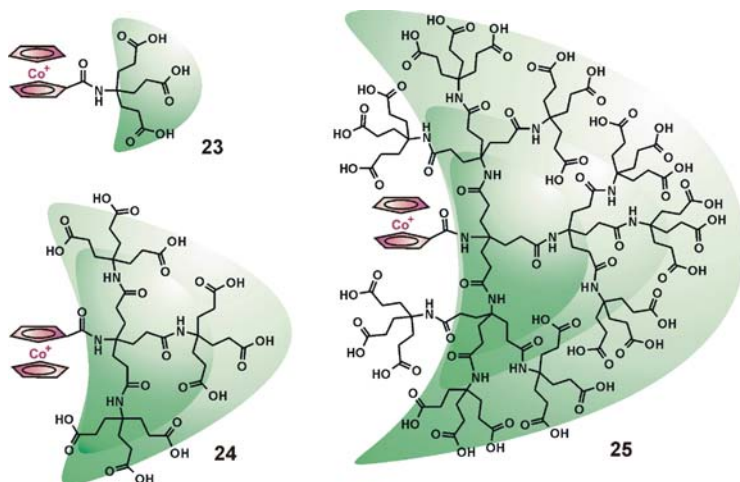
Table 4 Equilibrium association constants[a] (M^{-1}) at 25°C measured in aqueous media between dendronized metallocenes and the CB7 host

Guest	At pH 2	At pH 7
8	3.9×10^4	n.b.[b]
9	4.2×10^6	3.8×10^5
10	Insol.[c]	7.7×10^5
23	3.2×10^5	1.0×10^4
24	1.1×10^7	3.4×10^6
25	4.0×10^5	4.0×10^5

[a]Error margin: $\pm 12\%$; [b]No binding detected; [c]Insoluble under these conditions

In analogy with the anionic derivative **20**, the first-generation ferrocenyl dendrimer **8** is not bound by CB7 at pH 7, where its three carboxylic acid groups are ionized [57]. In contrast, the same compound is bound at pH 2 because protonation removes the negative charges on the carboxylic acid groups. The intensity of these electrostatic effects decreases as the dendron increases its size. Therefore, the second-generation ferrocenyl dendrimer **9** is bound at both solution pH values, although the binding affinity is higher at pH 2. We must point out that a similar pH effect was also visible in the data for the dendronized viologens (Table 3). Unfortunately, the complex between **10** and CB7 was insoluble in pH 2 solution, which prevents us from completing this comparison for the larger ferrocenyl dendrimer. The dendronized cobaltocenium derivatives followed similar binding affinity trends. More stable CB7 complexes are formed at pH 2 than at pH 7 solutions, presumably reflecting the electrostatic repulsions between the terminal carboxylates on the dendrimer and the cavity openings in the host [55]. Electrostatics are not enough in this case, to prevent the formation of a stable complex between CB7 and the first-generation compound **23**, even at pH 7 where the three terminal carboxylates on the dendron are fully ionized. A comparison between guests **8** and **23** at neutral pH indicates that the presence of a positive charge on the metallocene binding site stabilizes the CB7 complex. This is also consistent with the fact that the dendronized cobaltocenium complexes are more stable in all cases than the corresponding ferrocene complexes. Overall, the binding data between CB7 and dendronized metallocenes suggest that electrostatic effects play a significant role in the overall stability of the complexes, while charge effects play a minor role, if any, when β-CD serves as the freely diffusing host in similar experiments.

6   Cucurbit[8]uril-Mediated Dendrimer Self-Assembly

Increasing the size of the CB host cavity opens up a number of interesting possibilities. Kim pioneered the use of CB8 and realized that this receptor has a cavity large enough to host two aromatic compounds simultaneously, giving rise to ternary
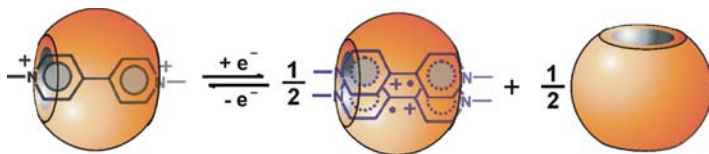
Fig. 6 CB8-mediated dimerization of methylviologen upon one-electron reduction

complexes. One of the first reports on this interesting binding property saw the light in 2002 [58]. Kim et al. demonstrated that, while CB8 forms a very stable 1:1 complex with methylviologen, one-electron reduction of the guest gives rise to the formation of an extremely stable ternary complex in which CB8 encapsulates two methylviologen cation radicals (Fig. 6). Dimerization of viologen cation radicals was, of course, well known before Kim's report. However, the extent of dimerization was found to vary widely depending on the nature of the solvent and the substituents attached to the viologen nucleus. Kim's report opened up the possibility of using CB8-mediated dimerization of viologen cation radicals as a mechanism to drive the formation of interesting supramolecular structures.

Application of these phenomena to the dendronized viologens **16–18** was of immediate interest to us because it may afford a novel mechanism for dimerization of dendrimers under redox control. Therefore, we investigated the one-electron reduction of these compounds in the presence of CB8 [59]. Our experiments provided clear evidence for a similar mechanism operating with the dendronized viologens. For instance, reduction of the second-generation dendrimer **17** in the presence of CB8 leads to a deeply colored blue solution, whose electronic absorption spectrum has the anticipated features of the cation radical dimer and shows essentially no evidence for the presence of monomeric cation radicals. In the absence of CB8 or in the presence of the smaller host CB7, one-electron viologen reduction does not lead to any significant degree of cation radical dimerization. The cyclic voltammetric behavior of **17** also supports extensive dimerization of the cation radical form, as the difference between the half-wave potentials for the two consecutive one-electron viologen reductions increases considerably from what is observed in the absence of CB8. Our experimental results confirm the dimerization of the cation radical form of the dendrimers in all cases, even in solutions containing mixtures of two different dendronized viologens [59]. Detailed analysis of the visible spectra shows that the dimerization of one-electron reduced **18** does take place, but the extent of dimerization is significantly lower than with smaller dendrimers. This was rationalized as a result of the large number of negative charges present on the surface of **18** at the neutral pH in which these experiments were conducted. Overall, our results verify the proposed mechanism (Fig. 7) which constitutes a novel example of the use of redox conversions to control dendrimer assembly.

The success of this approach gave us a powerful reason to explore related mechanisms that may also rely on the binding properties of CB8. For instance, it is well-known that CB8 forms ternary complexes in which electron acceptor and electron donor aromatic groups are simultaneously bound inside the host cavity [10].
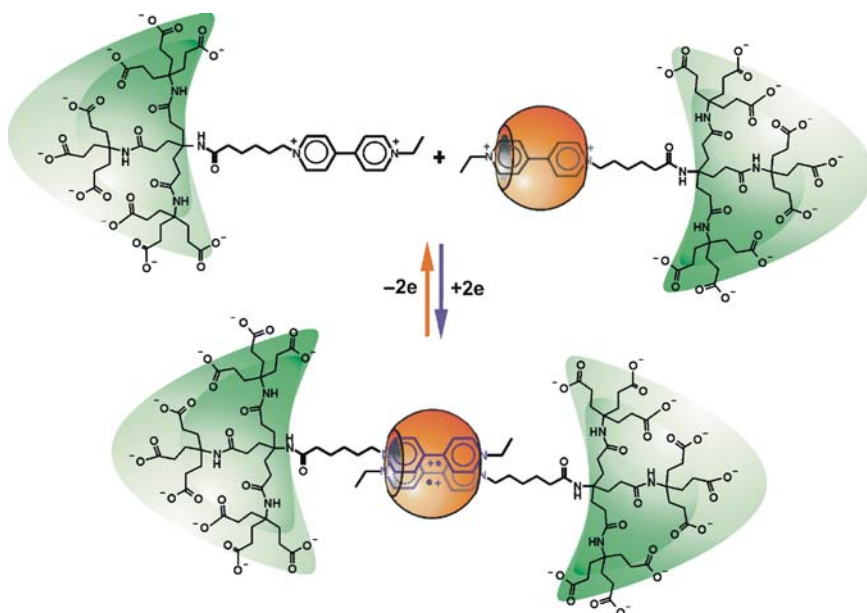
Fig. 7 Redox control on the CB8-mediated dimerization of dendronized viologens

We reasoned that the interplay between viologen cation radical dimerization and viologen-π donor interaction could be utilized to develop more sophisticated mechanisms of dendrimer assembly under redox control. Driven by this hypothesis, we prepared a new series of dendrimers, similar to **16–18**, but containing a dialkoxybenzene aromatic donor residue instead of the electron acceptor viologen moiety [60]. The new series of dendronized dialkoxybenzene derivatives (**26–28**) is shown below.
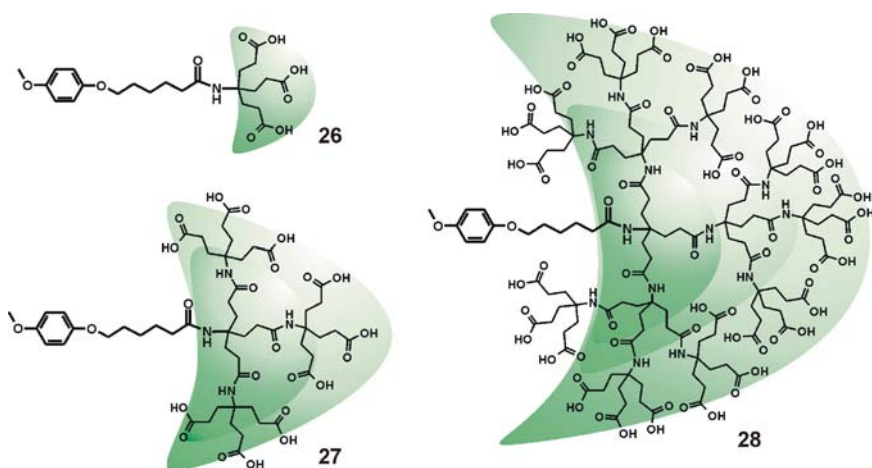
Mixing of equimolar amounts of **27** and the second-generation viologen analogue (compound **17**) in pH 7 aqueous solution may give rise to the formation of a charge transfer complex between the viologen acceptor and dialkoxybenzene donor residues. Not surprisingly, complexation is not observed at millimolar concentrations of both dendrimers, since the equilibrium association constants for these charge transfer complexes are typically quite low ($< 50M^{-1}$). However, addition of CB8 leads to the formation of the charge transfer complex as observed by the development of a visible band at 492 nm. In fact, the absorbance at this wavelength increases linearly with the added concentration of CB8, until 1.0 equiv. of the host is present in solution. After this point, the band does not develop any further. This finding reflects the high stability of the complex formed between the two dendrimers and CB8, in which the host includes the charge transfer complex composed by the two (acceptor + donor) aromatic units. ^{1}H NMR spectroscopy confirms the formation of a viologen–dialkoxybenzene charge transfer complex inside the CB8 cavity, as both sets of aromatic protons shift to higher field as gradually increasing amounts of the host are added to the solution [60]. Similar results are observed when any dendronized viologen is mixed with any dendronized dialkoxybenzene in the presence of CB8. What would be the effect of one-electron viologen reduction on these dendrimer assemblies? It is well known that one-electron reduction of a viologen residue decreases considerably its electron acceptor character and tends to break up any charge transfer complexes with aromatic donors. In this case, the generation of viologen cation radicals may also lead to their dimerization inside the CB8 cavity. In other words, our working hypothesis was that one-electron reduction of the dendronized viologen would cause the dissociation of the charge transfer complex with the dendronized dialkoxybenzene and give rise to self-dimerization, thus effecting a redox-driven change of partner. We verified that this is indeed the case using cyclic voltammetric and electronic absorption spectroscopic data. The cyclic voltammograms obtained with solutions containing equimolar concentrations of **17**, **27**, and CB8 are essentially identical to those obtained if **27** is not present in the solution, reflecting the fact that the current-potential response is controlled by the viologen cation radical dimerization process. Furthermore, one-electron reduction of solutions containing the three components gives rise to visible spectra fully dominated by the features of the viologen cation radical dimer. Similar results were obtained with all other dendrimer combinations [60]. However, we also observed that the efficiency of the dendrimer assembly (before and after viologen reduction) tends to decrease as the size of the involved dendrimers increases. Figure 8 illustrates a situation in which redox control on the partner translates into size selection of the assembly, which is the most attractive aspect of this dendrimer association scheme.

We are currently investigating the extension of this redox-controlled scheme to multivalent dendrimers, having multiple copies of an aromatic donor unit on their surface, and simple dendronized viologens in order to amplify the size selection aspects of this mechanism.
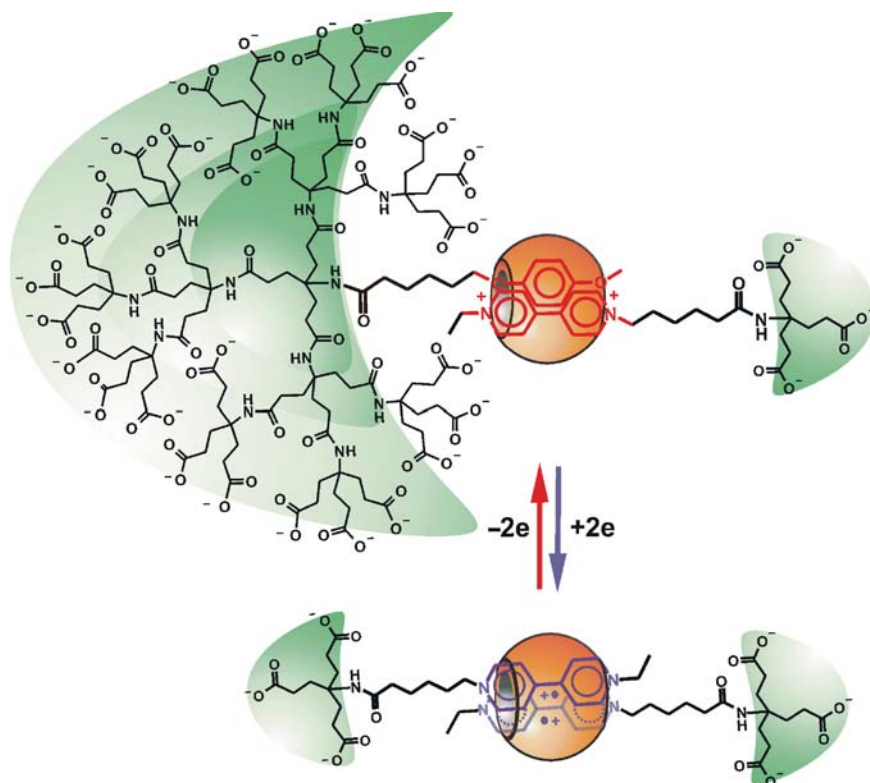
Fig. 8 Redox control on the size of CB8-mediated dendrimer assemblies

7 Related Phenomena

Binding interactions of dendronized guest residues with other hosts have also been investigated. Although space considerations limit how deeply we can address this topic, we will briefly mention here that binding studies of dendronized viologens by a crown ether host afforded data that can be used to distinguish the space-filling properties of different types of dendrons (Newkome vs. Fréchet) covalently attached to the viologen residues [61].

Dendrimers have also been proposed as gene transfection agents and, in 2001, Baker and coworkers showed that complexation with β-CD improves the efficiency of DNA membrane transport by polyamidoamino (PAMAM) dendrimers [62]. This was thought to be due to the smaller size of the dendrimer-DNA particles that form in the presence of β-CD. A similar concept has been developed extensively by Uekama's group, although they elected to prepare covalent conjugates of PAMAM dendrimers with β-CD [63–65]. Kim and coworkers have also reported on the use of cucurbiturils to improve the gene transfection efficiency of dendrimers [66].

8 Conclusions and Outlook

The work summarized herein shows that considerable progress has been made in just a few years at understanding the binding interactions between dendrimers and cyclodextrin and cucurbituril hosts. An important finding in this body of work is that multivalency can be used to develop very stable binding interactions between dendrimers and organized assemblies of suitable receptors, leading to the concept of the molecular printboard, as developed by Reinhoudt and coworkers. The author's group has investigated extensively the binding interactions between dendrimers containing a single and accessible guest residue and CD and CB hosts. Our findings show a surprising diversity of binding affinity trends as a function of dendrimer size. We have also shown that the host properties of CB8 are extremely useful to develop novel schemes for dendrimer self-assembly under redox control. This body of research has been carried out with relatively simple dendrimers. Increasing the synthetic and structural complexity of the dendrimer components may add further levels of interest to this research work. Developments in the chemistry of cucurbiturils, which may eventually allow their peripheral functionalization, will also add new dimensions to these research efforts.

References

1. Lo S-C, Burn PL (2007) Development of dendrimers: macromolecules for use in organic light-emitting diodes and solar cells. Chem Rev 107:1097–1116
2. Hwang S-H, Shreiner CD, Moorefield CN, Newkome GR (2007) Recent progress and applications for metallodendrimers. New J Chem 31:1192–1217
3. Smith DK (2006) Dendritic gels – many arms make light work. Adv Mater 18:2773–2778
4. Boas U, Christensen JB, Heegaard PMH (2006) Dendrimers: design, synthesis and chemical properties. J Mater Chem 16:3785–3798
5. Caminade A-M, Maraval A, Majoral J-P (2006) Phosphorus-containing dendrons: synthesis, reactivity, properties, and use as building blocks for various dendritic architectures. Eur J Inorg Chem 887–901
6. Smith DK (2006) Dendritic supermolecules–towards controllable nanomaterials. Chem Commun 35:34–44
7. Kaifer AE (2007) Electron transfer and molecular recognition in metallocene-containing dendrimers. Eur J Inorg Chem 5015–5027
8. Ong W, Gómez-Kaifer M, Kaifer AE (2004) Dendrimers as guests in molecular recognition phenomena. Chem Commun 1677–1683
9. Connors KA (1997) The stability of cyclodextrin complexes in solution. Chem Rev 97:1325–1358
10. Lee JW, Samal S, Selvapalam N, Kim H-J, Kim K (2003) Cucurbituril homologues and derivatives: new opportunities in supramolecular chemistry. Acc Chem Res 36:621–630

11. Lagona J, Mukhopadhyay P, Chakrabartri S, Isaacs L (2005) The cucurbit[*n*]uril family. Angew Chem Int Ed 44:4844–4870
12. Jeon WS, Moon K, Park SH, Chun H, Ko YH, Lee JY, Lee ES, Samal S, Selvapalam N, Rekharsky MV, Sindelar V, Sobransingh D, Inoue Y, Kaifer AE, Kim K (2005) Complexation of ferrocene derivatives by the cucurbit[7]uril host: a comparative study of the cucurbituril and cyclodextrin host families. J Am Chem Soc 127:12984–12989
13. Rekharsky MV, Inoue Y (1998) Complexation thermodynamics of cyclodextrins. Chem Rev 98:1875–1917
14. Rekharsky MV, Mori T, Yang C, Ko YH, Selvapalam N, Kim H, Sobransingh D, Kaifer AE, Liu S, Isaacs L, Chen W, Moghaddam S, Gilson MK, Kim K, Inoue Y (2007) A synthetic host-guest system achieves avidin-biotin affinity by overcoming enthalpy-entropy compensation. Proc Nat Acad Sci U S A 104:20737–20742
15. Breslow R, Dong SD (1998) Biomimetic reactions catalyzed by cyclodextrins and their derivatives. Chem Rev 98:1997–2011
16. D'Souza VT (2003) Modification of cyclodextrins for use as artificial enzymes. Supramol Chem 15:221–229
17. Jon SY, Selvapalam N, Oh DH, Kang J-K, Kim S-Y, Jeon YJ, Lee JW, Kim K (2003) Facile synthesis of cucurbit[*n*]uril derivatives via direct functionalization: expanding utilization of cucurbit[*n*]uril. J Am Chem Soc 125:10186–10187
18. Ahern C, Darcy R, O'Keeffe F, Schwinte P (1996) 6-Hydroxyalkylamino-6-deoxy-cyclodextrins: towards dendrimeric host molecules. J Incl Phenom 25:43–46
19. Suh J, Hah SS, Lee SH (1997) Dendrimer poly(ethylenimine)s linked to β-cyclodextrin. Bioorg Chem 25:63–75
20. Newkome GR, Godínez LA, Moorefield CN (1998) Molecular recognition using β-cyclodextrin-modified dendrimers: novel building blocks for convergent self-assembly. Chem Commun 1821–1822
21. Baussanne I, Benito JM, Mellet CO, Fernández JMG, Law H, Defaye J (2000) Synthesis and comparative lectin-binding affinity of mannosyl-coated β-cyclodextrin-dendrimer constructs. Chem Commun 1489–1490
22. Ortega-Caballero F, Giménez-Martínez JJ, García-Fuentes L, Ortiz-Salmerón E, Santoyo-Gonzplez F, Vargas-Berenguel A (2001) Binding affinity Properties of dendritic glycosides based on a β-cyclodextrin core toward guest molecules and concanavalin A. J Org Chem 66:7786–7795
23. Vargas-Berenguel A, Ortega-Caballero F, Santoyo-González F, García-López JJ, Giménez-Martínez JJ, García-Fuentes L, Ortiz-Salmerón E (2002) Dendritic galactosides based on a β-cyclodextrin core for the construction of site-specific molecular delivery systems: synthesis and molecular recognition studies. Chem Eur J 8:812–827
24. Benito JM, Gómez-García M, Ortiz Mellet C, Baussanne I, Defaye J, García Fernández JM (2004) Optimizing saccharide-directed molecular delivery to biological receptors: design, synthesis, and biological evaluation of glycodendrimer-cyclodextrin conjugates. J Am Chem Soc 126:10355–10363
25. Gómez-García M, Benito JM, Rodríguez-Lucena D, Yu J-X, Chmurski K, Ortiz Mellet C, Gutierrez Gallego R, Maestre A, Defaye J, García Fernández JM (2005) Probing secondary carbohydrate-protein interactions with highly dense cyclodextrin-centered heteroglycoclusters: the heterocluster effect. J Am Chem Soc 127:7970–7971
26. Isnin R, Salam C, Kaifer AE (1991) Bimodal cyclodextrin complexation of ferrocene derivatives containing n-alkyl chains of varying length. J Org Chem 56:35–41
27. Godínez LA, Schwartz L, Criss CM, Kaifer AE (1997) Thermodynamic studies on the complexation of aromatic and aliphatic guests in water and water-urea mixtures. Experimental evidence for the interaction of urea with arene surfaces. J Phys Chem B 101:3376–3380
28. Alonso B, Cuadrado I, Morán M, Losada J (1994) Organometallic silicon dendrimers. J Chem Soc Chem Commun 2575–2576
29. Cuadrado I, Morán M, Casado CM, Alonso B, Lobete F, García B, Ibisate M, Losada J (1996) Ferrocenyl-functionalized poly(propylenimine) dendrimers. Organometallics 15:5278–5280

30. Castro R, Cuadrado I, Alonso B, Casado CM, Morán M, Kaifer AE (1997) Multisite inclusion complexation of redox active dendrimer guests. J Am Chem Soc 119:5760–5761
31. Valerio C, Fillaut J-L, Ruiz J, Guittard J, Blais J-C, Astruc D (1997) The dendritic effect in molecular recognition: ferrocene dendrimers and their use as supramolecular redox sensors for the recognition of small inorganic anions. J Am Chem Soc 119:2588–2589
32. Moozyckine AU, Bookham JL, Deary ME, Davies DM (2001) Structure and stability of cyclodextrin inclusion complexes with the ferrocenium cation in aq. solution: ^{1}H NMR studies. J Chem Soc Perkin Trans 2:1858–1862
33. Wang Y, Mendoza S, Kaifer AE (1998) Electrochemical reduction of cobaltocenium in the presence of β-cyclodextrin. Inorg Chem 37:317–320
34. González B, Casado CM, Alonso B, Cuadrado I, Morán M, Wang Y, Kaifer AE (1998) Synthesis, electrochemistry and cyclodextrin binding of novel cobaltocenium-functionalized dendrimers. Chem Commun 2569–2570
35. González, B, Cuadrado I, Alonso B, Casado CM, Morán M, Kaifer AE (2002) Mixed cobaltocenium-ferrocene heterobimetallic complexes and their binding interactions with β-cyclodextrin. A three-state, host-guest system under redox control. Organometallics 21:3544–3551
36. Casado C, González B, Cuadrado I, Alonso B, Morán M, Losada J (2000) Mixed ferrocene-cobaltocenium dendrimers: the most stable organometallic redox systems combined in a dendritic molecule. Angew Chem Int Ed 39:2135–2138
37. Michels JJ, Baars MWPL, Meijer EW, Huskens J, Reinhoudt DN (2000) Well-defined assemblies of adamantyl-terminated poly(propyleneimine) dendrimers and β-cyclodextrin in water. J Chem Soc Perkin Trans 2:1914–1918
38. Huskeens J, Deij MA, Reinhoudt DN (2002) Attachment of molecules at a molecular printboard by multiple host-guest interactions. Angew Chem Int Ed 41:4467–4471
39. Ludden MJW, Reinhoudt DN, Huskens J (2006) Molecular printboards: versatile platforms for the creation and positioning of supramolecular assemblies and materials. Chem Soc Rev 35:1122–1134
40. Cameron CS, Gorman CB (2002) Effects of site encapsulation on electrochemical behavior of redox-active core dendrimers. Adv Funct Mater 12:17–20
41. Cardona CM, Kaifer AE (1998) Asymmetric redox-active dendrimers containing a ferrocene subunit. Preparation, characterization, and electrochemistry. J Am Chem Soc 120:4023–4024
42. Cardona CM, McCarley TD, Kaifer AE (2000) Synthesis, electrochemistry, and interactions with β-cyclodextrin of dendrimers containing a single ferrocene subunit located "off-center". J Org Chem 65:1857–1864
43. Newkome GR, Behera RK, Moorefield CN, Baker GR (1991) Chemistry of micelles. 18. Cascade polymers: syntheses and characterization of one-directional arborols based on adamantane. J Org Chem 56:7162–7167
44. Wang Y, Cardona CM, Kaifer AE (1999) Molecular orientation effects on the rates of heterogeneous electron transfer of unsymmetric dendrimers. J Am Chem Soc 121:9756–9757
45. Cardona CM, Alvarez J, Kaifer AE, McCarley TD, Pandey S, Baker GA, Bonzagni NJ, Bright FV (2000) Dendrimers functionalized with a single fluorescent dansyl group attached "off center:" Synthesis and photophysical studies. J Am Chem Soc 122:6139–6144
46. Ashton PR, Balzani V, Clemente-Leon M, Colonna B, Credi A, Jayaraman N, Raymo FM, Stoddart JF, Venturi M (2002) Ferrocene-containing carbohydrate dendrimers. Chem Eur J 8:673–684
47. Newkome GR, Kotta KK, Moorefield CN (2006) Design, synthesis and characterization of conifer-shaped dendritic architectures. Chem Eur J 12:3726–3734
48. Chechik V, Ionita G (2006) Supramolecular complexes of spin-labelled cyclodextrins. Org Biomol Chem 4:3505–3510
49. Lee JW, Ko YH, Park S-H, Yamaguchi K, Kim K (2001) Novel pseudorotaxane-terminated dendrimers: supramolecular modification of dendrimer periphery. Angew Chem Int Ed 40:746–749
50. Ong W, Gomez-Kaifer M, Kaifer AE (2002) Cucurbit[7]uril: a very effective host for viologens and their cation radicals. Org Lett 4:1791–1794

51. Ong W, Kaifer AE (2004) Salt effects on the apparent stability of the cucurbit[7]uril-methyl viologen inclusion complex. J Org Chem 69:1383–1385
52. Ong W, Kaifer AE (2002) Unusual electrochemical properties of unsymmetric viologen dendrimers. J Am Chem Soc 124:9358–9359
53. Ong W, Kaifer AE (2003) Molecular encapsulation by cucurbit[7]uril of the apical 4,4″-bipyridinium residue in Newkome-type dendrimers. Angew Chem Int Ed 42:2164–2167
54. Ong W, Kaifer AE (2003) Unusual electrochemical properties of the inclusion complexes of ferrocenium and cobaltocenium with cucurbit[7]uril. Organometallics 22:4181–4183
55. Sobransingh D, Kaifer AE (2006) New dendrimers containing a single cobaltocenium unit covalently attached to the apical position of newkome dendrons: electrochemistry and guest binding interactions with cucurbit[7]uril. Langmuir 22:10540–10544
56. Liu S, Ruspic C, Mukhopadhyay P, Chakrabarti S, Zavalij PY, Isaacs L (2005) The cucurbit[n]uril family: prime components for self-sorting systems. J Am Chem Soc 127:15959–15967
57. Sobransingh D, Kaifer AE (2005) Binding interactions between the host cucurbit[7]uril and dendrimer guests containing a single ferrocenyl residue. Chem Commun 5071–5073
58. Jeon WS, Kim H-J, Lee C, Kim K (2002) Control of the stoichiometry in host-guest complexation by redox chemistry of guests: inclusion of methylviologen in cucurbit[8]uril. Chem Commun 1828–1829
59. Moon K, Grindstaff J, Sobransingh D, Kaifer AE (2004) Cucurbit[8]uril-mediated redox-controlled self-assembly of viologen-containing dendrimers. Angew Chem Int Ed 43:5496–5499
60. Wang W, Kaifer AE (2006) Electrochemical switching and size selection in cucurbit[8]uril-mediated dendrimer self-assembly. Angew Chem Int Ed 45:7042–7046
61. Ong W, Grindstaff J, Sobransingh D, Toba R, Quintela JM, Peinador C, Kaifer AE (2005) Electrochemical and guest binding properties of Fréchet- and Newkome-type dendrimers with a single viologen unit located at their apical positions. J Am Chem Soc 127:3353–3361
62. Roessler BJ, Bielinska AU, Janczak K, Lee I, Baker JR (2001) Substituted β-cyclodextrins interact with PAMAM dendrimer-DNA complexes and modify transfection efficiency. Biochem Biophys Res Commun 283:12–129
63. Arima H, Kihara F, Hirayama F, Uekama K (2001) Enhancement of gene expression by polyamidoamine dendrimer conjugates with gα−, β-, and gγ-cyclodextrins. Bioconjugate Chem 12:476–484
64. Kihara F, Arima H, Tsutsumi T, Hirayama F, Uekama K (2002) Effects of structure of polyamidoamine dendrimer on gene transfer efficiency of the dendrimer conjugate with α-cyclodextrin. Bioconjugate Chem 13:1211–1219
65. Tsutumi T, Arima H, Hirayama F, Uekama K (2006) Potential use of dendrimer/a-cyclodextrin conjugate as a novel carrier for small interfering RNA (siRNA). J Incl Phenom 56:81–84
66. Lim Y, Kim T, Lee JW, Kim S, Kim H-J, Kim K, Park J (2002) Self-assembled ternary complex of cationic dendrimer, cucurbituril, and DNA: noncovalent strategy in developing a gene delivery carrier. Bioconjugate Chem 13:1181–1185

Index